Data Release Report for Source Physics Experiments 2 and 3 (SPE-2 and SPE-3) Nevada National Security Site

January 2014

Prepared for:

U.S. Department of Energy
National Nuclear Security Administration
Defense Nuclear Nonproliferation Research and Development
National Center for Nuclear Security

Compiled by:

Margaret Townsend and Curtis Obi

Underground Test Area and Boreholes Programs and Operations
National Security Technologies, LLC
Las Vegas, Nevada

DISCLAIMER STATEMENT

Reference herein to any specific commercial product, process, or service by trade name, trademark, manufacturer, or otherwise, does not necessarily constitute or imply its endorsement, recommendation, or favoring by the U.S. Government or any agency thereof or its contractors or subcontractors.

AVAILABILITY STATEMENT

Available for sale to the public, in paper, from–

U.S. Department of Commerce
National Technical Information Service
5301 Shawnee Road
Alexandria, VA 22312
Telephone: 800.553.6847
Fax: 703.605.6900
E-mail: orders@ntis.gov
Online ordering: http://www.ntis.gov/help/ordermethods.aspx

Available electronically at http://www.osti.gov/bridge.

Available for a processing fee to U.S. Department of Energy and its contractors, in paper, from–

U.S. Department of Energy
Office of Scientific and Technical Information
P.O. Box 62
Oak Ridge, TN 37831-0062
Telephone: 865.576.8401
Fax: 865.576.5728
E-mail: reports@adonis.osti.gov

Data Release Report for Source Physics Experiments 2 and 3 (SPE-2 and SPE-3) Nevada National Security Site

Compiled by:
Margaret Townsend and Curtis Obi
National Security Technologies, LLC

With contributions from:

Robert Abbott, Sandia National Laboratories
Robert Mellors, Lawrence Livermore National Laboratory
Ken Smith, Nevada Seismology Laboratory, University of Nevada, Reno
David Steedman, Los Alamos National Laboratory
William Walter, Lawrence Livermore National Laboratory

January 2015

The near-field data for SPE-2 are found in **Assembled Data Set 14-067***, and near field data for SPE-3 are found in* **Assembled Data Set 14-068**. *Both data sets also include this report. The far-field data were submitted directly using the Nevada Seismological Laboratory's "SN" network code and merged directly in the IRIS archive.*

Source Physics Experiments 2 and 3
Principal Investigators:

Lawrence Livermore National Laboratory

Tarabay Antoun   William Walter

Los Alamos National Laboratory

Christopher Bradley   Wendee Brunish (ret.)   David Coblentz
Howard Patton   David Steedman   Aviva Sussman
                       Rodney Whitaker

Sandia National Laboratories

Robert Abbott   Scott Broome   Kyle Jones

Defense Threat Reduction Agency

Kiran Shah

Air Force Technical Applications Center

Chandan Saikia

National Security Technologies, LLC

Catherine Snelson (now at Los Alamos National Laboratory)

Other Major Contributors:

Lawrence Livermore National Laboratory

Sean Ford   Lew Glenn   Ilya Lomov
Robert Mellors   Phil Harben   Artie Rodgers
J. P. Lewis   Oleg Vorobiev   Teresa Hauk
Souheil Ezzedine   Moira Pyle   Jeff Wagoner

Los Alamos National Laboratory

Earl Knight   Carene Larmat   Esteban Rougier
Charlotte Rowe   Tom Sandoval   Emily Schultz-Fellenz
Jennifer Wilson   Reece Wilson   David Yang

Sandia National Laboratories

Dave Aldridge   Nedra Bonal   Hunter Knox   Leiph Preston   David Yocky

Nevada Seismological Laboratory, University of Nevada, Reno

Ken Smith   Gabe Plank

National Security Technologies, LLC

Ryan Emmitt   Curtis Obi   Scot Tibbets   Margaret Townsend   Robert White

Executive Summary

The second Source Physics Experiment shot (SPE-2) was conducted in Nevada on October 25, 2011, at 1900:00.011623 Greenwich Mean Time (GMT). The explosive source was 997 kilograms (kg) trinitrotoluene (TNT) equivalent of sensitized heavy ammonium fuel oil (SHANFO) detonated at a depth of 45.7 meters (m). The third Source Physics Experiment shot (SPE-3) was conducted in Nevada on July 24, 2012, at 1800:00.44835 GMT. The explosive source was 905 kg TNT equivalent of SHANFO detonated at a depth of 45.8 m. Both shots were recorded by an extensive set of instrumentation that includes sensors both at near-field (less than 100 m) and far-field (100 m or greater) distances. The near-field instruments consisted of three-component accelerometers deployed in boreholes at 15, 46, and 55 m depths around the shot and a set of single-component vertical accelerometers on the surface. The far-field network was composed of a variety of seismic and acoustic sensors, including short-period geophones, broadband seismometers, three-component accelerometers, and rotational seismometers at distances of 100 m to 25 kilometers. This report coincides with the release of these data for analysts and organizations that are not participants in this program. This report describes the second and third Source Physics Experiment shots and the various types of near-field and far-field data that are available.

This page intentionally left blank.

Table of Contents

List of Appendices

List of Figures

List of Acronyms and Abbreviations

AFTAC	Air Force Technical Applications Center
AP	Access Point
CORRTEX	Continuous Reflectometry Radius versus Time Experiment
cm	centimeter(s)
DOB	depth of burial
DTRA	Defense Threat Reduction Agency
E	east
GMT	Greenwich Mean Time
HDD	hard disk drive
Hz	hertz
IML-ST	Inter-Mountain Labs
IRIS	Incorporated Research Institutions for Seismology
kg	kilogram(s)
km	kilometer(s)
L	lateral
LANL	Los Alamos National Laboratory
LLNL	Lawrence Livermore National Laboratory
m	meter(s)
N	north
NNSS	Nevada National Security Site
NSL	Nevada Seismological Laboratory
PASSCAL	Program for Array Seismic Studies of the Continental Lithosphere
R	radial
SCS	Systems Computing Server
SEED	Standard for the Exchange of Earthquake Data
SGZ	surface ground zero
SHANFO	sensitized heavy ammonium nitrate and fuel oil
SNL	Sandia National Laboratories
SPC	State Plane Coordinates
SPE	Source Physics Experiment
sps	samples per second
T	tangential
TNT	trinitrotoluene
UNLV	University of Nevada, Las Vegas
UNR	University of Nevada, Reno
Z	vertical

This page intentionally left blank.

1 Introduction

1.1 Project Description

The Source Physics Experiment (SPE) is a series of chemical explosive tests. SPE Phase I was constructed in granitic rock of the Climax stock, in northern Yucca Flat at the Nevada National Security Site (NNSS; formerly known as the Nevada Test Site) in 2010–2011 (Figure 1). These tests are sponsored by the U.S. Department of Energy, National Nuclear Security Administration's Office of Defense Nonproliferation Research and Development. The SPE test series is primarily designed to study the generation and propagation of seismic waves, and will provide data that will improve the predictive capability of numerical models for detecting and characterizing underground explosions (e.g., Ford and Walter, 2013; Snelson et al., 2012; 2013). These validated, improved seismic-acoustic models and simulations will enhance the U.S. ability to detect and discriminate "low-yield" nuclear explosions.
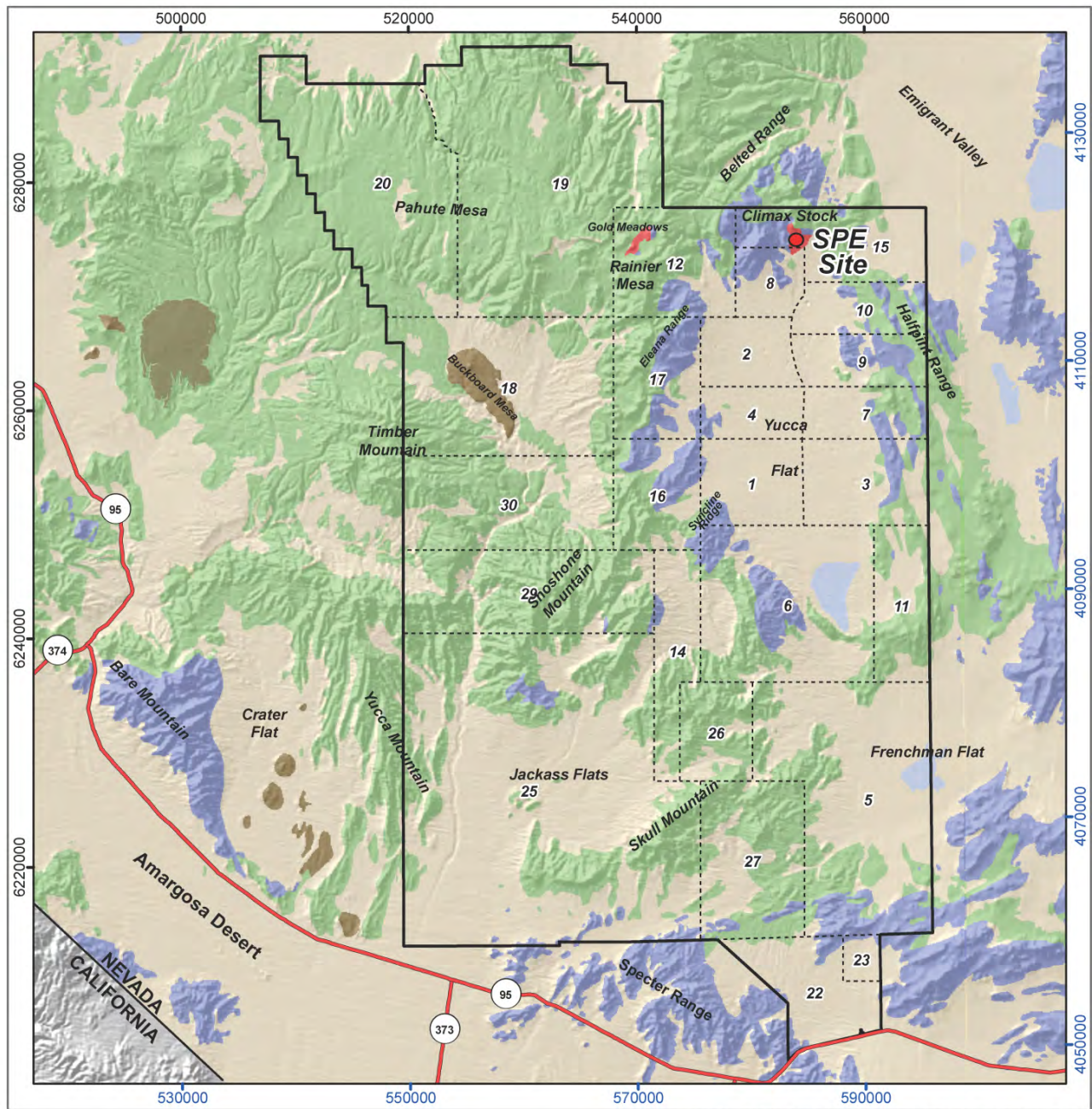
The SPE tests are designed and conducted by a consortium of organizations, including Los Alamos National Laboratory (LANL), Lawrence Livermore National Laboratory (LLNL), Sandia National Laboratories (SNL), and the Defense Threat Reduction Agency (DTRA), in conjunction with National Security Technologies, LLC (NSTec), the Management and Operations contractor at the NNSS. The University of Nevada, Reno (UNR) assisted in data acquisition and compilation. Other organizations, including the Air Force Technical Applications Center (AFTAC) and ENSCO, participated in data acquisition efforts as well.

The first SPE test (SPE-1) was conducted in May 2011, SPE-2 was conducted in October 2011, and SPE-3 was conducted in July 2012. New tests are being planned. The vast majority of data acquired under the SPE program is unclassified/unlimited but subject to a 2-year hold, similar to the policy of the U.S. National Science Foundation. The SPE-2 and SPE-3 time-dependent data (strong motion and seismo-acoustic) have now been released for public access. This report presents information that will aid in the proper understanding and use of the SPE-2 and SPE-3 data sets. (See NSTec [2014] for a description of the SPE-1 experiment, for which data were released in April 2014.)
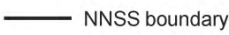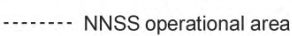
Jesse Bonner, NSTec point of contact (bonnerjl@nv.doe.gov), or Catherine M. Snelson, the SPE test scientist for these data sets, now at LANL (snelsonc@lanl.gov), can be contacted for further information, including information about other data collected at the SPE site.

1.2 Test Description

The SPE-2 test had a larger shot size than SPE-1 (NSTec, 2014). It was designed so that signals could be recorded to 100 kilometers (km) and to investigate depth of burial (DOB) effects. The SPE-3 shot was conducted within the damage zone created by the SPE-2 shot to investigate damage zone effects. The two shots were similar in yield and DOB. Both tests provided data for research and development of simulation capability at both near- and far-field distances. In general, the near field is expected to include inelastic nonlinear effects, while the far field can be considered primarily elastic (or visco-elastic). A detailed description of the sources is provided in Section 2.1.

Figure 1
Map Showing Location of the SPE Experiments at the Nevada National Security Site

A comprehensive set of strong-motion and seismo-acoustic instrumentation was deployed for both shots. The near-field (< 100 meters [m] from the shot point) instrumentation included high-sample-rate, three-component accelerometers deployed in boreholes. A set of single-component surface accelerometers was also installed. At distances at and beyond 100 m (far-field), a comprehensive set of seismic and acoustic sensors were deployed at distances up to 25 kilometers (km). The data and metadata were compiled, archived, and distributed by the technical members of the Nevada Seismological Laboratory (NSL) at UNR. Records for stations at greater distances are available from the permanent UNR seismic network.

The full data sets for SPE-2 and SPE-3, along with associated metadata, are available from the Incorporated Research Institutions for Seismology (IRIS) Data Management Center. The near-field and far-field data sets were submitted separately because they are in different formats. The high sample rates for the near-field recordings are not compatible with the miniSEED format used for the far-field data, and so were submitted separately in SAC format. The near-field data for SPE-2 were assigned the assembled data set number 14-067, with the short name "SPE2." The near-field data for SPE-3 were assigned the assembled data set number 14-068, with the short name "SPE3." The far-field data were submitted directly using NSL's "SN" network code and were merged directly into the IRIS archive. This report is intended to complement the two data sets and provide ancillary information, including selected metadata. However, all data users should verify they are using the full current metadata, including the SN network dataless SEED volume from IRIS for the far-field data, and/or the CSS3.0 metadata from the assembled data sets for the near-field sites.

1.3 Site Description

The SPE test bed consists of a pad excavated and filled on the side of a hill that slopes to the southeast. The setting is weathered granite with a thin but variable cover of unconsolidated soil over bedrock. A 0.91 m diameter source hole was drilled in the center of the test bed, and is surrounded by two rings of 0.20 m diameter instrument holes. The site is identified by the NNSS designator U-15n, with the source hole labeled U-15n, and instrument holes labeled U-15n#1, U-15n#2, and so on in the order they were drilled.

Holes U-15n#1 through #6 had been drilled and instrumented for the SPE-1 shot (NSTec, 2014). All holes were drilled to depths ranging from 57.9 to 60.7 m. Prior to the SPE-2 shot, replacement hole U-15n#1A was drilled to replace the failed instrumentation in U-15n#1. Following the SPE-2 shot and before SPE-3, four new instrument holes were drilled and instrumented similar to the first seven, but deeper, in anticipation of recording the future deeper SPE-4 shot.

1.4 Test Bed Construction

The source hole was drilled to a depth of 60.7 m over a period of several months in late 2010 and early 2011. The first six instrument holes were drilled in August and September 2010, with the addition of a replacement hole in August 2011, prior to SPE-2. The next four instrument holes were added in February 2012, after SPE-2 and prior to SPE-3.

The inner ring of instrument holes (U-15n#1, #2, #3, and #8) are each 10 m from the source hole, and the outer ring of holes (U-15n#4, #5, #6, #7, and #9) are each 20 m from the source hole. Hole U-15n#11 is located 51.2 m northeast of the source hole. After the SPE-2 shot, hole U-15n#10 was

drilled at an angle from the surface to the SPE-2 shot location to document and sample the damaged rock adjacent to the shot point.

Appendix 1 includes construction data for the U-15n source hole and instrument holes. Appendix C in Townsend et al. (2012) contains detailed information about the construction of the first six instrument holes at the SPE site. Figure 2 shows an aerial view of the SPE-2 test bed with the locations of the source hole and instrument holes marked. Figure 3 shows the configuration of the test bed for SPE-3. Figure 4 provides a cut-away view of the test bed for SPE-2 and SPE-3.

1.5 Geology

The Climax stock was selected as the site of the first set of SPE tests because its granite lithology provides a relatively "homogenous" medium and because, as the site of three historical underground nuclear tests, abundant geologic, seismic, and ground shock data are available for comparison to expected SPE test data.

1.5.1 Geologic Setting

The Climax stock is a composite granitic intrusive of Cretaceous age, which intrudes sedimentary rocks of Paleozoic and Precambrian age. The granite body is exposed at the base of Oak Spring Butte, in extreme northern Yucca Flat (Figure 5). The surface exposures of the granite are weathered to depths ranging from about 7.6 to 38.1 m (Townsend et al., 2012).

The Climax stock is moderately to highly fractured. Three major faults define the structure of the Climax area, the Tippinip fault on the west and the Boundary and Yucca faults on the east and south. The SPE site is located approximately 245 m northwest, at closest approach, from the Boundary fault, which separates the surface exposure of the granitic rocks from the alluvium of the Yucca Flat basin. The Boundary fault dips steeply to the southeast, and offset on it is inferred from gravity data to be approximately 245 m down to the east near the SPE site. The offset apparently decreases to the northeast along the fault trace, as it approaches the junction with the Yucca fault to become the Butte fault (Orkild et al., 1983).

A perched groundwater table is present at the SPE site. The top of groundwater averages about 22.4 to 24.1 m below the ground surface.

1.5.2 Geologic Characterization Data

A core hole was drilled in granite (quartz monzonite) from the ground surface to the depth of 60 m at the location of the source hole, and drill cuttings were collected during drilling of the first six boreholes drilled for instrumentation. Data summarized in this section is from Townsend et al. (2012), where additional information can be found.

A suite of geophysical logs (listed below) was run in the core hole and all instrument holes to characterize the hole and surrounding rock.

- Caliper
- Deviation
- Natural Gamma
- Resistivity (core hole only)

- Full-wave Sonic/Travel Time
- Acoustic Televiewer
- Optical Televiewer (instrument holes only
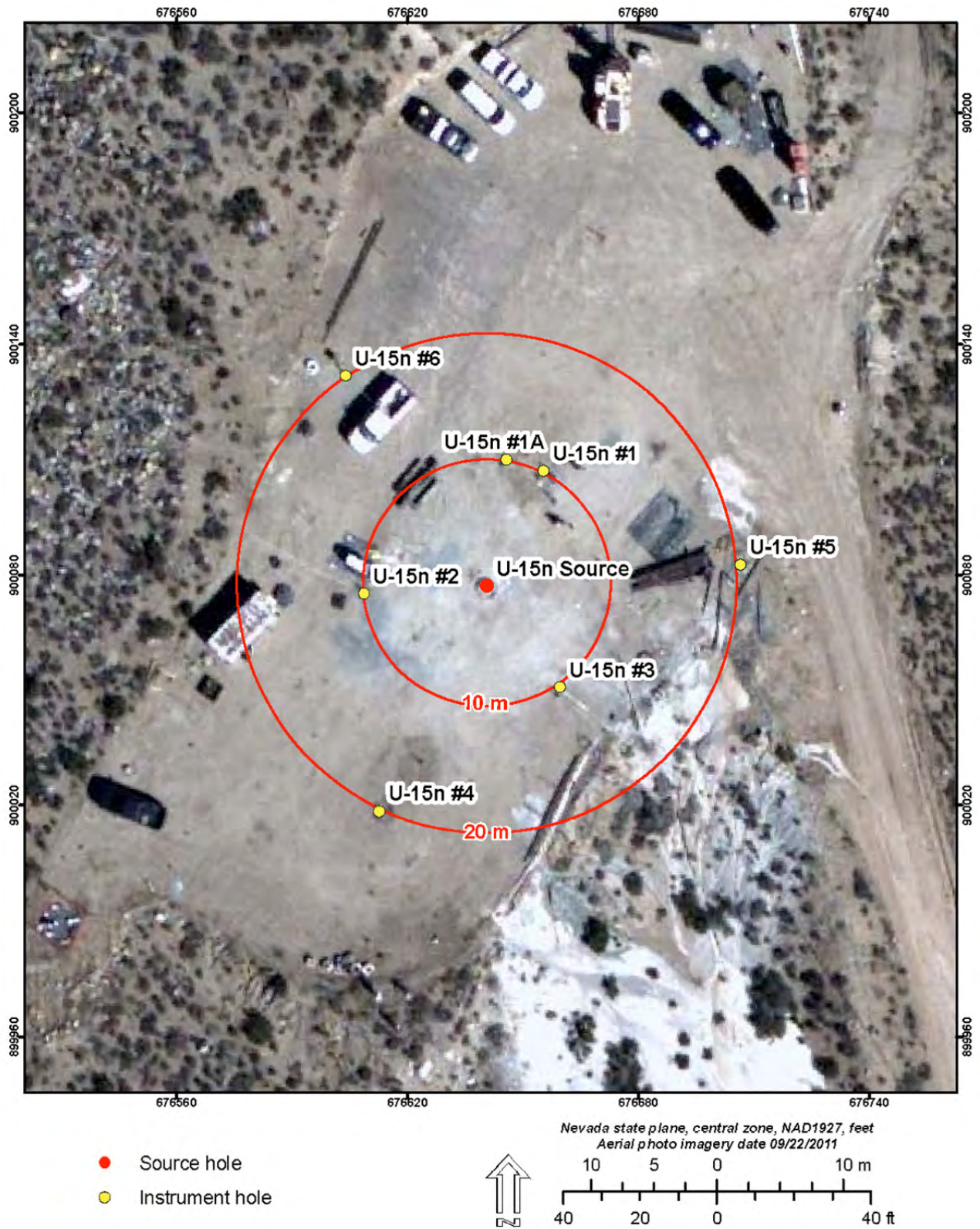
Figure 2
Aerial Photo of the SPE-2 Test Bed Showing Locations of Source Hole and Instrument Holes
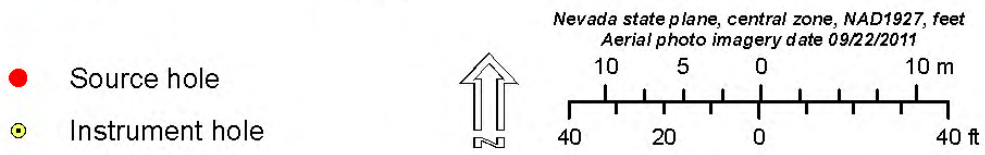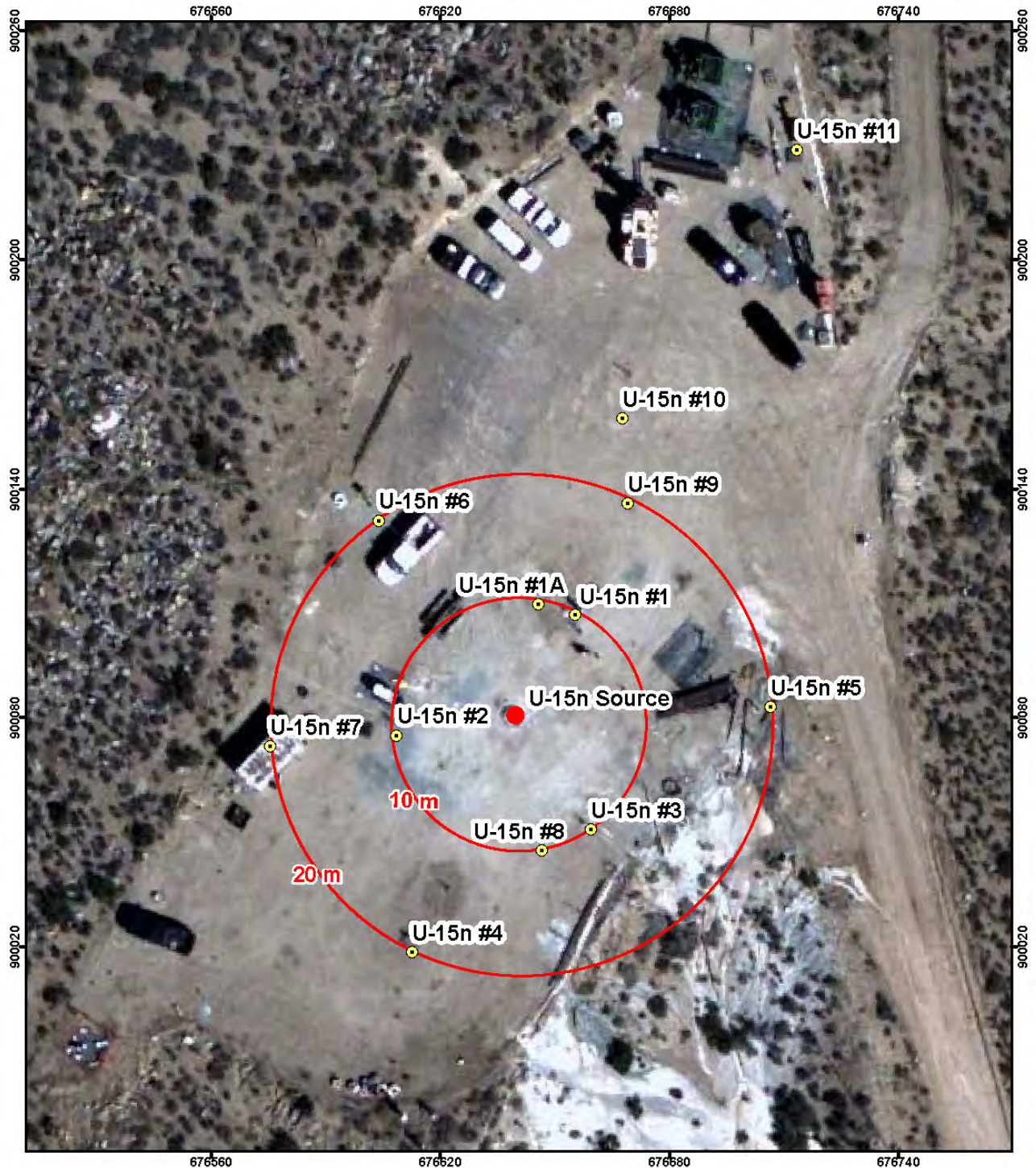
Figure 3
Aerial Photo of the SPE-3 Test Bed Showing Locations of the Source Hole and Instrument Holes
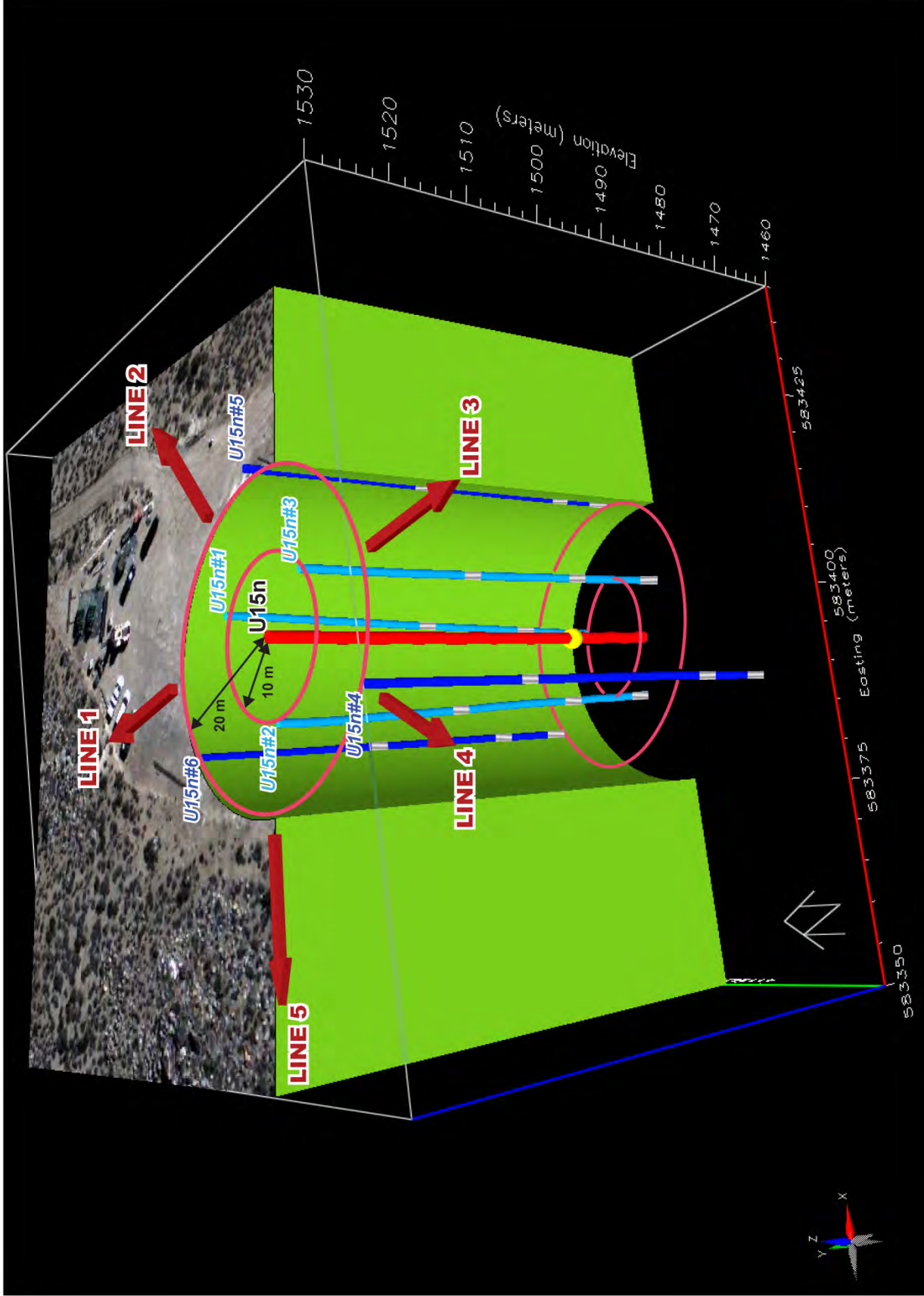
Figure 4
Sketch Showing Cut-Away View of Test Bed for SPE-2 and SP-3
(All instrument holes not shown.)
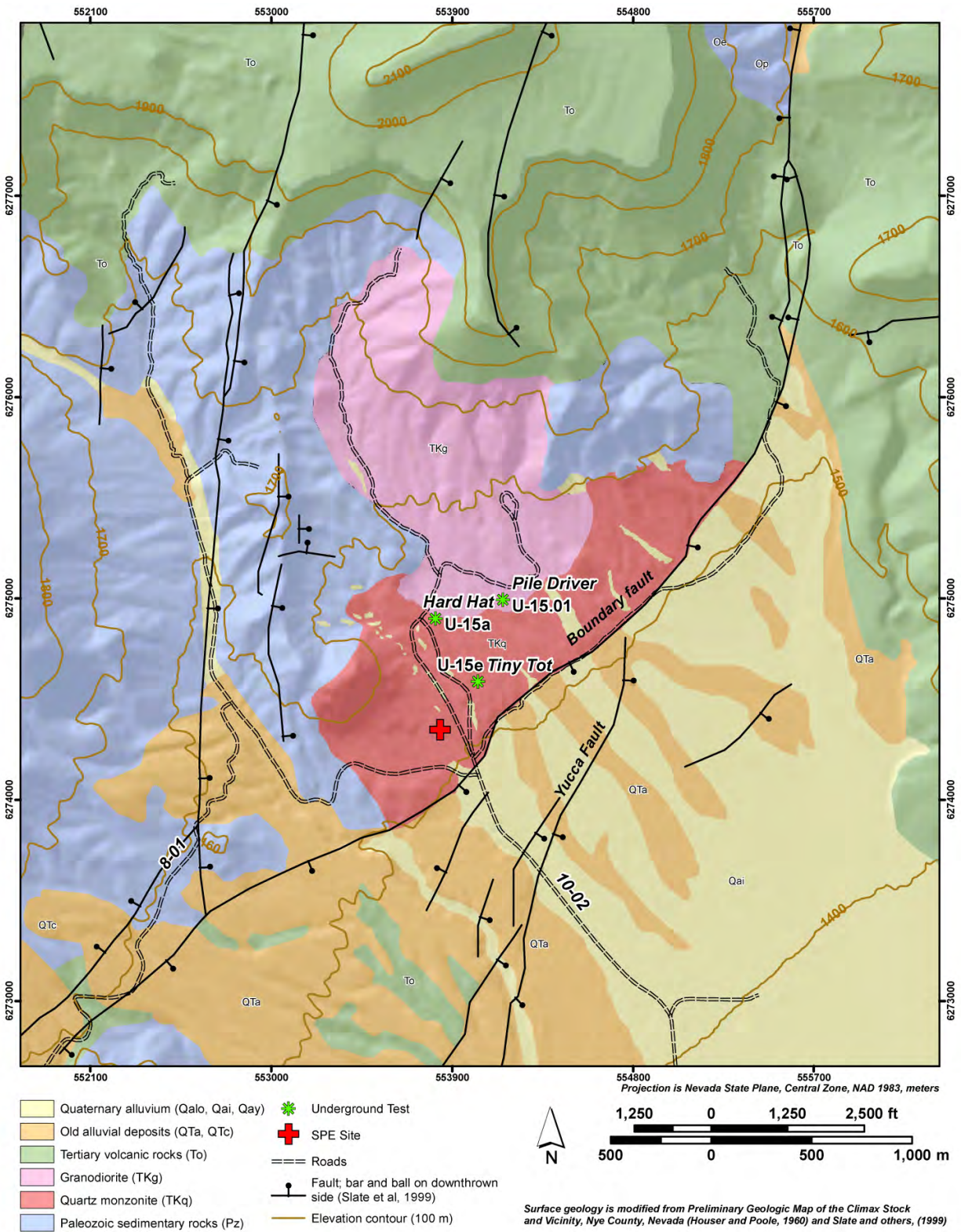
Figure 5
Surface Geologic Map of the Climax Stock Area

Legend:
- Quaternary alluvium (Qalo, Qai, Qay)
- Old alluvial deposits (QTa, QTc)
- Tertiary volcanic rocks (To)
- Granodiorite (TKg)
- Quartz monzonite (TKq)
- Paleozoic sedimentary rocks (Pz)
- Underground Test
- SPE Site
- === Roads
- Fault; bar and ball on downthrown side (Slate et al, 1999)
- Elevation contour (100 m)

Projection is Nevada State Plane, Central Zone, NAD 1983, meters

Surface geology is modified from Preliminary Geologic Map of the Climax Stock and Vicinity, Nye County, Nevada (Houser and Poole, 1960) and Slate and others, (1999)

Physical and mechanical properties were measured by SNL on samples from the core hole, as listed below (Broome and Pfeifle, 2011).

- Bulk density
- Unconfined compressive strength
- Compressional and shear wave velocity
- Direct shear

- Triaxial shear
- Triaxial compression
- Dynamic Brazilian Tension

2 SPE-2 and SPE-3 Test Descriptions

2.1 Explosive Sources

The explosive source for both shots was trinitrotoluene (TNT) equivalent, sensitized heavy ammonium nitrate and fuel oil (SHANFO).

2.1.1 SPE-2 Source and Insertion

The SPE-2 source was 991 kilograms (kg) of SHANFO with two 2.9 kg pentolite boosters for a total TNT equivalent shot of 997 kg. The SHANFO was loaded into a 1.27-centimeter (cm) thick aluminum canister at the surface and lowered to a depth of 47.2 m in the source hole. The canister was a right circular cylinder with a height of 3 m and diameter of 0.8 m, for a length-to-diameter ratio of about 4 to 1.

To fully confine the explosive source, the canister with the SHANFO was cemented in place with a grout mixture up to the depth of 43 m below ground surface. The remaining hole was then stemmed with the following materials: 1.2 m of sand, 11 m of pea gravel, 12 m of concrete, 15 m of sand, and 1.5 m of concrete to 1.5 m below ground surface (Figure 6).

The SPE-2 shot was detonated on October 25 (day 298), 2011, at 19:00:00.011623 Greenwich Mean Time (GMT). The location was 37.221207, –116.0608674 and at a centroid depth of 45.7 m.

The shot was fully confined; only SHANFO gases were released from the source hole and from one of the instrumentation holes.

2.1.2 SPE-3 Source and Insertion

The SPE-3 source was 899 kg of SHANFO with two 2.9 kg pentolite boosters for a total TNT equivalent shot of 905 kg. The SHANFO was loaded into a 1.27-cm thick aluminum canister at the surface and lowered to a depth of 47.2 m in the source hole. The canister was a right circular cylinder with a height of 2.7 m and diameter of 0.8 m, for a length-to-diameter ratio of about 3.5 to 1.

To fully confine the explosive source, the canister with the SHANFO was cemented in place with a grout mixture up to the depth of 43 m below ground surface. The remaining hole was then stemmed with the following materials: 1.2 m of sand, 35 m of pea gravel, 0.6 m of sand, and 4.5 m of concrete to 1.5 m below ground surface (Figure 7).

The shot was detonated on July 24 (day 206), 2012, at 18:00:00.44835 GMT. The location was 37.221207, –116.0608674 and at a centroid depth of 45.8 m.

The shot was fully confined; only SHANFO gases were released from the source hole along and from two of the instrumentation holes.

Ground surface

42–in. carbon–steel casing to 2.1 m (7.0 ft)

1.5 m (5 ft)

121.9–cm (48–in.) borehole to 2.3 m (7.5 ft)

18.3 m (60 ft)

Static water level approximately 23.5 m (77 ft)

91.4–cm (36–in.) borehole to TD

SPE–1 Cement to 47.4 m (155.6 ft)

Center of SPE–1 (expended) at 55.1 m (180.9 ft)

Total depth: 60.7 m (199 ft)

Horizontal scale = 12X vertical scale

All depths are below ground surface

SPE–2

30.5 m (100.0 ft)
31.1 m (102.0 ft)

41.1 m (135.0 ft)

42.7 m (140.3 ft)

SPE-2

Shot Point 45.7 m (149.9 ft)

47.4 m (155.6 ft)

Horizontal scale = 5X vertical scale

Concrete   Grout   SPE–1 Cement

Sand tube wadding (SPE–1)   Fill   Sand   Gravel

Figure 6
Schematic Drawing Showing Placement of Explosives Canister and Stemming in the SPE-2 Source Hole

Figure 7
Schematic Drawing Showing Placement of Explosives Canister and Stemming
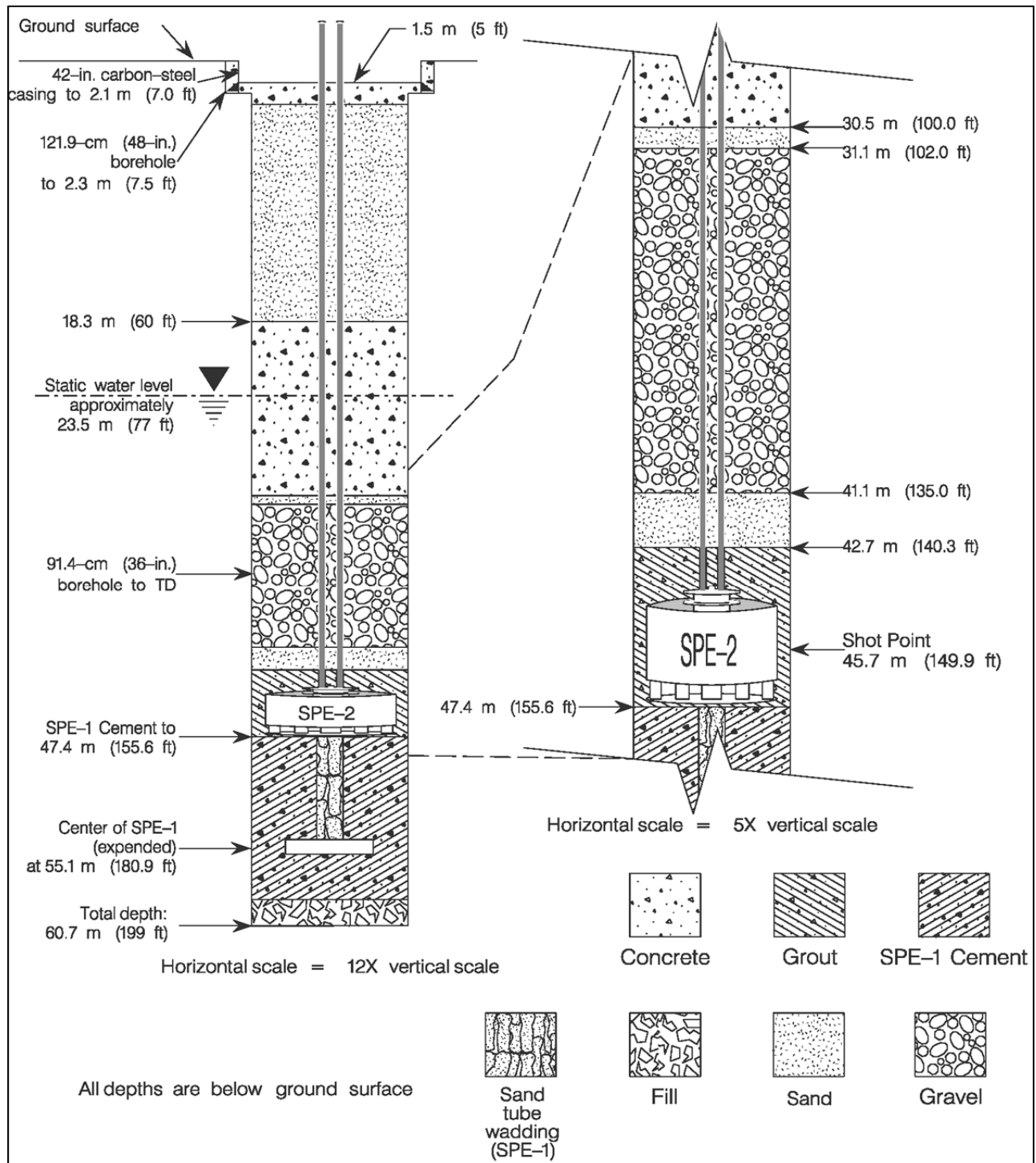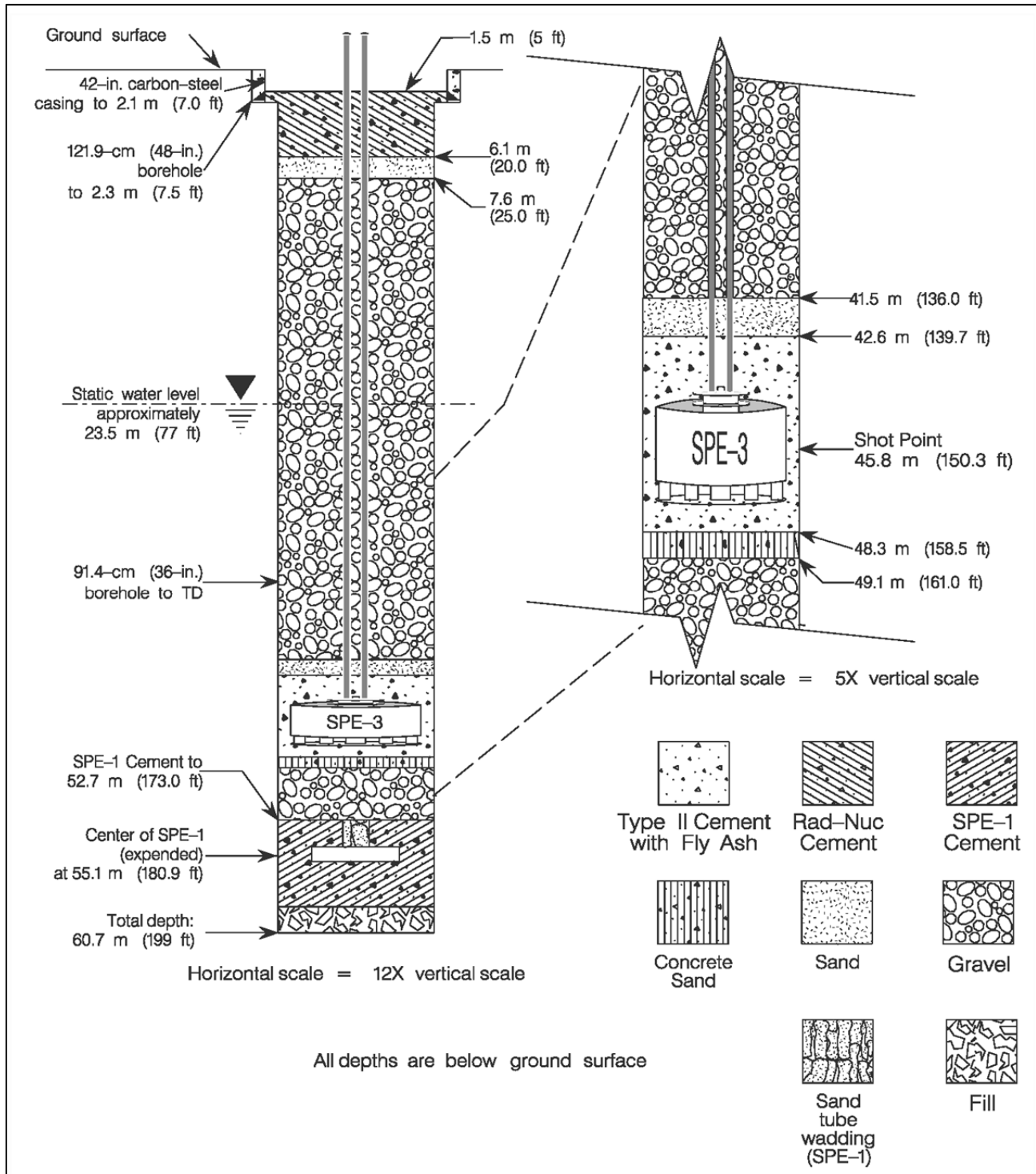**in the SPE-3 Source Hole**

2.2 Diagnostic Instrumentation

Instrumentation for both the SPE-2 and SPE-3 tests was installed in and on the explosives canister in the source hole to provide near-field diagnostic data for the detonation. These were CORRTEX (Continuous Reflectometry Radius versus Time Experiment), time of arrival, and velocity of detonation. These diagnostics provide a sense of the symmetry of the blast that can be used to distinguish between the effects of the blast and effects of discontinuities within the formation.

2.2.1 Near-Field Instrumentation for SPE-2

The instrumentation included an array of near-field accelerometers installed in boreholes to record the response of the near-field region (defined as less than 100 m from the source). Instrument holes U15n#1/1A, #2, and #3 are on a nominally 10 m radius circle, and holes U15n#4, #5, and #6 are on a nominally 20 m radius circle (Figures 2 and 3). The inner and outer rings of instrument holes are offset from one other to maximize azimuthal coverage. Instrumentation in these holes was designed to be in place for multiple SPE shots at different depths in the same source hole; the arrangement of the gauge packages reflects this purpose, as described in the following sections. Appendix 2 provides information about sensors in place for the SPE-2 test. However, all data users should verify they are using the full current metadata posted with the sensor data.

2.2.2 Near-Field Instrumentation for SPE-3

The SPE-2 instrumentation remained in place for the SPE-3 shot, and four new vertical instrument holes were added to the test bed. Holes U-15n#7 and #8 were added to the 20 m and 10 m rings, respectively. Hole U-15n#11 was positioned 51.2 m from the charge hole and had gauge depths identical to the older holes. Hole U-15n#9 on the 20 m ring had gauge packages at those depths as well as at 27.4 m and 36.6 m from the ground surface. The post-SPE-2 angle hole, U-15n#10, was instrumented with a single radial (i.e., in the line of the hole axis) transducer at a distance of 12 m from the charge. Appendix 3 provides information about sensors in place for the SPE-3 test. However, all data users should verify they are using the full current metadata posted with the sensor data.

2.2.3 Borehole Gauge Designations for SPE-2 and SPE-3

All instrument holes except U-15n #10 (as described above) contained three each three-component accelerometer gauge packages set at various depths. For each hole, gauge package 1 was set at the SPE-1 shot depth (55 m below ground surface), gauge package 2 was set 46 m below ground surface (the depth of the SPE-2 and SPE-3 shots), and gauge package 3 was set 15 m below ground surface. In addition to gauge packages 1, 2, and 3, hole U-15n#9, in place for the SPE-3 shot, also included gauge package 4, set at the depth of 36.6 m, and gauge package 5, set at the depth of 27.4 m. Each package has one radial component, one transverse component, and one longitudinal component.

Gauge packages are referred to by their respective hole and depth (e.g., package 2-1 is in hole U-15n#2 at depth 1). Further, each individual accelerometer in the package is labeled by the first letter of its component (e.g., measurement 2-1-R is the radial measurement in package 2-1). Figures 8 and 9 illustrate the SPE-2 and SPE-3 gauge package arrangement.
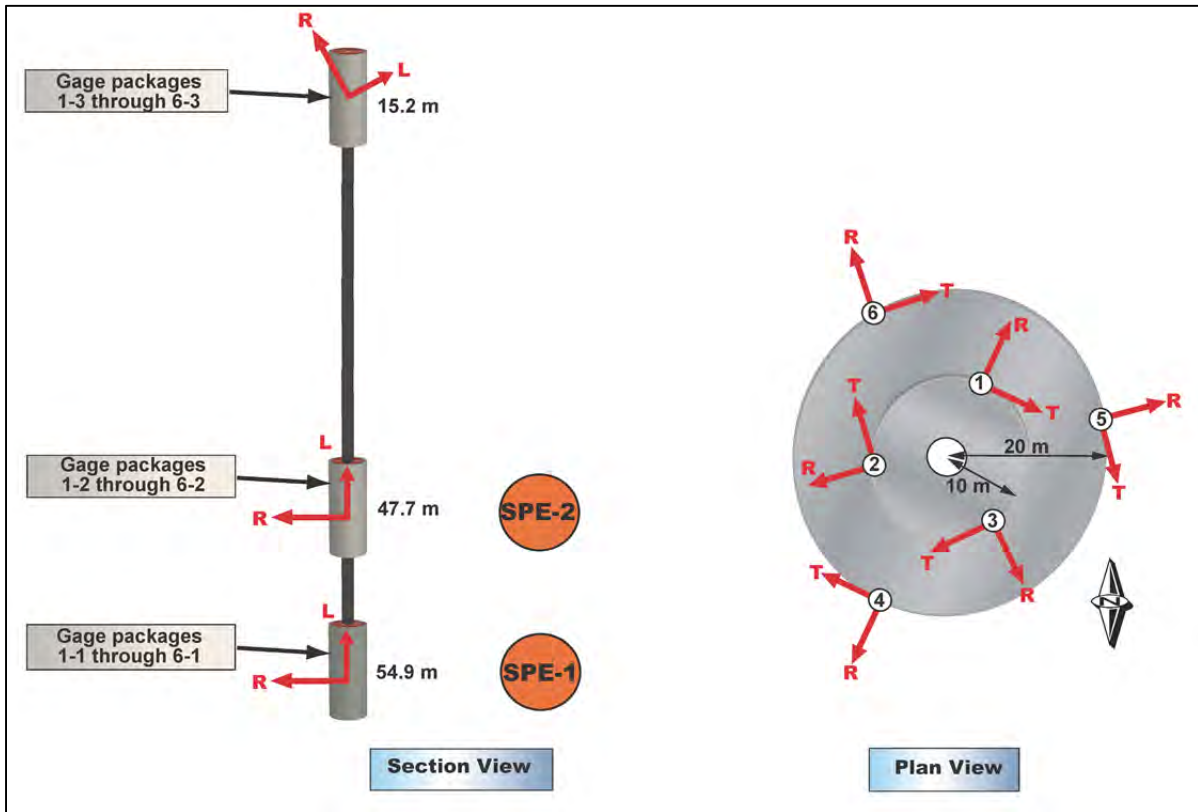
Figure 8
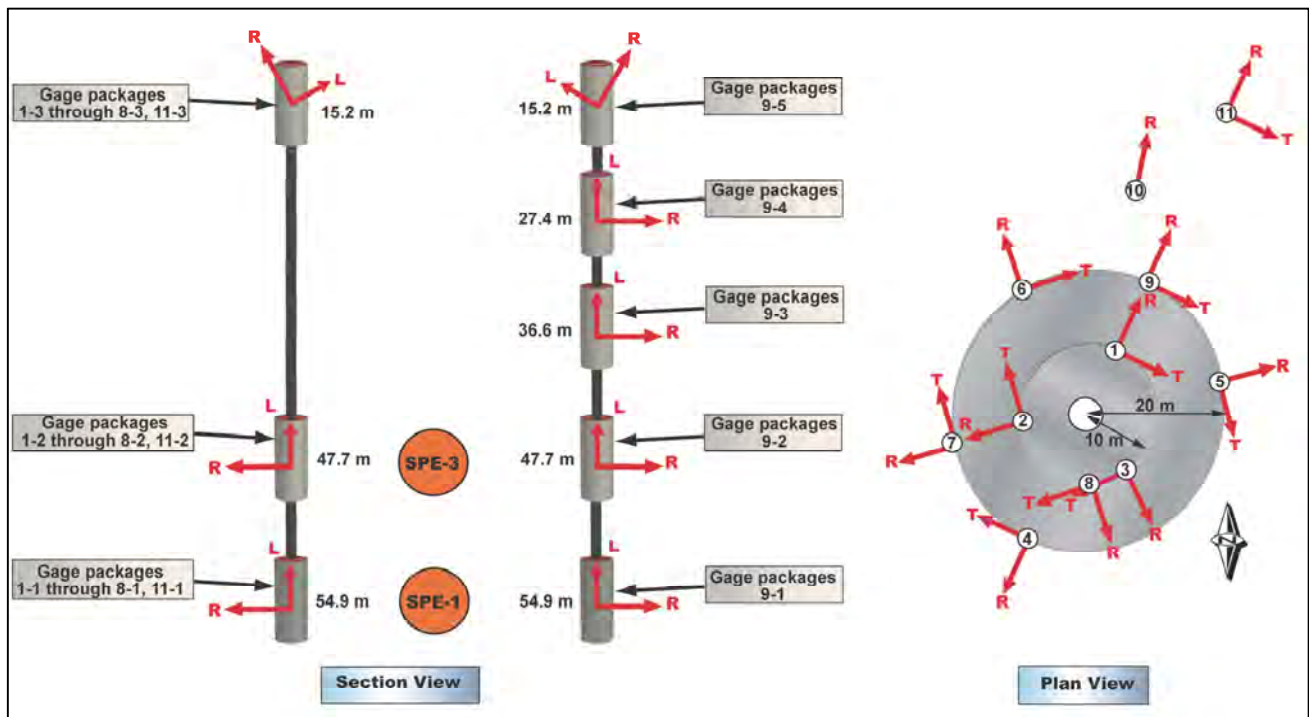**Diagrams Showing Typical Near-Field Gauge Package Arrangement for SPE-2**

Figure 9
Diagrams Showing Typical Near-Field Gauge Package Arrangement for SPE-3

NOTE: Neither figure is drawn to scale. In both figures, the arrows point in the positive direction.

2.2.3.1 Near-Field Gauge Placement Relative to the Source

Due to the complex deployment geometry of the test bed, these components need further description. The gauge packages at depths 1 and 2 are placed in a cylindrical coordinate system about the axis of the source hole. The "radial" gauges at these depths are, strictly speaking, horizontal outward measuring transducers, so for SPE-2 and SPE-3 only the R gauges at the SPE-2/3 depth (i.e., depth 2) are radial. For example, gauge 2-2-R is a radial measurement for SPE-2. However, gauge 2-1-R at the SPE-1 depth is more accurately described as measuring the horizontal component of the spherically propagating shock for SPE-2/3. Similarly, the longitudinal component is vertical, and gauge 2-2-L is a true longitudinal (or vertically oriented tangential) measurement for SPE-2/3, while gauge 2-1-L is the vertical component of the spherically propagating shock in this test. The tangential measurement is a horizontal component normal to the R–L plane.

The gauge packages at depth 3 are oriented in a spherical coordinate system with the origin at the SPE-2/3 shot point. So, the radial gauge at depth 3 is a truly radial measurement for SPE-2 and SPE-3. Similarly, the longitudinal and transverse gauges at depth 3 are orthogonal tangential measurements on a sphere centered at the SPE-2/3 shot point. Appendices 4 and 5 provide information about the borehole sensors, including locations, elevations, and type of instruments installed.

For both the SPE-2 and SPE-3 shots, vertically sensing accelerometers were mounted on the surface with gauges of 100- and 500-g sensitivity. These included a ring of transducers at the 15-m range from the surface ground zero (SGZ) on various azimuths. There was a single transducer 30 m southeast from SGZ. There was a line of accelerometers on an azimuth southwest from SGZ, beginning 30 m from SGZ and extending to 90 m from SGZ in 15-m increments.

2.2.3.2 As-Built Adjustments of Near-Field Gauge Positions

The description above provides nominal distances and directions between the gauges and the source, as if the source hole and instrumentation boreholes were perfectly vertical. However, due to the nature of the drilling process, none of the boreholes on the SPE test bed is truly vertical. The orientation ("deviation" from vertical) of each hole was measured after drilling, and the deviation data can be used to determine the exact position of each gauge position and its distance from the source. These data are included with the SPE-2 and SPE-3 data packages, and are also listed in Appendices 4 and 5 for each gauge. These data should be used for determining as-built locations of both the charge and the accelerometers.

2.2.4 Far-Field Instrumentation

Two primary types of far-field sensors (seismic and infrasound) were deployed for the SPE-2 and SPE-3 shots, as described below.

2.2.4.1 Seismic Instrumentation

To characterize the far-field seismic wavefield (defined as 100 m or more from the source), a number of different instrument arrays were deployed starting at a distance of 100 m from the SGZ and extending to distances as great as 25 km (Figures 10 and 11). Most seismic sensors were
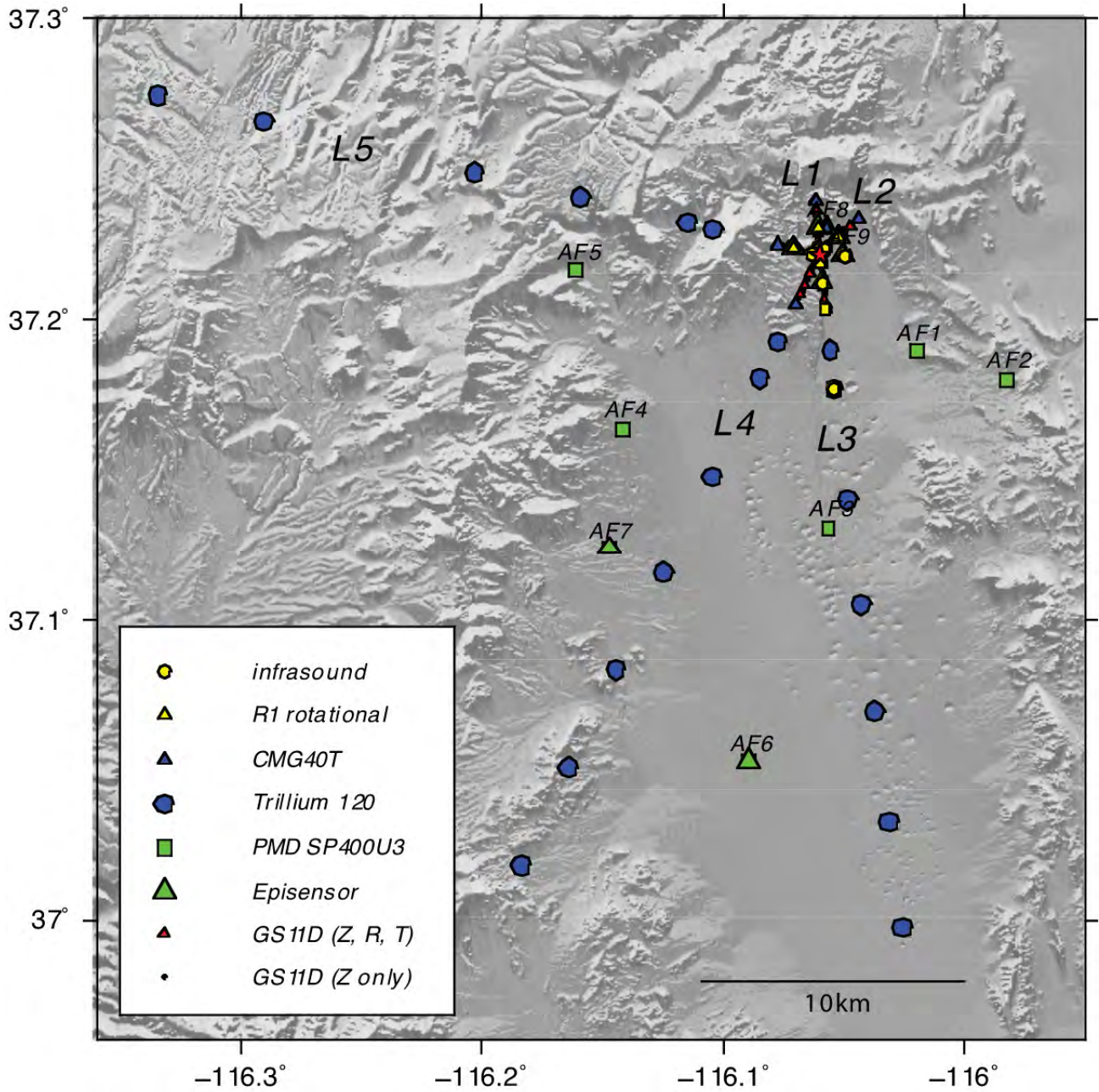
Figure 10
Location Map of Far-Field Instrumentation Layout

Map shows configuration for SPE-3, which included a small six-element geophone array east of SGZ.
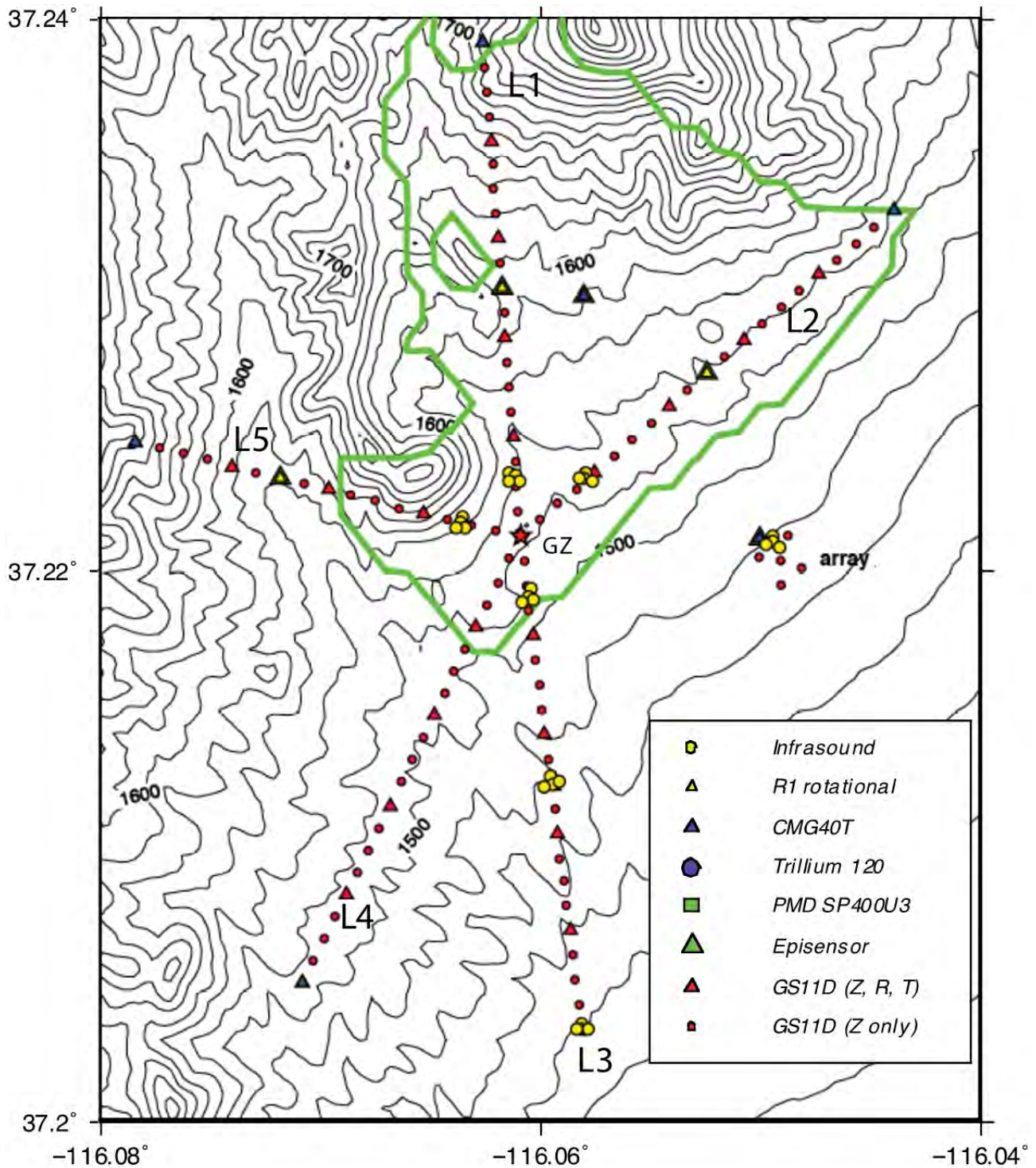
Figure 11
**Map Showing Locations of Geophones Placed within Approximately 2 Kilometers
of the SPE-2/SPE-3 Shot-point**

Small six-element geophone array east of SGZ was in place for SPE-3 only. Nominal
distance between instruments is 100 meters. The green line is the approximate outline of the
granite body at the surface.

16

installed in five radial lines extending out from the source. Line 1 extends to the north, and Line 2 extends to the northeast; both lines are relatively short due to proximity to the boundaries of the NNSS. Lines 3 and 4 extend to the south and southwest, while Line 5 extends roughly northwest. Instrument density on Line 5 is lower than on the other lines because steep topographic gradients hindered deployment. A small array of six geophones was deployed to the southeast of SGZ in Yucca Flat for SPE-3.

Recording was conducted on 6-channel RefTek 130 digitizers. For the sensors within 2 km, typically several stations at different locations were recorded on one digitizer, which led to long (100 m) cable runs in some cases. The digitizers were powered by batteries trickle-charged by solar panels. Data were stored to disk and collected manually at intervals.

It is important to note that data polarity standards for geophones and seismometers differ. Geophones produce negative voltages for upward ground motion, while the seismometers and accelerometers produce positive voltages for upward ground motion. This polarity standard is extended to three components in the case of three-component geophones. Geophone polarity follows a right-hand-rule standard with vertical pointing into the earth. The data in this collection are exactly as recorded by the sensors.

Characteristics of the instruments installed along the five geophone lines are summarized below. Exact details such as sensor type and response can be found in the metadata as well. Appendices 6 and 7 contain a summary of location and instrument information for each surface sensor site. However, all data users should verify they are using the full current metadata posted with the data.

Geospace GS-11D 4.5-hertz (Hz) geophones were deployed in five linear arrays, radiating from SGZ from 100 m to 1.9 km. Nominal station spacing is 100 m, with some expected locations skipped due to steep topography (mostly along Line 5). Every fourth geophone in each line is a three-component sensor oriented radial, transverse, and vertical to SGZ. The remaining geophones are vertical only. The geophones are buried less than 0.5 m deep in native material, with sandbags placed on top.

Guralp CMG 40T three-component seismometers are installed at the ends of the five geophone lines, 2 km distant from SGZ. The components are oriented radial, transverse, and vertical. The Guralps are installed on a concrete pad set less than 10 cm into the soil.

Lines 1, 2, 3, and 5 each include one Kinemetrics Episensor accelerometer and one Eentec R-1 rotational seismometer installed 1 km from SGZ. The instruments are mounted on an aluminum plate, which was then embedded into the concrete pad.

Lines 3, 4, and 5 are extended beyond 2 km (to a maximum of 25 km) by either six or seven Nanometrics Trillium Compact seismometers each, oriented radial north-south, east-west, and vertical (Figure 7). The instruments are installed on a concrete pad set less than 10 cm into the soil. Two stations on Line 5 (L5-28 and L5-34) were very close (centimeters) to bedrock, so at those locations the broadband instruments were covered by a sensor case in an ice chest (not barometrically sealed) covered with sandbags.

For SPE-2, broadband Compact Trillium sensors on Lines 3, 4, and 5, channels 1, 2, and 3, were oriented positive, up, radial and transverse, respectively, whereas for SPE-3 channels 1, 2, and 3

were oriented positive, up, north, and east, respectively. Orientation was estimated visually in the field, and the error is estimated to be less than about 5 degrees, as checked by later precise orientation measurements. At the 2-km distance and beyond, sensor orientations are set with respect to cardinal directions and not radial/tangential. This difference is denoted in the channel names. Timing was established by Geographic Positioning System receivers at each cataloger/digitizer. RefTek logs were reviewed for timing errors during data compilation.

In addition to this instrumentation, AFTAC deployed instruments at nine sites. Two sites were within 2 km and were equipped with Kinemetrics Episensors and CMG 40 T broadband instruments. The remaining sites were at distances up to 15 km and varying azimuths and equipped with PMD SP400U3 isotropic seismometers. Two of the PMD sites also had Episensor accelerometers. All sites were equipped with Chaparral infrasound sensors. All sensors were oriented to north (N), east (E), and vertical (Z) and recorded on Reftek digitizers.

2.2.4.2 Infrasound Arrays

Prior to the SPE-2 shot, SNL deployed seven infrasound arrays around SGZ. Each array consists of four Inter-Mountain Labs (IML-ST) infrasound sensors. The data were recorded using Reftek RT-130 digitizers sampling at 500 Hz. Each station telemetered data in real time to the SNL trailer at the command center, located approximately 365 m southeast of SGZ.

The infrasound sensors were installed in a roughly triangular geometry, with one sensor and the digitizer at the center and the other three sensors arranged azimuthally (~120-degree increments) around the center element at a distance of about 30 m. Attached to each sensor were four sections of porous hose about 15 m long for wind noise reduction. The IML-ST sensors have a nominal sensitivity of 0.20 volts per pascal and a flat response from 30 Hz down to onset of the roll-off at about 2 Hz (Hart, 2007). Four arrays were installed azimuthally around the test pad approximately 0.25 km from SGZ, and at different elevations due to topography constraints. The remaining three arrays were located at 1, 2, and 5 km respectively linearly south-southeast of SGZ (Figure 12). See Jones et al. (2012) for additional information.

Due to the roll-off of the IML sensors, SNL chose to upgrade to Hyperion IFS-3000 sensors (www.hyperiontg.com) for SPE-3 and all future shots. The IFS-3000 has a flat response from 0.1 to 100 Hz (without porous hoses) and 0.1 to 40 Hz (with porous hoses) with a 100-pascal full scale range and a nominal sensitivity of 0.15 volts per pascal. The SPE-3 infrasound data were recorded on Geotech Instruments SMART-24 digitizers at 200 samples per second (sps). The sample rate was decreased from 500 sps (for SPE-1 and SPE-2) to 200 sps for SPE-3 because the majority of the acoustic energy is around 3 Hz, and the IFS-3000 response is flat only up to 100 Hz without a correction. SNL also installed an additional array 1 km east of SGZ for SPE-3. All other array locations and geometries were the same as for SPE-1 and SPE-2.
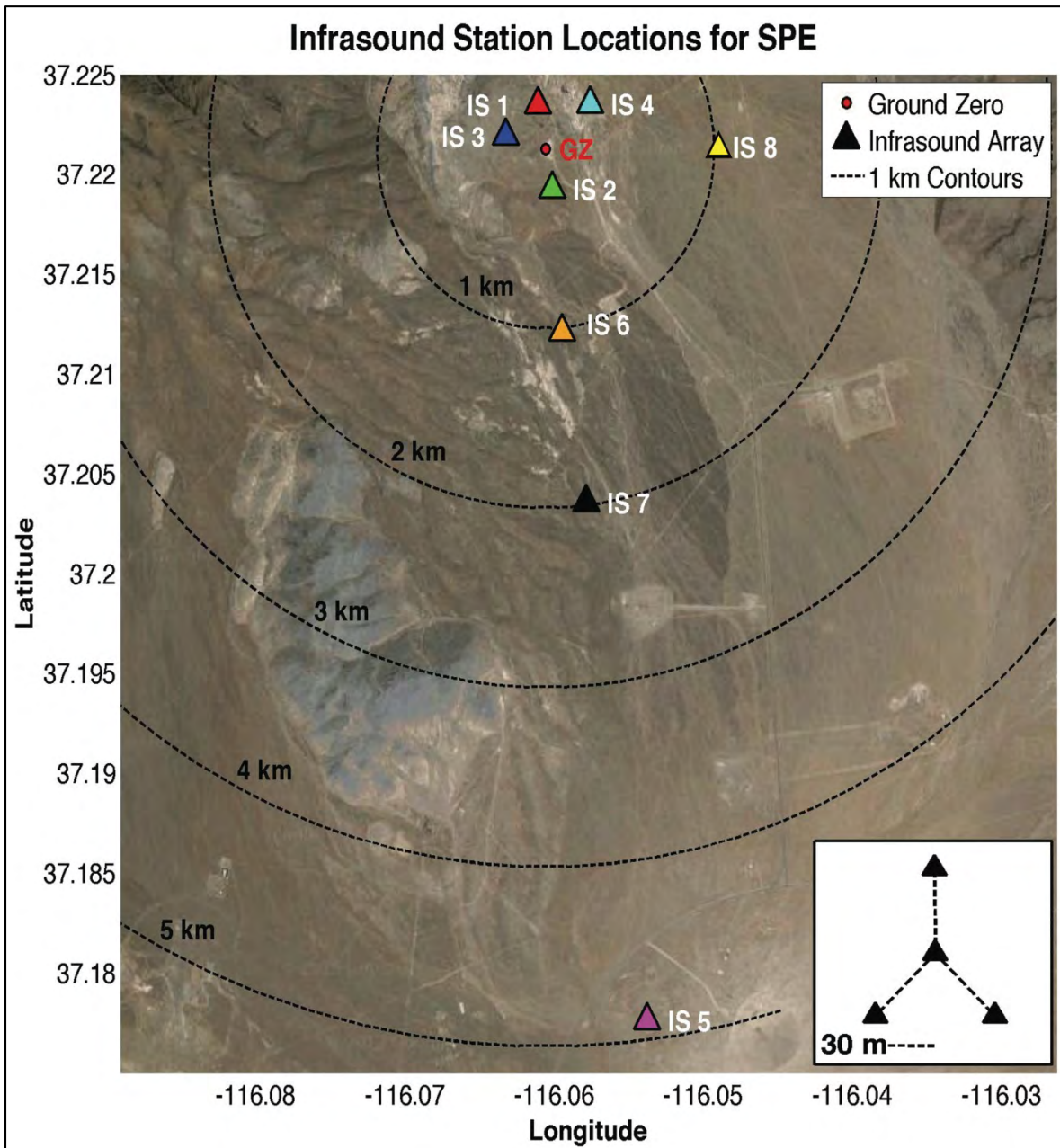
Figure 12
Map Showing Infrasound Array Locations (Triangles) around Surface Ground Zero (red)

Stations IS 1 through IS 7 were in place for SPE-1, SPE-2, and SPE-3. Station IS 8 was added after SPE-2. Dashed lines are 1-km contours from SGZ. Inset shows an example of the sensor geometry at each array.

3 Data Acquisition and Corrections

3.1 Near Field

3.1.1 Data Acquisition

The data packages for SPE-2 and SPE-3 include the raw acceleration-time pairs recorded for all accelerometers. These data are in the form of time-acceleration pairs. The files are in comma space variables in ASCII text format. For all records, time is in seconds and acceleration is in g units.

3.1.2 Data Corrections

Several standard and non-standard corrections were performed on the near-field data sets.

3.1.2.1 Corrections for Gauge Orientation

The SPE-2 and SPE-3 tests included an array of accelerometers (see Section 2.2) positioned near the source, intended to provide measurements of the strong ground motion, or "near field," regime. Some anomalous records were found during reviews of the SPE-1 and SPE-2 near-field data, which are suspected of having been caused by rotation of the gauges during installation in the boreholes. This is believed to have occurred in part because the deviation of the boreholes caused sections of the pipe on which the gauge packages were inserted to partially "unscrew" during insertion, thus changing the planned orientation of the gauges relative to the sources. The effect is believed to have occurred in gauges at the deeper "1" and "2" locations.

No corrections were applied to the packages at the "3" depth. These corrections apply to the original gauge installations (i.e., in instrumentation holes 1 through 6 plus 1A). Instrumentation in holes 7 through 11 was installed as a response to discovering the rotation issue and were subject to a more rigorous quality installation procedure.

Scientists at LANL and Applied Research Associates, a DTRA contractor, performed extensive analyses of the suspect data records and found that plots of uncorrected data (i.e., assuming that labeled components were pointed in the desired direction) are inconsistent with the shock environment expected from an explosive source. Further, the data histories exhibit considerable inconsistency between measurement locations, and the peak amplitudes of these data exhibit significant scatter.

A correction was performed by estimating the degree of rotation for each canister, and then correcting the gauge data to reflect the rotation. The resulting set of histories provides a self-consistent data set, and the peak amplitudes demonstrated considerably less scatter.

Those corrections were performed as described in detail in Steedman (2013) and summarized here (see also Appendix 8). The acceleration data were reviewed on a timestep-by-timestep basis. The radial and transverse records were resolved using trigonometric calculations, iterating on possible rotation angle, enabling the determination of the angle that provided the maximum outward radial motion for each location. The final reported radial and transverse records were altered to reflect this geometric correction.

The data corrected for canister rotation are included as Excel workbooks. Each workbook contains the data for all depths and all orientations available within the instrumentation hole listed in the file

name. Each worksheet within the workbook is a single transducer representing the depth and orientation listed in the worksheet tab name. The two data columns on each worksheet are time in seconds and acceleration in g units.

3.1.2.2   Baseline Shift Corrections

Appendices 8 and 9 discuss recommended baseline shift corrections for the borehole accelerometer data. These corrections were made in two stages:

- Correction for pre-arrival baseline shift
- Correction for post-arrival baseline shift

We do not provided data files with these corrections and leave it to the analyst to apply corrections at their discretion.

3.2 Far Field

Data were rapidly acquired and sent on a portable hard drive to NSL for reformatting and construction of metadata for those stations that were not telemetered.

An important note is that the signal polarity of the GS11D uses the Society of Exploration Geophysics standard: a downward ground motion yields a positive signal. The other instruments have the opposite polarity, i.e., upward ground motion yields a positive signal. Gains were set to unity on the Reftek instruments for the shots.

Data features:

- Difference in polarity between geophones and other instruments
- Data spikes (most obvious on data prior to shot); these were most likely due to issues with the cable power systems, although thunderstorms and lightning produce similar signals
- Possible cross-talk causing low amplitude signals on non-functioning channels

4   Post-Experiment Procedures

4.1 Aggregation, Merging, and Archiving of SPE-2 and SPE-3 Data

Post-experiment aggregation, merging, archiving, and distribution of SPE-2 and SPE-3 data were conducted at UNR by the technical members of the NSL. The process employed the Antelope data processing software system, version 4.11, from Boulder Real Time Technologies (Boulder, Colorado); the data processing suite from the Program for Array Seismic Studies of the Continental Lithosphere (PASSCAL); the CSS 3.0 database format; and Ubuntu-Linux-based servers at NSL data centers.

4.1.1   Data Aggregation

Data aggregation is the phase of acquiring raw metadata and time series data from project participants, reviewing the submissions, and conducting initial format conversions to standardize the media.

4.1.1.1 Metadata

Metadata were compiled prior to the SPE-2 and SPE-3 tests and refined during the merging and archival process. For each sensor, NSL asked SPE-2 and SPE-3 participants to submit the following items:

- Sensor make/model/type
- Sensor sensitivity factor
- Sensor serial number
- Sensor lat/long, decimal degrees
- Sensor frequency response file
- Sensor depth

- Sensor orientation
- Sensor on-time, off-time
- Sensor
- Data logger make/model
- Data logger serial number
- Data logger response file

- Data logger bit weight
- Data logger channel number
- Channel gain
- Channel sample rate
- Site name
- Site description

SPE investigators submitted these initial metadata to NSL through electronic transfer of spreadsheets, figures, and scanned drawings, which were then made available to all participants via document archives on the SPE data server.

4.1.1.2 Far-Field Waveform Aggregation Procedure

Far-field waveform data, recorded on RefTek RT130 data loggers on removable Secure Digital flash disks, were recovered by field technicians following the SPE-2 test. The native RefTek-formatted data were transferred to standard magnetic hard disk drives (HDDs), and the HDDs were delivered to the NSL Reno data center. Native-format data were duplicated to a redundant disk array, on a dedicated server, and converted to the RefTek "raw" format using PASSCAL's *rt130cut* conversion program. The "raw" output comprised one raw file per data logger per day. The "raw" formatted files were then converted to miniSEED format, using PASSCAL's *ref2mseed* program. The output from this conversion process was (1) one miniSEED file per data logger per hour, and (2) one log file per data logger per hour. The log files include recording parameters and state-of-health information for the recording periods. All logs and raw- and miniSEED-formatted files were then mirrored to a second disk array on a second dedicated server for data security and for distribution to project investigators for review.

4.1.1.3 Real-Time Telemetry for SPE-3

Real-time telemetry was implemented for some stations in place for SPE-3; no telemetry was in place for SPE-2. Real-time telemetry eliminates site visits for data downloads, allows real-time station diagnostics, provides capability to access stations remotely for parameter checks and adjustments, and ensures an overall increase in the level of data quality and data return rates over stand-alone portable stations. Telemetry sites for SPE-3 include:

Line 1:

L1-13, L1-14, L1-15, L1-16 (all GS11d geophones at 500 sps)

Line 3:

L3-23, L3-26, L3-36 (all Compact Trillium Broadband sensors at 250 sps)

Line 5:

L5-01 through L5-16 (all GS11d geophones at 500 sps)
L5-10 (Episensor accelerometer and Eentec rotational seismometer, both at 500 sps)

Figure 13 shows the telemetry paths that were in place for SPE-3 as red lines (white station paths on Figure 13 show the telemetry path configuration implemented after SPE-3). Data for SPE-3 were routed to the NSL microwave backbone site on Skull Mountain, with links directly to the University of Nevada, Las Vegas (UNLV), from NSL-spe-skull (Figure 13; triangle), referred to as Access Point 1 (AP1), the primary data collection point. Data are routed via microwave to UNLV, where they are transmitted on a fiber link to the NSL data center in Reno. Other secondary relay points installed due to line-of-site issues to AP1 include L5-15 (referred to as AP3) and NSL-spe-ap2 (referred to as AP2). Data rates from geophone sites, running at 500 sps, vary from 2 to 4 megabytes/day per channel, depending on noise level (data are transmitted in a compressed format
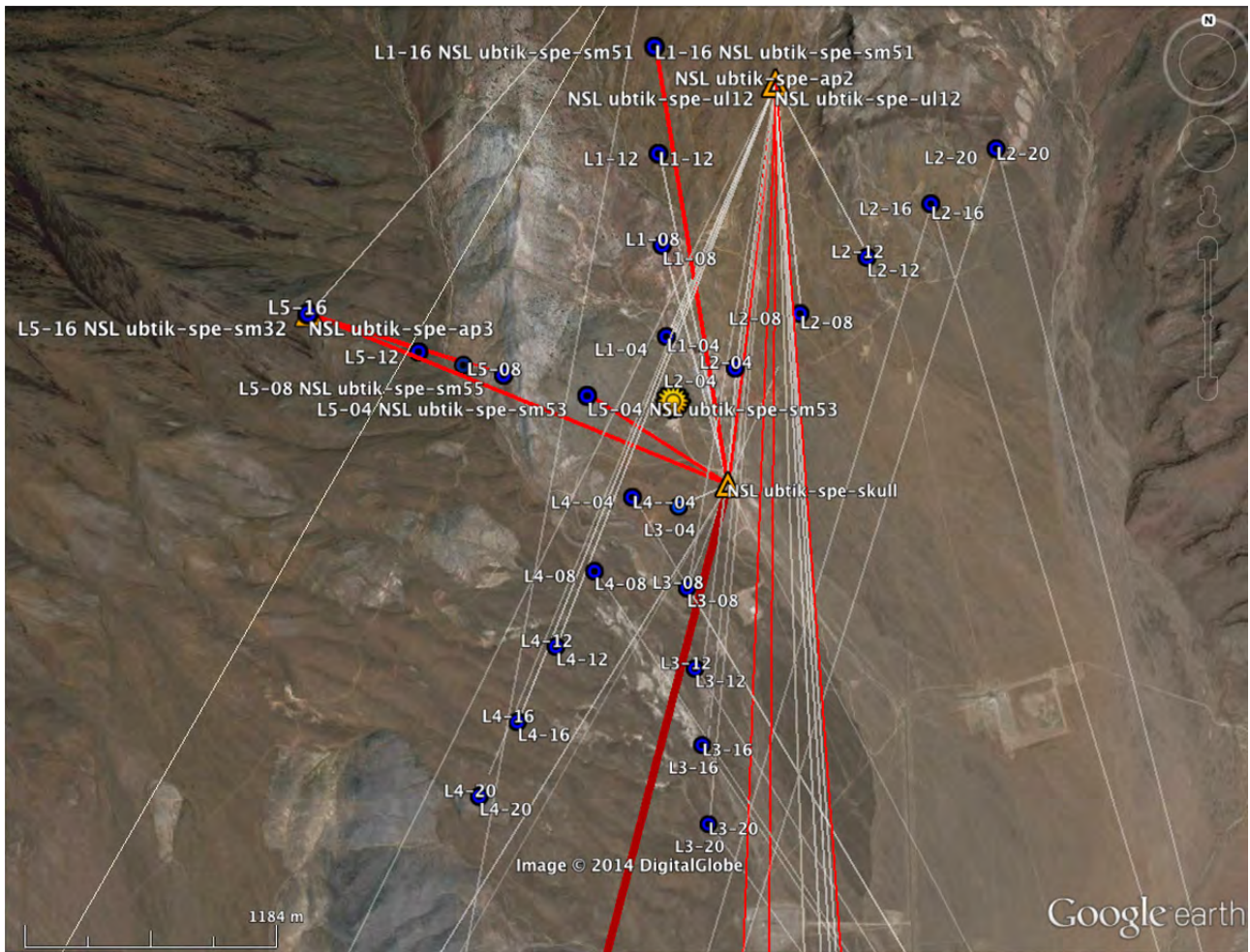

Figure 13
Telemetry Paths for SPE Geophones

Red lines indicate paths active for SPE-3; the white telemetry path configuration was installed after SPE-3. Relay Access Points (AP-collection points) are at L5-16, NSL-spe-ap2, and NSL-spe-skull. Thicker red line to the south-southwest is the link to the microwave backbone at Skull Mountain.

23

to reduce through-put). Broadband channels (Line 3) transmit at about 1 megabyte/day (250 sps). The far southern sites on Line 3 are not shown in Figure 13.

A data server with storage was established at a data center managed by the Nevada Systems of Higher Education Systems Computing Server (SCS), located on the UNLV campus, to provide access to all SPE data for project scientists. Real-time data from SPE-3 were transmitted and available to project scientists from the SCS-based data server, and currently (as of December 2014), all real-time data from the SPE array, NSL regional network, and Leo Brady network stations are available on the data server. The data server also functions as an access point for near-field and other spatial data collected by the project.

The telemetry link was to UNR, where data were collected into mini-SEED volumes using Antelope software. Data for the remaining stations were collected as in SPE-1 (NSTec, 2014).

4.1.1.4   Near-Field Waveform Data Aggregation Procedure

Near-field waveform data recorded on high-sample-rate multi-channel digitizers were recovered by project principal investigators and submitted to NSL by electronic file transfer. The data formats included (1) SAC, (2) four-byte integer, and (3) non-standard ASCII formats with accompanying scripts and other supporting metadata. For data received in SAC format, there was no required initial conversion procedure. Other formats required varying amounts of effort to convert to a common format.

4.1.2   Merging of Data Sets

Data merging is the phase of generating a valid CSS 3.0 metadata volume and modifying waveform file headers so that they will synchronize with the CSS 3.0 metadata format.

4.1.2.1   Metadata Merging

Upon receipt of metadata submissions, NSL staff distilled and standardized the information into ASCII files, one per station, in an open format that provides the input to Antelope's *dbbuild* program. The dbbuild format tracks station information changes through time (i.e., station histories), and allows for (1) rapid regeneration of an entire CSS 3.0 database as corrections and additions are required, (2) cross-institution database maintainability, (3) version control and revision history, and (4) a distributable and readable station record that can be useful even without proprietary tools.

4.1.2.1.1   Station Names and Descriptions

Upon submission, most metadata contained station descriptions and names that were meaningful only to the internal processes of the submitting institution. For the purpose of creating a single coherent volume, NSL technical staff created five-character station names that are compliant with the Standard for the Exchange of Earthquake Data (SEED). Where possible, the initial descriptions were preserved in the CSS 3.0 site descriptions to ensure new station names would be easily recognized by the various investigators. The file headers for the far-field stations (submitted as part of NSL's "SN" network) were changed to remove dashes (hyphens), which were replaced by zeroes to make them SEED compatible (Appendices 6 and 7).

4.1.2.1.2   Channel Codes

NSL staff created SEED-compliant channel codes describing the sample rate (band), instrument type, and orientation of each data channel. However, a collective decision was made by NSL and project investigators to leave the band code unchanged, even though per-instrument sample rates fluctuated from 100, to 500, to 250, to 200 sps. This was to avoid generating confusion for the large party of investigators who were not yet familiar with the CSS 3.0 database, which is sometimes terse and detailed and can become lengthy when many configuration changes are made across a large array during the course of recording. In addition, it was widely held as important that channel codes be tied to certain sensor types to facilitate rapid association of a channel's code with the sensor's location relative to the source.

4.1.2.1.3   Precision of Sensor Location

Sensor locations were submitted to NSL in State Plane Coordinates (SPC, feet) and geographic coordinates (decimal degrees). The submitted geographic coordinate submissions were merged directly into the CSS 3.0 metadata where station lat/long values were required. The SPC station locations were used to calculate northing and easting offsets in feet from the location of the SPE-2/3 source (station SP-01, northing 900077.22, easting 676640.6), and these offsets were then converted to meters using the conversion factor 1 m = 3.28084 feet.

4.1.2.1.4   Precision of Sensor Orientation

For the most part, measured sensor orientations were not submitted to NSL, with the exception of the vertical angles (in the radial direction) of the near-field borehole accelerometers. The remainder were submitted as orientation codes (N=North, E=East, Z=Vertical, R=Radial, T=Tangential, L=Lateral), and NSL calculated the azimuths of the sensor axes from the geographic coordinates. All azimuthal calculations were based on the assumption that the particular axis of the sensor was correctly aligned, e.g., that a radial orientation was indeed radial, and that the geographic coordinates are accurate to <0.3 m. The estimated error on horizontal orientation is <5 degrees.

4.1.2.1.5   Sensor Sensitivities

Sensitivity values were submitted per sensor for the near-field borehole (stations BH-) and surface accelerometers (stations DT- and SL-). Listed gauge sensitivities are measured, not nominal, as each accelerometer was tested at DTRA prior to deployment, with a tolerance of less than 2.4 percent. Far-field sensitivity values are nominal and were derived from manufacturer information sheets.

4.1.2.1.6   Gains

Pre-amplifier gains were also submitted per sensor for the near-field accelerometers. Accelerometer sensitivities varied by location in order to optimize response with respect to the estimated wavefield amplitudes. Where the gains were set larger (compared to predicted signal size) there will be a larger error due to increased amplification, which increases the signal-to-noise ratio. Gains for far-field RT130 seismic data were recovered from the logs generated from the raw RefTek to miniSEED by the data reduction process described above.

4.1.2.1.7 Calibration Factors

Calibration factors for near-field accelerometers in the CSS3.0 metadata were calculated from pre-amplifier gains (as above), a digitizer constant (bit weight), and sensitivity values (as above). All of these components are listed in the CSS3.0 *stage* table for the assembled near-field data sets. SL-* sensor calibration factors for SPE-2 also include a 10 percent cable-attenuation factor. Alternative calibration factors, supplied by DTRA for the near-field channels, are included with the assembled data sets in the file *calibrations.txt*. These calibration factors employ the raw vertical bit weight for each channel, and include base line averaging over 512 samples, but differ less than 2.4 percent from calculated values.

4.1.2.1.8 Instrument Response

Numerical (e.g., pole-and-zero) frequency responses are not available for the near-field accelerometers. Frequency response is expected to be essentially flat for frequencies of interest (Winningham, 2011) and is represented as constant in the metadata. Response data for the far-field sensors are redistributed from the versions supplied with the Antelope data processing system, except in the case of the infrasound sensors, and those responses were supplied in pole-zero format by SNL.

4.1.2.2 Merging Waveform Data

The procedure for merging waveforms included correcting waveform file headers to reflect the appropriate network-station-channel-location (net_sta_chan_loc) codes, and then using the Antelope *miniseed2db* or *sac2db* programs to generate a CSS 3.0 "wfdisc" table. The "wfdisc" table provides the mechanism to associate the time series data with the metadata set that describes the waveforms' response, sensor parameters, etc.

For miniSEED files, header modification was done using the PASSCAL *fixhdr* program. By default, the station and channel names in miniSEED file headers are set to the data logger serial number and stream codes. The data logger and channel codes are then mapped to SEED net_sta_chan_loc. The net_sta_chan_loc code maps were derived from the site metadata for each data logger configuration.

For SAC files, the header modifications were done using the SAC analysis software, distributed through IRIS.

4.1.3 Data Archiving

Archiving is the phase of presenting final data products. It includes completion of quality control procedures and generation of final product formats.

4.1.3.1 Metadata Formats

4.1.3.1.1 CSS 3.0

The CSS 3.0 metadata format is an industry/community standard and is the format supported by the Antelope system. It is a readable and open database system that allows for schema extensions and therefore is flexible, scalable, and adaptable to non-standard sensor array configurations.

The dataless SEED format is an industry/community standard for metadata that includes station histories as well as sensor and data logger response information. It is distributed as a single file, and can be read and imported by a wide variety of programs and applications. The volume distributed by NSL was generated from CSS 3.0 metadata using the Antelope application *db2sd*.

4.1.3.1.3   Dbbuild

The dbbuild format is an ASCII text-based format that documents site parameters throughout all epochs, or periods of distinct recording configurations. The dbbuild-based metadata comprise one text file per station, and while the files by themselves do not include sensor frequency response or data logger response, they do include sensor sensitivity factors. As input to the Antelope *dbbuild* program, which builds CSS 3.0 metadata (and in turn is converted to dataless SEED), the dbbuild-format files are the fundamental metadata records maintained by NSL for all SPE stations.

4.1.3.2   Time Series Formats

There are many time-series data formats, but for simplicity and for reusability of conversion and processing scripts, the technical staff at NSL resolved to create an archive based on either miniSEED or SAC formats. MiniSEED is the preferred format for data submissions to IRIS, and also the standard format for most Antelope-based programs and tools. SAC is the most widely known and used time-series format, and in some cases, such as with very high-sample-rate data (e.g., 1 million sps), it has capabilities that miniSEED does not.

4.1.3.3   Quality Control Measures

While the quality control of time-series data is left to SPE investigators (the near-field and far-field data committees), NSL is charged with creating a coherent database that is up to date and accurate with respect to the data submissions. As such, there are four quality control measures used to verify the data products for SPE-1.

4.1.3.3.1   Manual Inspection of dbbuild-Format Files

All metadata submissions are converted initially to the dbbuild-format. These files are reviewed for completeness and then checked in to the Concurrent Versioning System revision control system. The use of revision control allows NSL to track completeness of array-wide edits, and is important for tracking metadata errors and corrections.

4.1.3.3.2   Output Warnings and Errors from dbbuild Program

The dbbuild-format files are used by the *dbbuild* program to generate the CSS 3.0 metadata. All runs of *dbbuild* are conducted with the use of verbose warnings, the standard output is captured in a log, and the log is reviewed after the run completes. This process allows NSL to find and fix inconsistencies, incomplete entries, and mistakes in the dbbuild-format metadata that are not caught during manual review.

After generating a coherent CSS 3.0 metadata set that passes the first two levels of quality control, the data are examined for any additional problems using the Antelope *dbverify* program. This program performs consistency checks between database tables and is largely a tool for checking the validity of database schema and formats, rather than for finding omissions or typographic mistakes.

4.1.3.3.4   Output from dbjoin and dbfixids

The final step in each iterative generation of a CSS 3.0 metadata set is to synchronize the wfdisc table with the new channel identifiers, waveform identifiers, channel names, and calibration values that often change as metadata are refined and improved. This process not only corrects out-of-sync values in the wfdisc tables, but also warns when there are entries in the wfdisc table that do not join with the CSS 3.0 metadata. This reveals the case where waveforms have been submitted, but no metadata exist for the particular station. This situation can occur when new stations are added, or when data loggers are changed in the field without the updated information being submitted. Otherwise it can point up a case where NSL has missed a submission. This measure prompts staff to re-examine emails, contact field technicians, etc., to sort out why metadata are missing and contributes greatly to the completeness of the SPE-1 archive.

5   Summary

This report coincides with the official release of near- and far-field seismic station, gauge, and diagnostic data for SPE-2 and SPE-3. It describes the location of data and supporting documents on the SPE data server. The report includes a description of the experiment, the types of data and instruments, corrections made to the accelerometer data, and post-experiment data processing. This data release includes separate sets of these data, including the raw data as well as the data reflecting the application of the corrections.

6   Acknowledgements

7 References

Broome, S. T., and T. Pfeifle, 2011. Written communication prepared for the U.S. Department of Energy, National Nuclear Security Administration Nevada Site Office. Subject: "Phase 1 Mechanical Testing Results on Core from Borehole U-15n, Nevada National Security Site, in Support of NCNS Source Physics Experiment." Sandia National Laboratories, June 8, 2011.

Ford, S., and W. R. Walter, 2013. "An Explosion Model Comparison with Insights from the Source Physics Experiments," *Bull. Seism. Soc. Am.,* vol. 103, pp. 2937–2945, doi: 10.1785/0120130035.

Hart, D. M., 2007. *Evaluation of Inter-Mountain Labs Infrasound Sensors July 2007*. Sandia National Laboratories Technical Report, SAND2007-7020. Albuquerque, NM.

Jones, K. R., R. W. Whitaker, and S. J. Arrowsmith, 2012. "Infrasound Observations from the Source Physics Experiment (Tests 1 and 2) at the Nevada National Security Site." In: *Proceedings of the 2012 Monitoring Research Review: Ground-Based Nuclear Explosion Monitoring Technologies, Volume II*. Albuquerque, NM.

National Security Technologies, LLC, 2014. *Data Release Report for Source Physics Experiment 1 (SPE-1), Nevada National Security Site*. DOE/NV/25946--2018. Las Vegas, NV.

NSTec, see National Security Technologies, LLC.

Orkild, P. P., D. R. Townsend, M. J. Baldwin, D. L. Healey, G. D. Bath, C. E. Jahren, and J. G. Rosenbaum, 1983. *Geologic and Geophysical Investigations of Climax Stock Intrusive, Nevada*. Open-File Report 83-377. U. S. Geological Survey, Denver, CO.

Rougier, E., and D. Steedman, 2013. *SPE-1 Baseline Shift Corrections*. Los Alamos National Laboratory Report LA-UR-13-23956. Los Alamos, NM.

Snelson, C. M., V. D. Chipman, R. L. White, R. F. Emmitt, M. J. Townsend, D. L. Barker, and P. Lee, 2012. "An Overview of the Source Physics Experiment at the Nevada National Security Site." In: *Proceedings of the 2012 Monitoring Research Review: Ground-Based Nuclear Explosion Monitoring Technologies, Volume I*. Albuquerque, NM.

Snelson, C. M., R. Mellors, H. J. Patton, A. J. Sussman, M. J. Townsend, and W. R. Walter, 2013, "Source Physics Experiments to Validate a New Paradigm for Nuclear Test Monitoring," *Eos Trans., American Geophysical Union*, vol. 94, no. 27, pp. 237–239.

Steedman, D. W., 2013. *Review of Data from Shock Physics Experiments SPE-1, SPE-2, and SPE-3: Data Corrections and Phenomenology Analysis*. Los Alamos National Laboratory Report LA-UR-13-22561. Los Alamos, NM.

Townsend, M., L. Prothro, and C. Obi, 2012. *Geology of the Source Physics Experiment Site, Climax Stock, Nevada National Security Site*. DOE/NV/25946--1448. Prepared by National Security Technologies, LLC, Las Vegas, NV.

Winningham, K., Defense Threat Reduction Agency, 2011. Personal communication to K. Smith, University of Nevada, Reno Seismological Laboratory, regarding frequency response of borehole sensors.

List of Appendices

1. Construction Data for Holes Drilled at the U-15n Site

2. Instrument Metadata for SPE-2

3. Instrument Metadata for SPE-3

4. Selected Metadata for SPE-2 Borehole Sensors

5. Selected Metadata for SPE-3 Borehole Sensors

6. Selected Metadata for SPE-2 Surface Stations

7. Selected Metadata for SPE-3 Surface Stations

8. *SPE-1 Baseline Shift Corrections*, Los Alamos National Laboratory Report LA-UR-13-23956, prepared by E. Rougier and D. Steedman

9. *Review of Data from Source Physics Experiment-1: Data Corrections*, Los Alamos National Laboratory Report LA-UR-22561 (2013) prepared by D. Steedman

All data users should verify they are using the full current metadata, including the SN network dataless SEED volume from IRIS for the far-field data (surface sensors), and the CSS3.0 metadata from the assembled data sets for the near-field sites (boreholes).

Appendix 1

Construction Data for Holes Drilled at the U-15n Site

Appendix 1
Construction Data for Holes Drilled at the U-15n Site
(As-built coordinates and elevations as of March 8, 2012)

Hole Name	State Plane Coordinates at Collar [a]		UTM Coordinates at Collar [b]		Geographic Coordinates at Collar [c]		Ground Elevation [d]	Conductor Hole	Conductor Casing	Drilled Depth
	Northing (feet)	Easting (feet)	Northing (meters)	Easting (meters)	Latitude (degrees)	Longitude (degrees)	(feet)	Depth (feet)	Depth (feet)	(feet)
Boreholes used for SPE Shot-2										
U-15n Source	900,077.28	676,640.62	4,119,823.7	583,318.7	37.221195	-116.060867	5,001.87	7.5 [e]	7 [g]	199 [i]
U-15n#1	900,107.01	676,655.17	4,119,832.8	583,323.1	37.221276	-116.060816	5,002.00	7 [f]	6.5 [h]	190 [j]
U-15n#1A	900,109.89	676,645.66	4,119,833.7	583,320.2	37.221284	-116.060849	5,002.10	7 [f]	7	194 [j]
U-15n#2	900,075.27	676,608.54	4,119,823.1	583,308.9	37.221190	-116.060977	5,002.16	10 [f]	9.5 [h]	190 [j]
U-15n#3	900,050.67	676,659.48	4,119,815.6	583,324.5	37.221121	-116.060803	5,001.58	10 [f]	9.5 [h]	190 [j]
U-15n#4	900,018.48	676,612.53	4,119,805.8	583,310.2	37.221034	-116.060965	5,001.54	10 [f]	9.5 [h]	192 [j]
U-15n#5	900,082.71	676,706.51	4,119,825.5	583,338.8	37.221208	-116.060641	5,001.29	10 [f]	9.5 [h]	192 [j]
U-15n#6	900,131.75	676,603.86	4,119,840.3	583,307.4	37.221345	-116.060992	5,005.09	7 [f]	6.5 [h]	190 [j]
Additional boreholes used for SPE Shot-3										
U-15n#7	900,072.50	676,575.36	4,119,822.2	583,298.8	37.221183	-116.061091	5,002.87	10 [f]	7.5 [h]	305 [j]
U-15n#8	900,045.12	676,646.50	4,119,813.9	583,320.5	37.221106	-116.060848	5,001.59	10 [f]	10 [h]	305 [j]
U-15n#9	900,136.27	676,669.01	4,119,841.7	583,327.3	37.221356	-116.060768	5,002.00	10 [f]	7.4 [h]	305 [j]
U-15n#10	900,158.43	676,667.73	4,119,848.5	583,326.9	37.221417	-116.060772	5,002.59	10 [f,k]	7 [k,l]	174 [k,m]
U-15n#11	900,228.67	676,713.30	4,119,869.9	583,340.7	37.221609	-116.060614	5,003.48	10 [f]	6.5 [h]	305 [j]

NOTE
a. State Plane Coordinates, Central Nevada, North American Datum 1927
b. Univeral Transverse Mercator, Zone 11, North American Datum 1983
c. Latitude/Longitude, North American Datum 1983
d. National Geodetic Vertical Datum, 1929
e. 48-inch diameter hole
f. 12.25-inch diameter hole
g. 42-inch diameter steel casing
h. 10.75-inch diameter steel casing
i. 36-inch diameter hole
j. 8-inch diameter hole
k. Depth value shown for borehole angled 30 degrees from vertical is measured along inclined borehole axis from ground surface
l. 5.5-in diameter PVC casing
m. 3.9-inch diameter core hole

Appendix 2

Instrument Metadata for SPE-2

Appendix 2

Instrument Metadata for SPE-2

Instrument ID	Instrument Name	Instrument Code	Frequency Band	Sample Rate (samples/ second)	Response Type
1	Geospace GS-11D 380ohm/Reftek 130 Datalogger	gs11d	High frequency	500	Velocity
3	Geospace GS-11D 380ohm/Reftek 130 Datalogger	gs11d	High frequency	500	Velocity
6	Episensor 200 Hz 1.25 Volt per g/Reftek 130 Datalo	epi_1.	Broad-band	500	Acceleration
7	Eentec R1 Rotational Seismometer/Reftek 130 Datalo	eentec	Broad-band	500	Velocity
8	Episensor 200 Hz 1.25 Volt per g/Reftek 130 Datalo	epi_1.	Broad-band	250	Acceleration
11	Guralp CMG40T_30sec/Reftek 130 Datalogger	cmg40t	Broad-band	500	Velocity
12	Guralp CMG40T_30sec/Reftek 130 Datalogger	cmg40t	Broad-band	250	Velocity
19	Nanometrics Trillium 120 Compact/Reftek 130 Datalo	trilli	Broad-band	250	Velocity
20	Nanometrics Trillium 120 Compact/Reftek 130 Datalo	trilli	Broad-band	250	Velocity
26	Chapparral 2.5 microphone/Reftek 130 Datalogger	chapar	Long-period	250	Infrasound
27	IML ST Infrasound/Reftek 130 Datalogger	iml_st	Long-period	250	Infrasound
28	New Mexico Tech InfraNMT_xxC/Reftek 130 Datalogger	infran	Long-period	250	Infrasound
30	Chapparral 2.5 microphone/Reftek 130 Datalogger	chapar	Long-period	250	Infrasound
31	PMD SP400U3/Reftek 130 Datalogger	SP400U	Broad-band	250	Velocity
34	Episensor 200 Hz 1.25 Volt per g/Reftek 130 Datalo	epi_1.	Broad-band	250	Acceleration
36	7264B Accelerometer 2000g/DTRA Datalogger	e7264b	Broad-band	1000000	Acceleration
41	7264B Accelerometer 2000g/DTRA Datalogger	e7264b	Broad-band	1000000	Acceleration
42	EGE-73A Accelerometer 5000g/DTRA Datalogger	ege73a	Broad-band	1000000	Acceleration
43	7264C Accelerometer 500g/DTRA Datalogger	e7264c	Broad-band	1000000	Acceleration
44	7264C Accelerometer 500g/DTRA Datalogger	e7264c	Broad-band	1000000	Acceleration
49	7264B Accelerometer 2000g/DTRA Datalogger	e7264b	Broad-band	1000000	Acceleration
50	7264B Accelerometer 2000g/DTRA Datalogger	e7264b	Broad-band	1000000	Acceleration
57	EGE-73A Accelerometer 5000g/DTRA Datalogger	ege73a	Broad-band	1000000	Acceleration
58	EGE-73A Accelerometer 5000g/DTRA Datalogger	ege73a	Broad-band	1000000	Acceleration
59	7264B Accelerometer 2000g/DTRA Datalogger	e7264b	Broad-band	1000000	Acceleration
60	7264B Accelerometer 2000g/DTRA Datalogger	e7264b	Broad-band	1000000	Acceleration
61	EGE-73A Accelerometer 5000g/DTRA Datalogger	ege73a	Broad-band	1000000	Acceleration
62	7264C Accelerometer 500g/DTRA Datalogger	e7264c	Broad-band	1000000	Acceleration
63	7264C Accelerometer 500g/DTRA Datalogger	e7264c	Broad-band	1000000	Acceleration
80	EGE-73A Accelerometer 5000g/DTRA Datalogger	ege73a	Broad-band	1000000	Acceleration
81	7264B Accelerometer 2000g/DTRA Datalogger	e7264b	Broad-band	1000000	Acceleration
82	7264B Accelerometer 2000g/DTRA Datalogger	e7264b	Broad-band	1000000	Acceleration
83	EGE-73A Accelerometer 5000g/DTRA Datalogger	ege73a	Broad-band	1000000	Acceleration
84	7264C Accelerometer 500g/DTRA Datalogger	e7264c	Broad-band	1000000	Acceleration
85	7264C Accelerometer 500g/DTRA Datalogger	e7264c	Broad-band	1000000	Acceleration
98	7264B Accelerometer 2000g/DTRA Datalogger	e7264b	Broad-band	1000000	Acceleration
99	EGE-73A Accelerometer 5000g/DTRA Datalogger	ege73a	Broad-band	1000000	Acceleration
100	EGE-73A Accelerometer 5000g/DTRA Datalogger	ege73a	Broad-band	1000000	Acceleration
101	7264B Accelerometer 2000g/DTRA Datalogger	e7264b	Broad-band	1000000	Acceleration
102	EGE-73A Accelerometer 5000g/DTRA Datalogger	ege73a	Broad-band	1000000	Acceleration
103	EGE-73A Accelerometer 5000g/DTRA Datalogger	ege73a	Broad-band	1000000	Acceleration
104	7264C Accelerometer 500g/DTRA Datalogger	e7264c	Broad-band	1000000	Acceleration
105	EGE-73A Accelerometer 5000g/DTRA Datalogger	ege73a	Broad-band	1000000	Acceleration
106	EGE-73A Accelerometer 5000g/DTRA Datalogger	ege73a	Broad-band	1000000	Acceleration
120	7264B Accelerometer 2000g/DTRA Datalogger	e7264b	Broad-band	1000000	Acceleration
121	7264B Accelerometer 2000g/DTRA Datalogger	e7264b	Broad-band	1000000	Acceleration
122	7264B Accelerometer 2000g/DTRA Datalogger	e7264b	Broad-band	1000000	Acceleration
123	7264C Accelerometer 500g/DTRA Datalogger	e7264c	Broad-band	1000000	Acceleration
124	EGE-73A Accelerometer 5000g/DTRA Datalogger	ege73a	Broad-band	1000000	Acceleration
125	EGE-73A Accelerometer 5000g/DTRA Datalogger	ege73a	Broad-band	1000000	Acceleration
141	7264B Accelerometer 2000g/DTRA Datalogger	e7264b	Broad-band	1000000	Acceleration
142	7264B Accelerometer 2000g/DTRA Datalogger	e7264b	Broad-band	1000000	Acceleration
143	EGE-73A Accelerometer 5000g/DTRA Datalogger	ege73a	Broad-band	1000000	Acceleration
144	EGE-73A Accelerometer 5000g/DTRA Datalogger	ege73a	Broad-band	1000000	Acceleration
145	EGE-73A Accelerometer 5000g/DTRA Datalogger	ege73a	Broad-band	1000000	Acceleration
146	EGE-73A Accelerometer 5000g/DTRA Datalogger	ege73a	Broad-band	1000000	Acceleration
147	EGE-73A Accelerometer 5000g/DTRA Datalogger	ege73a	Broad-band	1000000	Acceleration

Appendix 2
Instrument Metadata for SPE-2

Instrument ID	Instrument Name	Instrument Code	Frequency Band	Sample Rate (samples/ second)	Response Type
194	EGE-73A Accelerometer 5000g/DTRA Datalogger	ege73a	Broad-band	1000000	Acceleration
195	7264B Accelerometer 2000g/DTRA Datalogger	e7264b	Broad-band	1000000	Acceleration
196	7264B Accelerometer 2000g/DTRA Datalogger	e7264b	Broad-band	1000000	Acceleration
197	EGE-73A Accelerometer 5000g/DTRA Datalogger	ege73a	Broad-band	1000000	Acceleration
198	7264B Accelerometer 2000g/DTRA Datalogger	e7264b	Broad-band	1000000	Acceleration
199	Endevco 7270A-2K/DTRA Datalogger	e7270	Broad-band	1000000	Acceleration
200	EGE-73A Accelerometer 5000g/DTRA Datalogger	ege73a	Broad-band	1000000	Acceleration
201	7264B Accelerometer 2000g/DTRA Datalogger	e7264b	Broad-band	1000000	Acceleration
202	7264B Accelerometer 2000g/DTRA Datalogger	e7264b	Broad-band	1000000	Acceleration
211	EGCS-D0-50g Accelerometer/DTRA Datalogger	egcsd0	Broad-band	1000000	Acceleration
213	EGCS-D0-100g Accel/DTRA Datalogger	egcsd0	Broad-band	1000000	Acceleration
215	EGCS-D0-100g Accel/DTRA Datalogger	egcsd0	Broad-band	1000000	Acceleration
217	EGCS-D0-100g Accel/DTRA Datalogger	egcsd0	Broad-band	1000000	Acceleration
220	EGCS-D0-50g Accelerometer/DTRA Datalogger	egcsd0	Broad-band	1000000	Acceleration
222	EGCS-D0-100g Accel/DTRA Datalogger	egcsd0	Broad-band	1000000	Acceleration
225	Endevco 7264B-500/SNL Datalogger	endevc	Broad-band	4000	Acceleration
234	IML ST Infrasound/Reftek 130 Datalogger	iml_st	Long-period	500	Infrasound

Appendix 3

Instrument Metadata for SPE-3

Appendix 3
Instrument Metadata for SPE-3

Instrument ID	Instrument Name	Instrument Code	Frequency Band	Sample Rate (samples/ second)	Response Type
1	Geospace GS-11D 380ohm/Reftek 130 Datalogger	gs11d	High frequency	500	Velocity
2	Geospace GS-11D 380ohm/Reftek 130 Datalogger	gs11d	High frequency	250	Velocity
3	Geospace GS-11D 380ohm/Reftek 130 Datalogger	gs11d	High frequency	500	Velocity
6	Episensor 200 Hz 1.25 Volt per g/Reftek 130 Datalo	epi_1.	Broad-band	500	Acceleration
8	Episensor 200 Hz 1.25 Volt per g/Reftek 130 Datalo	epi_1.	Broad-band	250	Acceleration
9	Eentec R1 Rotational Seismometer/Reftek 130 Datalo	eentec	Broad-band	250	Velocity
10	Guralp CMG40T_30sec/Reftek 130 Datalogger	cmg40t	Broad-band	500	Velocity
11	Guralp CMG40T_30sec/Reftek 130 Datalogger	cmg40t	Broad-band	500	Velocity
12	Guralp CMG40T_30sec/Reftek 130 Datalogger	cmg40t	Broad-band	250	Velocity
17	Nanometrics Trillium 120 Compact/Reftek 130 Datalo	trilli	Broad-band	500	Velocity
19	Nanometrics Trillium 120 Compact/Reftek 130 Datalo	trilli	Broad-band	250	Velocity
20	Nanometrics Trillium 120 Compact/Reftek 130 Datalo	trilli	Broad-band	250	Velocity
22	Episensor 200 Hz 1.25 Volt per g/Reftek 130 Datalo	epi_1.	Broad-band	500	Acceleration
23	Eentec R1 Rotational Seismometer/Reftek 130 Datalo	eentec	Broad-band	500	Velocity
26	Chapparral 2.5 microphone/Reftek 130 Datalogger	chapar	Long-period	250	Infrasound
27	IML ST Infrasound/Reftek 130 Datalogger	iml_st	Long-period	250	Infrasound
28	New Mexico Tech InfraNMT_xxC/Reftek 130 Datalogger	infran	Long-period	250	Infrasound
29	EMI BF6 magnetometer/Reftek 130 Datalogger	emi_bf	Broad-band	500	N
30	Chapparral 2.5 microphone/Reftek 130 Datalogger	chapar	Long-period	250	Infrasound
31	PMD SP400U3/Reftek 130 Datalogger	SP400U	Broad-band	250	Velocity
33	PMD SP400U3/Reftek 130 Datalogger	SP400U	Broad-band	250	Velocity
34	Episensor 200 Hz 1.25 Volt per g/Reftek 130 Datalo	epi_1.	Broad-band	250	Acceleration
45	EGE-73A Accelerometer 5000g/DTRA Datalogger	ege73a	Broad-band	500000	Acceleration
46	7264C Accelerometer 500g/DTRA Datalogger	e7264c	Broad-band	500000	Acceleration
47	7264C Accelerometer 500g/DTRA Datalogger	e7264c	Broad-band	500000	Acceleration
64	EGE-73A Accelerometer 5000g/DTRA Datalogger	ege73a	Broad-band	500000	Acceleration
65	7264B Accelerometer 2000g/DTRA Datalogger	e7264b	Broad-band	500000	Acceleration
66	7264B Accelerometer 2000g/DTRA Datalogger	e7264b	Broad-band	500000	Acceleration
67	7264B Accelerometer 2000g/DTRA Datalogger	e7264b	Broad-band	500000	Acceleration
68	7264B Accelerometer 2000g/DTRA Datalogger	e7264b	Broad-band	500000	Acceleration
69	EGE-73A Accelerometer 5000g/DTRA Datalogger	ege73a	Broad-band	500000	Acceleration
70	7264C Accelerometer 500g/DTRA Datalogger	e7264c	Broad-band	500000	Acceleration
71	7264C Accelerometer 500g/DTRA Datalogger	e7264c	Broad-band	500000	Acceleration
86	EGE-73A Accelerometer 5000g/DTRA Datalogger	ege73a	Broad-band	500000	Acceleration
87	7264C Accelerometer 500g/DTRA Datalogger	e7264c	Broad-band	500000	Acceleration
88	7264C Accelerometer 500g/DTRA Datalogger	e7264c	Broad-band	500000	Acceleration
107	7264B Accelerometer 2000g/DTRA Datalogger	e7264b	Broad-band	500000	Acceleration
108	7264B Accelerometer 2000g/DTRA Datalogger	e7264b	Broad-band	500000	Acceleration
109	EGE-73A Accelerometer 5000g/DTRA Datalogger	ege73a	Broad-band	500000	Acceleration
110	EGE-73A Accelerometer 5000g/DTRA Datalogger	ege73a	Broad-band	500000	Acceleration
111	7264C Accelerometer 500g/DTRA Datalogger	e7264c	Broad-band	500000	Acceleration
112	EGE-73A Accelerometer 5000g/DTRA Datalogger	ege73a	Broad-band	500000	Acceleration
113	EGE-73A Accelerometer 5000g/DTRA Datalogger	ege73a	Broad-band	500000	Acceleration
126	7264B Accelerometer 2000g/DTRA Datalogger	e7264b	Broad-band	500000	Acceleration
127	7264B Accelerometer 2000g/DTRA Datalogger	e7264b	Broad-band	500000	Acceleration
128	7264B Accelerometer 2000g/DTRA Datalogger	e7264b	Broad-band	500000	Acceleration
129	7264C Accelerometer 500g/DTRA Datalogger	e7264c	Broad-band	500000	Acceleration
130	EGE-73A Accelerometer 5000g/DTRA Datalogger	ege73a	Broad-band	500000	Acceleration
131	EGE-73A Accelerometer 5000g/DTRA Datalogger	ege73a	Broad-band	500000	Acceleration
148	7264B Accelerometer 2000g/DTRA Datalogger	e7264b	Broad-band	500000	Acceleration
149	EGE-73A Accelerometer 5000g/DTRA Datalogger	ege73a	Broad-band	500000	Acceleration
150	7264B Accelerometer 2000g/DTRA Datalogger	e7264b	Broad-band	500000	Acceleration
151	EGE-73A Accelerometer 5000g/DTRA Datalogger	ege73a	Broad-band	500000	Acceleration
152	EGE-73A Accelerometer 5000g/DTRA Datalogger	ege73a	Broad-band	500000	Acceleration
153	EGE-73A Accelerometer 5000g/DTRA Datalogger	ege73a	Broad-band	500000	Acceleration
154	EGE-73A Accelerometer 5000g/DTRA Datalogger	ege73a	Broad-band	500000	Acceleration
155	EGE-73A Accelerometer 5000g/DTRA Datalogger	ege73a	Broad-band	500000	Acceleration

Appendix 3
Instrument Metadata for SPE-3

Instrument ID	Instrument Name	Instrument Code	Frequency Band	Sample Rate (samples/ second)	Response Type
156	7264G Accelerometer 2000g/DTRA Datalogger	e7264g	Broad-band	500000	Acceleration
157	7264C Accelerometer 500g/DTRA Datalogger	e7264c	Broad-band	500000	Acceleration
158	7264C Accelerometer 500g/DTRA Datalogger	e7264c	Broad-band	500000	Acceleration
159	7264G Accelerometer 2000g/DTRA Datalogger	e7264g	Broad-band	500000	Acceleration
160	7264C Accelerometer 500g/DTRA Datalogger	e7264c	Broad-band	500000	Acceleration
161	7264C Accelerometer 500g/DTRA Datalogger	e7264c	Broad-band	500000	Acceleration
162	7264C Accelerometer 500g/DTRA Datalogger	e7264c	Broad-band	500000	Acceleration
163	EGE-73A Accelerometer 5000g/DTRA Datalogger	ege73a	Broad-band	500000	Acceleration
164	7264G Accelerometer 2000g/DTRA Datalogger	e7264g	Broad-band	500000	Acceleration
165	7264G Accelerometer 2000g/DTRA Datalogger	e7264g	Broad-band	500000	Acceleration
166	EGE-73A Accelerometer 5000g/DTRA Datalogger	ege73a	Broad-band	500000	Acceleration
167	7264G Accelerometer 2000g/DTRA Datalogger	e7264g	Broad-band	500000	Acceleration
168	7264C Accelerometer 500g/DTRA Datalogger	e7264c	Broad-band	500000	Acceleration
169	7264C Accelerometer 500g/DTRA Datalogger	e7264c	Broad-band	500000	Acceleration
170	7264C Accelerometer 500g/DTRA Datalogger	e7264c	Broad-band	500000	Acceleration
171	7264G Accelerometer 2000g/DTRA Datalogger	e7264g	Broad-band	500000	Acceleration
172	7264C Accelerometer 500g/DTRA Datalogger	e7264c	Broad-band	500000	Acceleration
173	7264C Accelerometer 500g/DTRA Datalogger	e7264c	Broad-band	500000	Acceleration
174	7264G Accelerometer 2000g/DTRA Datalogger	e7264g	Broad-band	500000	Acceleration
175	7264C Accelerometer 500g/DTRA Datalogger	e7264c	Broad-band	500000	Acceleration
176	7264C Accelerometer 500g/DTRA Datalogger	e7264c	Broad-band	500000	Acceleration
177	7264G Accelerometer 2000g/DTRA Datalogger	e7264g	Broad-band	500000	Acceleration
178	7264C Accelerometer 500g/DTRA Datalogger	e7264c	Broad-band	500000	Acceleration
179	7264C Accelerometer 500g/DTRA Datalogger	e7264c	Broad-band	500000	Acceleration
180	7264G Accelerometer 2000g/DTRA Datalogger	e7264g	Broad-band	500000	Acceleration
181	7264C Accelerometer 500g/DTRA Datalogger	e7264c	Broad-band	500000	Acceleration
182	7264C Accelerometer 500g/DTRA Datalogger	e7264c	Broad-band	500000	Acceleration
183	7264C Accelerometer 500g/DTRA Datalogger	e7264c	Broad-band	500000	Acceleration
184	7264C Accelerometer 500g/DTRA Datalogger	e7264c	Broad-band	500000	Acceleration
185	7264C Accelerometer 500g/DTRA Datalogger	e7264c	Broad-band	500000	Acceleration
186	EGCS-D0-50g Accelerometer/DTRA Datalogger	egcsd0	Broad-band	500000	Acceleration
187	7264C Accelerometer 500g/DTRA Datalogger	e7264c	Broad-band	500000	Acceleration
188	7264C Accelerometer 500g/DTRA Datalogger	e7264c	Broad-band	500000	Acceleration
189	7264C Accelerometer 500g/DTRA Datalogger	e7264c	Broad-band	500000	Acceleration
190	7264C Accelerometer 500g/DTRA Datalogger	e7264c	Broad-band	500000	Acceleration
191	7264C Accelerometer 500g/DTRA Datalogger	e7264c	Broad-band	500000	Acceleration
192	7264C Accelerometer 500g/DTRA Datalogger	e7264c	Broad-band	500000	Acceleration
193	7264C Accelerometer 500g/DTRA Datalogger	e7264c	Broad-band	500000	Acceleration
194	EGE-73A Accelerometer 5000g/DTRA Datalogger	ege73a	Broad-band	1000000	Acceleration
195	7264B Accelerometer 2000g/DTRA Datalogger	e7264b	Broad-band	1000000	Acceleration
196	7264B Accelerometer 2000g/DTRA Datalogger	e7264b	Broad-band	1000000	Acceleration
197	EGE-73A Accelerometer 5000g/DTRA Datalogger	ege73a	Broad-band	1000000	Acceleration
198	7264B Accelerometer 2000g/DTRA Datalogger	e7264b	Broad-band	1000000	Acceleration
199	Endevco 7270A-2K/DTRA Datalogger	e7270	Broad-band	1000000	Acceleration
200	EGE-73A Accelerometer 5000g/DTRA Datalogger	ege73a	Broad-band	1000000	Acceleration
201	7264B Accelerometer 2000g/DTRA Datalogger	e7264b	Broad-band	1000000	Acceleration
202	7264B Accelerometer 2000g/DTRA Datalogger	e7264b	Broad-band	1000000	Acceleration
203	Endevco 7270A-2K/DTRA Datalogger	e7270	Broad-band	500000	Acceleration
204	EGE-73A Accelerometer 5000g/DTRA Datalogger	ege73a	Broad-band	500000	Acceleration
205	7264B Accelerometer 2000g/DTRA Datalogger	e7264b	Broad-band	500000	Acceleration
206	7264B Accelerometer 2000g/DTRA Datalogger	e7264b	Broad-band	500000	Acceleration
214	EGCS-D0-100g Accel/DTRA Datalogger	egcsd0	Broad-band	500000	Acceleration
216	EGCS-D0-100g Accel/DTRA Datalogger	egcsd0	Broad-band	500000	Acceleration
218	EGCS-D0-50g Accelerometer/DTRA Datalogger	egcsd0	Broad-band	500000	Acceleration
219	EGCS-D0-50g Accelerometer/DTRA Datalogger	egcsd0	Broad-band	500000	Acceleration
221	EGCS-D0-50g Accelerometer/DTRA Datalogger	egcsd0	Broad-band	500000	Acceleration
223	EGCS-D0-100g Accel/DTRA Datalogger	egcsd0	Broad-band	500000	Acceleration

Appendix 3
Instrument Metadata for SPE-3

Instrument ID	Instrument Name	Instrument Code	Frequency Band	Sample Rate (samples/ second)	Response Type
224	7264B Accelerometer 2000g/DTRA Datalogger	e7264b	Broad-band	500000	Acceleration
226	EGCS-D0-50g Accelerometer/DTRA Datalogger	egcsd0	Broad-band	500000	Acceleration
227	Endevco 7264B-500/DTRA Datalogger	endevc	Broad-band	500000	Acceleration
228	EGCS-D0-50g Accelerometer/DTRA Datalogger	egcsd0	Broad-band	500000	Acceleration
229	EGCS-D0-100g Accel/DTRA Datalogger	egcsd0	Broad-band	500000	Acceleration
230	7264B Accelerometer 2000g/DTRA Datalogger	e7264b	Broad-band	500000	Acceleration
231	EGCS-D0-50g Accelerometer/DTRA Datalogger	egcsd0	Broad-band	500000	Acceleration
232	EGCS-D0-100g Accel/DTRA Datalogger	egcsd0	Broad-band	500000	Acceleration
233	EGCS-D0-50g Accelerometer/DTRA Datalogger	egcsd0	Broad-band	500000	Acceleration
235	Hyperion IFS3000 Infrasound/Geotech Smart24 DAS	hifs3k	Long-period	200	Infrasound

Appendix 4

Selected Metadata for SPE-2 Borehole Sensors

Appendix 4
Selected Metadata for SPE-2 Borehole Sensors

SPE Borehole Station	Channel	SPE2 Instrument[a] ID	SPE2 edepth[b] km	Northing	Easting	Elevation	Latitude	Longitude	Elevation
				SPC NAD27 ft		NGVD29 ft	GEO NAD83 dec deg		NAVD88 m
				NSTec Survey & Colog Deviation[c]			USACE Corpscon6 Conversion[d]		
BH-01	FNT-1	36	0.0549	900,103.3	676,651.3	4,822.47	37.22127	116.06083	1,470.9
BH-01	FNT-2	41	0.0457	900,102.6	676,650.8	4,852.47	37.22126	116.06083	1,480.0
BH-01	FNR-3	42	0.0152	900,106.2	676,653.9	4,952.47	37.22127	116.06082	1,510.5
BH-01	FNT-3	43	0.0152	900,106.2	676,653.9	4,952.47	37.22127	116.06082	1,510.5
BH-01	FNL-3	44	0.0152	900,106.2	676,653.9	4,952.47	37.22127	116.06082	1,510.5
BH-01A	FNR_1	194	0.0549	900,109.7	676,645.3	4,822.47	37.22128	116.06085	1,470.9
BH-01A	FNT_1	195	0.0549	900,109.7	676,645.3	4,822.47	37.22128	116.06085	1,470.9
BH-01A	FNL_1	196	0.0549	900,109.7	676,645.3	4,822.47	37.22128	116.06085	1,470.9
BH-01A	FNR_2	197	0.0457	900,109.8	676,645.2	4,852.47	37.22128	116.06085	1,480.0
BH-01A	FNT_2	199	0.0457	900,109.8	676,645.2	4,852.47	37.22128	116.06085	1,480.0
BH-01A	FNL_2	199	0.0457	900,109.8	676,645.2	4,852.47	37.22128	116.06085	1,480.0
BH-01A	FNR_3	200	0.0152	900,103.3	676,645.5	4,952.47	37.22127	116.06085	1,510.5
BH-01A	FNT_3	201	0.0152	900,103.3	676,645.5	4,952.47	37.22127	116.06085	1,510.5
BH-01A	FNL_3	202	0.0152	900,103.3	676,645.5	4,952.47	37.22127	116.06085	1,510.5
BH-02	FNR_1	57	0.0549	900,076.4	676,614.2	4,822.47	37.22119	116.06096	1,470.9
BH-02	FNT_1	49	0.0549	900,076.4	676,614.2	4,822.47	37.22119	116.06096	1,470.9
BH-02	FNL_1	50	0.0549	900,076.4	676,614.2	4,822.47	37.22119	116.06096	1,470.9
BH-02	FNR_2	58	0.0457	900,076.4	676,613.4	4,852.47	37.22119	116.06096	1,480.0
BH-02	FNT_2	59	0.0457	900,076.4	676,613.4	4,852.47	37.22119	116.06096	1,480.0
BH-02	FNL_2	60	0.0457	900,076.4	676,613.4	4,852.47	37.22119	116.06096	1,480.0
BH-02	FNR_3	61	0.0152	900,075.8	676,609.5	4,952.47	37.22119	116.06097	1,510.5
BH-02	FNT_3	62	0.0152	900,075.8	676,609.5	4,952.47	37.22119	116.06097	1,510.5
BH-02	FNL_3	63	0.0152	900,075.8	676,609.5	4,952.47	37.22119	116.06097	1,510.5
BH-03	FNR_2	80	0.0457	900,051.6	676,660.6	4,852.47	37.22112	116.06080	1,480.0
BH-03	FNT_2	81	0.0457	900,051.6	676,660.6	4,852.47	37.22112	116.06080	1,480.0
BH-03	FNL_2	82	0.0457	900,051.6	676,660.6	4,852.47	37.22112	116.06080	1,480.0
BH-03	FNR_3	83	0.0152	900,051.1	676,659.5	4,952.47	37.22112	116.06080	1,510.5
BH-03	FNT_3	84	0.0152	900,051.1	676,659.5	4,952.47	37.22112	116.06080	1,510.5
BH-03	FNL_3	85	0.0152	900,051.1	676,659.5	4,952.47	37.22112	116.06080	1,510.5
BH-04	FNR_1	98	0.0549	900,015.0	676,612.6	4,822.47	37.22102	116.06096	1,470.9
BH-04	FNT_1	99	0.0549	900,015.0	676,612.6	4,822.47	37.22102	116.06096	1,470.9
BH-04	FNL_1	100	0.0549	900,015.0	676,612.6	4,822.47	37.22102	116.06096	1,470.9
BH-04	FNR_2	101	0.0457	900,015.9	676,612.8	4,852.47	37.22103	116.06096	1,480.0
BH-04	FNT_2	102	0.0457	900,015.9	676,612.8	4,852.47	37.22103	116.06096	1,480.0
BH-04	FNL_2	103	0.0457	900,015.9	676,612.8	4,852.47	37.22103	116.06096	1,480.0
BH-04	FNR_3	104	0.0152	900,018.1	676,612.7	4,952.47	37.22103	116.06096	1,510.5
BH-04	FNT_3	105	0.0152	900,018.1	676,612.7	4,952.47	37.22103	116.06096	1,510.5
BH-04	FNL_3	106	0.0152	900,018.1	676,612.7	4,952.47	37.22103	116.06096	1,510.5
BH-05	FNR_2	120	0.0457	900,083.6	676,706.5	4,852.47	37.22121	116.06064	1,480.0
BH-05	FNT_2	121	0.0457	900,083.6	676,706.5	4,852.47	37.22121	116.06064	1,480.0
BH-05	FNL_2	122	0.0457	900,083.6	676,706.5	4,852.47	37.22121	116.06064	1,480.0
BH-05	FNR_3	123	0.0152	900,083.1	676,706.6	4,952.47	37.22121	116.06064	1,510.5
BH-05	FNT_3	124	0.0152	900,083.1	676,706.6	4,952.47	37.22121	116.06064	1,510.5
BH-05	FNL_3	125	0.0152	900,083.1	676,706.6	4,952.47	37.22121	116.06064	1,510.5
BH-06	FNR_1	141	0.0549	900,131.2	676,604.9	4,822.47	37.22134	116.06099	1,470.9
BH-06	FNT_1	99	0.0549	900,131.2	676,604.9	4,822.47	37.22134	116.06099	1,470.9
BH-06	FNR_2	142	0.0457	900,131.4	676,604.7	4,852.47	37.22134	116.06099	1,480.0
BH-06	FNT_2	143	0.0457	900,131.4	676,604.7	4,852.47	37.22134	116.06099	1,480.0
BH-06	FNL_2	144	0.0457	900,131.4	676,604.7	4,852.47	37.22134	116.06099	1,480.0
BH-06	FNR_3	145	0.0152	900,131.7	676,604.0	4,952.47	37.22134	116.06099	1,510.5
BH-06	FNT_3	146	0.0152	900,131.7	676,604.0	4,952.47	37.22134	116.06099	1,510.5
BH-06	FNL_3	147	0.0152	900,131.7	676,604.0	4,952.47	37.22134	116.06099	1,510.5

NOTES

a. See Appendix 2 for key to instruments.

b. Depth in kilometers at which the instrument is positioned, relative to the ground surface elevation at the borehole collar.

c. State Plane Coordinates at sensor location based on the borehole collar location, as surveyed by NSTec,
corrected for borehole deviation, along borehole path, as measured by IDS Colog Group.

d. Conversion of NSTec State Plane coordinates to latitude/longitude using USACE "Corpscon6" application.

Appendix 4
Selected Metadata for SPE-2 Borehole Sensors

SPE Borehole Station	Channel	SPE2 Instrument[a] ID	SPE2 edepth[b] km	Northing	Easting	Elevation	Latitude	Longitude	Elevation
				SPC NAD27 ft		NGVD29 ft	GEO NAD83 dec deg		NAVD88 m
				NSTec Survey & Colog Deviation[c]			USACE Corpscon6 Conversion[d]		

ABBREVIATIONS

SPC	State Plane Cordinate Systems, Zone 2702 Nevada Central
NAD27	North American Datum 1927
ft	U.S. Survey Feet
NGVD29	National Geodetic Vertical Datum 1929
NSTec	National Security Technologies, Inc.
GEO	Geographic Coordinate System
NAD83	North American Datum 1983
NAVD88	North American Vertical Datum 1988
m	Meters
USACE	U.S. Army Corps of Engineers

Appendix 5

Selected Metadata for SPE-3 Borehole Sensors

Appendix 5
Selected Metadata for SPE-3 Borehole Sensors

SPE Borehole Station	Channel	SPE3 Instrument[a] ID	SPE3 edepth[b] km	Northing	Easting	Elevation	Latitude	Longitude	Elevation
				SPC NAD27 ft		NGVD29 ft	GEO NAD83 dec deg		NAVD88 m
				NSTec Survey & Colog Deviation[c]			USACE Corpscon6 Conversion[d]		
BH-01	GNR-3	45	0.0152	900,106.2	676,653.9	4,952.47	37.22127	116.06082	1,510.5
BH-01	GNT-3	46	0.0152	900,106.2	676,653.9	4,952.47	37.22127	116.06082	1,510.5
BH-01	GNL-3	47	0.0152	900,106.2	676,653.9	4,952.47	37.22127	116.06082	1,510.5
BH-01A	FNR_1	194	0.0549	900,109.7	676,645.3	4,822.47	37.22128	116.06085	1,470.9
BH-01A	FNT_1	195	0.0549	900,109.7	676,645.3	4,822.47	37.22128	116.06085	1,470.9
BH-01A	FNL_1	196	0.0549	900,109.7	676,645.3	4,822.47	37.22128	116.06085	1,470.9
BH-01A	FNR_2	197	0.0457	900,109.8	676,645.2	4,852.47	37.22128	116.06085	1,480.0
BH-01A	FNT_2	198	0.0457	900,109.8	676,645.2	4,852.47	37.22128	116.06085	1,480.0
BH-01A	FNL_2	199	0.0457	900,109.8	676,645.2	4,852.47	37.22128	116.06085	1,480.0
BH-01A	GNL_2	203	0.0457	900,109.8	676,645.2	4,852.47	37.22128	116.06085	1,480.0
BH-01A	FNR_3	200	0.0152	900,103.3	676,645.5	4,952.47	37.22127	116.06085	1,510.5
BH-01A	FNT_3	201	0.0152	900,103.3	676,645.5	4,952.47	37.22127	116.06085	1,510.5
BH-01A	FNL_3	202	0.0152	900,103.3	676,645.5	4,952.47	37.22127	116.06085	1,510.5
BH-01A	GNR_3	204	0.0152	900,103.3	676,645.5	4,952.47	37.22127	116.06085	1,510.5
BH-01A	GNT_3	205	0.0152	900,103.3	676,645.5	4,952.47	37.22127	116.06085	1,510.5
BH-01A	GNL_3	206	0.0152	900,103.3	676,645.5	4,952.47	37.22127	116.06085	1,510.5
BH-02	GNR_1	64	0.0549	900,076.4	676,614.2	4,822.47	37.22119	116.06096	1,470.9
BH-02	GNT_1	67	0.0549	900,076.4	676,614.2	4,822.47	37.22119	116.06096	1,470.9
BH-02	GNL_1	66	0.0549	900,076.4	676,614.2	4,822.47	37.22119	116.06096	1,470.9
BH-02	GNT_2	67	0.0457	900,076.4	676,613.4	4,852.47	37.22119	116.06096	1,480.0
BH-02	GNL_2	68	0.0457	900,076.4	676,613.4	4,852.47	37.22119	116.06096	1,480.0
BH-02	GNR_3	69	0.0152	900,075.8	676,609.5	4,952.47	37.22119	116.06097	1,510.5
BH-02	GNT_3	70	0.0152	900,075.8	676,609.5	4,952.47	37.22119	116.06097	1,510.5
BH-02	GNL_3	71	0.0152	900,075.8	676,609.5	4,952.47	37.22119	116.06097	1,510.5
BH-03	GNR_3	86	0.0152	900,051.1	676,659.5	4,952.47	37.22112	116.06080	1,510.5
BH-03	GNT_3	87	0.0152	900,051.1	676,659.5	4,952.47	37.22112	116.06080	1,510.5
BH-03	GNL_3	88	0.0152	900,051.1	676,659.5	4,952.47	37.22112	116.06080	1,510.5
BH-04	GNR_1	107	0.0549	900,015.0	676,612.6	4,822.47	37.22102	116.06096	1,470.9
BH-04	GNR_2	108	0.0457	900,015.9	676,612.8	4,852.47	37.22103	116.06096	1,480.0
BH-04	GNT_2	109	0.0457	900,015.9	676,612.8	4,852.47	37.22103	116.06096	1,480.0
BH-04	GNL_2	110	0.0457	900,015.9	676,612.8	4,852.47	37.22103	116.06096	1,480.0
BH-04	GNR_3	111	0.0152	900,018.1	676,612.7	4,952.47	37.22103	116.06096	1,510.5
BH-04	GNT_3	112	0.0152	900,018.1	676,612.7	4,952.47	37.22103	116.06096	1,510.5
BH-04	GNL_3	113	0.0152	900,018.1	676,612.7	4,952.47	37.22103	116.06096	1,510.5
BH-05	GNR_2	126	0.0457	900,083.6	676,706.5	4,852.47	37.22121	116.06064	1,480.0
BH-05	GNT_2	127	0.0457	900,083.6	676,706.5	4,852.47	37.22121	116.06064	1,480.0
BH-05	GNL_2	128	0.0457	900,083.6	676,706.5	4,852.47	37.22121	116.06064	1,480.0
BH-05	GNR_3	129	0.0152	900,083.1	676,706.6	4,952.47	37.22121	116.06064	1,510.5
BH-05	GNT_3	130	0.0152	900,083.1	676,706.6	4,952.47	37.22121	116.06064	1,510.5
BH-05	GNL_3	131	0.0152	900,083.1	676,706.6	4,952.47	37.22121	116.06064	1,510.5
BH-06	GNR_1	148	0.0549	900,131.2	676,604.9	4,822.47	37.22134	116.06099	1,470.9
BH-06	GNT_1	149	0.0549	900,131.2	676,604.9	4,822.47	37.22134	116.06099	1,470.9
BH-06	GNR_2	150	0.0457	900,131.4	676,604.7	4,852.47	37.22134	116.06099	1,480.0
BH-06	GNT_2	151	0.0457	900,131.4	676,604.7	4,852.47	37.22134	116.06099	1,480.0
BH-06	GNL_2	152	0.0457	900,131.4	676,604.7	4,852.47	37.22134	116.06099	1,480.0
BH-06	GNR_3	153	0.0152	900,131.7	676,604.0	4,952.47	37.22134	116.06099	1,510.5
BH-06	GNT_3	154	0.0152	900,131.7	676,604.0	4,952.47	37.22134	116.06099	1,510.5
BH-06	GNL_3	155	0.0152	900,131.7	676,604.0	4,952.47	37.22134	116.06099	1,510.5
BH-07	GNR_1	156	0.0549	900,073.1	676,576.1	4,822.47	37.22118	116.06109	1,470.9
BH-07	GNT_1	157	0.0549	900,073.1	676,576.1	4,822.47	37.22118	116.06109	1,470.9
BH-07	GNL_1	158	0.0549	900,073.1	676,576.1	4,822.47	37.22118	116.06109	1,470.9
BH-07	GNR_2	159	0.0457	900,072.2	676,577.6	4,852.47	37.22118	116.06108	1,480.0
BH-07	GNT_2	160	0.0457	900,072.2	676,577.6	4,852.47	37.22118	116.06108	1,480.0
BH-07	GNL_2	160	0.0457	900,072.2	676,577.6	4,852.47	37.22118	116.06108	1,480.0
BH-07	GNR_3	163	0.0152	900,072.6	676,576.0	4,952.47	37.22118	116.06109	1,510.5
BH-07	GNT_3	162	0.0152	900,072.6	676,576.0	4,952.47	37.22118	116.06109	1,510.5
BH-07	GNL_3	111	0.0152	900,072.6	676,576.0	4,952.47	37.22118	116.06109	1,510.5
BH-08	GNR_1	163	0.0549	900,045.4	676,649.1	4,822.47	37.22111	116.06084	1,470.9
BH-08	GNT_1	164	0.0549	900,045.4	676,649.1	4,822.47	37.22111	116.06084	1,470.9
BH-08	GNL_1	165	0.0549	900,045.4	676,649.1	4,822.47	37.22111	116.06084	1,470.9
BH-08	GNR_2	166	0.0457	900,045.4	676,647.6	4,852.47	37.22111	116.06084	1,480.0
BH-08	GNT_2	167	0.0457	900,045.4	676,647.6	4,852.47	37.22111	116.06084	1,480.0

SPE Borehole Station	Channel	SPE3 Instrument[a] ID	SPE3 edepth[b] km	Northing	Easting	Elevation	Latitude	Longitude	Elevation
				SPC NAD27 ft		NGVD29 ft	GEO NAD83 dec deg		NAVD88 m
				NSTec Survey & Colog Deviation[c]			USACE Corpscon6 Conversion[d]		
BH-08	GNL_2	167	0.0457	900,045.4	676,647.6	4,852.47	37.22111	116.06084	1,480.0
BH-08	GNR_3	168	0.0152	900,045.4	676,646.3	4,952.47	37.22111	116.06085	1,510.5
BH-08	GNT_3	169	0.0152	900,045.4	676,646.3	4,952.47	37.22111	116.06085	1,510.5
BH-08	GNL_3	170	0.0152	900,045.4	676,646.3	4,952.47	37.22111	116.06085	1,510.5
BH-09	GNR_1	171	0.0549	900,135.4	676,670.2	4,822.47	37.22135	116.06076	1,470.9
BH-09	GNT_1	172	0.0549	900,135.4	676,670.2	4,822.47	37.22135	116.06076	1,470.9
BH-09	GNL_1	173	0.0549	900,135.4	676,670.2	4,822.47	37.22135	116.06076	1,470.9
BH-09	GNR_2	174	0.0457	900,135.9	676,670.0	4,852.47	37.22136	116.06077	1,480.0
BH-09	GNT_2	175	0.0457	900,135.9	676,670.0	4,852.47	37.22136	116.06077	1,480.0
BH-09	GNL_2	176	0.0457	900,135.9	676,670.0	4,852.47	37.22136	116.06077	1,480.0
BH-09	GNR_3	177	0.0366	900,136.2	676,669.7	4,882.47	37.22136	116.06077	1,489.2
BH-09	GNT_3	178	0.0366	900,136.2	676,669.7	4,882.47	37.22136	116.06077	1,489.2
BH-09	GNL_3	179	0.0366	900,136.2	676,669.7	4,882.47	37.22136	116.06077	1,489.2
BH-09	GNR_4	180	0.0274	900,136.1	676,669.4	4,912.47	37.22136	116.06077	1,498.3
BH-09	GNT_4	181	0.0274	900,136.1	676,669.4	4,912.47	37.22136	116.06077	1,498.3
BH-09	GNL_4	182	0.0274	900,136.1	676,669.4	4,912.47	37.22136	116.06077	1,498.3
BH-09	GNR_5	183	0.0152	900,136.2	676,669.1	4,952.47	37.22136	116.06077	1,510.5
BH-09	GNT_5	184	0.0152	900,136.2	676,669.1	4,952.47	37.22136	116.06077	1,510.5
BH-09	GNL_5	185	0.0152	900,136.2	676,669.1	4,952.47	37.22136	116.06077	1,510.5
BH-10	GNR	186	0.0146	900,098.1	676,648.2	4,893.74	37.22125	116.06084	1,492.6
BH-11	GNR_1	189	0.0549	900,227.2	676,716.7	4,822.47	37.22160	116.06060	1,470.9
BH-11	GNT_1	188	0.0549	900,227.2	676,716.7	4,822.47	37.22160	116.06060	1,470.9
BH-11	GNL_1	189	0.0549	900,227.2	676,716.7	4,822.47	37.22160	116.06060	1,470.9
BH-11	GNR_2	190	0.0457	900,227.5	676,716.2	4,852.47	37.22161	116.06060	1,480.0
BH-11	GNL_2	191	0.0457	900,227.5	676,716.2	4,852.47	37.22161	116.06060	1,480.0
BH-11	GNR_3	192	0.0152	900,228.3	676,714.3	4,952.47	37.22161	116.06061	1,510.5
BH-11	GNT_3	193	0.0152	900,228.3	676,714.3	4,952.47	37.22161	116.06061	1,510.5

NOTES

a. See Appendix 3 for key to instruments.

b. Depth in kilometers at which the instrument is positioned, relative to the ground surface elevation at the borehole collar.

c. State Plane Coordinates at sensor location based on the borehole collar location, as surveyed by NSTec,
corrected for borehole deviation, along borehole path, as measured by IDS Colog Group.

d. Conversion of NSTec State Plane coordinates to latitude/longitude using USACE "Corpscon6" application.

ABBREVIATIONS

SPC	State Plane Cordinate Systems, Zone 2702 Nevada Central
NAD27	North American Datum 1927
ft	U.S. Survey Feet
NGVD29	National Geodetic Vertical Datum 1929
NSTec	National Security Technologies, Inc.
GEO	Geographic Coordinate System
NAD83	North American Datum 1983
NAVD88	North American Vertical Datum 1988
m	Meters
USACE	U.S. Army Corps of Engineers

Appendix 6

Selected Metadata for SPE-2 Surface Stations

Appendix 6
Selected Metadata for SPE-2 Surface Stations

Station Name	Station Header ID[a]	Channel	Estimated Latitude (degrees)	Estimated Longitude (degrees)	Estimated Elevation (km amsl)	Station Full Name
Near Field						
DT-13	DT-13	FNZ	37.2215	-116.0608	1.5246	NNSS-SPE DTRA Surface A8 sp2 30m NE
DT-15	DT-15	FNZ	37.2208	-116.0611	1.5219	NNSS-SPE DTRA Surface A4 sp2 45m SW
DT-16	DT-16	FNZ	37.2207	-116.0612	1.5213	NNSS-SPE DTRA Surface A3 sp2 60m SW
DT-17	DT-17	FNZ	37.2206	-116.0612	1.5221	NNSS-SPE DTRA Surface A2 sp2 75m SW
DT-18	DT-18	FNZ	37.2205	-116.0613	1.5229	NNSS-SPE DTRA Surface A1 sp2 90m SW
DT-14	DT-14	FNZ	37.2213	-116.0612	1.5273	NNSS-SPE DTRA Surface A9 sp2 30m NW
SL-07	SL-07	CNZ	37.2210	-116.0610	1.5243	NNSS-SPE Sandia NL surface A5 sp2 30m SW
SL-08	SL-08	CNZ	37.2211	-116.0609	1.5244	NNSS-SPE Sandia NL surface A6 sp2 15m SW
SL-09	SL-09	CNZ	37.2213	-116.0608	1.5246	NNSS-SPE Sandia NL surface A7 sp2 15m NE
SL-10	SL-10	CNZ	37.2213	-116.0610	1.5251	NNSS-SPE Sandia NL surface A10 sp2 15m NW
SL-11	SL-11	CNZ	37.2212	-116.0607	1.5244	NNSS-SPE Sandia NL surface A11 sp2 15m SE
SL-12	SL-12	CNZ	37.2211	-116.0606	1.5222	NNSS-SPE Sandia NL surface A12 30m SE
Far Field						
L1-01	L1001	CLZ	37.2221	-116.0610	1.5290	NNSS-SPE Line 1 site 01
L1-02	L1002	CLZ	37.2230	-116.0611	1.5370	NNSS-SPE Line 1 site 02
L1-03	L1003	CLZ	37.2239	-116.0611	1.5400	NNSS-SPE Line 1 site 03
L1-04	L1004	CLZ	37.2248	-116.0612	1.5370	NNSS-SPE Line 1 site 04
		CLR				
		CLT				
L1-05	L1005	CLZ	37.2257	-116.0613	1.5500	NNSS-SPE Line 1 site 05
L1-06	L1006	CLZ	37.2266	-116.0614	1.5580	NNSS-SPE Line 1 site 06
L1-07	L1007	CLZ	37.2275	-116.0615	1.5590	NNSS-SPE Line 1 site 07
L1-08	L1008	CLZ	37.2284	-116.0616	1.5720	NNSS-SPE Line 1 site 08
		CLR				
		CLT				
L1-09	L1009	CLZ	37.2293	-116.0616	1.5890	NNSS-SPE Line 1 site 09
L1-10	L1010	CNZ	37.2302	-116.0617	1.5850	NNSS-SPE Line 1 site 10
		CNR				
		CNT				
		DJZ				
		DJR				
		DJT				
		CLZ				
L1-11	L1011	CLZ	37.2311	-116.0618	1.5970	NNSS-SPE Line 1 site 11
L1-12	L1012	CLZ	37.2320	-116.0619	1.6040	NNSS-SPE Line 1 site 12
		CLR				
		CLT				
L1-13	L1013	CLZ	37.2329	-116.0620	1.6160	NNSS-SPE Line 1 site 13
L1-14	L1014	CLZ	37.2338	-116.0621	1.6330	NNSS-SPE Line 1 site 14
L1-15	L1015	CLZ	37.2347	-116.0621	1.6560	NNSS-SPE Line 1 site 15
L1-16	L1016	CLZ	37.2355	-116.0622	1.6740	NNSS-SPE Line 1 site 16
		CLR				
		CLT				
L1-17	L1017	CLZ	37.2364	-116.0623	1.7060	NNSS-SPE Line 1 site 17
L1-18	L1018	CLZ	37.2373	-116.0624	1.7390	NNSS-SPE Line 1 site 18
L1-19	L1019	CLZ	37.2382	-116.0625	1.7380	NNSS-SPE Line 1 site 19
L1-20	L1020	DHZ	37.2391	-116.0626	1.7520	NNSS-SPE Line 1 site 20
		DHR				
		DHT				
L2-01	L2001	CLZ	37.2218	-116.0600	1.5200	NNSS-SPE Line 2 site 01
L2-02	L2002	CLZ	37.2224	-116.0592	1.5150	NNSS-SPE Line 2 site 02
L2-03	L2003	CLZ	37.2229	-116.0583	1.5280	NNSS-SPE Line 2 site 03

Appendix 6
Selected Metadata for SPE-2 Surface Stations

Station Name	Station Header ID[a]	Channel	Estimated Latitude (degrees)	Estimated Longitude (degrees)	Estimated Elevation (km amsl)	Station Full Name
L2-04	L2004	CLZ	37.2235	-116.0575	1.5280	NNSS-SPE Line 2 site 04
		CLR				
		CLT				
L2-05	L2005	CLZ	37.2241	-116.0566	1.5320	NNSS-SPE Line 2 site 05
L2-06	L2006	CLZ	37.2247	-116.0558	1.5310	NNSS-SPE Line 2 site 06
L2-07	L2007	CLZ	37.2253	-116.0549	1.5300	NNSS-SPE Line 2 site 07
L2-08	L2008	CLZ	37.2259	-116.0541	1.5300	NNSS-SPE Line 2 site 08
		CLR				
		CLT				
L2-09	L2009	CLZ	37.2265	-116.0533	1.5370	NNSS-SPE Line 2 site 09
L2-10	L2010	CNZ	37.2271	-116.0524	1.5310	NNSS-SPE Line 2 site 10
		CNR				
		CNT				
		DJZ				
		DJR				
		DJT				
		CLZ				
L2-11	L2011	CLZ	37.2277	-116.0516	1.5370	NNSS-SPE Line 2 site 11
L2-12	L2012	CLZ	37.2283	-116.0507	1.5370	NNSS-SPE Line 2 site 12
		CLR				
		CLT				
L2-13	L2013	CLZ	37.2289	-116.0499	1.5360	NNSS-SPE Line 2 site 13
L2-14	L2014	CLZ	37.2295	-116.0490	1.5410	NNSS-SPE Line 2 site 14
L2-15	L2015	CLZ	37.2301	-116.0482	1.5430	NNSS-SPE Line 2 site 15
L2-16	L2016	CLZ	37.2307	-116.0473	1.5360	NNSS-SPE Line 2 site 16
		CLR				
		CLT				
L2-17	L2017	CLZ	37.2312	-116.0465	1.5490	NNSS-SPE Line 2 site 17
L2-18	L2018	CLZ	37.2318	-116.0456	1.5480	NNSS-SPE Line 2 site 18
L2-19	L2019	CLZ	37.2324	-116.0448	1.5520	NNSS-SPE Line 2 site 19
L2-20	L2020	DHZ	37.2330	-116.0439	1.5330	NNSS-SPE Line 2 site 20
		DHR				
		DHT				
L3-01	L3001	CLZ	37.2203	-116.0607	1.5160	NNSS-SPE Line 3 site 01
L3-02	L3002	CLZ	37.2194	-116.0606	1.5120	NNSS-SPE Line 3 site 02
L3-03	L3003	CLZ	37.2185	-116.0605	1.5120	NNSS-SPE Line 3 site 03
L3-04	L3004	CLZ	37.2176	-116.0603	1.4960	NNSS-SPE Line 3 site 04
		CLR				
		CLT				
L3-05	L3005	CLZ	37.2167	-116.0602	1.4960	NNSS-SPE Line 3 site 05
L3-06	L3006	CLZ	37.2158	-116.0600	1.4940	NNSS-SPE Line 3 site 06
L3-07	L3007	CLZ	37.2149	-116.0599	1.4870	NNSS-SPE Line 3 site 07
L3-08	L3008	CLZ	37.2140	-116.0598	1.4840	NNSS-SPE Line 3 site 08
		CLR				
		CLT				
L3-09	L3009	CLZ	37.2131	-116.0596	1.4690	NNSS-SPE Line 3 site 09
L3-10	L3010	CNZ	37.2122	-116.0595	1.4810	NNSS-SPE Line 3 site 10
		CNR				
		CNT				
		DJZ				
		DJR				
		DJT				
		CLZ				
L3-11	L3011	CLZ	37.2113	-116.0593	1.4750	NNSS-SPE Line 3 site 11

Appendix 6
Selected Metadata for SPE-2 Surface Stations

Station Name	Station Header ID[a]	Channel	Estimated Latitude (degrees)	Estimated Longitude (degrees)	Estimated Elevation (km amsl)	Station Full Name
L3-12	L3012	CLZ	37.2104	-116.0592	1.4640	NNSS-SPE Line 3 site 12
		CLR				
		CLT				
L3-13	L3013	CLZ	37.2095	-116.0591	1.4590	NNSS-SPE Line 3 site 13
L3-14	L3014	CLZ	37.2087	-116.0589	1.4630	NNSS-SPE Line 3 site 14
L3-15	L3015	CLZ	37.2078	-116.0588	1.4530	NNSS-SPE Line 3 site 15
L3-16	L3016	CLZ	37.2069	-116.0586	1.4370	NNSS-SPE Line 3 site 16
		CLR				
		CLT				
L3-17	L3017	CLZ	37.2060	-116.0585	1.4310	NNSS-SPE Line 3 site 17
L3-18	L3018	CLZ	37.2051	-116.0584	1.4340	NNSS-SPE Line 3 site 18
L3-19	L3019	CLZ	37.2042	-116.0582	1.4280	NNSS-SPE Line 3 site 19
L3-20	L3020	DHZ	37.2033	-116.0581	1.4230	NNSS-SPE Line 3 site 20
		DHR				
		DHT				
L3-23	L3023	CHZ	37.1899	-116.0560	1.3450	NNSS-SPE Line 3 site 23
		CH1				
		CH2				
		CHZ_04				
		CH1_05				
		CH2_06				
L3-26	L3026	CHZ	37.1770	-116.0539	1.3100	NNSS-SPE Line 3 site 26
		CH1				
		CH2				
L3-28	L3028	CHZ	37.1407	-116.0482	1.2850	NNSS-SPE Line 3 site 28
		CH1				
		CH2				
		CHZ_04				
		CH1_05				
		CH2_06				
L3-30	L3030	CHZ	37.1049	-116.0426	1.2740	NNSS-SPE Line 3 site 30
		CH1				
		CH2				
L3-32	L3032	CHZ	37.0697	-116.0370	1.2360	NNSS-SPE Line 3 site 32
		CH1				
		CH2				
L3-34	L3034	CHZ	37.0330	-116.0314	1.2180	NNSS-SPE Line 3 site 34
		CH1				
		CH2				
L3-36	L3036	CHZ	36.9976	-116.0258	1.2040	NNSS-SPE Line 3 site 36
		CH1				
		CH2				
L4-01	L4001	CLZ	37.2204	-116.0614	1.5230	NNSS-SPE Line 4 site 01
L4-02	L4002	CLZ	37.2195	-116.0619	1.5210	NNSS-SPE Line 4 site 02
L4-03	L4003	CLZ	37.2187	-116.0624	1.5320	NNSS-SPE Line 4 site 03
L4-04	L4004	CLZ	37.2179	-116.0629	1.5230	NNSS-SPE Line 4 site 04
		CLR				
		CLT				
L4-05	L4005	CLZ	37.2171	-116.0634	1.5020	NNSS-SPE Line 4 site 05
L4-06	L4006	CLZ	37.2163	-116.0639	1.4990	NNSS-SPE Line 4 site 06
L4-07	L4007	CLZ	37.2155	-116.0643	1.5130	NNSS-SPE Line 4 site 07
L4-08	L4008	CLZ	37.2147	-116.0648	1.5050	NNSS-SPE Line 4 site 08
		CLR				
		CLT				

Station Name	Station Header ID[a]	Channel	Estimated Latitude (degrees)	Estimated Longitude (degrees)	Estimated Elevation (km amsl)	Station Full Name
L4-09	L4009	CLZ	37.2139	-116.0653	1.5070	NNSS-SPE Line 4 site 09
L4-10	L4010	CLZ	37.2131	-116.0658	1.5040	NNSS-SPE Line 4 site 10
L4-11	L4011	CLZ	37.2123	-116.0663	1.5080	NNSS-SPE Line 4 site 11
L4-12	L4012	CLZ	37.2114	-116.0668	1.5110	NNSS-SPE Line 4 site 12
		CLR				
		CLT				
L4-13	L4013	CLZ	37.2106	-116.0673	1.5120	NNSS-SPE Line 4 site 13
L4-14	L4014	CLZ	37.2098	-116.0678	1.5110	NNSS-SPE Line 4 site 14
L4-15	L4015	CLZ	37.2090	-116.0683	1.5140	NNSS-SPE Line 4 site 15
L4-16	L4016	CLZ	37.2082	-116.0688	1.5140	NNSS-SPE Line 4 site 16
		CLR				
		CLT				
L4-17	L4017	CLZ	37.2074	-116.0693	1.5120	NNSS-SPE Line 4 site 17
L4-18	L4018	CLZ	37.2066	-116.0698	1.5080	NNSS-SPE Line 4 site 18
L4-19	L4019	CLZ	37.2058	-116.0703	1.5130	NNSS-SPE Line 4 site 19
L4-20	L4020	DHZ	37.2050	-116.0708	1.5070	NNSS-SPE Line 4 site 20
		DHR				
		DHT				
L4-23	L4023	CHZ	37.1928	-116.0782	1.4400	NNSS-SPE Line 4 site 23
		CH1				
		CH2				
L4-26	L4026	CHZ	37.1807	-116.0856	1.3800	NNSS-SPE Line 4 site 26
		CH1				
		CH2				
L4-28	L4028	CHZ	37.1483	-116.1053	1.3550	NNSS-SPE Line 4 site 28
		CH1				
		CH2				
L4-30	L4030	CHZ	37.1159	-116.1250	1.3780	NNSS-SPE Line 4 site 30
		CH1				
		CH2				
L4-32	L4032	CHZ	37.0835	-116.1447	1.4210	NNSS-SPE Line 4 site 32
		CH1				
		CH2				
L4-34	L4034	CHZ	37.0510	-116.1644	1.5680	NNSS-SPE Line 4 site 34
		CH1				
		CH2				
L4-36	L4036	CHZ	37.0186	-116.1841	1.5270	NNSS-SPE Line 4 site 36
		CH1				
		CH2				
L5-01	L5001	CLZ	37.2214	-116.0620	1.5390	NNSS-SPE Line 5 site 01
L5-02	L5002	CLZ	37.2216	-116.0631	1.5560	NNSS-SPE Line 5 site 02
L5-03	L5003	CLZ	37.2218	-116.0642	1.5770	NNSS-SPE Line 5 site 03
L5-04	L5004	CLZ	37.2220	-116.0653	1.6220	NNSS-SPE Line 5 site 04
		CLR				
		CLT				
L5-05	L5005	CLZ	37.2222	-116.0664	1.6410	NNSS-SPE Line 5 site 05
L5-06	L5006	CLZ	37.2225	-116.0675	1.6190	NNSS-SPE Line 5 site 06
L5-07	L5007	CLZ	37.2227	-116.0686	1.6120	NNSS-SPE Line 5 site 07
L5-08	L5008	CLZ	37.2229	-116.0696	1.5890	NNSS-SPE Line 5 site 08
		CLR				
		CLT				
L5-09	L5009	CLZ	37.2231	-116.0707	1.5790	NNSS-SPE Line 5 site 09

Station Name	Station Header ID[a]	Channel	Estimated Latitude (degrees)	Estimated Longitude (degrees)	Estimated Elevation (km amsl)	Station Full Name
L5-10	L5010	CNZ	37.2233	-116.0718	1.5680	NNSS-SPE Line 5 site 10
		CNR				
		CNT				
		DJZ				
		DJR				
		DJT				
		CLZ				
L5-11	L5011	CLZ	37.2235	-116.0729	1.5660	NNSS-SPE Line 5 site 11
L5-12	L5012	CLZ	37.2237	-116.0740	1.5860	NNSS-SPE Line 5 site 12
		CLR				
		CLT				
L5-13	L5013	CLZ	37.2240	-116.0751	1.6120	NNSS-SPE Line 5 site 13
L5-14	L5014	CLZ	37.2242	-116.0762	1.6420	NNSS-SPE Line 5 site 14
L5-15	L5015	CLZ	37.2244	-116.0773	1.6780	NNSS-SPE Line 5 site 15
L5-16	L5016	DHZ	37.2246	-116.0784	1.7250	NNSS-SPE Line 5 site 16
		DHR				
		DHT				
L5-24	L5024	CHZ	37.2297	-116.1047	1.7670	NNSS-SPE Line 5 site 24
		CH1				
		CH2				
L5-26	L5026	CHZ	37.2319	-116.1156	1.8080	NNSS-SPE Line 5 site 26
		CH1				
		CH2				
L5-28	L5028	CHZ	37.2404	-116.1594	1.9110	NNSS-SPE Line 5 site 28
		CH1				
		CH2				
L5-30	L5030	CHZ	37.2490	-116.2032	2.0740	NNSS-SPE Line 5 site 30
		CH1				
		CH2				
L5-34	L5034	CHZ	37.2660	-116.2909	2.0770	NNSS-SPE Line 5 site 34
		CH1				
		CH2				
L5-36	L5036	CHZ	37.2745	-116.3347	2.1000	NNSS-SPE Line 5 site 36
		CH1				
		CH2				
A7-01	A7001	CDF_01	37.0996	-116.0416	1.2469	NNSS-SPE Area 7 Inf-N no.1
A7-02	A7002	CDF_02	37.0993	-116.0412	1.2476	NNSS-SPE Area 7 Inf-E no.2
A7-03	A7003	CDF_03	37.0989	-116.0417	1.2464	NNSS-SPE Area 7 Inf-S no.3
A7-04	A7004	CDF_04	37.0993	-116.0421	1.2455	NNSS-SPE Area 7 Inf-W no.4
A7-05	A7005	CDF_05	37.0993	-116.0416	1.2467	NNSS-SPE Area 7 Inf-C no.5
AX-01	AX001	CDF_01	37.1776	-116.0541	1.2842	NNSS-SPE Area 10 Sedan-N no.6
AX-02	AX002	CDF_02	37.1772	-116.0540	1.2840	NNSS-SPE Area 10 Sedan-SE no.7
AX-03	AX003	CDF_03	37.1773	-116.0544	1.2837	NNSS-SPE Area 10 Sedan-SW no.8
AX-04	AX004	CDF_01	37.2036	-116.0581	1.4004	NNSS-SPE Area 10 NMT-2K-N no.9
AX-05	AX005	CDF_02	37.2033	-116.0578	1.3934	NNSS-SPE Area 10 NMT-2K-E no.10
AX-06	AX006	CDF_03	37.2033	-116.0584	1.3993	NNSS-SPE Area 10 NMT-2K-W no.11
AF-01	AF001	CDF	37.2160	-116.1611	1.6371	NNSS-SPE AFTAC site 01
		CHZ				
		CHN				
		CHE				
AF-02	AF002	CDF	37.1640	-116.1423	1.4941	NNSS-SPE AFTAC site 02
		CHZ				
		CHN				
		CHE				

Appendix 6
Selected Metadata for SPE-2 Surface Stations

Station Name	Station Header ID[a]	Channel	Estimated Latitude (degrees)	Estimated Longitude (degrees)	Estimated Elevation (km amsl)	Station Full Name
AF-03	AF003	CDF	37.1313	-116.0573	1.2618	NNSS-SPE AFTAC site 03
		CHZ				
		CHN				
		CHE				
AF-04	AF004	CDF	37.1801	-115.9834	1.4370	NNSS-SPE AFTAC site 04
		CHZ				
		CHN				
		CHE				
AF-05	AF005	CDF	37.1894	-116.0204	1.3372	NNSS-SPE AFTAC site 05
		CHZ				
		CHN				
		CHE				
AF-06	AF006	CNZ	37.0531	-116.0903	1.2484	NNSS-SPE AFTAC site 06
		CNN				
		CNE				
AF-07	AF007	CDF	37.1239	-116.1478	1.4521	NNSS-SPE AFTAC site 07
		CHZ				
		CHN				
		CHE				
AF-08	AF008	CNZ	37.2211	-116.0496	1.4539	NNSS-SPE AFTAC site 08
		CNN				
		CNE				
		DHZ				
		DHN				
		DHE				
AF-09	AF009	CNZ	37.2299	-116.0577	1.5490	NNSS-SPE AFTAC site 09
		CNN				
		CNE				
		DHZ				
		DHN				
		DHE				
IS11	IS11	CDF_1	37.2235	-116.0614	1.5451	NNSS-SPE Sandia Inf 250 m N
IS12	IS12	CDF_2	37.2234	-116.0611	1.5419	NNSS-SPE Sandia Inf 233 m N
IS13	IS13	CDF_3	37.2232	-116.0609	1.5385	NNSS-SPE Sandia Inf 208 m N
IS14	IS14	CDF_4	37.2232	-116.0614	1.5451	NNSS-SPE Sandia Inf 218 m N
		CDF_5				
IS21	IS21	CDF_1	37.2193	-116.0604	1.5138	NNSS-SPE Sandia Inf 226 m S
IS22	IS22	CDF_2	37.2190	-116.0605	1.5163	NNSS-SPE Sandia Inf 251 m S
IS23	IS23	CDF_3	37.2189	-116.0603	1.5120	NNSS-SPE Sandia Inf 271 m S
IS24	IS24	CDF_4	37.2188	-116.0608	1.5182	NNSS-SPE Sandia Inf 270 m S
		CDF_5				
IS31	IS31	CDF_1	37.2219	-116.0635	1.5704	NNSS-SPE Sandia Inf 249 m W
IS32	IS32	CDF_2	37.2217	-116.0636	1.5659	NNSS-SPE Sandia Inf 251 m W
IS33	IS33	CDF_3	37.2215	-116.0634	1.5597	NNSS-SPE Sandia Inf 229 m W
IS34	IS34	CDF_4	37.2215	-116.0638	1.5627	NNSS-SPE Sandia Inf 261 m W
		CDF_5				
IS41	IS41	CDF_1	37.2235	-116.0579	1.5325	NNSS-SPE Sandia Inf 363 m E
IS42	IS42	CDF_2	37.2233	-116.0580	1.5315	NNSS-SPE Sandia Inf 339 m E
IS43	IS43	CDF_3	37.2232	-116.0576	1.5301	NNSS-SPE Sandia Inf 353 m E
IS44	IS44	CDF_4	37.2233	-116.0582	1.5301	NNSS-SPE Sandia Inf 320 m E
		CDF_5				
IS51	IS51	CDF_1	37.1776	-116.0541	1.3107	NNSS-SPE Sandia Inf 5 Km S
IS52	IS52	CDF_2	37.1773	-116.0542	1.3107	NNSS-SPE Sandia Inf 5 Km S
IS53	IS53	CDF_3	37.1771	-116.0540	1.3107	NNSS-SPE Sandia Inf 5 Km S

Appendix 6
Selected Metadata for SPE-2 Surface Stations

Station Name	Station Header ID[a]	Channel	Estimated Latitude (degrees)	Estimated Longitude (degrees)	Estimated Elevation (km amsl)	Station Full Name
IS54	IS54	CDF_4	37.1773	-116.0545	1.3106	NNSS-SPE Sandia Inf 5 Km S
		CDF_5				
IS61	IS61	CDF_1	37.2125	-116.0595	1.4833	NNSS-SPE Sandia Inf 1 Km S
IS62	IS62	CDF_2	37.2122	-116.0594	1.4826	NNSS-SPE Sandia Inf 1 Km S
IS63	IS63	CDF_3	37.2123	-116.0591	1.4809	NNSS-SPE Sandia Inf 1 Km S
IS64	IS64	CDF_4	37.2121	-116.0598	1.4821	NNSS-SPE Sandia Inf 1 Km S
		CDF_5				
IS71	IS71	CDF_1	37.2035	-116.0581	1.4267	NNSS-SPE Sandia Inf 2 Km S
IS72	IS72	CDF_2	37.2033	-116.0581	1.4253	NNSS-SPE Sandia Inf 2 Km S
IS73	IS73	CDF_3	37.2033	-116.0578	1.4201	NNSS-SPE Sandia Inf 2 Km S
IS74	IS74	CDF_4	37.2033	-116.0583	1.4261	NNSS-SPE Sandia Inf 2 Km S
		CDF_5				

NOTES

a. Station Header IDs of far-field stations have been changed with hyphens removed and replaced by zeros.   Station Header IDs of ne
   stations retain the hyphen, as they are being submitted as an assembled data set with it's own meta-data volume in CSS3.0

ABBREVIATIONS

km   kilometers
amsl   above mean sea level

Appendix 6
List of Known Poor Data Channels on Source Physics Experiment 2 Far-Field
(>100 m) Geophone Lines

Station	Channel	Potential Issue
Line 1		
L1-14	CLZ	No signal
L1-10	CNR,T	Orientation
Line 2		
L2-09	CLZ	No signal
L2-10	CNZ,R,T	No signal
L2-13	CLZ	No signal
Line 3		
L3-13	CLZ	Low amplitude
L3-10	DJR,H,T	No signal
L3-20	DHR	No signal
L3-23	CHZ,1,2	Low amplitude
L3-28	CHZ	No Signal
Line 4		
L4-07	CLZ	No signal
L4-26	CHZ	No signal
L4-28	CHZ	No signal
Line 5		
L5-01	CLZ	Clipped
L5-02	CLZ	Clipped
L5-03	CLZ	Clipped
L5-10	CNR,CNT	Orientations
L5-12	CLZ	No signal
L5-24	CHZ,1,2	No signal
L5-26	CH1,2	Orientation
L5-28	CH1,2	Orientation
L5-30	CH1,2	Orientation
L5-34	CH1,2	Orientation
L5-36	CH1,2	Orientation
AFTAC Sites		
AF-01	CHZ	No signal
AF-02	CHZ	No signal
AF-05	CHE	No signal
AF-06	CNZ,N,E	No signal

Appendix 7

Selected Metadata for SPE-3 Surface Stations

Appendix 7
Selected Metadata for SPE-3 Surface Stations

Station Name	Station Header ID[a]	Channel	Estimated Latitude (degrees)	Estimated Longitude (degrees)	Estimated Elevation (km amsl)	Station Full Name
Near Field						
DT-13	DT-13	GNZ	37.2215	-116.0608	1.5246	NNSS-SPE DTRA Surface A8 sp2 30m NE
DT-15	DT-15	GNZ	37.2208	-116.0611	1.5219	NNSS-SPE DTRA Surface A4 sp2 45m SW
DT-16	DT-16	GNZ	37.2207	-116.0612	1.5213	NNSS-SPE DTRA Surface A3 sp2 60m SW
DT-17	DT-17	GNZ	37.2206	-116.0612	1.5221	NNSS-SPE DTRA Surface A2 sp2 75m SW
DT-18	DT-18	GNZ	37.2205	-116.0613	1.5229	NNSS-SPE DTRA Surface A1 sp2 90m SW
DT-14	DT-14	GNZ / GNZ_sl	37.2213	-116.0612	1.5273	NNSS-SPE DTRA Surface A9 sp2 30m NW
SL-07	SL-07	GNZ	37.221	-116.061	1.5243	NNSS-SPE Sandia NL surface A5 sp2 30m SW
SL-08	SL-08	GNZ / GNZ_dt	37.2211	-116.0609	1.5244	NNSS-SPE Sandia NL surface A6 sp2 15m SW
SL-09	SL-09	GNZ	37.2213	-116.0608	1.5246	NNSS-SPE Sandia NL surface A7 sp2 15m NE
SL-10	SL-10	GNZ / GNZ_dt	37.2213	-116.061	1.5251	NNSS-SPE Sandia NL surface A10 sp2 15m NW
SL-11	SL-11	GNZ	37.2212	-116.0607	1.5244	NNSS-SPE Sandia NL surface A11 sp2 15m SE
SL-12	SL-12	GNZ	37.2211	-116.0606	1.5222	NNSS-SPE Sandia NL surface A12 30m SE
Far Field						
L1-01	L1001	CLZ / CLZ	37.2221	-116.0610	1.5290	NNSS-SPE Line 1 site 01
L1-02	L1002	CLZ / CLZ	37.2230	-116.0611	1.5370	NNSS-SPE Line 1 site 02
L1-03	L1003	CLZ / CLZ	37.2239	-116.0611	1.5400	NNSS-SPE Line 1 site 03
L1-04	L1004	CLZ / CLR / CLT / CLZ / CLR / CLT	37.2248	-116.0612	1.5370	NNSS-SPE Line 1 site 04
L1-05	L1005	CLZ / CLZ	37.2257	-116.0613	1.5500	NNSS-SPE Line 1 site 05
L1-06	L1006	CLZ / CLZ	37.2266	-116.0614	1.5580	NNSS-SPE Line 1 site 06
L1-07	L1007	CLZ / CLZ	37.2275	-116.0615	1.5590	NNSS-SPE Line 1 site 07
L1-08	L1008	CLZ / CLR / CLT / CLZ / CLR / CLT	37.2284	-116.0616	1.5720	NNSS-SPE Line 1 site 08
L1-09	L1009	CLZ / CLZ	37.2293	-116.0616	1.5890	NNSS-SPE Line 1 site 09
L1-10	L1010	CNZ / CNR / CNT / DJZ / DJR / DJT / CLZ / CLZ	37.2302	-116.0617	1.5850	NNSS-SPE Line 1 site 10
L1-11	L1011	CLZ / CLZ	37.2311	-116.0618	1.5970	NNSS-SPE Line 1 site 11

Appendix 7
Selected Metadata for SPE-3 Surface Stations

Station Name	Station Header ID[a]	Channel	Estimated Latitude (degrees)	Estimated Longitude (degrees)	Estimated Elevation (km amsl)	Station Full Name
L1-12	L1012	CLZ CLR CLT CLZ CLR CLT	37.2320	-116.0619	1.6040	NNSS-SPE Line 1 site 12
L1-13	L1013	CLZ CLZ	37.2329	-116.0620	1.6160	NNSS-SPE Line 1 site 13
L1-14	L1014	CLZ CLZ	37.2338	-116.0621	1.6330	NNSS-SPE Line 1 site 14
L1-15	L1015	CLZ CLZ	37.2347	-116.0621	1.6560	NNSS-SPE Line 1 site 15
L1-16	L1016	CLZ CLR CLT CLZ CLR CLT	37.2355	-116.0622	1.6740	NNSS-SPE Line 1 site 16
L1-17	L1017	CLZ CLZ	37.2364	-116.0623	1.7060	NNSS-SPE Line 1 site 17
L1-18	L1018	CLZ CLZ	37.2373	-116.0624	1.7390	NNSS-SPE Line 1 site 18
L1-19	L1019	CLZ CLZ	37.2382	-116.0625	1.7380	NNSS-SPE Line 1 site 19
L1-20	L1020	DHZ DHR DHT DHZ DHR DHT	37.2391	-116.0626	1.7520	NNSS-SPE Line 1 site 20
L2-01	L2001	CLZ CLZ	37.2218	-116.0600	1.5200	NNSS-SPE Line 2 site 01
L2-02	L2002	CLZ CLZ	37.2224	-116.0592	1.5150	NNSS-SPE Line 2 site 02
L2-03	L2003	CLZ CLZ	37.2229	-116.0583	1.5280	NNSS-SPE Line 2 site 03
L2-04	L2004	CLZ CLR CLT CLZ CLR CLT	37.2235	-116.0575	1.5280	NNSS-SPE Line 2 site 04
L2-05	L2005	CLZ CLZ	37.2241	-116.0566	1.5320	NNSS-SPE Line 2 site 05
L2-06	L2006	CLZ CLZ	37.2247	-116.0558	1.5310	NNSS-SPE Line 2 site 06
L2-07	L2007	CLZ CLZ	37.2253	-116.0549	1.5300	NNSS-SPE Line 2 site 07
L2-08	L2008	CLZ CLR CLT CLZ CLR CLT	37.2259	-116.0541	1.5300	NNSS-SPE Line 2 site 08

Appendix 7

Selected Metadata for SPE-3 Surface Stations

Station Name	Station Header ID[a]	Channel	Estimated Latitude (degrees)	Estimated Longitude (degrees)	Estimated Elevation (km amsl)	Station Full Name
L2-09	L2009	CLZ	37.2265	-116.0533	1.5370	NNSS-SPE Line 2 site 09
		CLZ				
L2-10	L2010	CNZ	37.2271	-116.0524	1.5310	NNSS-SPE Line 2 site 10
		CNR				
		CNT				
		CLZ_4				
		CLR_5				
		CLT_6				
		CLZ				
		CLZ				
L2-11	L2011	CLZ	37.2277	-116.0516	1.5370	NNSS-SPE Line 2 site 11
		CLZ				
L2-12	L2012	CLZ	37.2283	-116.0507	1.5370	NNSS-SPE Line 2 site 12
		CLR				
		CLT				
		CLZ				
		CLR				
		CLT				
L2-13	L2013	CLZ	37.2289	-116.0499	1.5360	NNSS-SPE Line 2 site 13
		CLZ				
L2-14	L2014	CLZ	37.2295	-116.0490	1.5410	NNSS-SPE Line 2 site 14
		CLZ				
L2-15	L2015	CLZ	37.2301	-116.0482	1.5430	NNSS-SPE Line 2 site 15
		CLZ				
L2-16	L2016	CLZ	37.2307	-116.0473	1.5360	NNSS-SPE Line 2 site 16
		CLR				
		CLT				
		CLZ				
		CLR				
		CLT				
L2-17	L2017	CLZ	37.2312	-116.0465	1.5490	NNSS-SPE Line 2 site 17
		CLZ				
L2-18	L2018	CLZ	37.2318	-116.0456	1.5480	NNSS-SPE Line 2 site 18
		CLZ				
L2-19	L2019	CLZ	37.2324	-116.0448	1.5520	NNSS-SPE Line 2 site 19
		CLZ				
L2-20	L2020	DHZ	37.2330	-116.0439	1.5330	NNSS-SPE Line 2 site 20
		DHR				
		DHT				
		DHZ				
		DHR				
		DHT				
L3-01	L3001	CLZ	37.2203	-116.0607	1.5160	NNSS-SPE Line 3 site 01
		CLZ				
L3-02	L3002	CLZ	37.2194	-116.0606	1.5120	NNSS-SPE Line 3 site 02
		CLZ				
L3-03	L3003	CLZ	37.2185	-116.0605	1.5120	NNSS-SPE Line 3 site 03
		CLZ				
L3-04	L3004	CLZ	37.2176	-116.0603	1.4960	NNSS-SPE Line 3 site 04
		CLR				
		CLT				
		CLZ				
		CLR				
		CLT				

Appendix 7
Selected Metadata for SPE-3 Surface Stations

Station Name	Station Header ID[a]	Channel	Estimated Latitude (degrees)	Estimated Longitude (degrees)	Estimated Elevation (km amsl)	Station Full Name
L3-05	L3005	CLZ	37.2167	-116.0602	1.4960	NNSS-SPE Line 3 site 05
		CLZ				
L3-06	L3006	CLZ	37.2158	-116.0600	1.4940	NNSS-SPE Line 3 site 06
		CLZ				
L3-07	L3007	CLZ	37.2149	-116.0599	1.4870	NNSS-SPE Line 3 site 07
		CLZ				
L3-08	L3008	CLZ	37.2140	-116.0598	1.4840	NNSS-SPE Line 3 site 08
		CLR				
		CLT				
		CLZ				
		CLR				
		CLT				
L3-09	L3009	CLZ	37.2131	-116.0596	1.4690	NNSS-SPE Line 3 site 09
		CLZ				
L3-10	L3010	CLZ	37.2122	-116.0595	1.4810	NNSS-SPE Line 3 site 10
		CLZ				
L3-11	L3011	CLZ	37.2113	-116.0593	1.4750	NNSS-SPE Line 3 site 11
		CLZ				
L3-12	L3012	CLZ	37.2104	-116.0592	1.4640	NNSS-SPE Line 3 site 12
		CLR				
		CLT				
		CLZ				
		CLR				
		CLT				
L3-13	L3013	CLZ	37.2095	-116.0591	1.4590	NNSS-SPE Line 3 site 13
		CLZ				
L3-14	L3014	CLZ	37.2087	-116.0589	1.4630	NNSS-SPE Line 3 site 14
		CLZ				
L3-15	L3015	CLZ	37.2078	-116.0588	1.4530	NNSS-SPE Line 3 site 15
		CLZ				
L3-16	L3016	CLZ	37.2069	-116.0586	1.4370	NNSS-SPE Line 3 site 16
		CLR				
		CLT				
		CLZ				
		CLR				
		CLT				
L3-17	L3017	CLZ	37.2060	-116.0585	1.4310	NNSS-SPE Line 3 site 17
		CLZ				
L3-18	L3018	CLZ	37.2051	-116.0584	1.4340	NNSS-SPE Line 3 site 18
		CLZ				
L3-19	L3019	CLZ	37.2042	-116.0582	1.4280	NNSS-SPE Line 3 site 19
		CLZ				
L3-20	L3020	DHZ	37.2033	-116.0581	1.4230	NNSS-SPE Line 3 site 20
		DHR				
		DHT				
		DHZ				
		DHR				
		DHT				
L3-23	L3023	CHZ	37.1899	-116.0560	1.3450	NNSS-SPE Line 3 site 23
		CH1				
		CH2				
		CHZ				
		CH1				
		CH2				

Station Name	Station Header ID[a]	Channel	Estimated Latitude (degrees)	Estimated Longitude (degrees)	Estimated Elevation (km amsl)	Station Full Name
L3-26	L3026	CHZ	37.1770	-116.0539	1.3100	NNSS-SPE Line 3 site 26
		CH1				
		CH2				
		CHZ				
		CH1				
		CH2				
L3-28	L3028	CHZ	37.1407	-116.0482	1.2850	NNSS-SPE Line 3 site 28
		CH1				
		CH2				
L3-30	L3030	CHZ	37.1049	-116.0426	1.2740	NNSS-SPE Line 3 site 30
		CH1				
		CH2				
L3-32	L3032	CHZ	37.0697	-116.0370	1.2360	NNSS-SPE Line 3 site 32
		CH1				
		CH2				
L3-34	L3034	CHZ	37.0330	-116.0314	1.2180	NNSS-SPE Line 3 site 34
		CH1				
		CH2				
L3-36	L3036	CHZ	36.9976	-116.0258	1.2040	NNSS-SPE Line 3 site 36
		CH1				
		CH2				
L4-01	L4001	CLZ	37.2204	-116.0614	1.5230	NNSS-SPE Line 4 site 01
		CLZ				
L4-02	L4002	CLZ	37.2195	-116.0619	1.5210	NNSS-SPE Line 4 site 02
		CLZ				
L4-03	L4003	CLZ	37.2187	-116.0624	1.5320	NNSS-SPE Line 4 site 03
		CLZ				
L4-04	L4004	CLZ	37.2179	-116.0629	1.5230	NNSS-SPE Line 4 site 04
		CLR				
		CLT				
		CLZ				
		CLR				
		CLT				
L4-05	L4005	CLZ	37.2171	-116.0634	1.5020	NNSS-SPE Line 4 site 05
		CLZ				
L4-06	L4006	CLZ	37.2163	-116.0639	1.4990	NNSS-SPE Line 4 site 06
		CLZ				
L4-07	L4007	CLZ	37.2155	-116.0643	1.5130	NNSS-SPE Line 4 site 07
		CLZ				
L4-08	L4008	CLZ	37.2147	-116.0648	1.5050	NNSS-SPE Line 4 site 08
		CLR				
		CLT				
		CLZ				
		CLR				
		CLT				
L4-09	L4009	CLZ	37.2139	-116.0653	1.5070	NNSS-SPE Line 4 site 09
		CLZ				
L4-10	L4010	CLZ	37.2131	-116.0658	1.5040	NNSS-SPE Line 4 site 10
		CLZ				
L4-11	L4011	CLZ	37.2123	-116.0663	1.5080	NNSS-SPE Line 4 site 11
		CLZ				

Appendix 7
Selected Metadata for SPE-3 Surface Stations

Station Name	Station Header ID[a]	Channel	Estimated Latitude (degrees)	Estimated Longitude (degrees)	Estimated Elevation (km amsl)	Station Full Name
L4-12	L4012	CLZ	37.2114	-116.0668	1.5110	NNSS-SPE Line 4 site 12
		CLR				
		CLT				
		CLZ				
		CLR				
		CLT				
L4-13	L4013	CLZ	37.2106	-116.0673	1.5120	NNSS-SPE Line 4 site 13
		CLZ				
L4-14	L4014	CLZ	37.2098	-116.0678	1.5110	NNSS-SPE Line 4 site 14
		CLZ				
L4-15	L4015	CLZ	37.2090	-116.0683	1.5140	NNSS-SPE Line 4 site 15
		CLZ				
L4-16	L4016	CLZ	37.2082	-116.0688	1.5140	NNSS-SPE Line 4 site 16
		CLR				
		CLT				
		CLZ				
		CLR				
		CLT				
L4-17	L4017	CLZ	37.2074	-116.0693	1.5120	NNSS-SPE Line 4 site 17
		CLZ				
L4-18	L4018	CLZ	37.2066	-116.0698	1.5080	NNSS-SPE Line 4 site 18
		CLZ				
L4-19	L4019	CLZ	37.2058	-116.0703	1.5130	NNSS-SPE Line 4 site 19
		CLZ				
L4-20	L4020	DHZ	37.2050	-116.0708	1.5070	NNSS-SPE Line 4 site 20
		DHR				
		DHT				
		DHZ				
		DHR				
		DHT				
L4-23	L4023	CHZ	37.1928	-116.0782	1.4400	NNSS-SPE Line 4 site 23
		CH1				
		CH2				
L4-26	L4026	CHZ	37.1807	-116.0856	1.3800	NNSS-SPE Line 4 site 26
		CH1				
		CH2				
L4-28	L4028	CHZ	37.1483	-116.1053	1.3550	NNSS-SPE Line 4 site 28
		CH1				
		CH2				
L4-30	L4030	CHZ	37.1159	-116.1250	1.3780	NNSS-SPE Line 4 site 30
		CH1				
		CH2				
L4-32	L4032	CHZ	37.0835	-116.1447	1.4210	NNSS-SPE Line 4 site 32
		CH1				
		CH2				
L4-34	L4034	CHZ	37.0510	-116.1644	1.5680	NNSS-SPE Line 4 site 34
		CH1				
		CH2				
L4-36	L4036	CHZ	37.0186	-116.1841	1.5270	NNSS-SPE Line 4 site 36
		CH1				
		CH2				
L5-01	L5001	CLZ	37.2214	-116.0620	1.5390	NNSS-SPE Line 5 site 01
L5-02	L5002	CLZ	37.2216	-116.0631	1.5560	NNSS-SPE Line 5 site 02
L5-03	L5003	CLZ	37.2218	-116.0642	1.5770	NNSS-SPE Line 5 site 03

Station Name	Station Header ID[a]	Channel	Estimated Latitude (degrees)	Estimated Longitude (degrees)	Estimated Elevation (km amsl)	Station Full Name
L5-04	L5004	CLZ	37.2220	-116.0653	1.6220	NNSS-SPE Line 5 site 04
		CLR				
		CLT				
L5-05	L5005	CLZ	37.2222	-116.0664	1.6410	NNSS-SPE Line 5 site 05
		CLZ				
L5-06	L5006	CLZ	37.2225	-116.0675	1.6190	NNSS-SPE Line 5 site 06
		CLZ				
L5-07	L5007	CLZ	37.2227	-116.0686	1.6120	NNSS-SPE Line 5 site 07
		CLZ				
L5-08	L5008	CLZ	37.2229	-116.0696	1.5890	NNSS-SPE Line 5 site 08
		CLR				
		CLT				
		CLZ				
		CLR				
		CLT				
L5-09	L5009	CLZ	37.2231	-116.0707	1.5790	NNSS-SPE Line 5 site 09
		CLZ				
L5-10	L5010	CNZ	37.2233	-116.0718	1.5680	NNSS-SPE Line 5 site 10
		CNR				
		CNT				
		DJZ				
		DJR				
		DJT				
		CLZ				
		CLZ				
L5-11	L5011	CLZ	37.2235	-116.0729	1.5660	NNSS-SPE Line 5 site 11
		CLZ				
L5-12	L5012	CLZ	37.2237	-116.0740	1.5860	NNSS-SPE Line 5 site 12
		CLR				
		CLT				
		CLZ				
		CLR				
		CLT				
L5-13	L5013	CLZ	37.2240	-116.0751	1.6120	NNSS-SPE Line 5 site 13
L5-14	L5014	CLZ	37.2242	-116.0762	1.6420	NNSS-SPE Line 5 site 14
L5-15	L5015	CLZ	37.2244	-116.0773	1.6780	NNSS-SPE Line 5 site 15
L5-16	L5016	DHZ	37.2246	-116.0784	1.7250	NNSS-SPE Line 5 site 16
		DHR				
		DHT				
L5-24	L5024	CHZ	37.2297	-116.1047	1.7670	NNSS-SPE Line 5 site 24
		CH1				
		CH2				
L5-26	L5026	CHZ	37.2319	-116.1156	1.8080	NNSS-SPE Line 5 site 26
		CH1				
		CH2				
L5-28	L5028	CHZ	37.2404	-116.1594	1.9110	NNSS-SPE Line 5 site 28
		CH1				
		CH2				
L5-30	L5030	CHZ	37.2490	-116.2032	2.0740	NNSS-SPE Line 5 site 30
		CH1				
		CH2				
L5-34	L5034	CHZ	37.2660	-116.2909	2.0770	NNSS-SPE Line 5 site 34
		CH1				
		CH2				

Appendix 7
Selected Metadata for SPE-3 Surface Stations

Station Name	Station Header ID[a]	Channel	Estimated Latitude (degrees)	Estimated Longitude (degrees)	Estimated Elevation (km amsl)	Station Full Name
L5-36	L5036	CHZ	37.2745	-116.3347	2.1000	NNSS-SPE Line 5 site 36
		CH1				
		CH2				
A7-01	A7001	CDF_01	37.0996	-116.0416	1.2469	NNSS-SPE Area 7 Inf-N no.1
A7-02	A7002	CDF_02	37.0993	-116.0412	1.2476	NNSS-SPE Area 7 Inf-E no.2
A7-03	A7003	CDF_03	37.0989	-116.0417	1.2464	NNSS-SPE Area 7 Inf-S no.3
A7-04	A7004	CDF_04	37.0993	-116.0421	1.2455	NNSS-SPE Area 7 Inf-W no.4
A7-05	A7005	CDF_05	37.0993	-116.0416	1.2467	NNSS-SPE Area 7 Inf-C no.5
AS-01	AS001	CLZ_1	37.2203	-116.0490	1.4467	NNSS-SPE SP3 Asymmetric Array site 01
AS-02	AS002	CLZ_2	37.2212	-116.0487	1.4503	NNSS-SPE SP3 Asymmetric Array site 02
AS-03	AS003	CLZ_3	37.2201	-116.0481	1.4414	NNSS-SPE SP3 Asymmetric Array site 03
AS-04	AS004	CLZ_4	37.2194	-116.0490	1.4414	NNSS-SPE SP3 Asymmetric Array site 04
AS-05	AS005	CLZ_5	37.2204	-116.0500	1.4507	NNSS-SPE SP3 Asymmetric Array site 05
AS-06	AS006	CLZ_6	37.2210	-116.0496	1.4531	NNSS-SPE SP3 Asymmetric Array site 06
AX-01	AX001	CDF_01	37.1776	-116.0541	1.2842	NNSS-SPE Area 10 Sedan-N no.6
AX-02	AX002	CDF_02	37.1772	-116.0540	1.2840	NNSS-SPE Area 10 Sedan-SE no.7
AX-03	AX003	CDF_03	37.1773	-116.0544	1.2837	NNSS-SPE Area 10 Sedan-SW no.8
AX-04	AX004	CDF_01	37.2036	-116.0581	1.4004	NNSS-SPE Area 10 NMT-2K-N no.9
AX-05	AX005	CDF_02	37.2033	-116.0578	1.3934	NNSS-SPE Area 10 NMT-2K-E no.10
AX-06	AX006	CDF_03	37.2033	-116.0584	1.3993	NNSS-SPE Area 10 NMT-2K-W no.11
EM-01	EM001	CFZ_01	37.2210	-116.0610	1.4992	NNSS-SPE LLNL EMP 30m SP3
		CFR_02				
		CFT_03				
EM-02	EM002	CFZ_04	37.2207	-116.0611	1.4960	NNSS-SPE LLNL EMP 60m SP3
		CFR_05				
		CFT_06				
AF-01	AF001	CDF	37.2160	-116.1611	1.6371	NNSS-SPE AFTAC site 01
		CHZ				
		CHN				
		CHE				
AF-02	AF002	CDF	37.1640	-116.1423	1.4941	NNSS-SPE AFTAC site 02
		CHZ				
		CHN				
		CHE				
AF-03	AF003	CDF	37.1313	-116.0573	1.2618	NNSS-SPE AFTAC site 03
		CHZ				
		CHN				
		CHE				
AF-04	AF004	CDF	37.1801	-115.9834	1.4370	NNSS-SPE AFTAC site 04
		CHZ				
		CHN				
		CHE				
AF-05	AF005	CDF	37.1894	-116.0204	1.3372	NNSS-SPE AFTAC site 05
		CHZ				
		CHN				
		CHE				
AF-06	AF006	CNZ	37.0531	-116.0903	1.2484	NNSS-SPE AFTAC site 06
		CNN				
		CNE				
AF-07	AF007	CDF	37.1239	-116.1478	1.4521	NNSS-SPE AFTAC site 07
		CHZ				
		CHN				
		CHE				

Station Name	Station Header ID[a]	Channel	Estimated Latitude (degrees)	Estimated Longitude (degrees)	Estimated Elevation (km amsl)	Station Full Name
AF-08	AF008	CNZ	37.2211	-116.0496	1.4539	NNSS-SPE AFTAC site 08
		CNN				
		CNE				
		DHZ				
		DHN				
		DHE				
AF-09	AF009	CNZ	37.2299	-116.0577	1.5490	NNSS-SPE AFTAC site 09
		CNN				
		CNE				
		DHZ				
		DHN				
		DHE				
IS11	IS11	CDF_1	37.2235	-116.0614	1.5451	NNSS-SPE Sandia Inf 250 m N
IS12	IS12	CDF_2	37.2234	-116.0611	1.5419	NNSS-SPE Sandia Inf 233 m N
IS13	IS13	CDF_3	37.2232	-116.0609	1.5385	NNSS-SPE Sandia Inf 208 m N
IS14	IS14	CDF_4	37.2232	-116.0614	1.5451	NNSS-SPE Sandia Inf 218 m N
IS21	IS21	CDF_1	37.2193	-116.0604	1.5138	NNSS-SPE Sandia Inf 226 m S
IS22	IS22	CDF_2	37.2190	-116.0605	1.5163	NNSS-SPE Sandia Inf 251 m S
IS23	IS23	CDF_3	37.2189	-116.0603	1.5120	NNSS-SPE Sandia Inf 271 m S
IS24	IS24	CDF_4	37.2188	-116.0608	1.5182	NNSS-SPE Sandia Inf 270 m S
IS31	IS31	CDF_1	37.2219	-116.0635	1.5704	NNSS-SPE Sandia Inf 249 m W
IS32	IS32	CDF_2	37.2217	-116.0636	1.5659	NNSS-SPE Sandia Inf 251 m W
IS33	IS33	CDF_3	37.2215	-116.0634	1.5597	NNSS-SPE Sandia Inf 229 m W
IS34	IS34	CDF_4	37.2215	-116.0638	1.5627	NNSS-SPE Sandia Inf 261 m W
IS41	IS41	CDF_1	37.2235	-116.0579	1.5325	NNSS-SPE Sandia Inf 363 m E
IS42	IS42	CDF_2	37.2233	-116.0580	1.5315	NNSS-SPE Sandia Inf 339 m E
IS43	IS43	CDF_3	37.2232	-116.0576	1.5301	NNSS-SPE Sandia Inf 353 m E
IS44	IS44	CDF_4	37.2233	-116.0582	1.5301	NNSS-SPE Sandia Inf 320 m E
IS51	IS51	CDF_1	37.1776	-116.0541	1.3107	NNSS-SPE Sandia Inf 5 Km S
IS52	IS52	CDF_2	37.1773	-116.0542	1.3107	NNSS-SPE Sandia Inf 5 Km S
IS53	IS53	CDF_3	37.1771	-116.0540	1.3107	NNSS-SPE Sandia Inf 5 Km S
IS54	IS54	CDF_4	37.1773	-116.0545	1.3106	NNSS-SPE Sandia Inf 5 Km S
IS61	IS61	CDF_1	37.2125	-116.0595	1.4833	NNSS-SPE Sandia Inf 1 Km S
IS62	IS62	CDF_2	37.2122	-116.0594	1.4826	NNSS-SPE Sandia Inf 1 Km S
IS63	IS63	CDF_3	37.2123	-116.0591	1.4809	NNSS-SPE Sandia Inf 1 Km S
IS64	IS64	CDF_4	37.2121	-116.0598	1.4821	NNSS-SPE Sandia Inf 1 Km S
IS71	IS71	CDF_1	37.2035	-116.0581	1.4267	NNSS-SPE Sandia Inf 2 Km S
IS72	IS72	CDF_2	37.2033	-116.0581	1.4253	NNSS-SPE Sandia Inf 2 Km S
IS73	IS73	CDF_3	37.2033	-116.0578	1.4201	NNSS-SPE Sandia Inf 2 Km S
IS74	IS74	CDF_4	37.2033	-116.0583	1.4261	NNSS-SPE Sandia Inf 2 Km S
IS81	IS81	CDF_1	37.2212	-116.0494	1.4803	NNSS-SPE Sandia Inf 1 Km E
IS82	IS82	CDF_2	37.2210	-116.0494	1.4787	NNSS-SPE Sandia Inf 1 Km E
IS83	IS83	CDF_3	37.2208	-116.0491	1.4766	NNSS-SPE Sandia Inf 1 Km E
IS84	IS84	CDF_4	37.2209	-116.0497	1.4787	NNSS-SPE Sandia Inf 1 Km E

NOTES

a. Station Header IDs of far-field stations have been changed with hyphens removed and replaced by zeros.   Station Header IDs of ne
    stations retain the hyphen, as they are being submitted as an assembled data set with it's own meta-data volume in CSS3.0

ABBREVIATIONS

km   kilometers
amsl   above mean sea level

Appendix 7
List of Known Poor Data Channels on Source Physics Experiment 3 Far-Field (>100 m) Geophone Lines

Station	Channel	Potential Issue
Line 1		
L1-17	CLZ	Low amplitude
L1-18	CLZ	Low amplitude
L1-19	CLZ	Low amplitude
Line 2		
L2-01	CLZ	No signal
L2-03	CLZ	No signal
L2-09	CLZ	No signal
L2-10	CNZ,R,T	No signal
L2-13	CLZ	Low amplitude
L2-14	CLZ	Low amplitude
Line 3		
L3-03	CLZ	No signal
L3-20	DHR	No signal
L3-28	CHZ, 1,2	Low amplitude
Line 4		
L4-07	CLZ	No signal
Line 5		
L5-09	CLZ	No signal
L5-12	CLZ	No signal
L5-24	CH2	No signal
L5-26	CH1	Orientation
L5-28	CH2	No signal
L5-30	CH1,2	Orientation
L5-34	CH1,2	Orientation
L5-36	CH1,2	Orientation
AFTAC Sites		
AF-01	CHZ,N,E	No data
AF-03	CHN	Low amplitude
AF-05	CHE	Low amplitude
AF-07	CHZ,CHE	No signal

Appendix 8

SPE-1 Baseline Shift Corrections
LA-UR-13-23956

Prepared by E. Rougier and D. Steedman
Los Alamos National Laboratory

Title: SPE-1 BASELINE SHIFT CORRECTIONS

Author(s):   Rougier, Esteban
                Steedman, David W.

Intended for: Report

Issued: 2013-05-30 (Draft)

SPE-1 BASELINE SHIFT CORRECTIONS

E. Rougier and D. W. Steedman
Geophysics Group, Los Alamos National Laboratory

Acknowledgements

Disclaimer

The baseline shift corrections presented in this report have been made following a set of practices considered by the authors to be appropriate. This report is intended to document those corrections which were made to support subsequent analyses by the authors.

1. BASELINE SHIFT CORRECTION PROCESS

The acceleration data obtained from the free-field accelerometers nominally located at the 10-m and 20-m range from ground zero (GZ) require baseline shift correction prior to analysis (*e.g.,* comparison with hydrodynamic calculation results, seismic-related analysis, *etc*.).

We used as our starting point the accelerometer data that were corrected in the manner of References 1 and 2 for gauge rotations that were described by Reference 3. These records are referred to herein as a^{orig}.

The baseline shift corrections presented in this work were made in two main stages:

- Correction for pre-arrival baseline shift.
- Correction for post-arrival baseline shift.

1.1. Correction for pre-arrival baseline shift

A typical accelerometer record will display a DC shift caused by electronic drift in the measurement and recording system. This appears as a constant offset from the expected pre-shock 0. acceleration. The cumulative offset during integration for velocity renders the data useless and must be corrected to achieve accurate portrayal of the velocity positive phase. To compensate, the pre-arrival baseline

shift acceleration was computed from the data and then subtracted from all points in the record. For each of the components of the acceleration the correction was made as shown in equation (1).

$$a^{pre} = a^{orig} + a^{c-pre} \qquad (1)$$

where $a^{c\text{-}pre}$ is the pre-arrival acceleration baseline shift correction and a^{pre} is the acceleration record corrected by this pre-arrival shift.

1.2. Correction for post-arrival baseline shift

A second shift occurs in many accelerometer records as the explosive wave shocks the instruments. This phenomenon has little noticeable effect on the outward phase velocity (either peak or duration) and is often neglected. However, some analysis (e.g., Ref. 4) is based on displacement records and this analysis is greatly facilitated by accomplishing a second correction for this post-shock shift. This second correction was made in the velocity domain. In other words, the acceleration data were integrated with respect to time in order to obtain the velocity waveforms. The time interval considered in this analysis goes from 0.0s (shot time) to 0.1s. Each component of the velocity waveforms was corrected so that the waveform reaches a condition as close as possible to steady state; *i.e.,* zero velocity as shown in Figure 1. The correction on the acceleration was derived from the correction on the velocity by performing a simple derivation. The final acceleration records for each component were obtained by adding the post-arrival correction on the acceleration to the pre-arrival corrected acceleration, as shown in equation (2).

$$a^{final} = a^{pre} + a^{c-post} \qquad (2)$$

where a^{final} is the final (corrected) acceleration record, a^{pre} is obtained from equation (1) and $a^{c\text{-}post}$ is the post-arrival acceleration baseline shift.
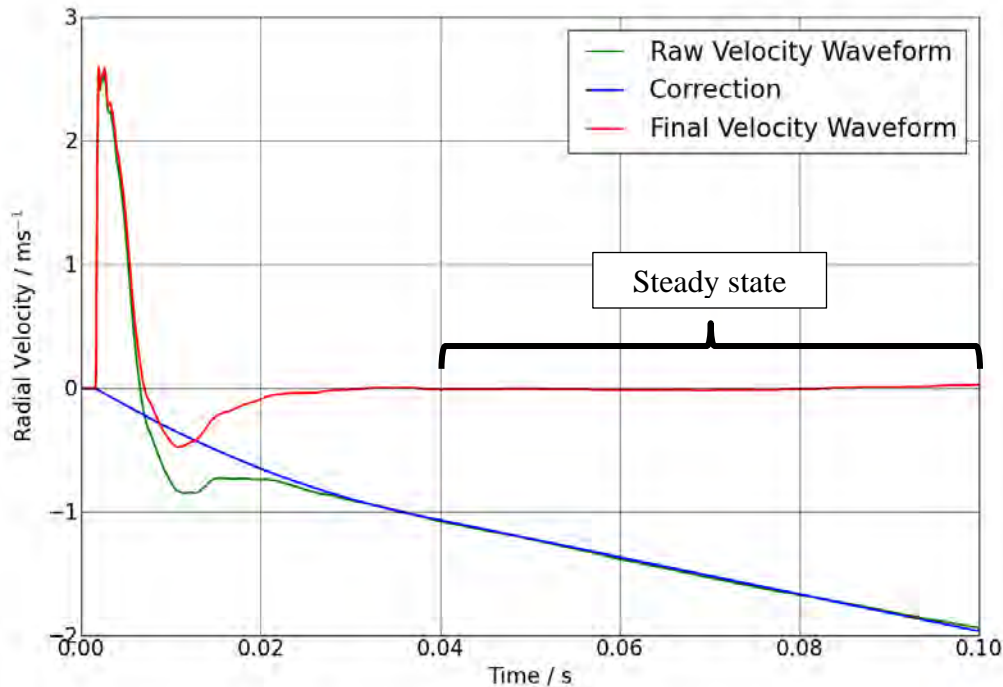
Figure 1. Example of velocity correction.

2.   FIGURES

In this section we present the velocity and displacement waveforms for the three components of the corrected data. The affected data records are listed in the following table.

Depth	Component	Borehole #					
		1	2	3	4	5	6
1 (180 ft)	R	✓	✓		✓		✓
	T	✓	✓		✓		✓
	L		✓		✓		✓
2 (150 ft)	R		✓	✓	✓		✓
	T		✓	✓	✓		✓
	L		✓	✓	✓		✓
3 (50 ft)	R	✓	✓	✓	✓	✓	✓
	T	✓	✓	✓	✓	✓	✓
	L	✓	✓	✓	✓	✓	✓

2.1.   Records corrected for pre-arrival baseline shift

The key to the legend in the graphs presented in this section is the following:

- v^{orig} represents the velocity waveform obtained by integrating the accelerometer data that were corrected in the manner of References 1 and 2 to for gauge rotations that were described by Reference 3.
- $v^{c\text{-}pre}$ represents the pre-arrival baseline shift acceleration correction in the velocity space.
- v^{pre} represents the velocity waveforms corrected for the pre-arrival baseline shift.
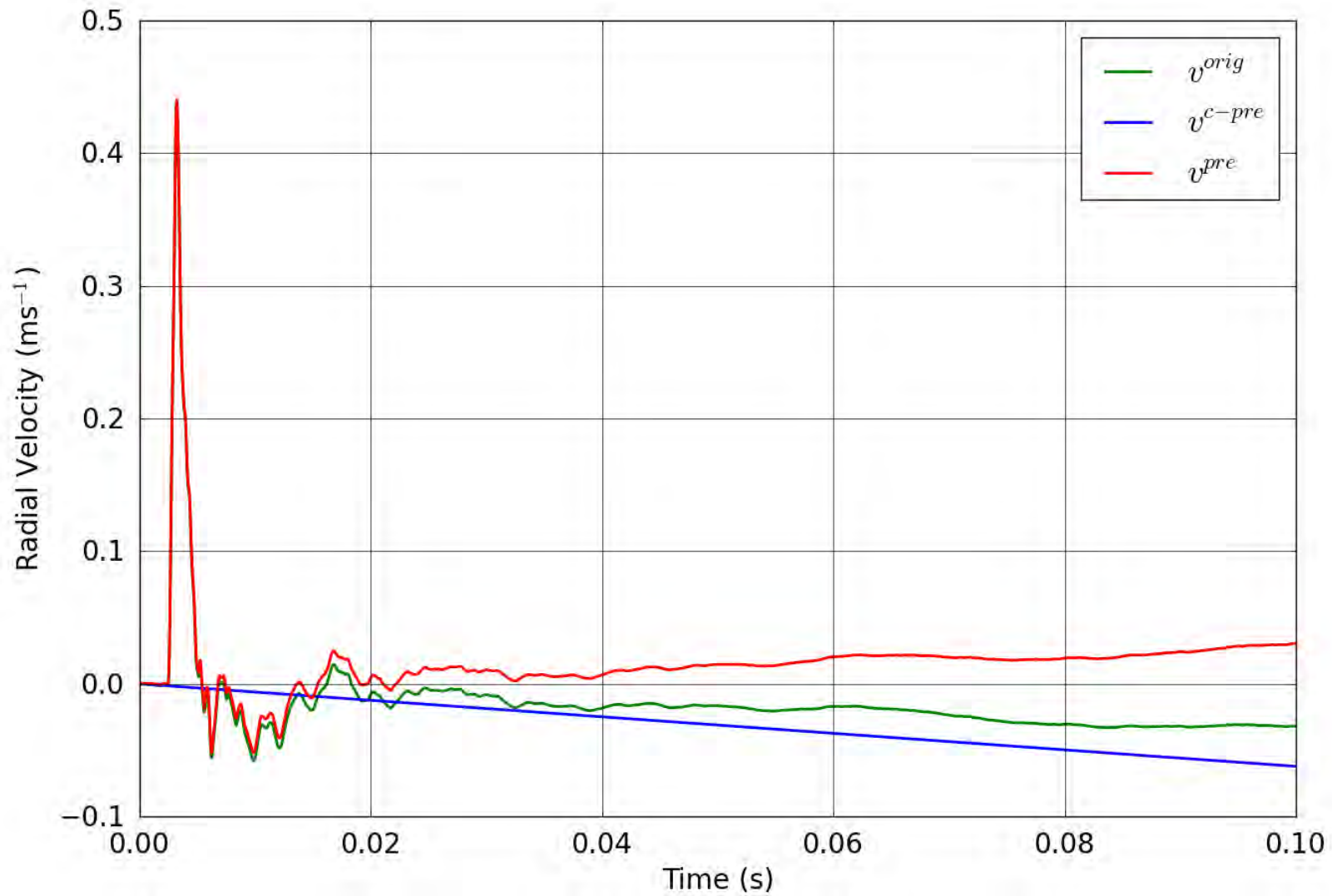
Figure 2. SPE-1 Gauge 1-1-R – Pre-shot baseline correction of the radial velocity.
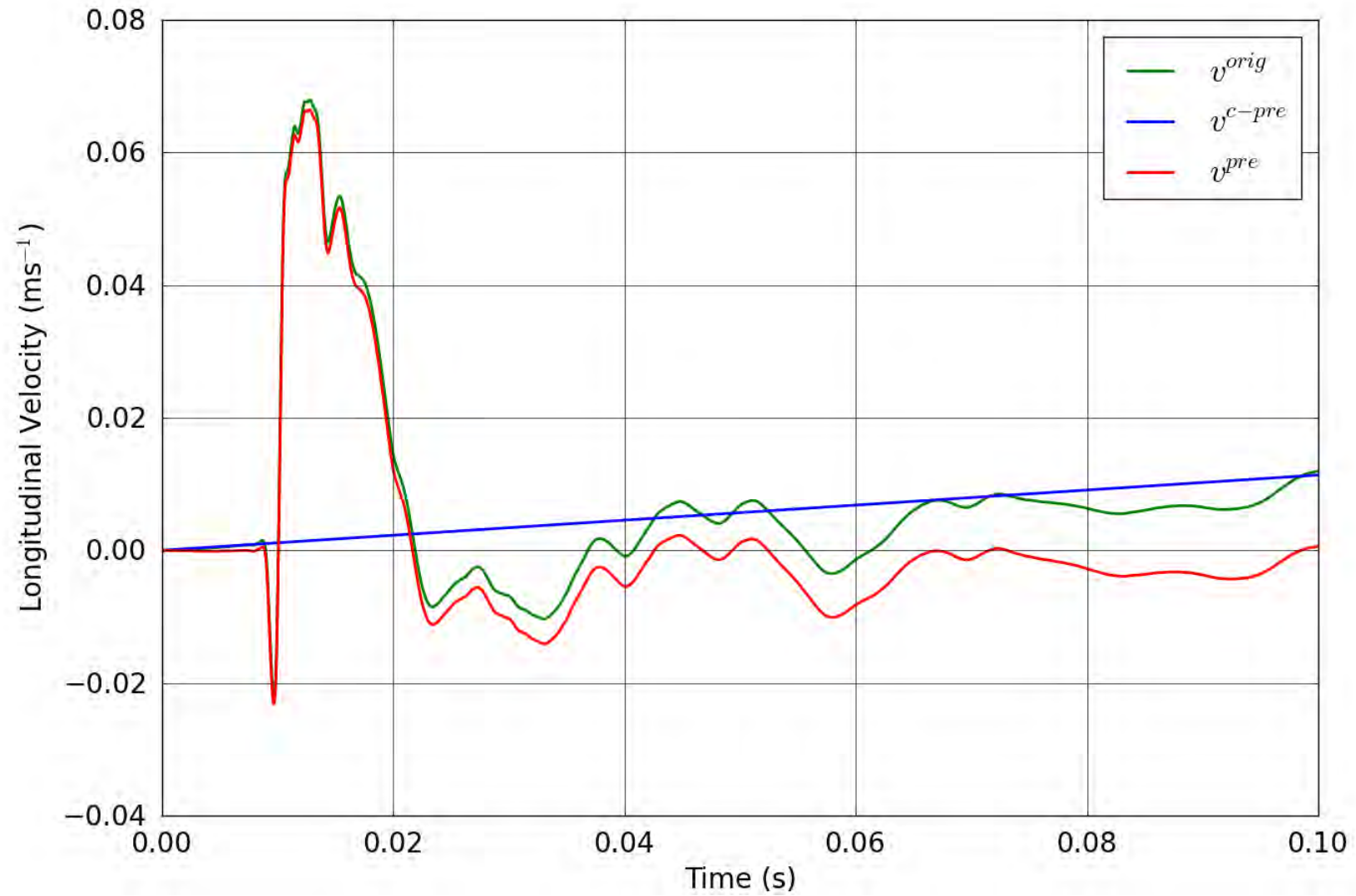
Figure 3. SPE-1 Gauge 1-3-L – Pre-shot baseline correction of the longitudinal velocity.
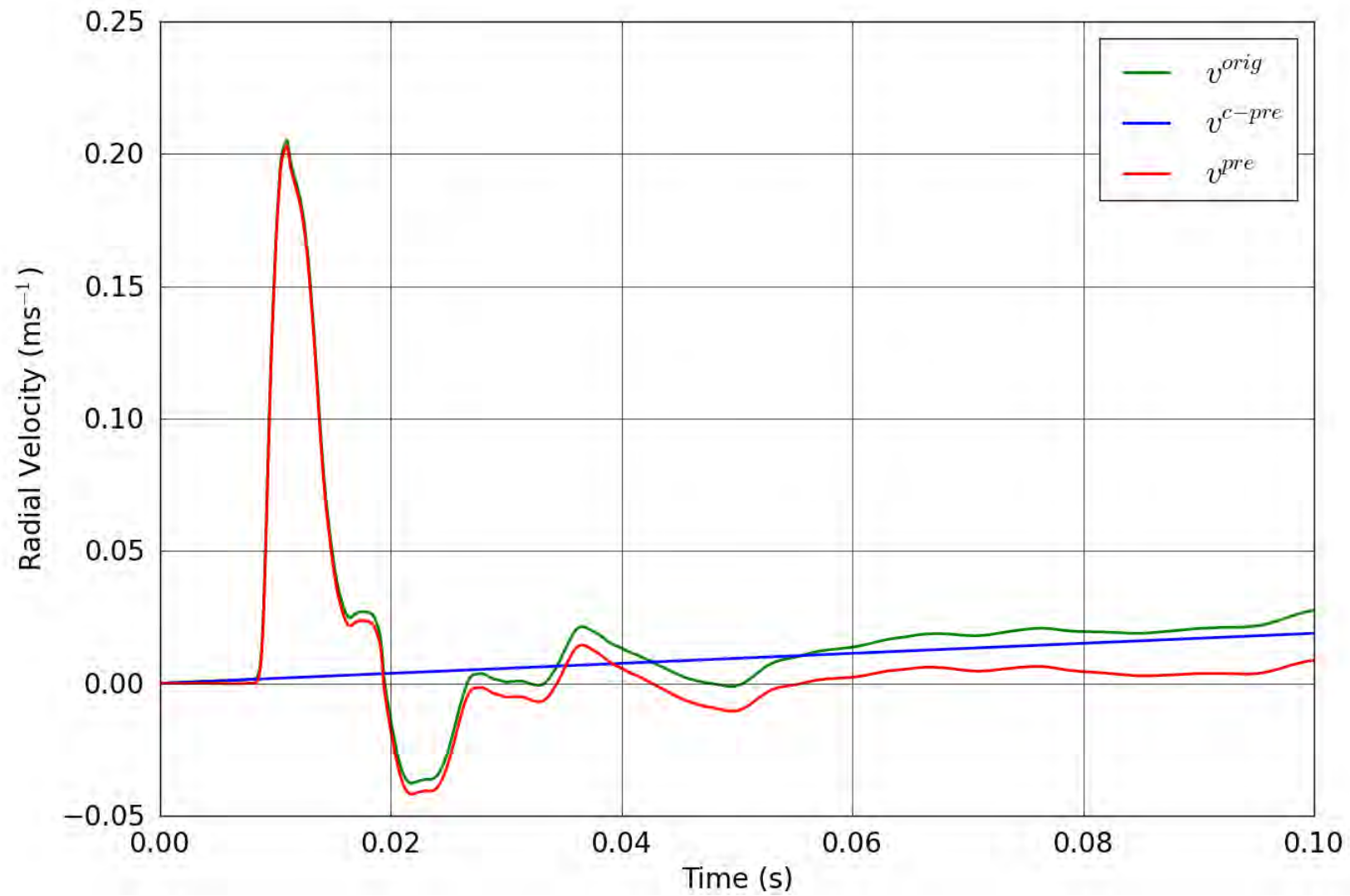
Figure 4. SPE-1 Gauge 1-3-R – Pre-shot baseline correction of the radial velocity.
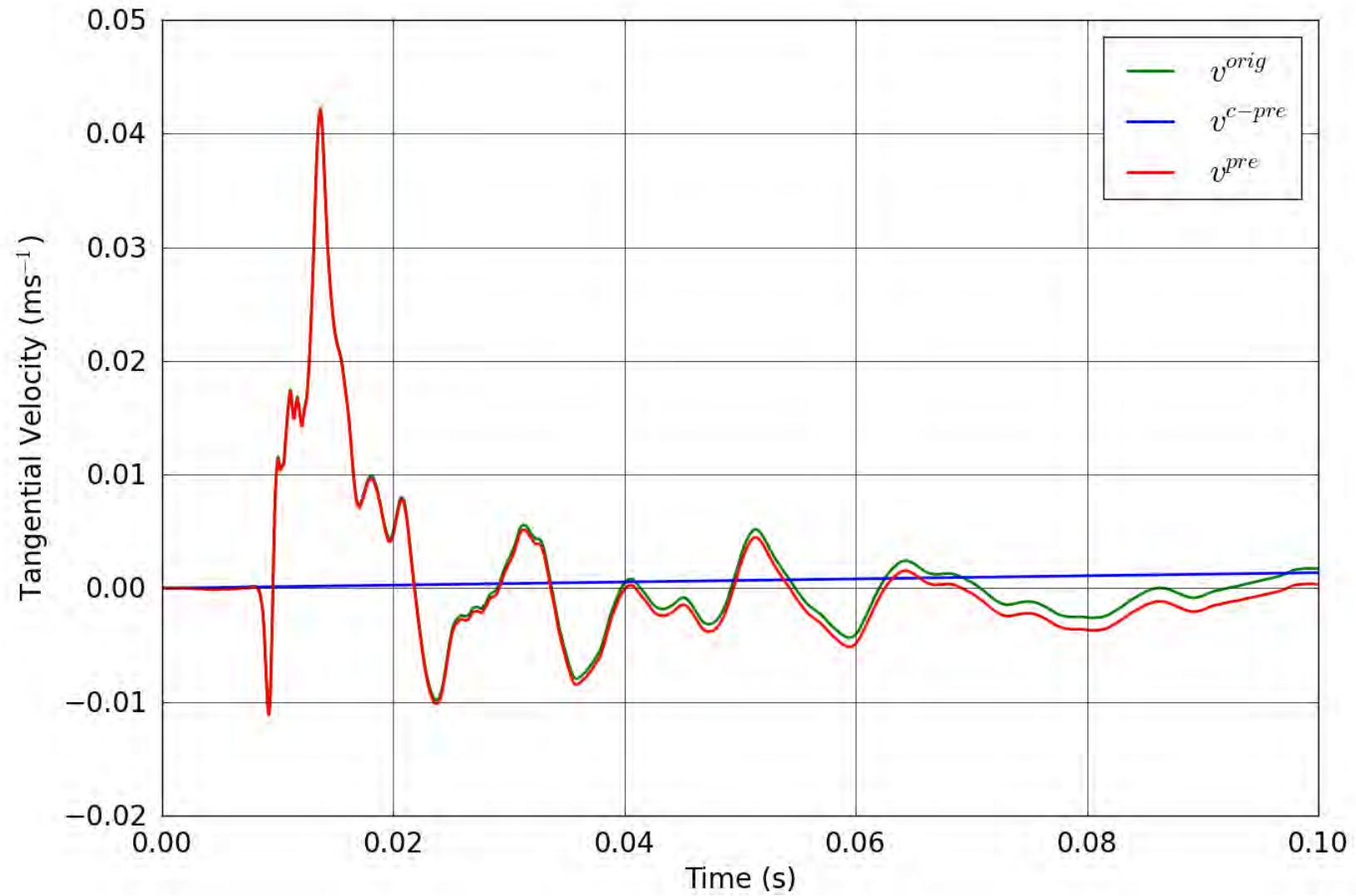
Figure 5. SPE-1 Gauge 1-3-T – Pre-shot baseline correction of the tangential velocity.
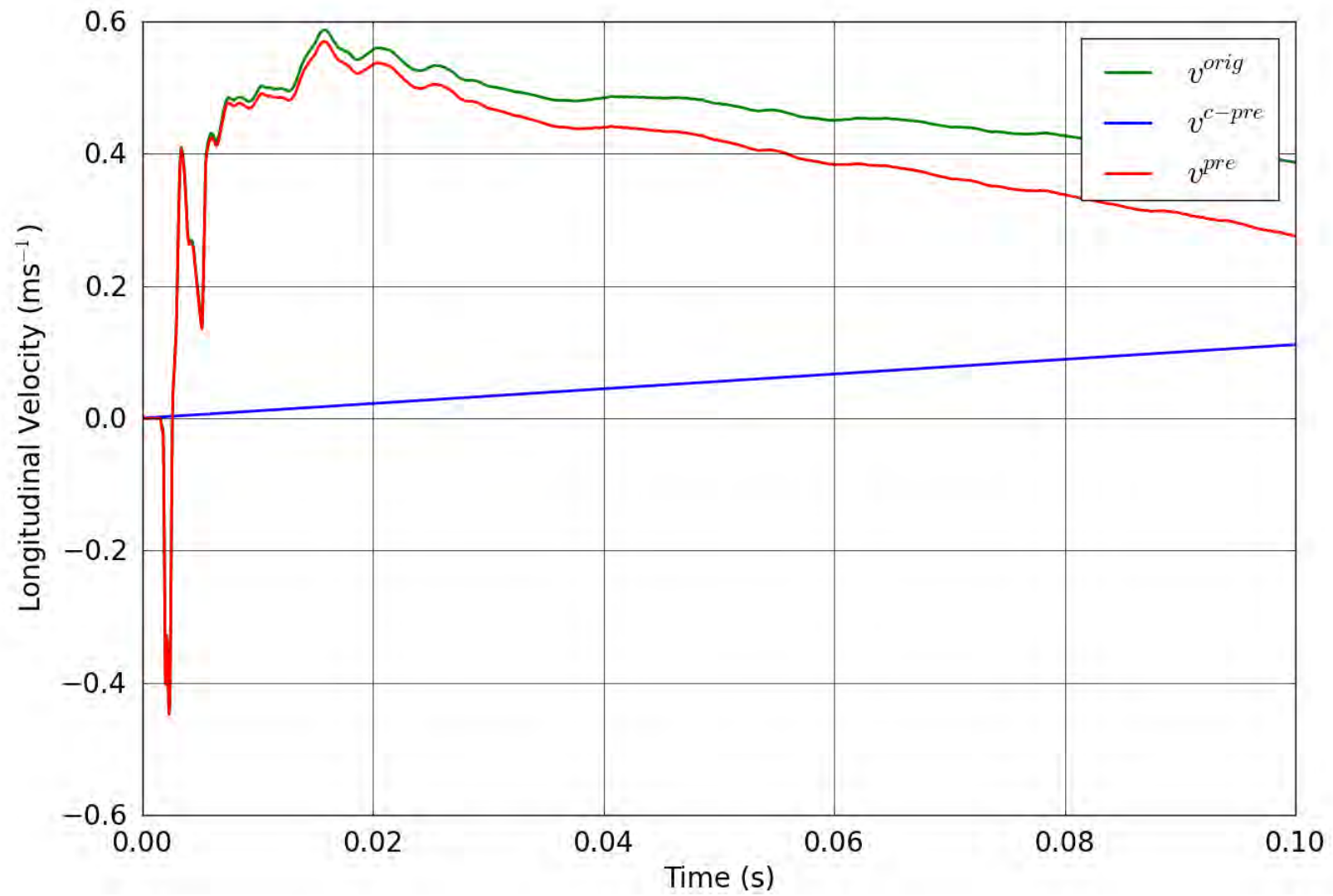
Figure 6. SPE-1 Gauge 2-1-L – Pre-shot baseline correction of the longitudinal velocity.
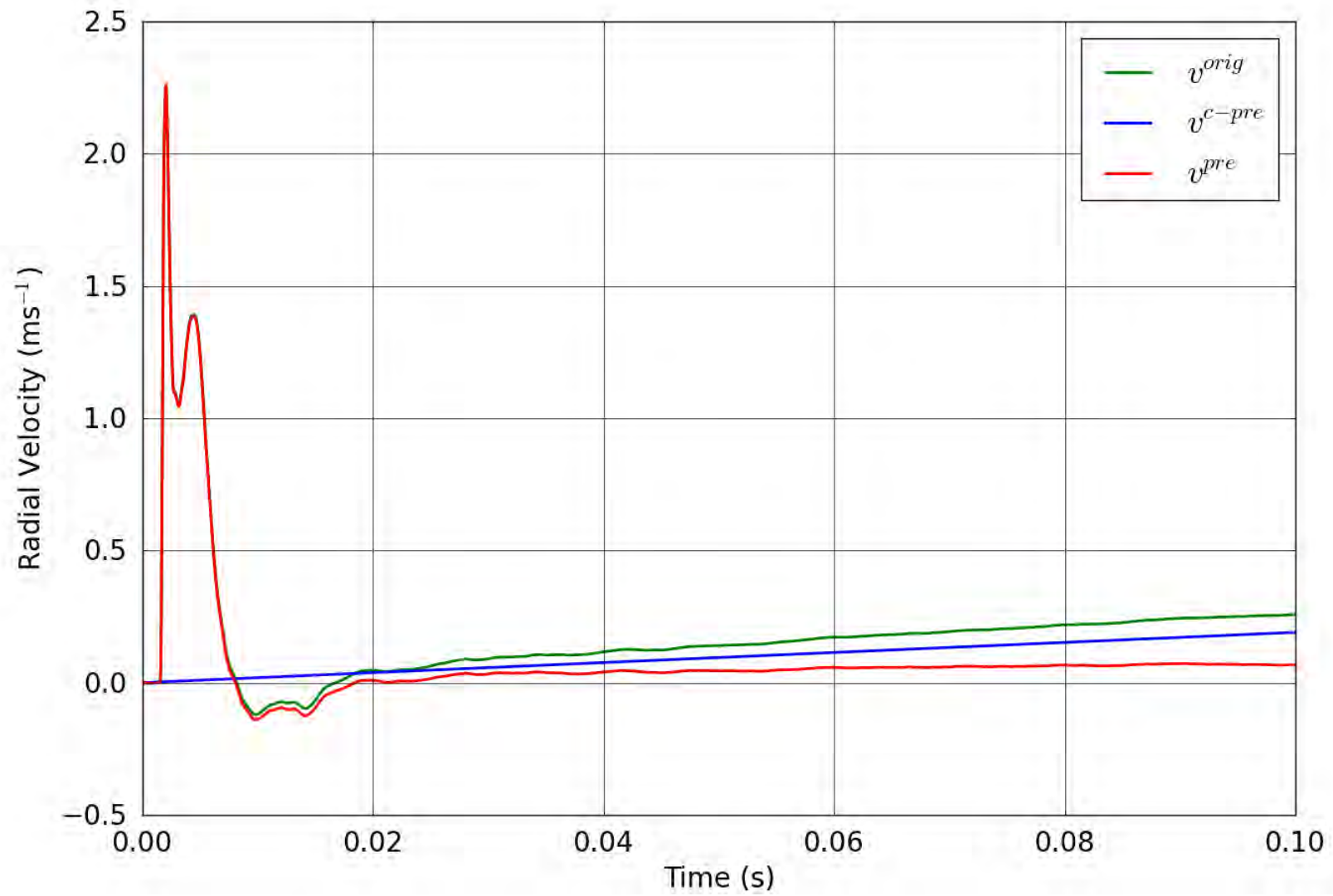
Figure 7. SPE-1 Gauge 2-1-R – Pre-shot baseline correction of the radial velocity.
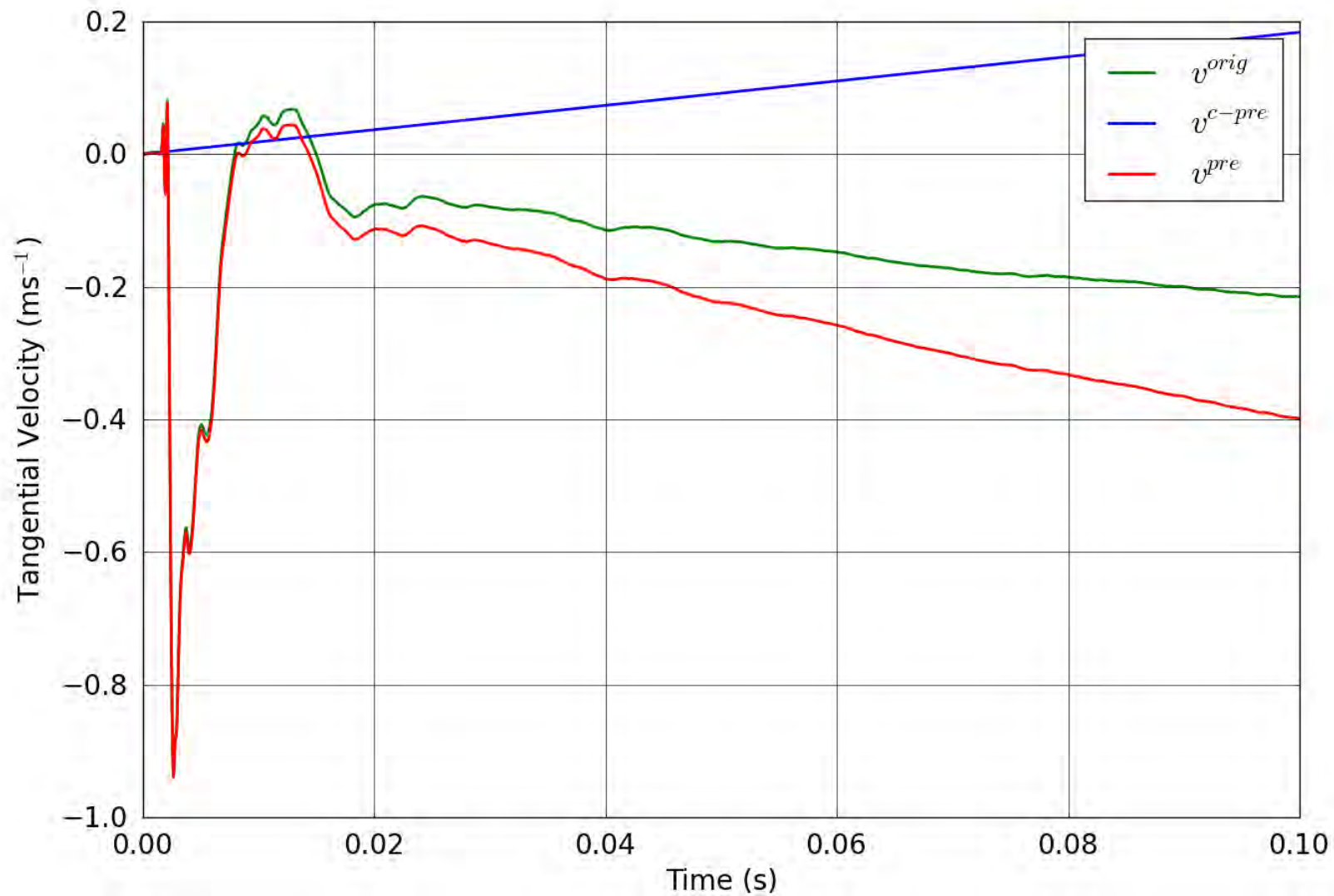
Figure 8. SPE-1 Gauge 2-1-T – Pre-shot baseline correction of the tangential velocity.
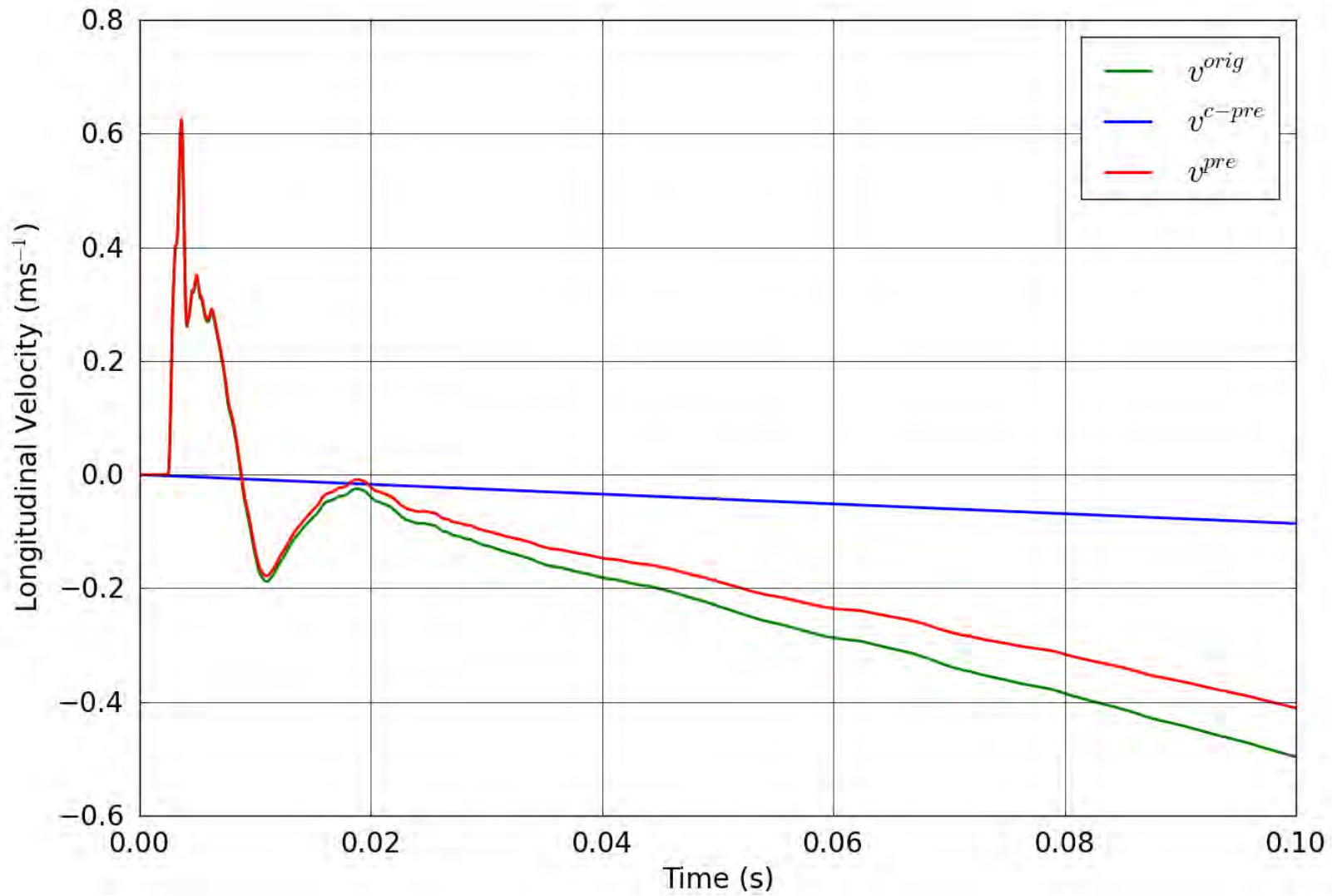
Figure 9. SPE-1 Gauge 2-2-L – Pre-shot baseline correction of the longitudinal velocity.
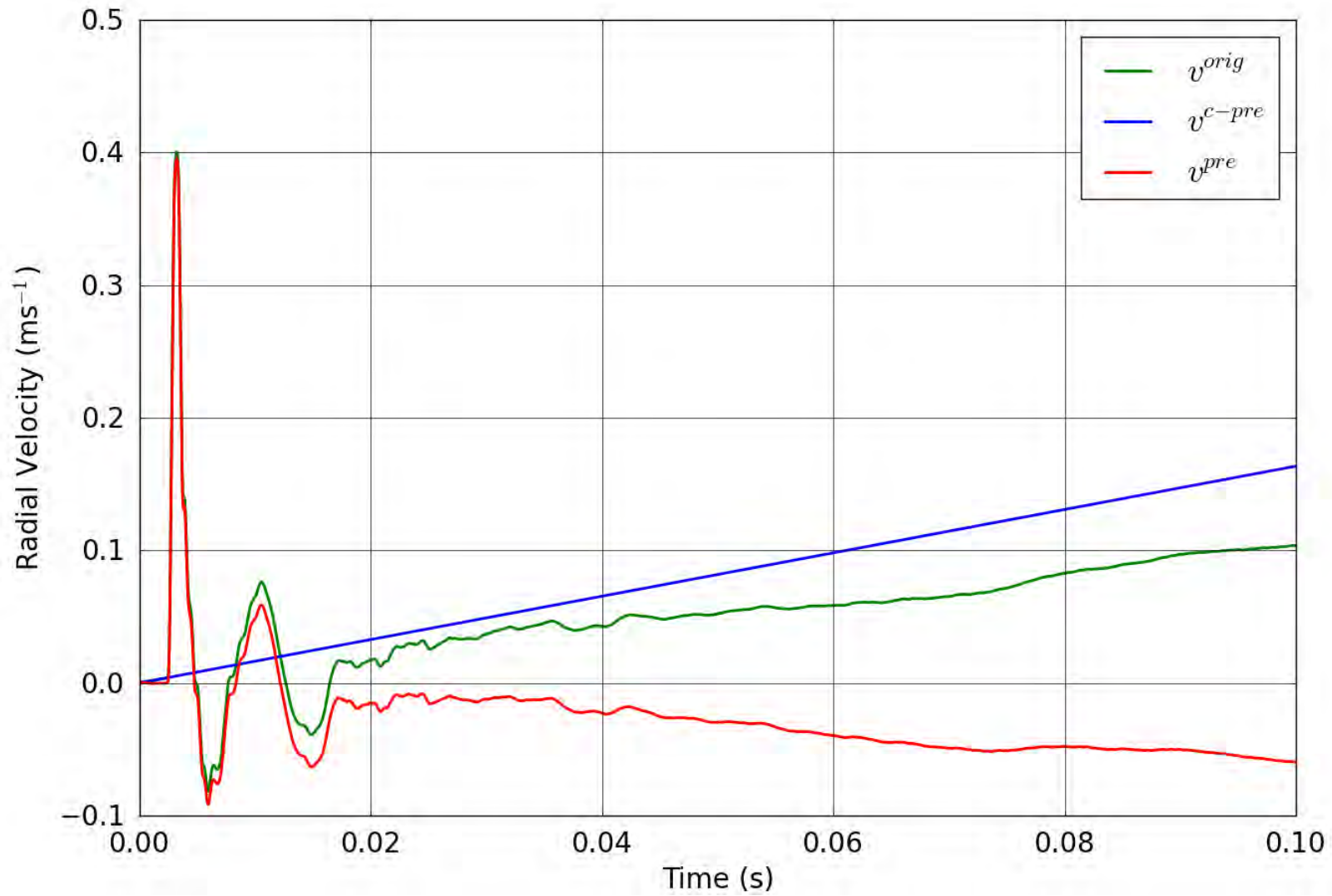
Figure 10. SPE-1 Gauge 2-2-R – Pre-shot baseline correction of the radial velocity.
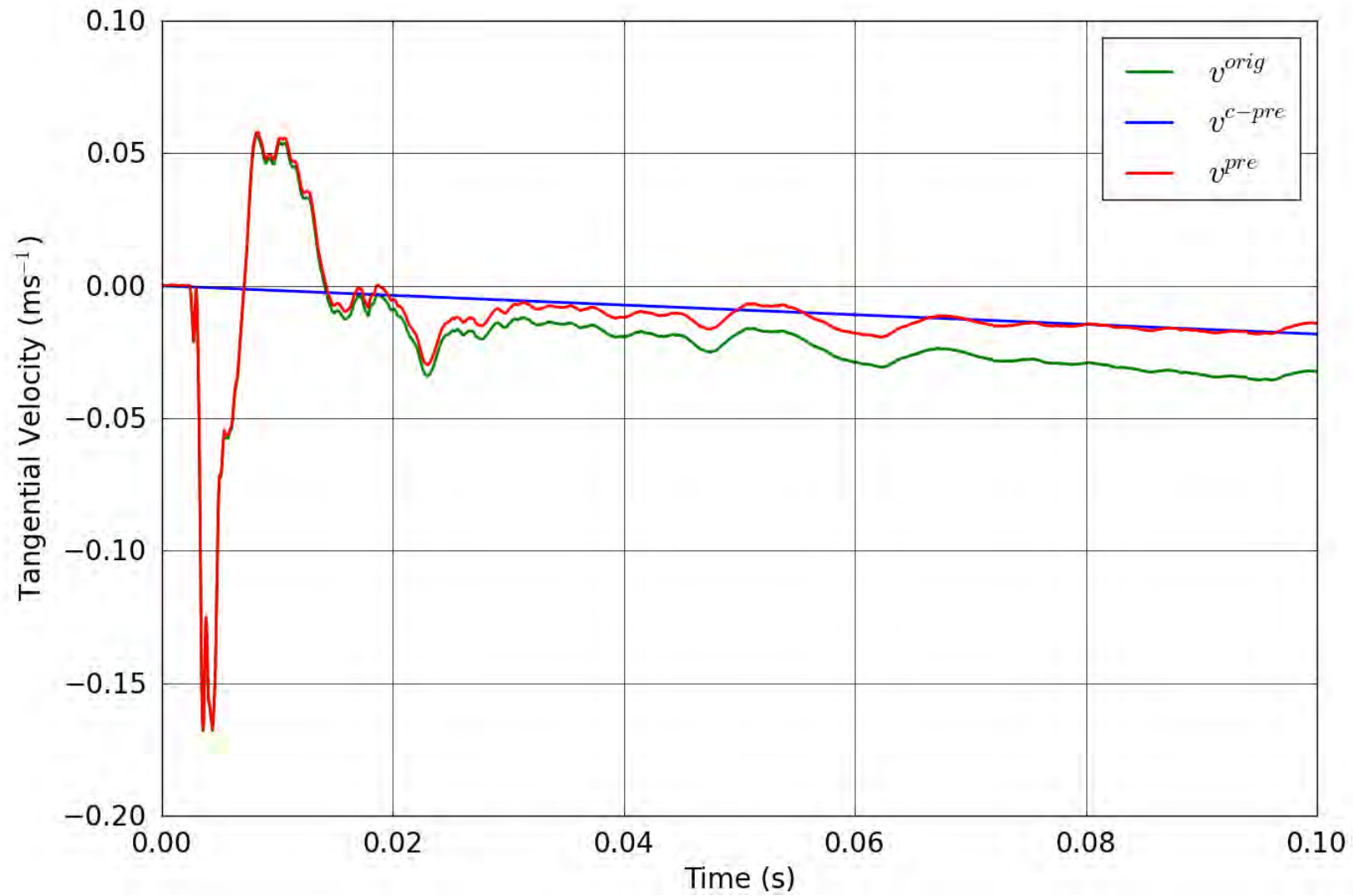
Figure 11. SPE-1 Gauge 2-2-T – Pre-shot baseline correction of the tangential velocity.
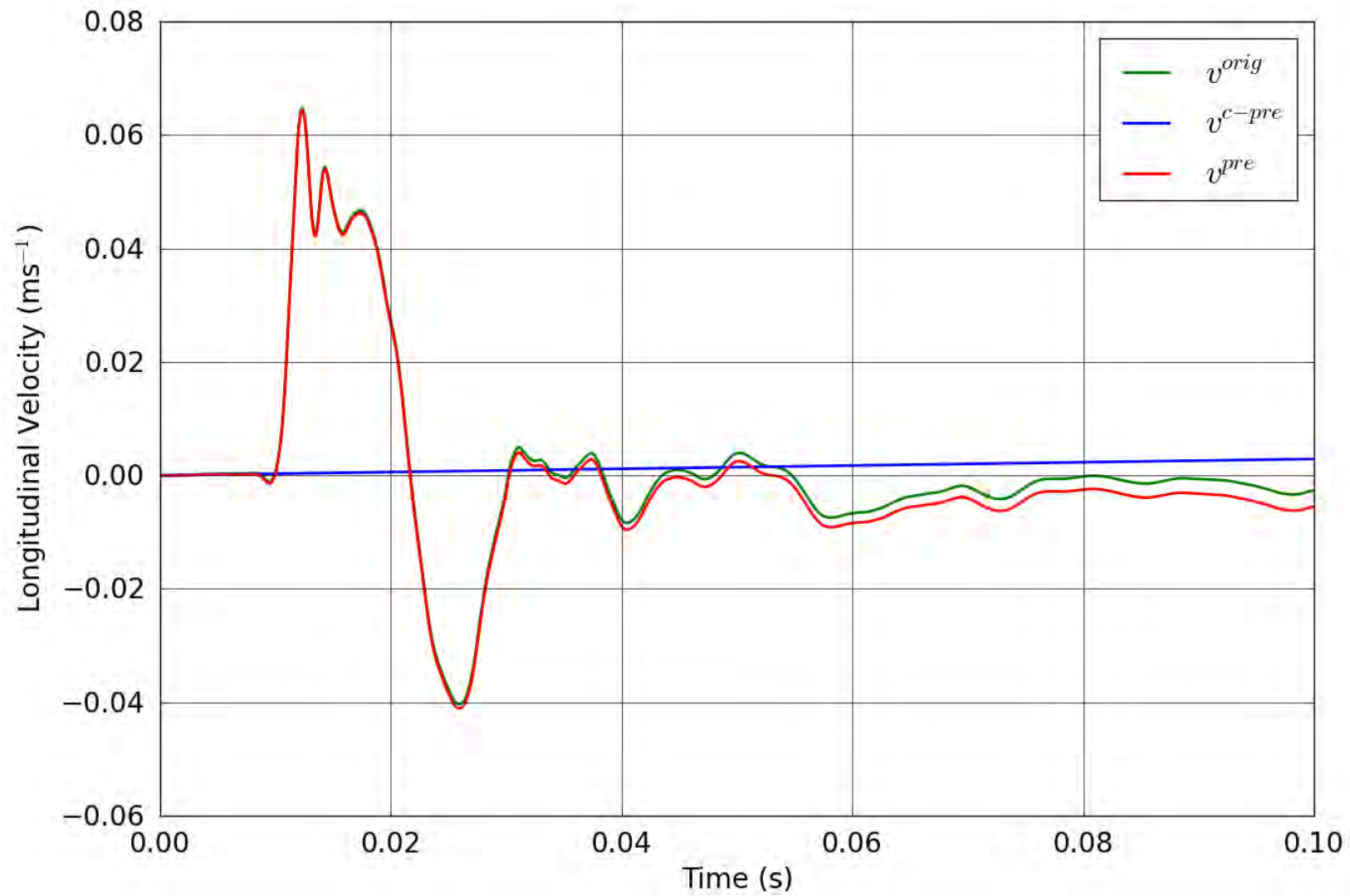
Figure 12. SPE-1 Gauge 2-3-L – Pre-shot baseline correction of the longitudinal velocity.
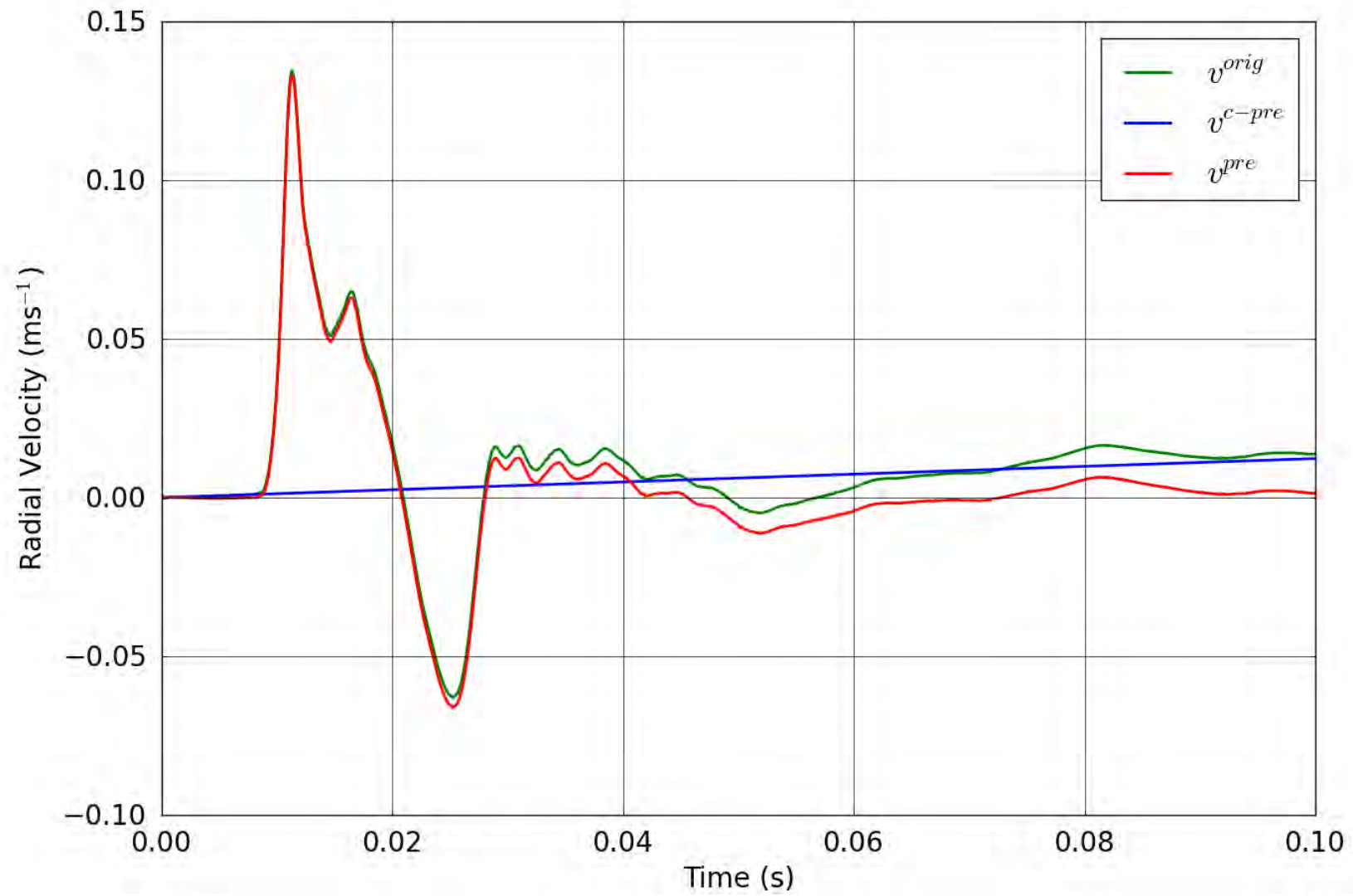
Figure 13. SPE-1 Gauge 2-3-R – Pre-shot baseline correction of the radial velocity.
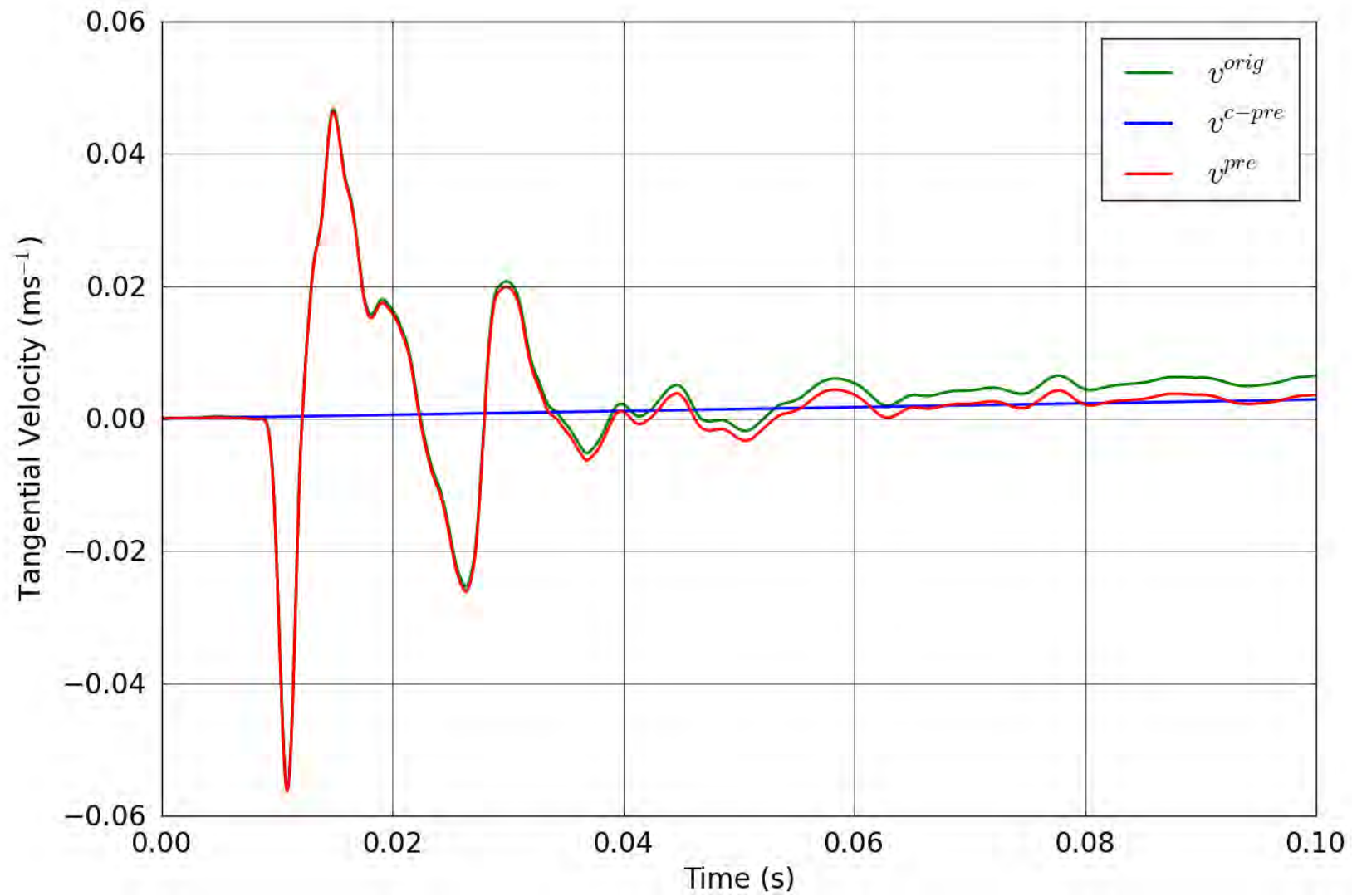
Figure 14. SPE-1 Gauge 2-3-T – Pre-shot baseline correction of the tangential velocity.
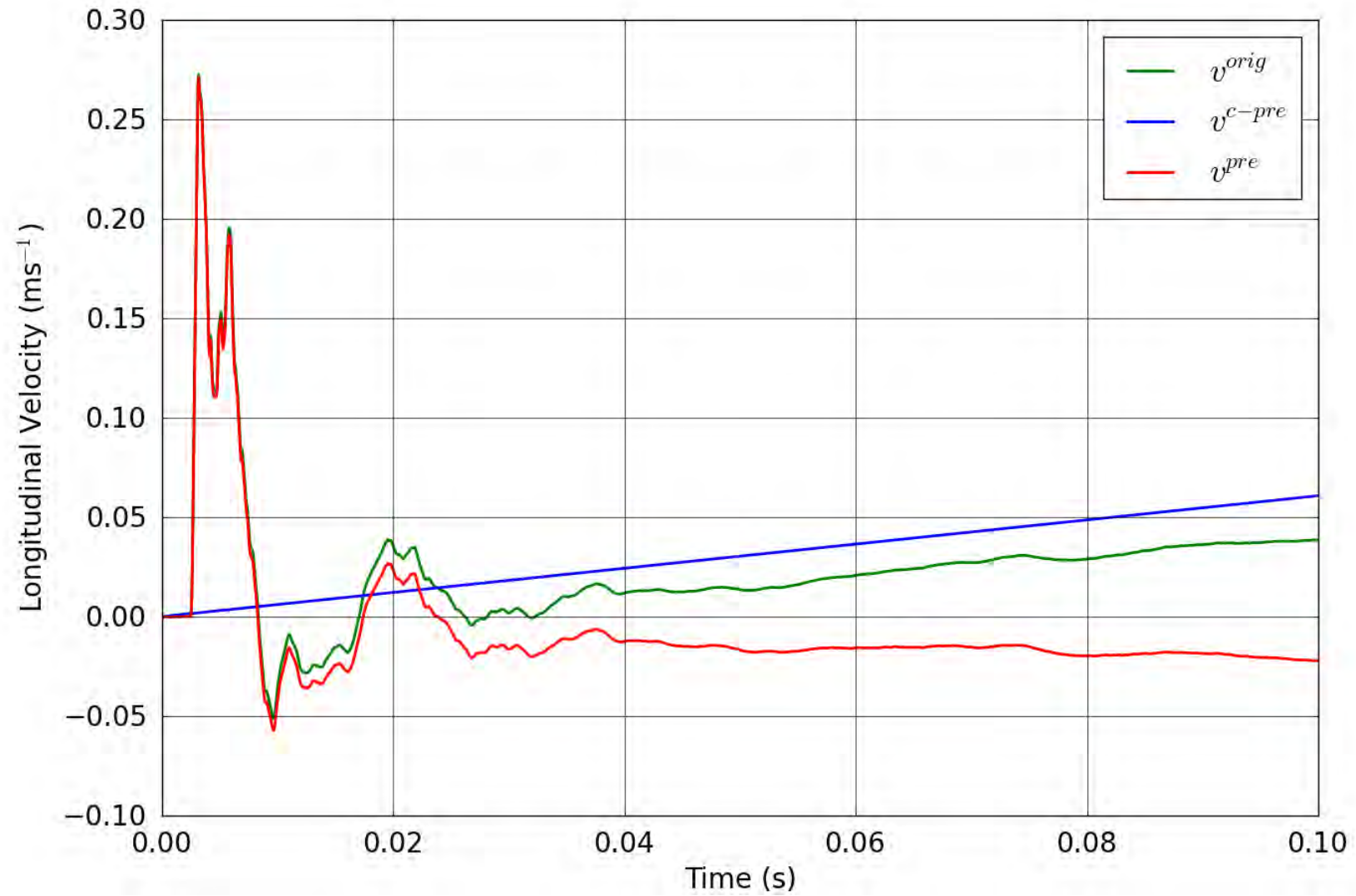
Figure 15. SPE-1 Gauge 3-2-L – Pre-shot baseline correction of the longitudinal velocity.
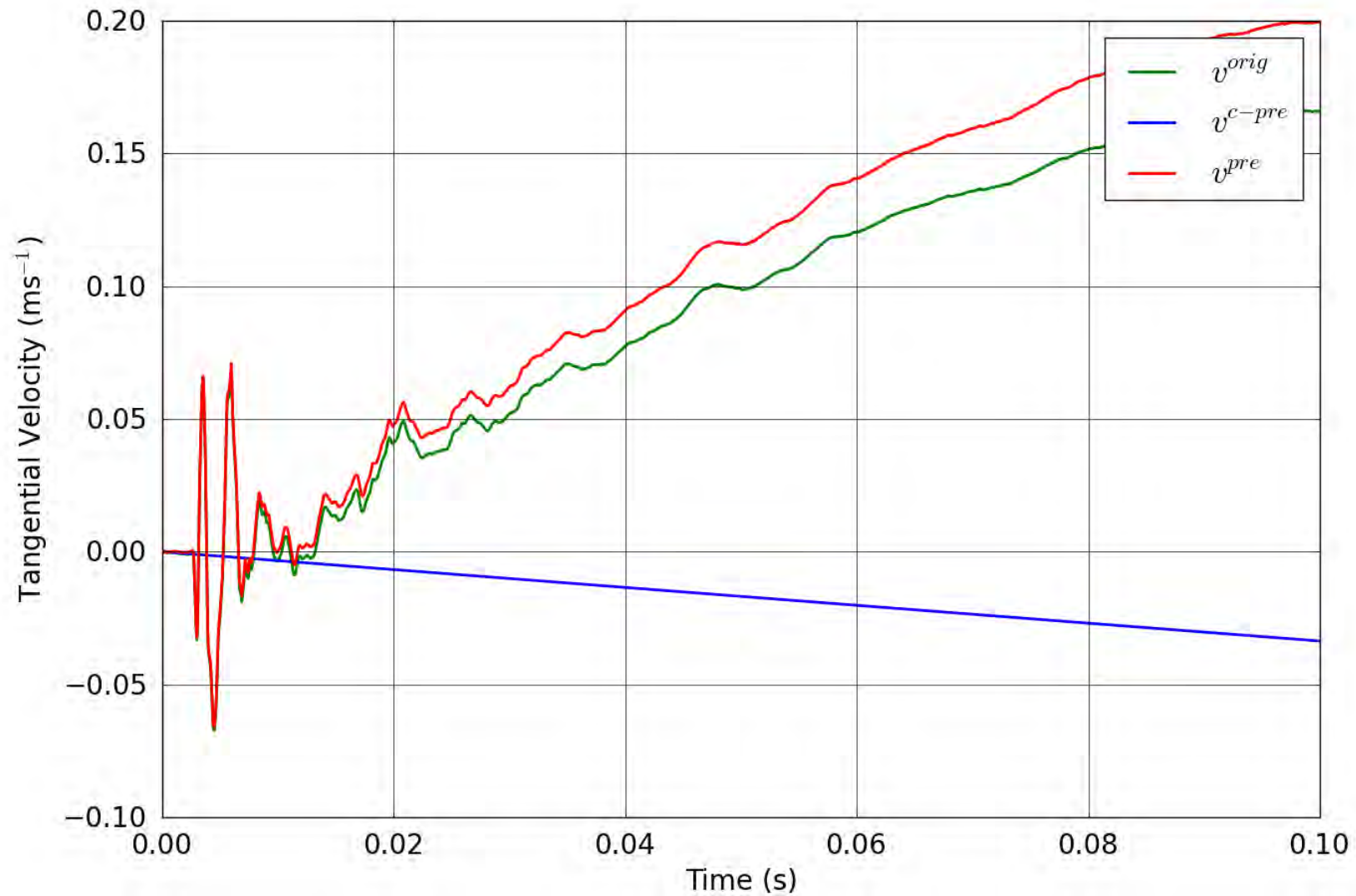
Figure 16. SPE-1 Gauge 3-2-T – Pre-shot baseline correction of the tangential velocity.
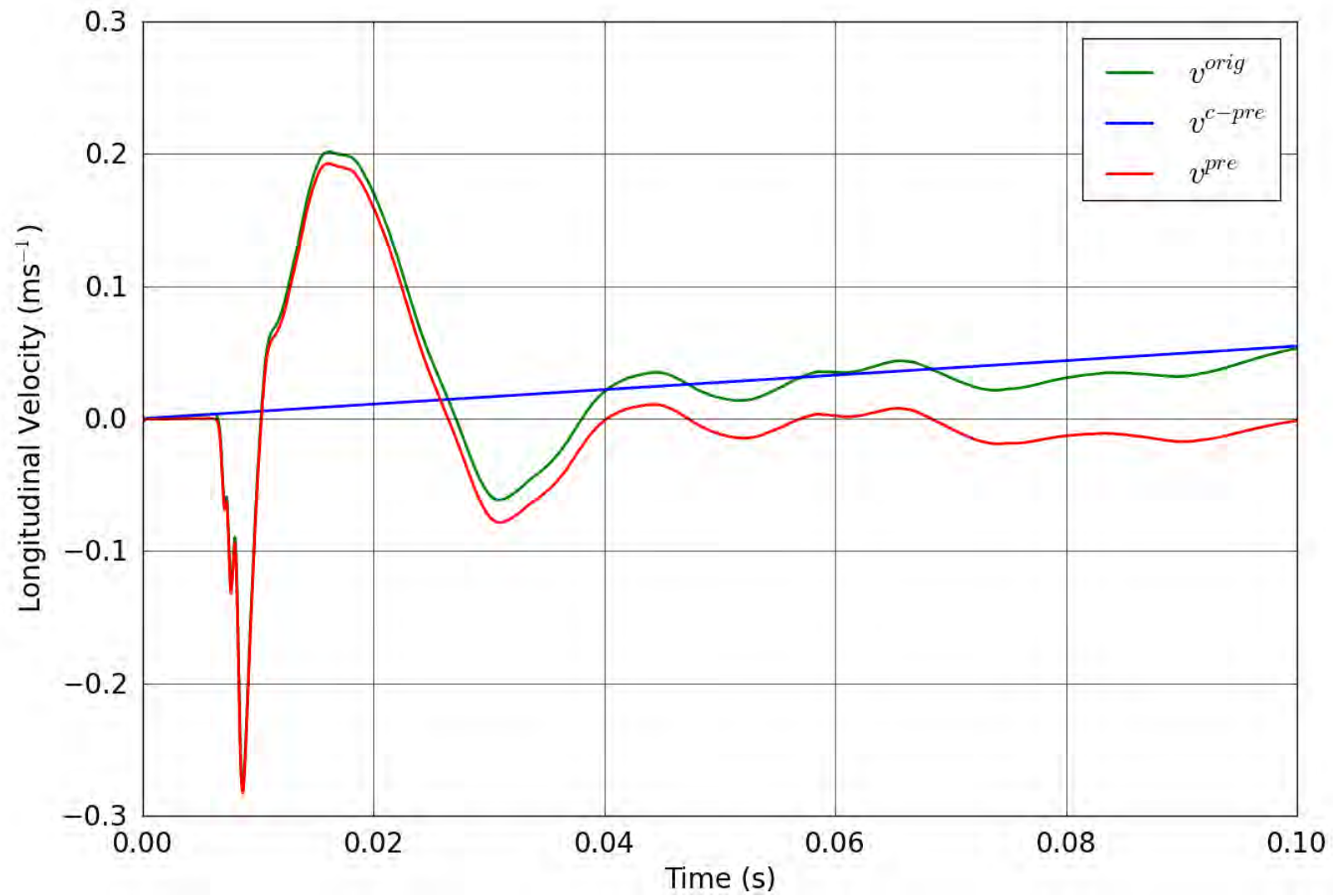
Figure 17. SPE-1 Gauge 3-3-L – Pre-shot baseline correction of the longitudinal velocity.
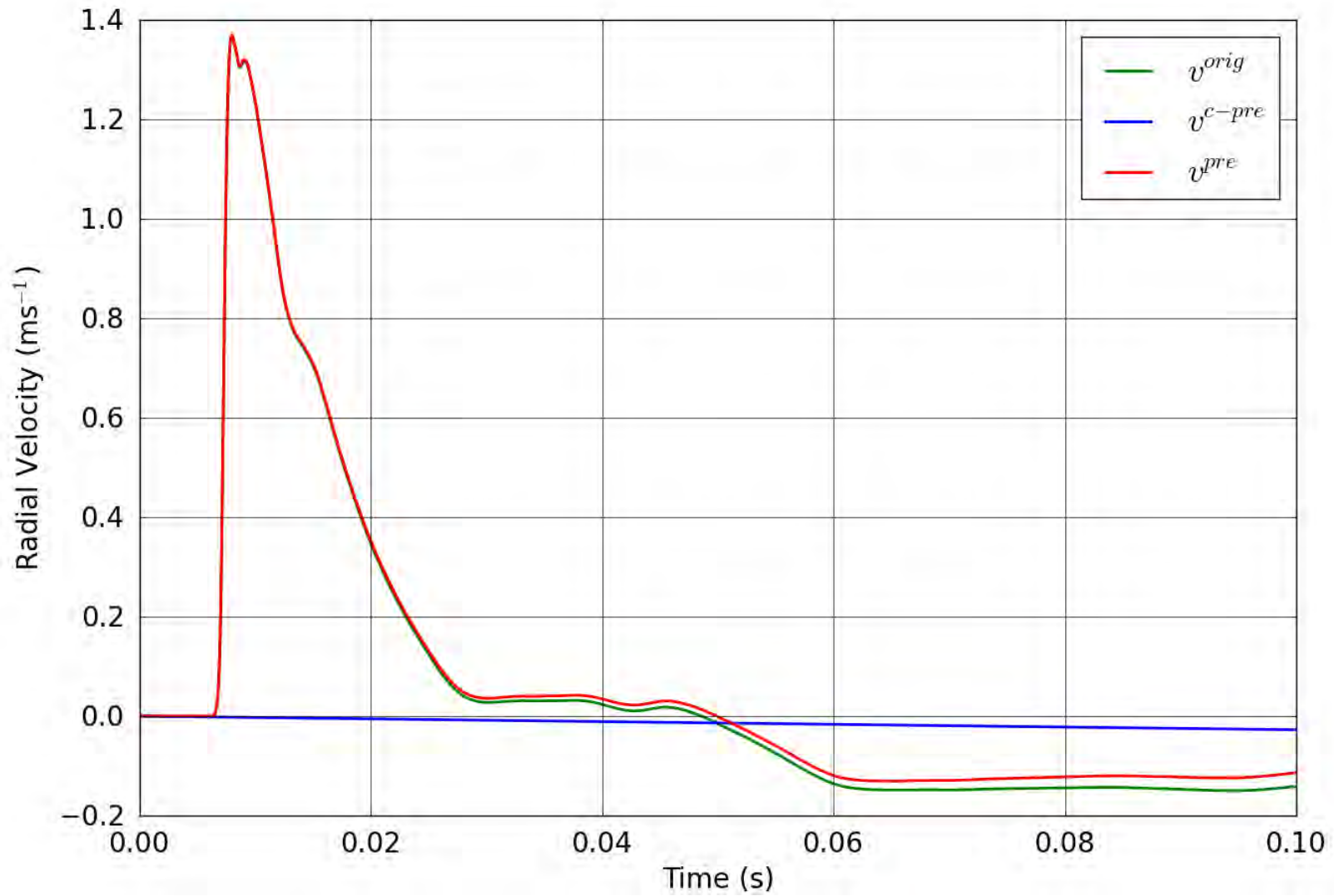
Figure 18. SPE-1 Gauge 3-3-R – Pre-shot baseline correction of the radial velocity.
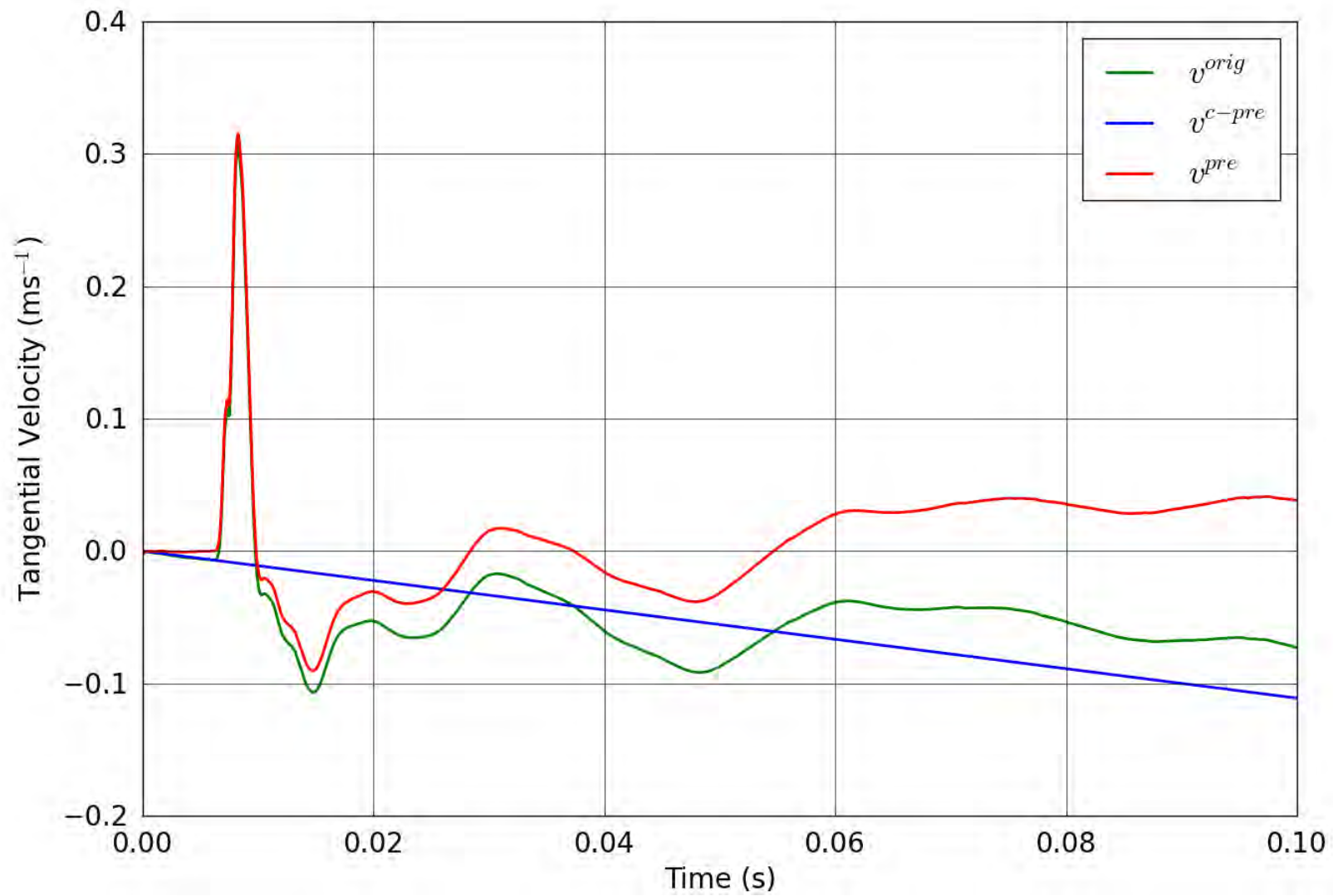
Figure 19. SPE-1 Gauge 3-3-T – Pre-shot baseline correction of the tangential velocity.
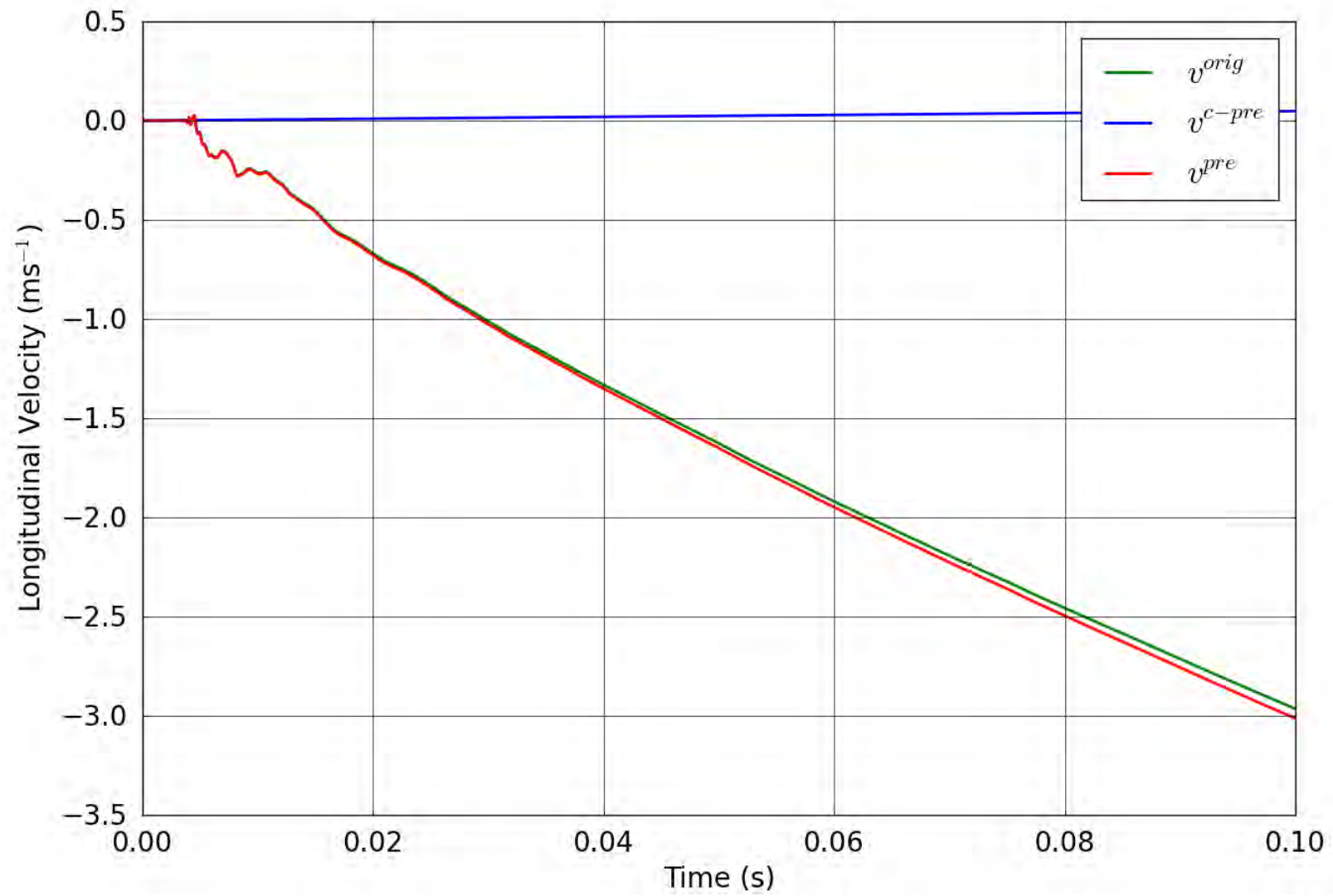
Figure 20. SPE-1 Gauge 4-1-L – Pre-shot baseline correction of the longitudinal velocity.
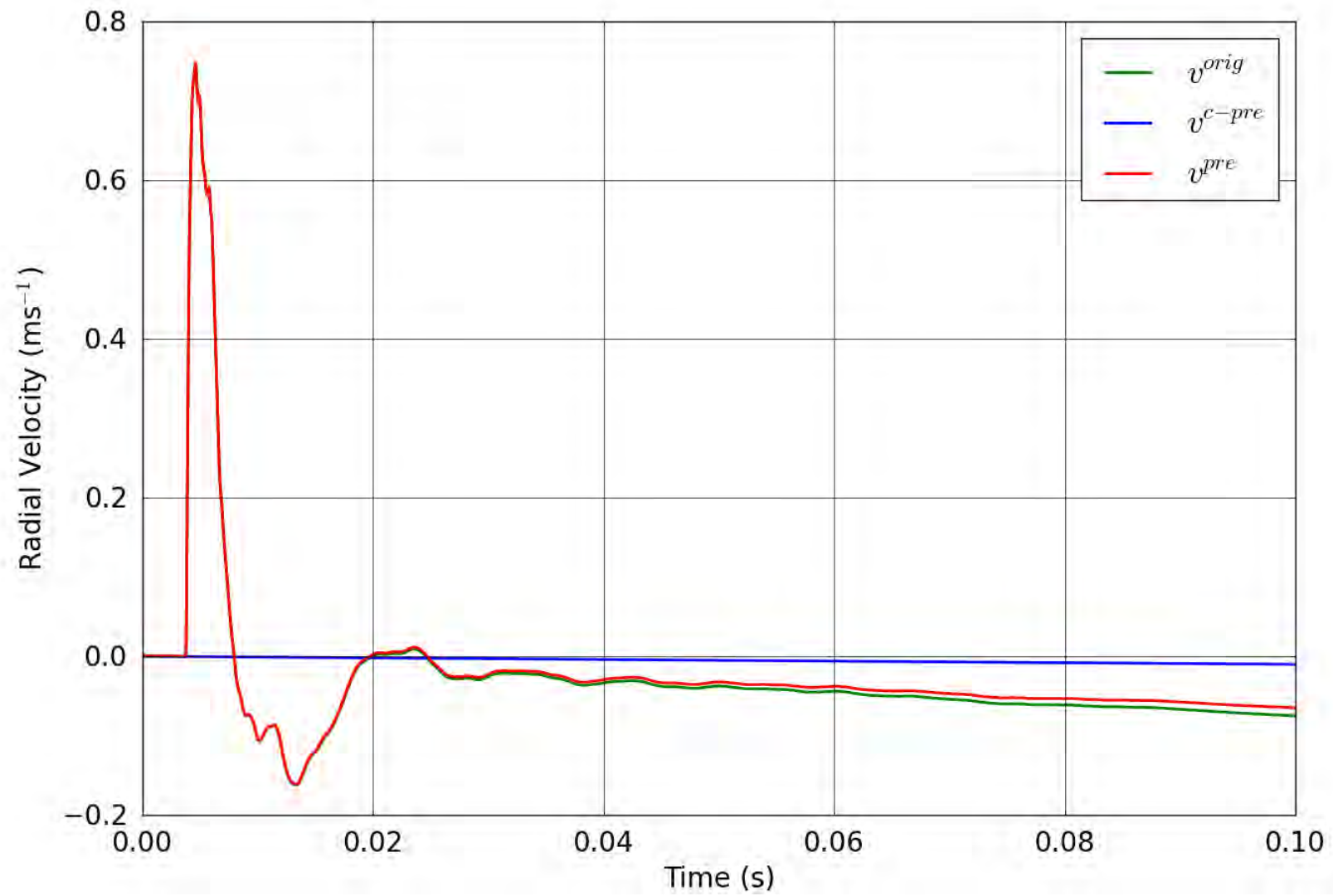
Figure 21. SPE-1 Gauge 4-1-R – Pre-shot baseline correction of the radial velocity.
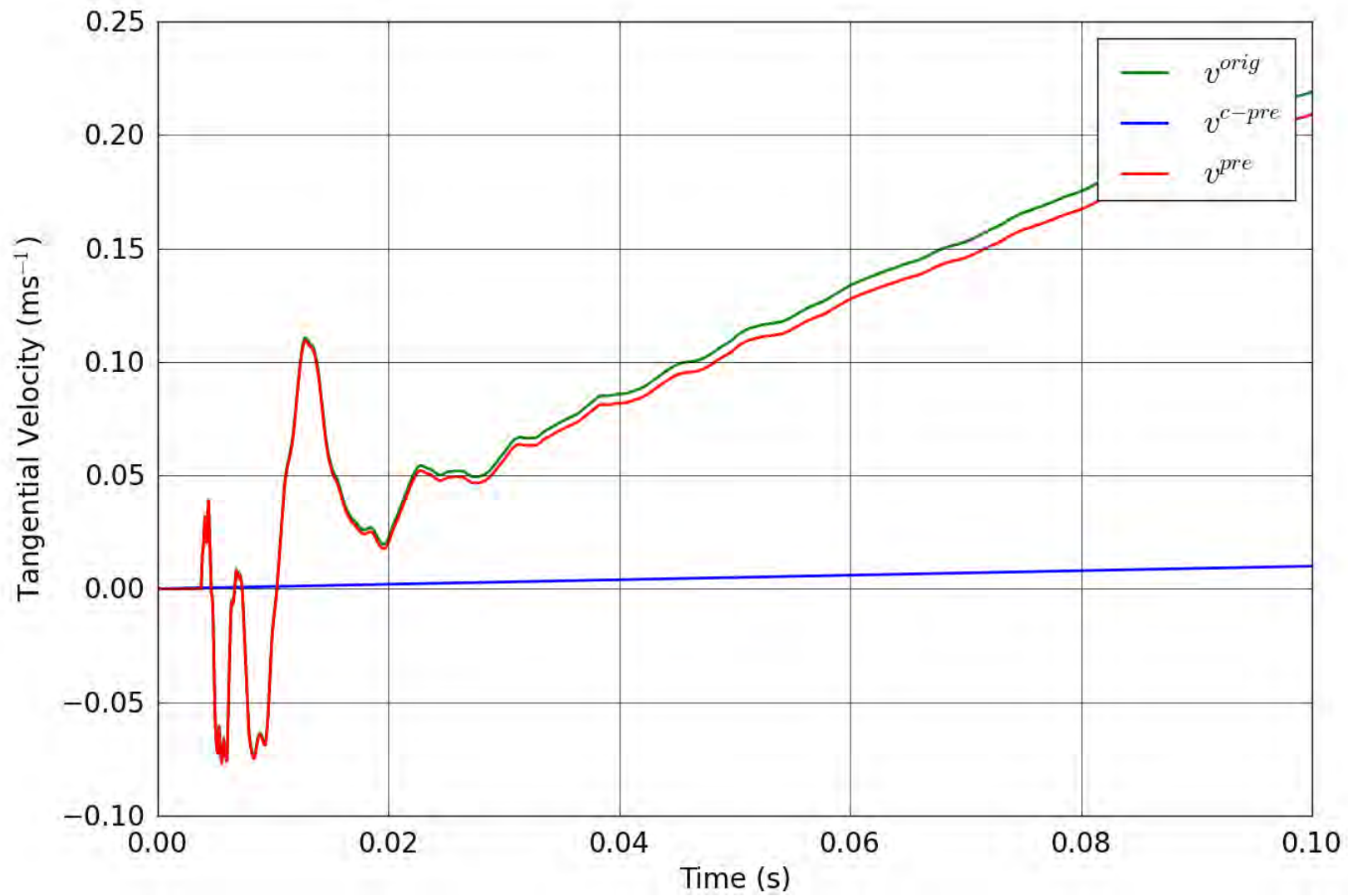
Figure 22. SPE-1 Gauge 4-1-T – Pre-shot baseline correction of the tangential velocity.
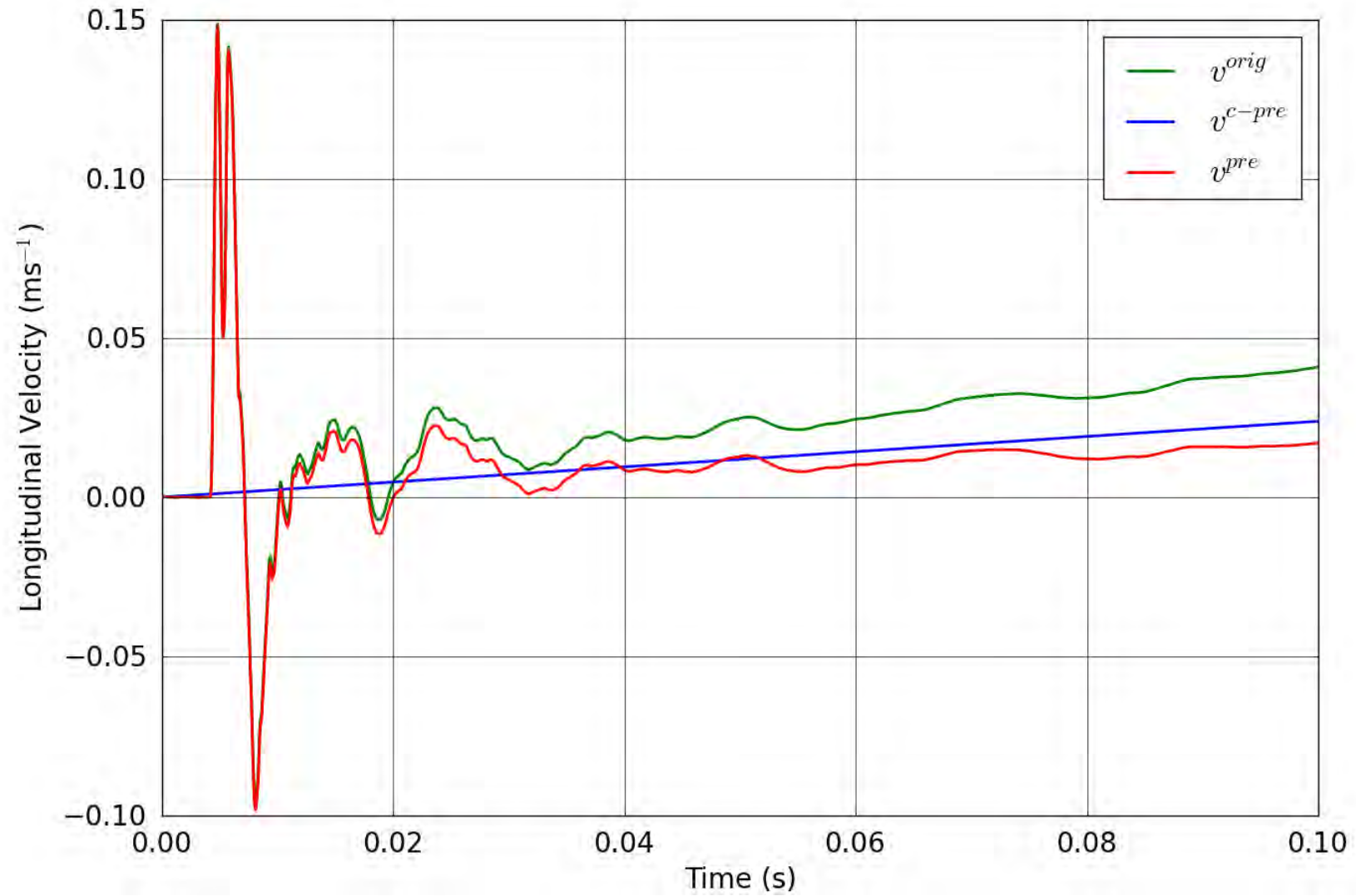
Figure 23. SPE-1 Gauge 4-2-L – Pre-shot baseline correction of the longitudinal velocity.
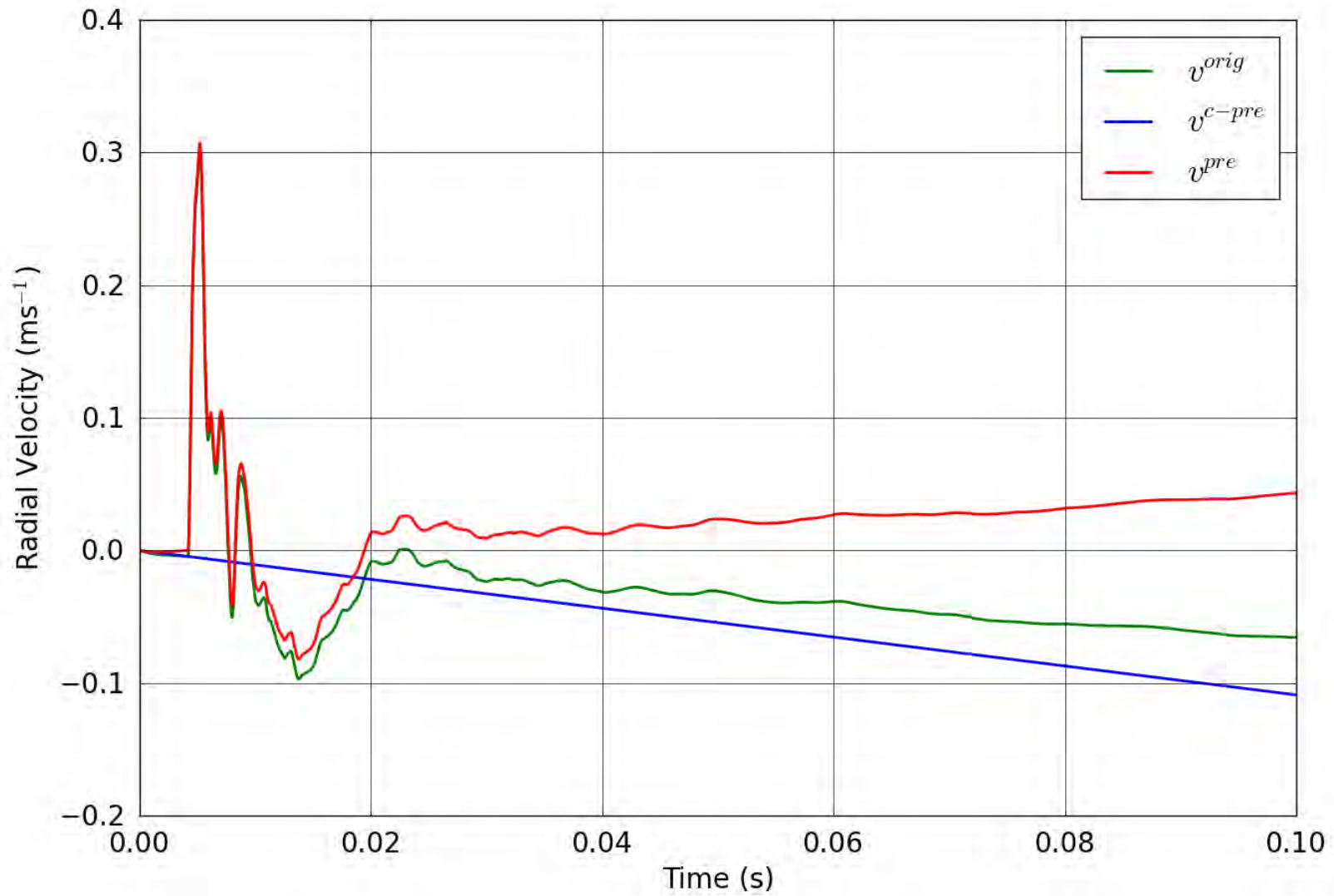
Figure 24. SPE-1 Gauge 4-2-R – Pre-shot baseline correction of the radial velocity.
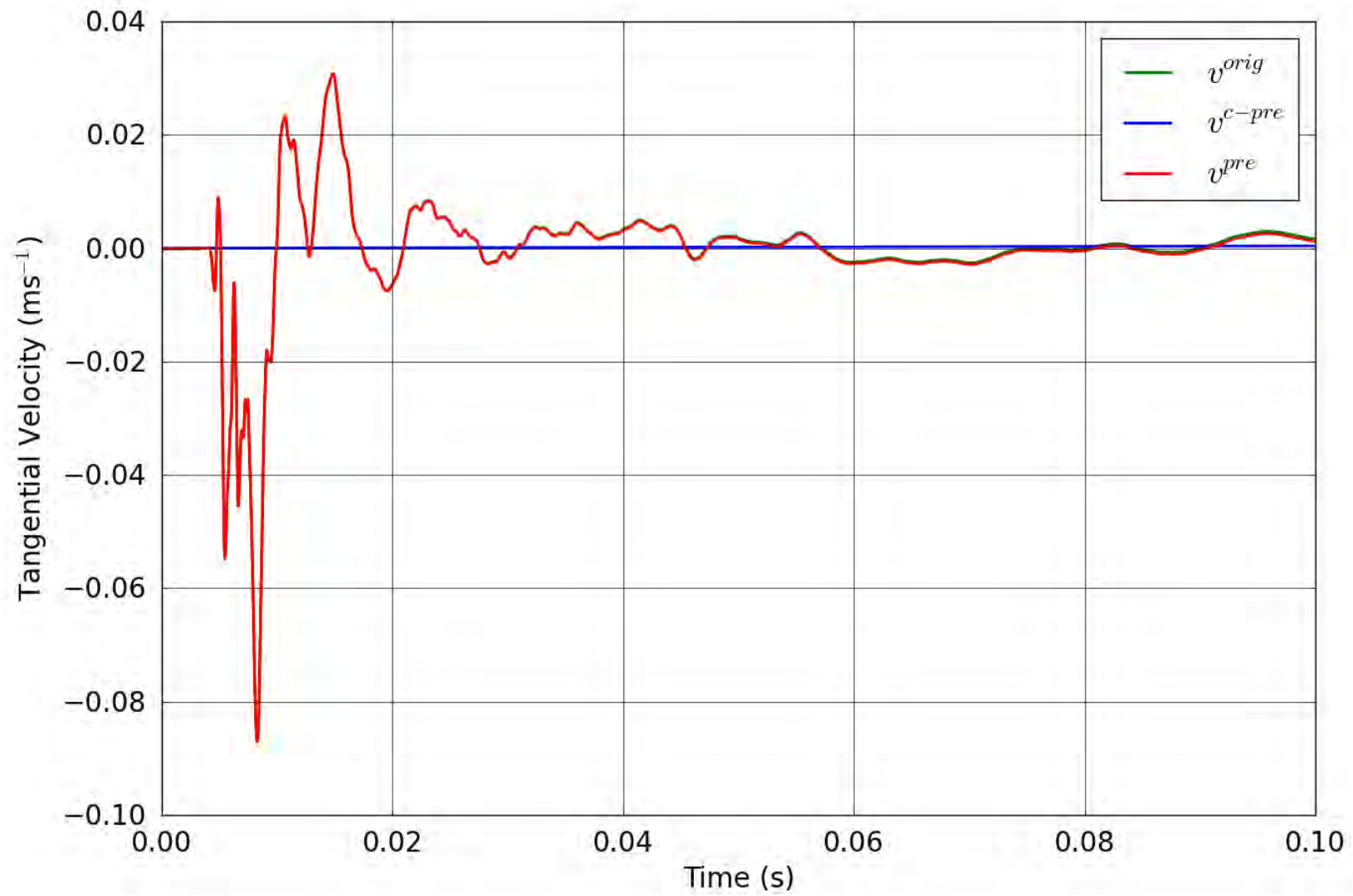
Figure 25. SPE-1 Gauge 4-2-T – Pre-shot baseline correction of the tangential velocity.
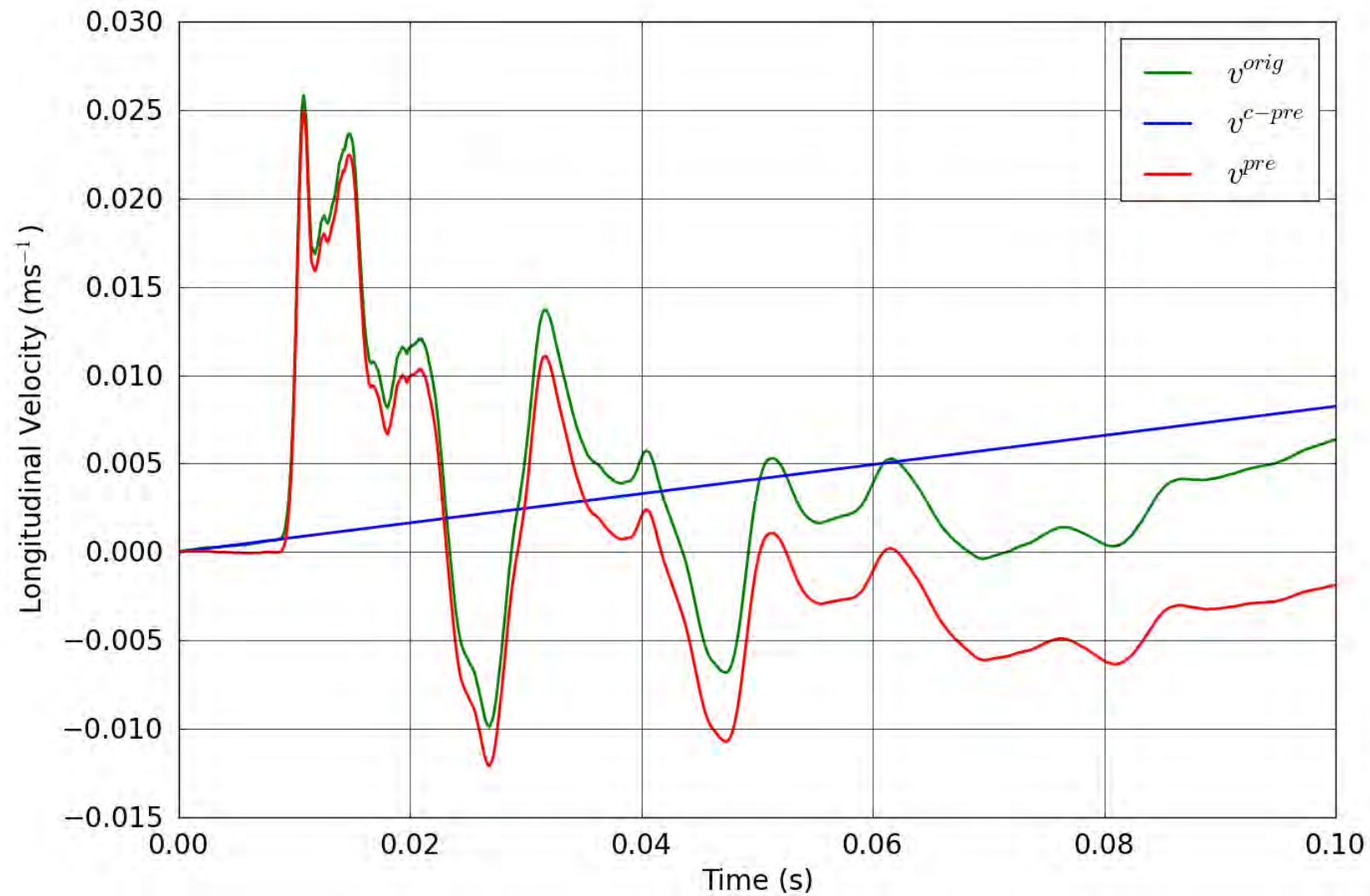
Figure 26. SPE-1 Gauge 4-3-L – Pre-shot baseline correction of the longitudinal velocity.
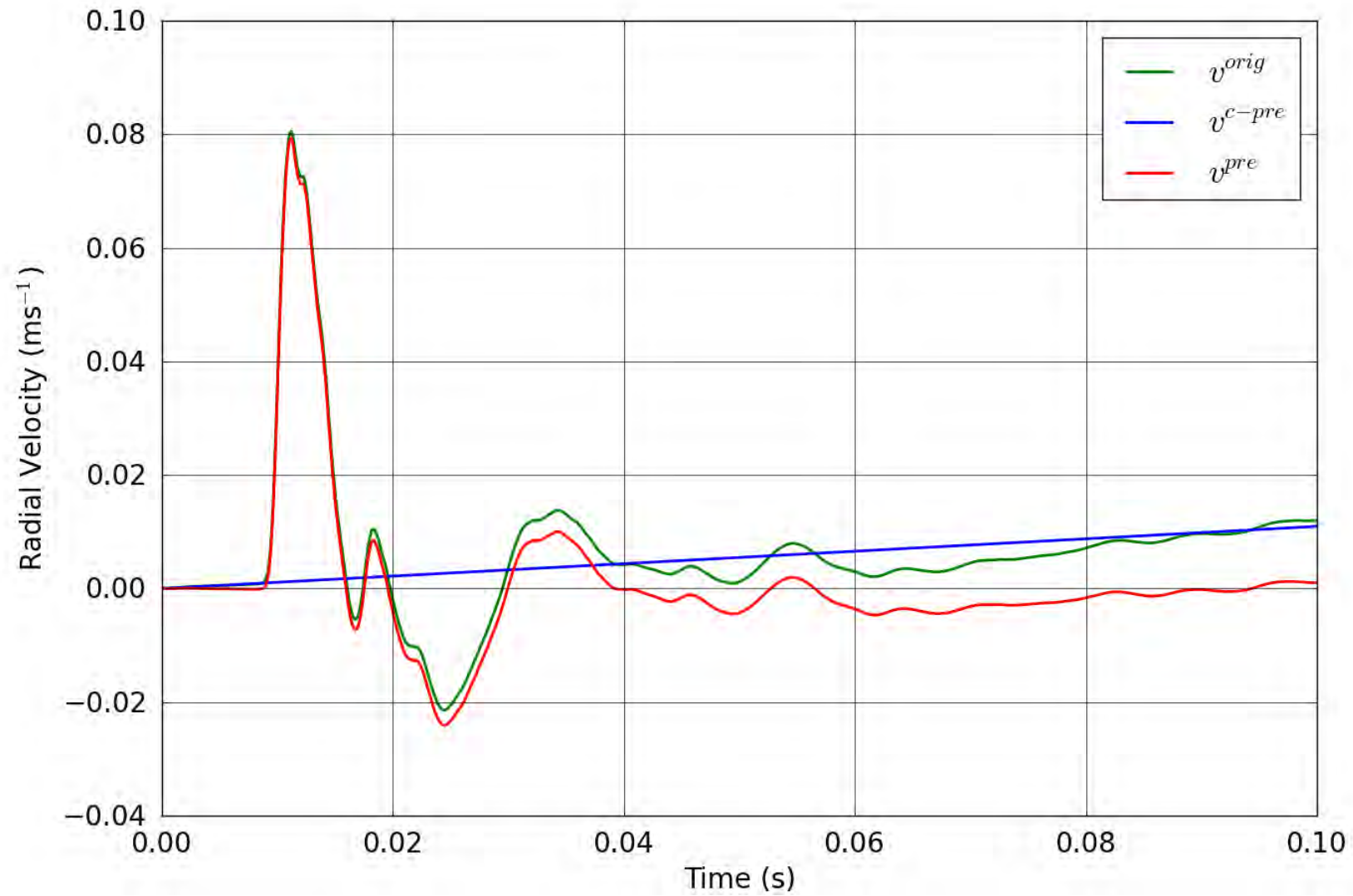
Figure 27. SPE-1 Gauge 4-3-R – Pre-shot baseline correction of the radial velocity.
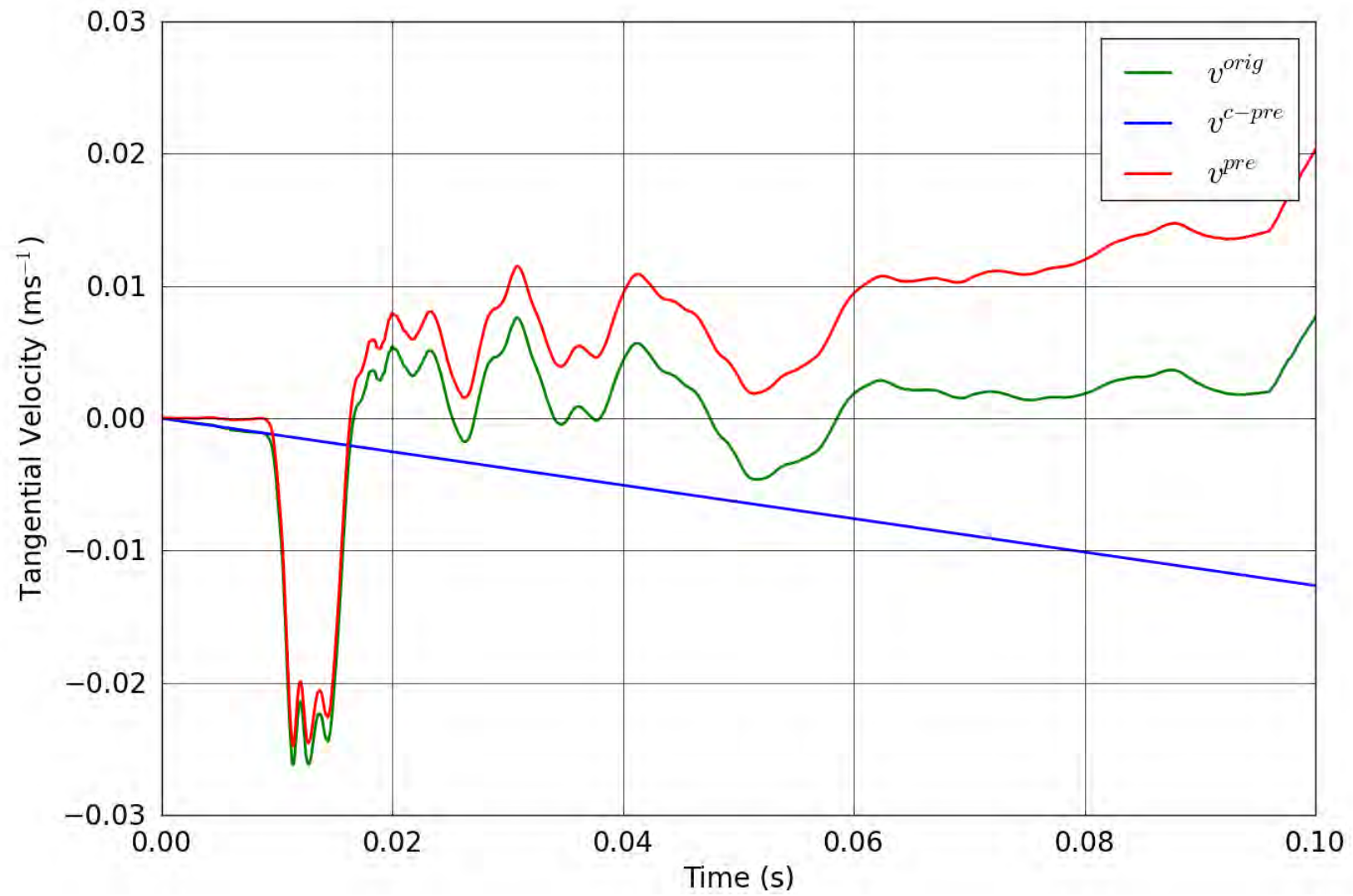
Figure 28. SPE-1 Gauge 4-3-T – Pre-shot baseline correction of the tangential velocity.
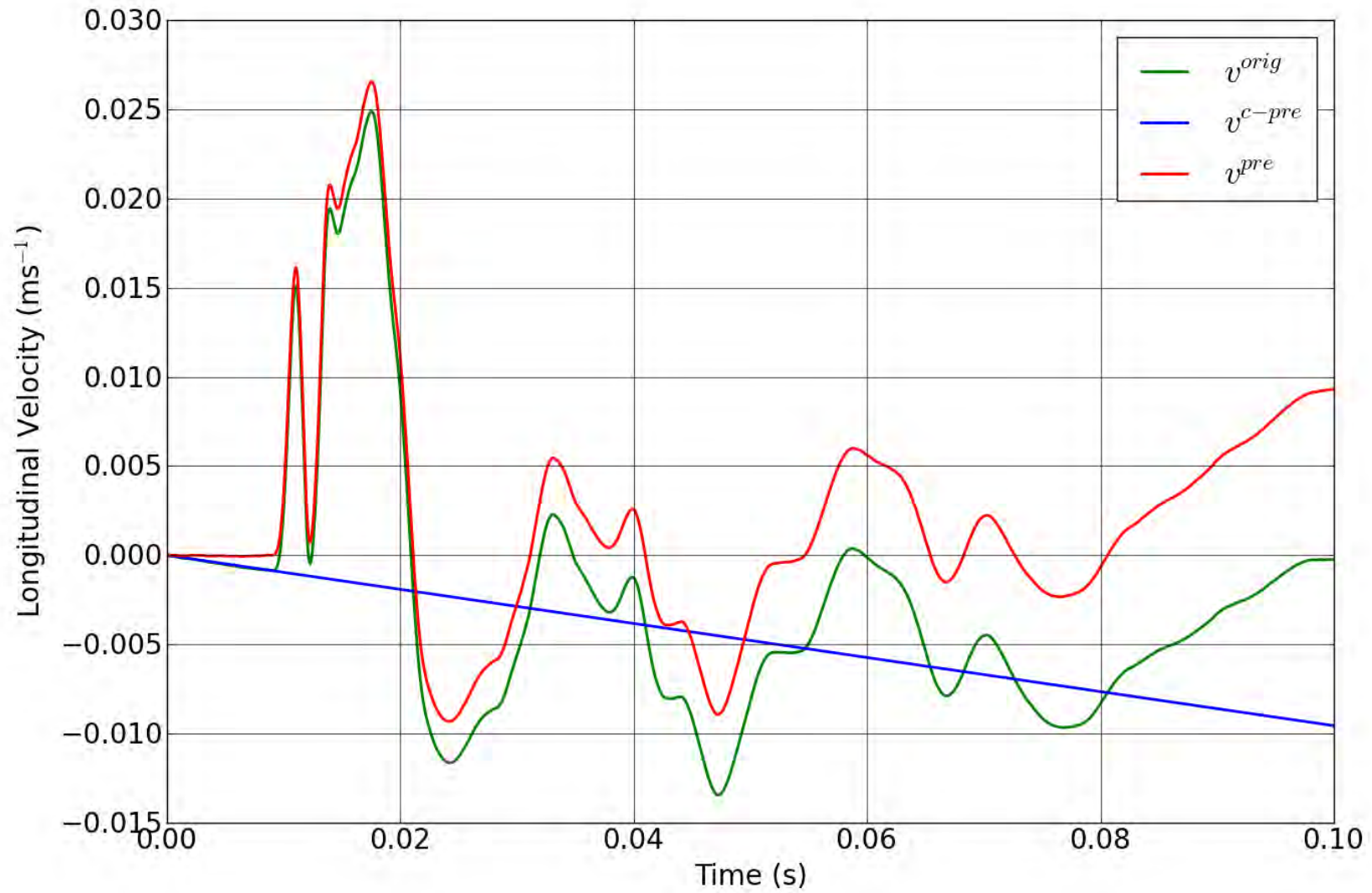
Figure 29. SPE-1 Gauge 5-3-L – Pre-shot baseline correction of the longitudinal velocity.
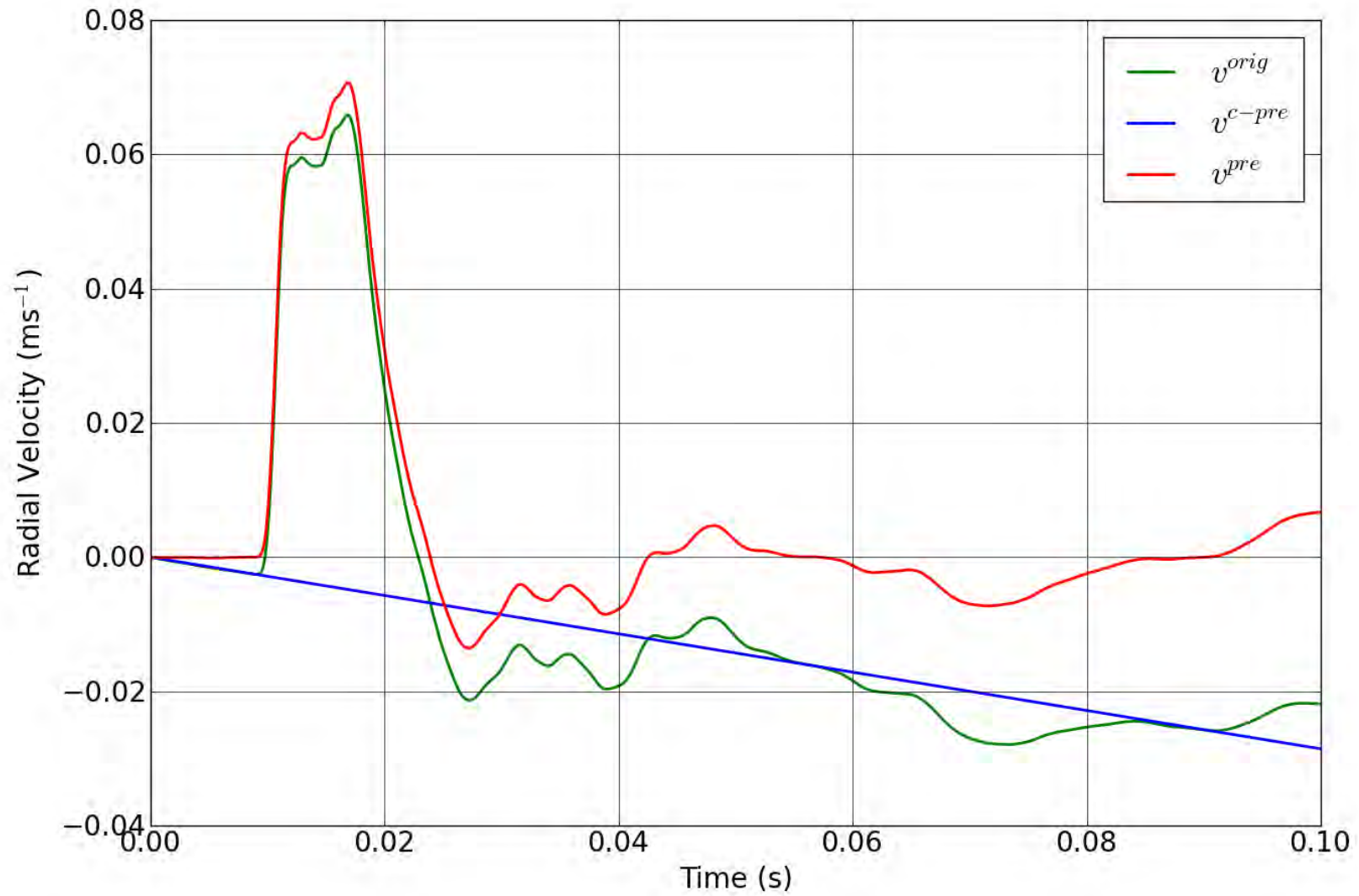
Figure 30. SPE-1 Gauge 5-3-R – Pre-shot baseline correction of the radial velocity.
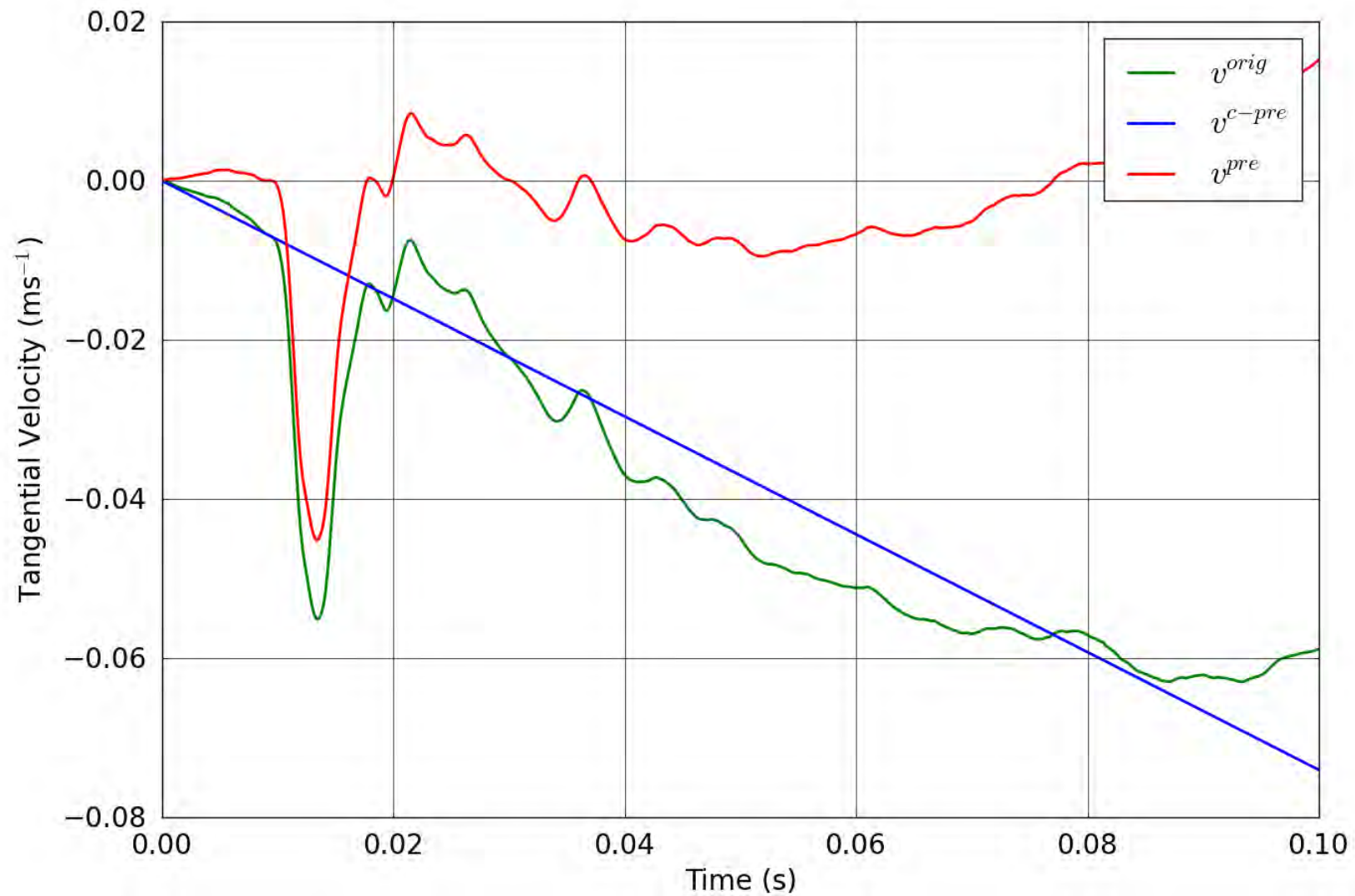
Figure 31. SPE-1 Gauge 5-3-T – Pre-shot baseline correction of the tangential velocity.
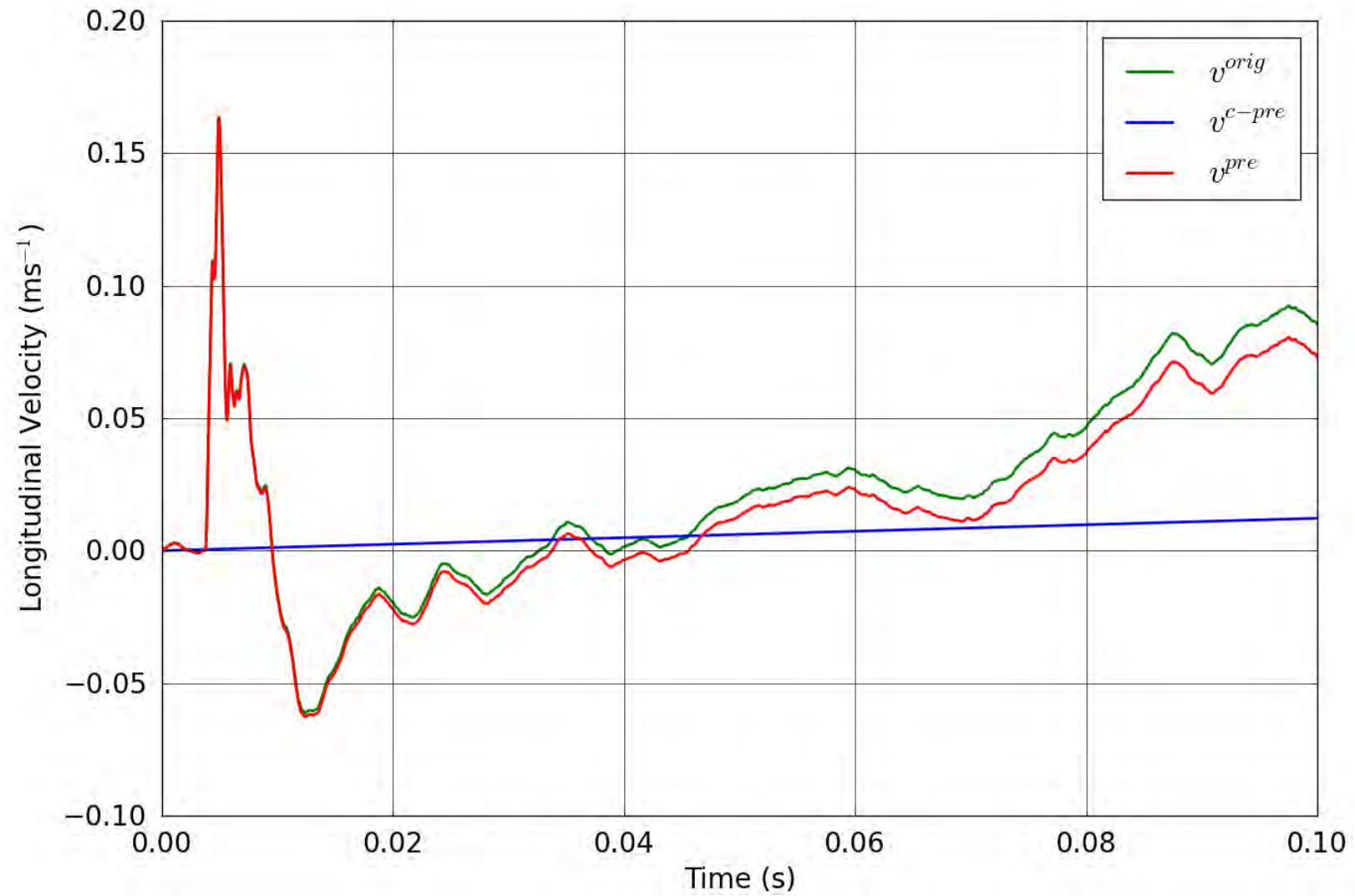
Figure 32. SPE-1 Gauge 6-1-L – Pre-shot baseline correction of the longitudinal velocity.
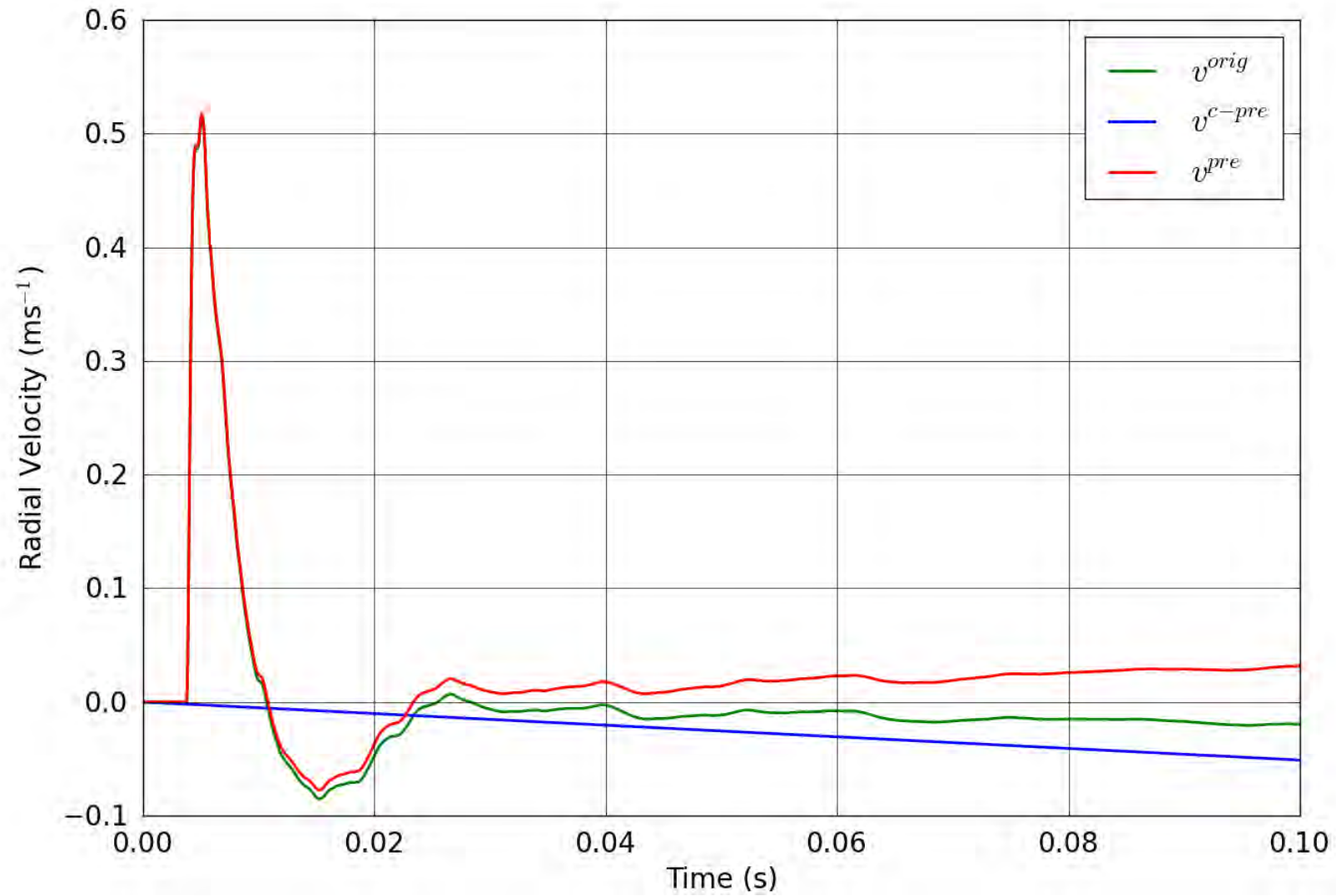
Figure 33. SPE-1 Gauge 6-1-R – Pre-shot baseline correction of the radial velocity.
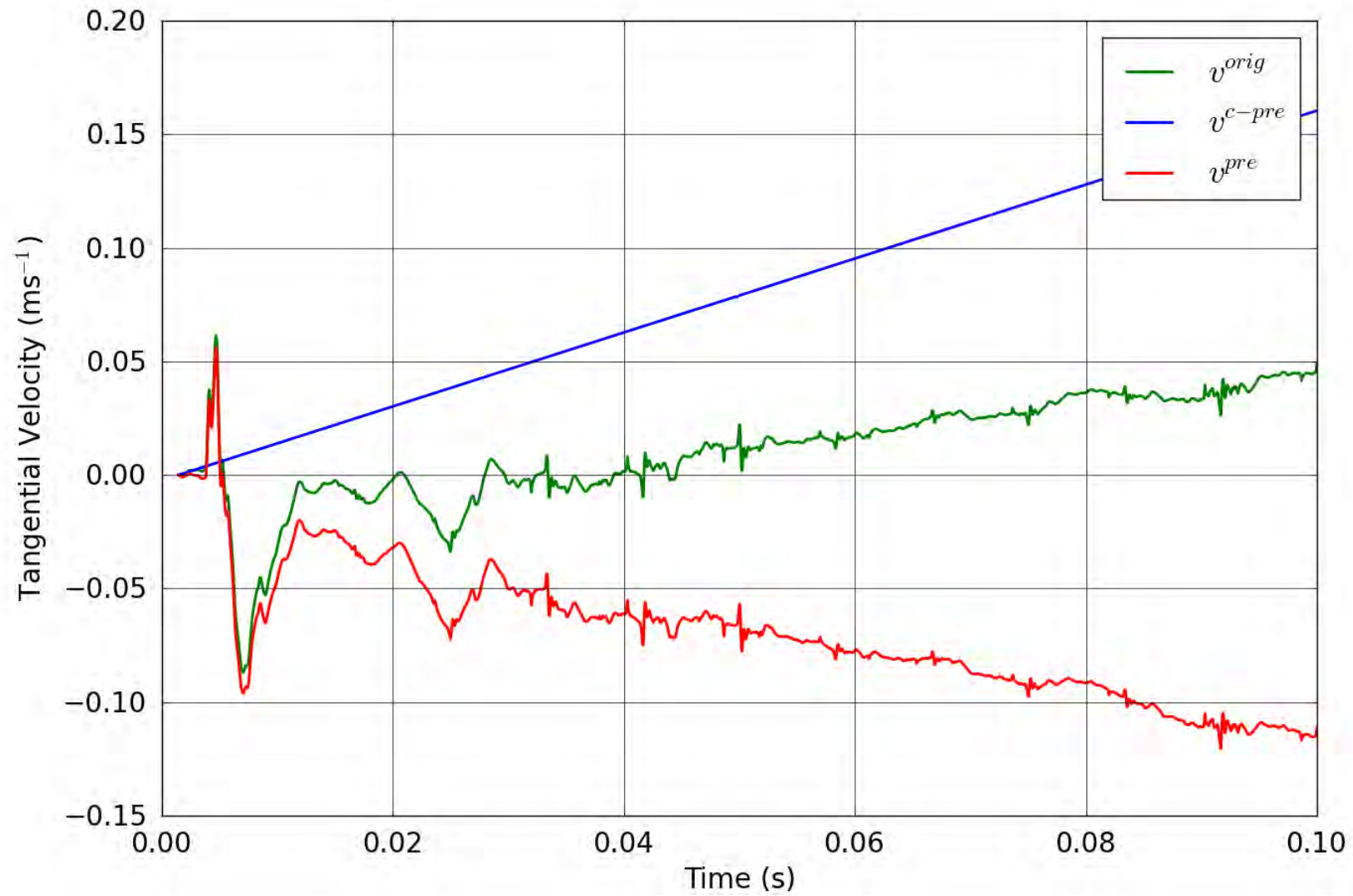
Figure 34. SPE-1 Gauge 6-1-T – Pre-shot baseline correction of the tangential velocity.
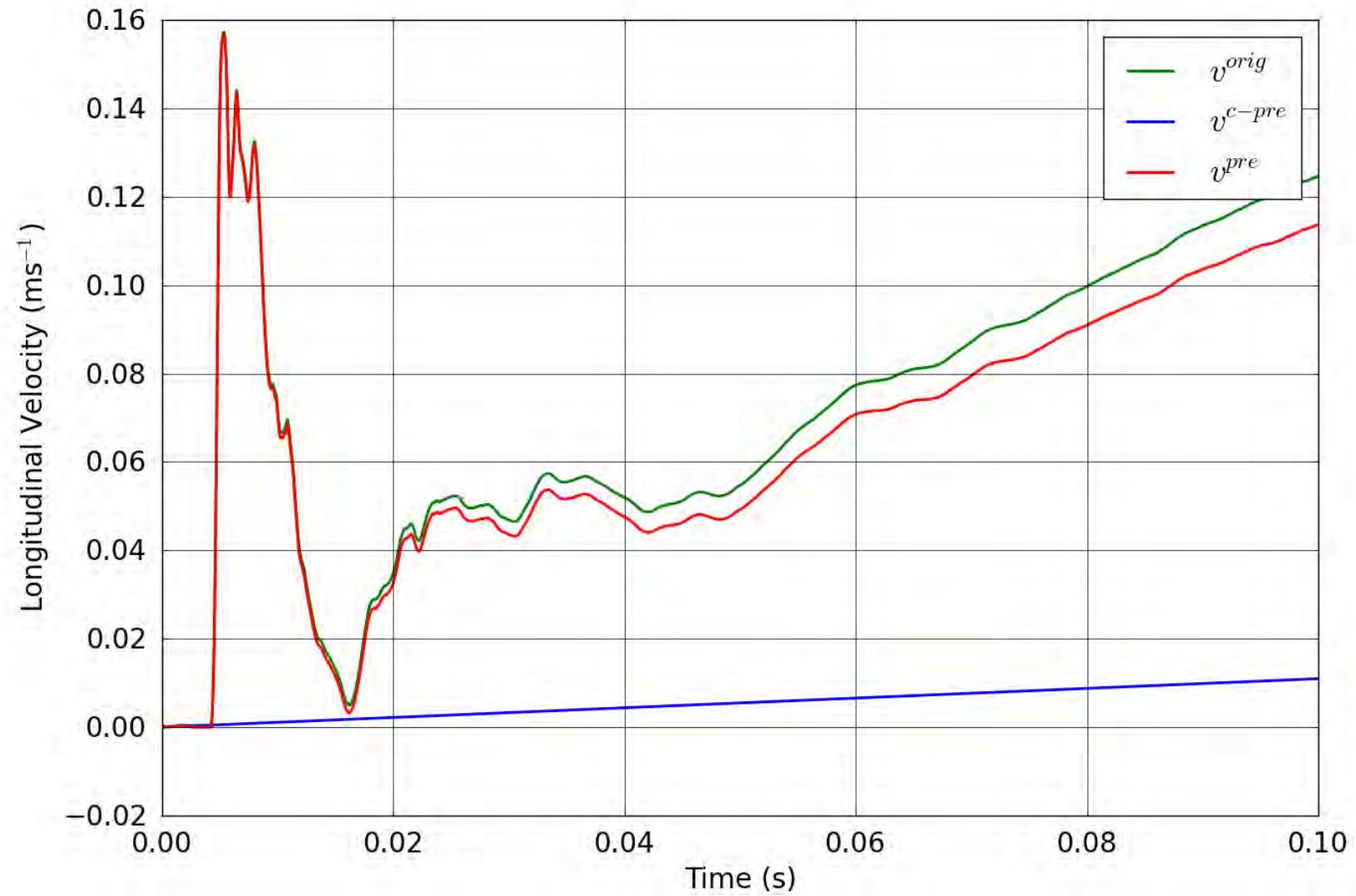
Figure 35. SPE-1 Gauge 6-2-L – Pre-shot baseline correction of the longitudinal velocity.
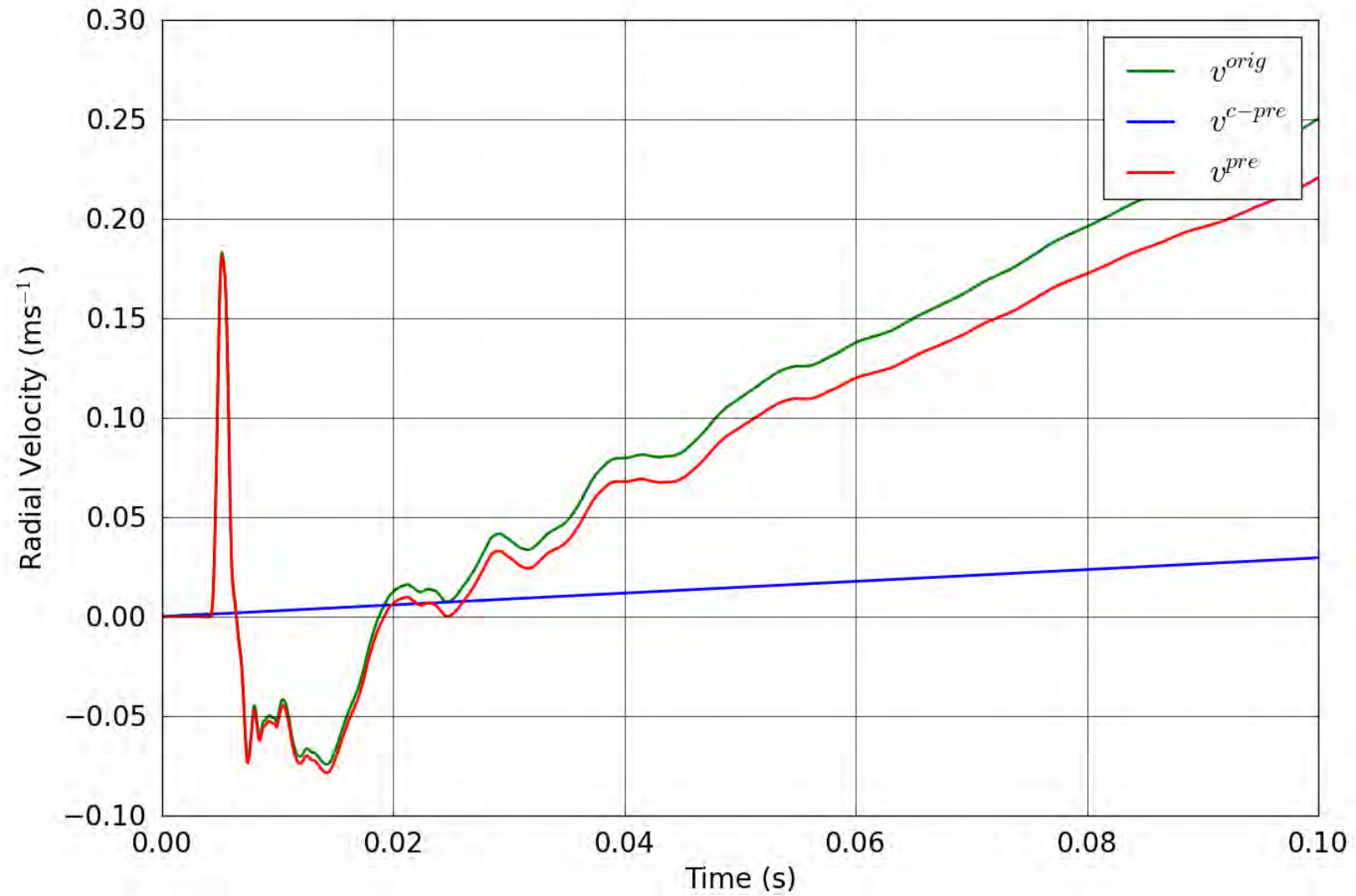
Figure 36. SPE-1 Gauge 6-2-R – Pre-shot baseline correction of the radial velocity.
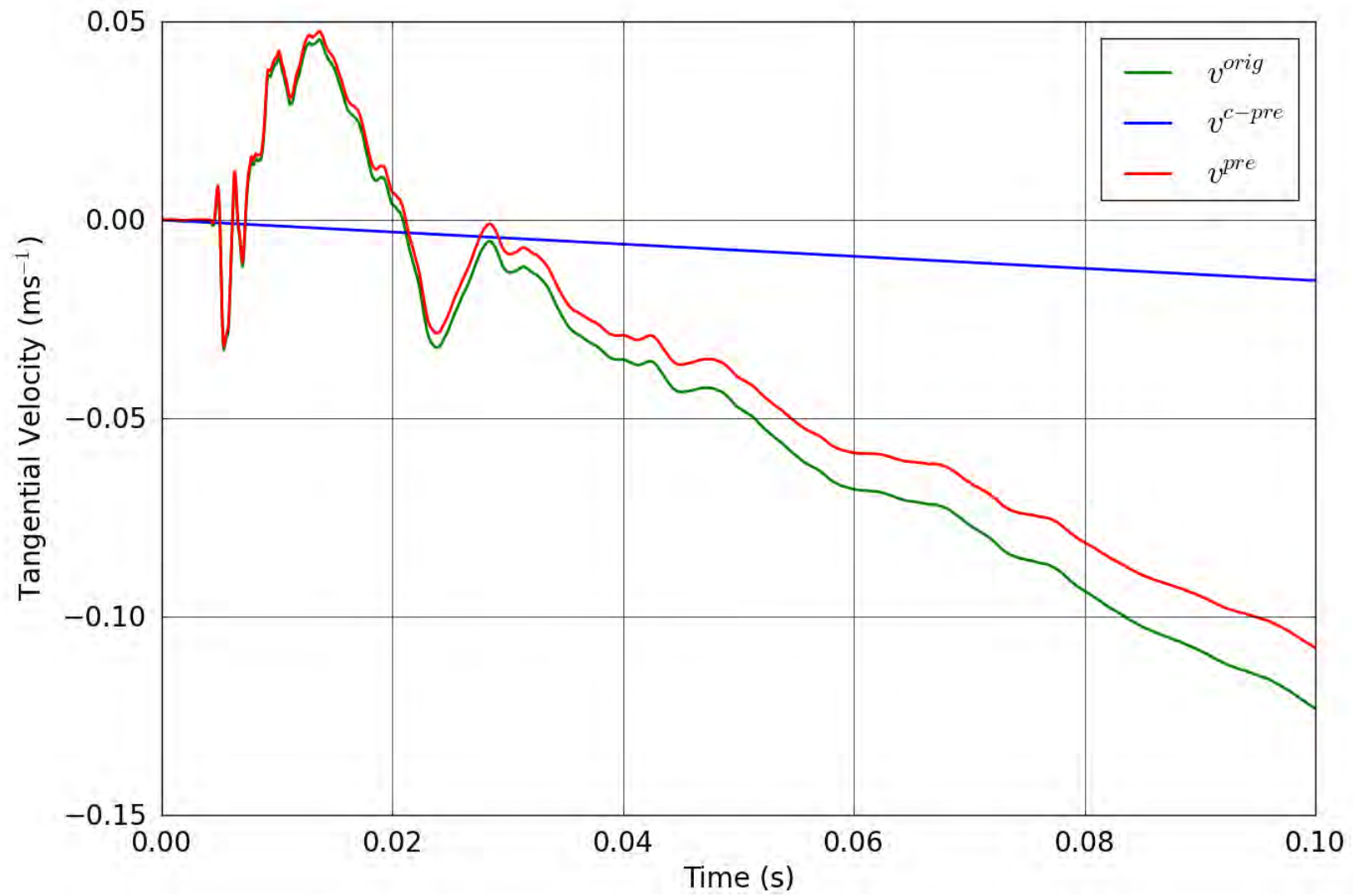
Figure 37. SPE-1 Gauge 6-2-T – Pre-shot baseline correction of the tangential velocity.
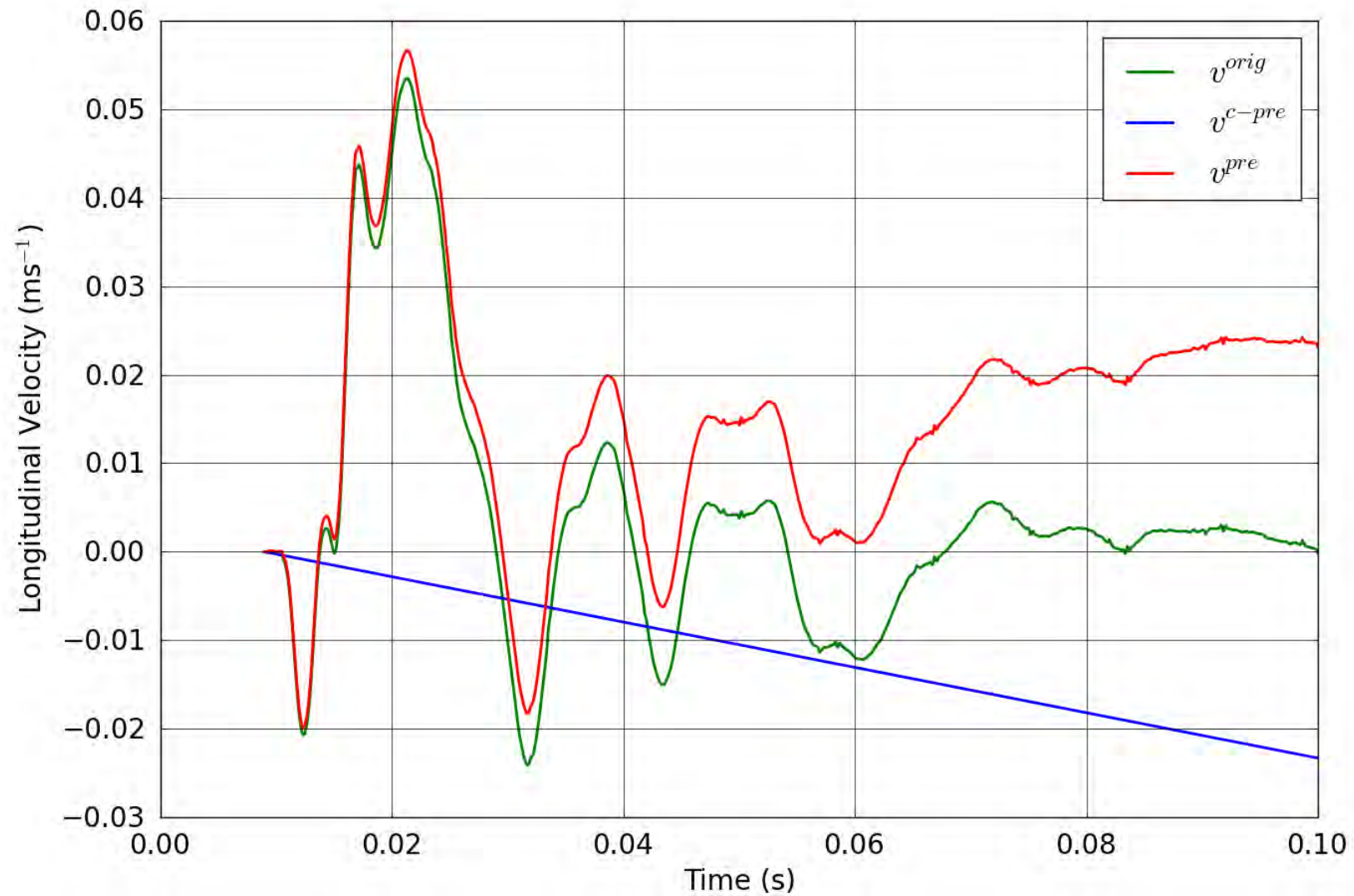
Figure 38. SPE-1 Gauge 6-3-L – Pre-shot baseline correction of the longitudinal velocity.
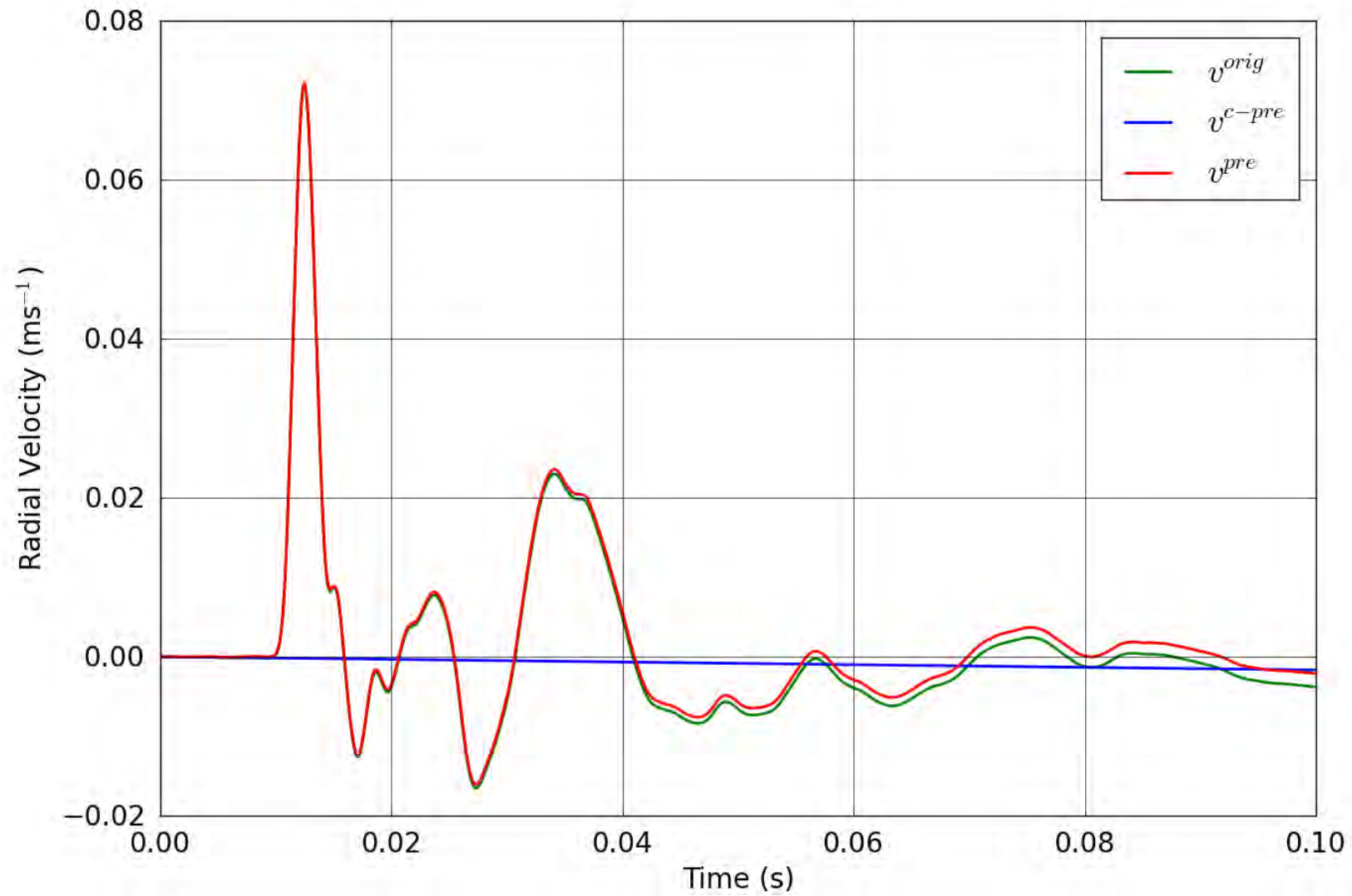
Figure 39. SPE-1 Gauge 6-3-R – Pre-shot baseline correction of the radial velocity.
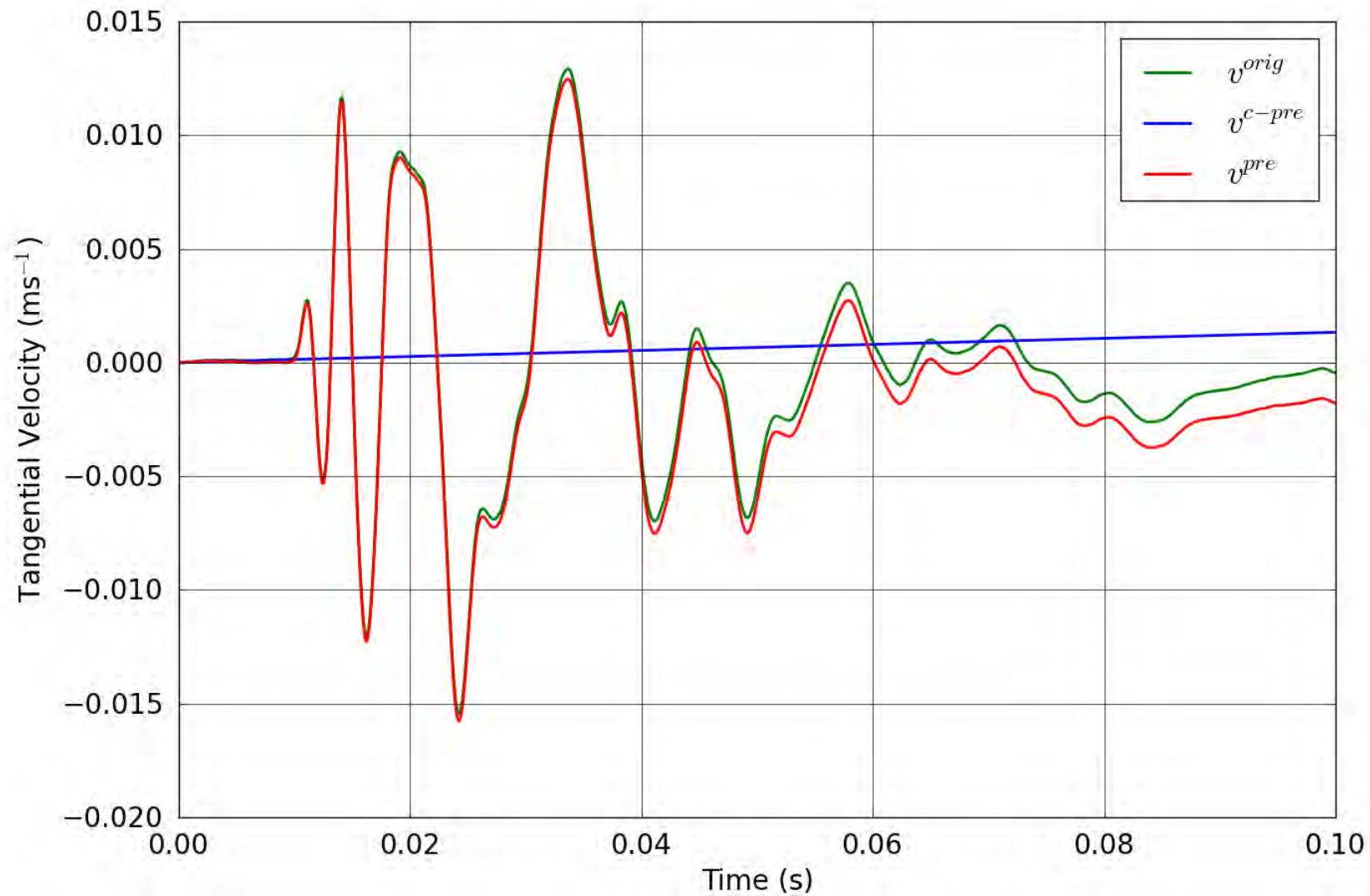
Figure 40. SPE-1 Gauge 6-3-T – Pre-shot baseline correction of the tangential velocity.

2.2. Records corrected for post-arrival baseline shift

The following plots reflect application of both the pre-arrival and the post-arrival baseline shifts. For each record we show the velocity waveform as displayed in Section 1.1 along with a plot of the post-arrival correction and the final velocity waveform. The velocity plot for each gauge is followed by the plot of displacement for this final correction.

The key to the legend in the graphs presented in this section is the following:

- v^{pre} represents the velocity waveforms corrected for the pre-arrival baseline shift.
- $v^{c\text{-}post}$ represents the post-arrival baseline shift acceleration correction in the velocity space.
- v^{final} represents the final velocity waveforms corrected for pre- and post-arrival baseline shifts.
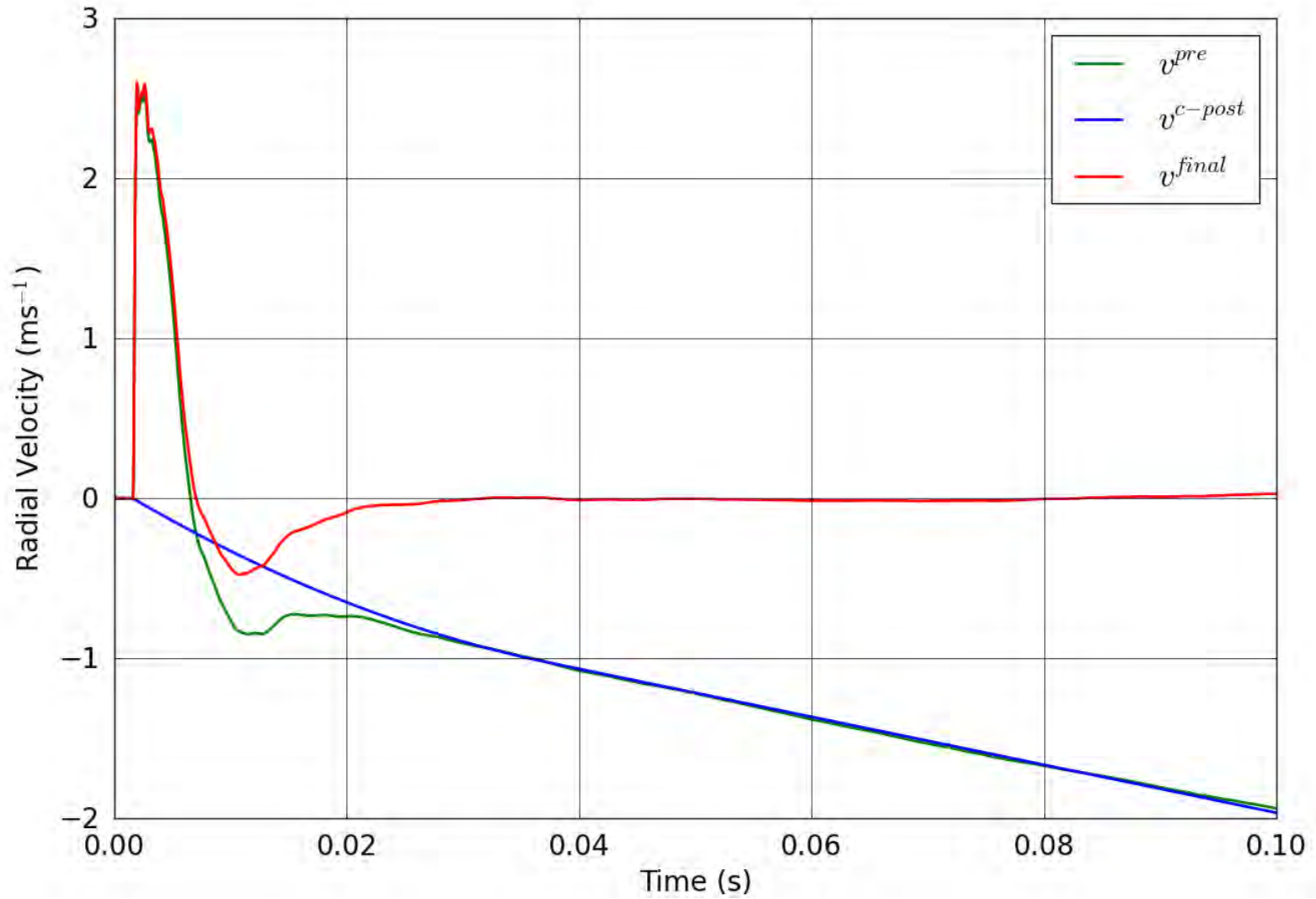
Figure 41. SPE-1 Gauge 1-1-R – Correction of the radial velocity.
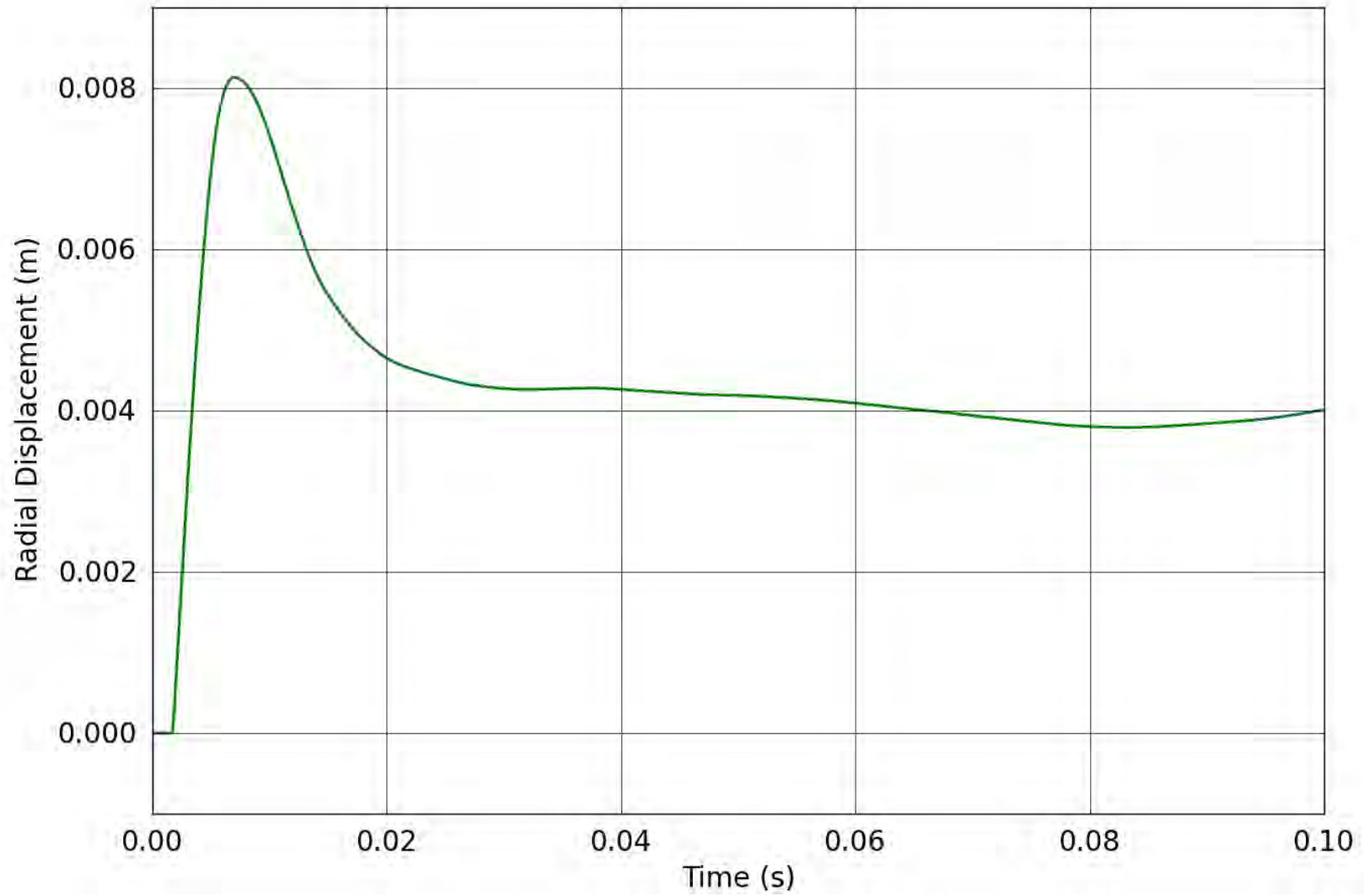
Figure 42. SPE-1 Gauge 1-1-R – Radial displacement obtained from the corrected radial velocity.
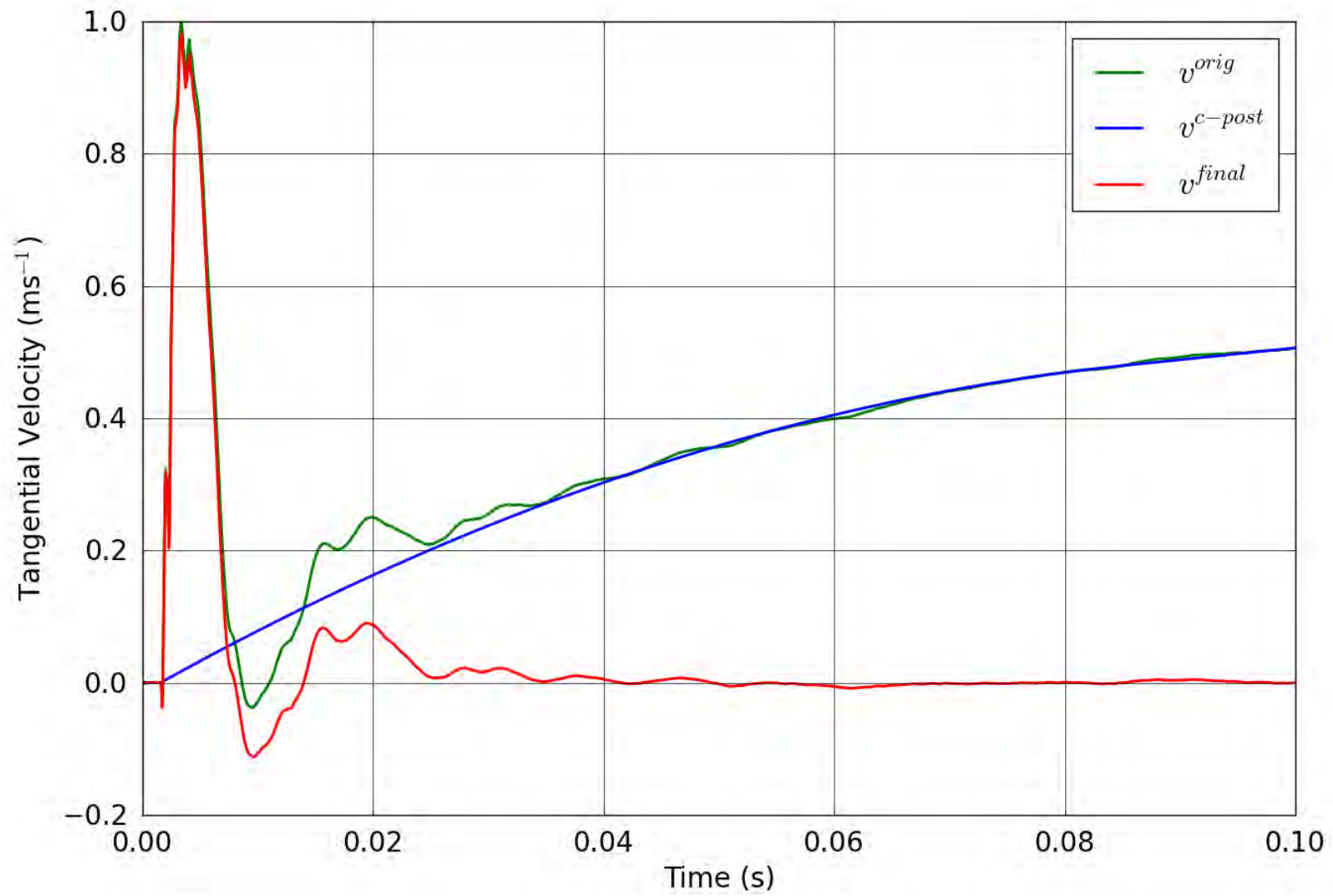
Figure 43. SPE-1 Gauge 1-1-T – Correction of the tangential velocity.
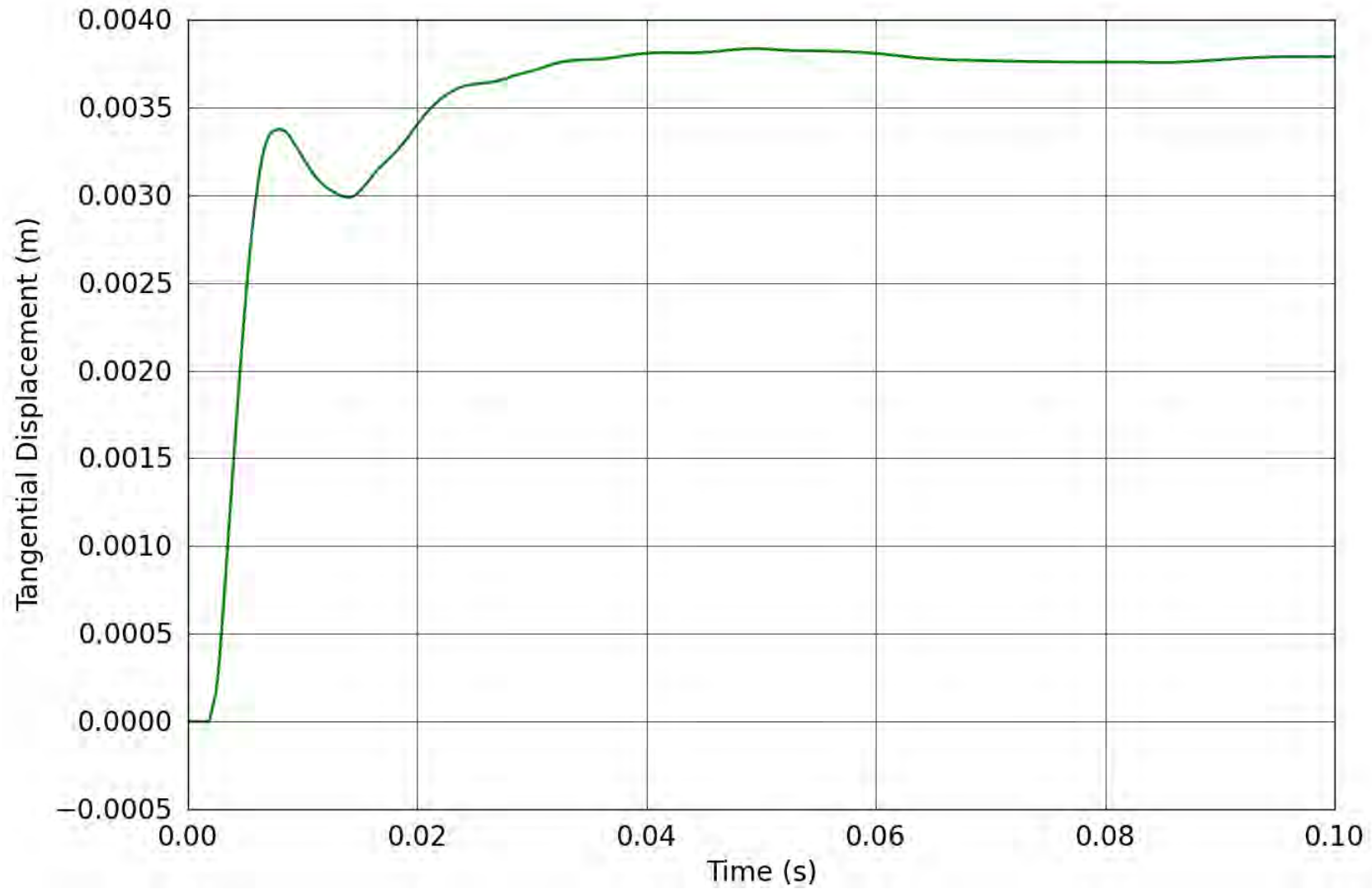
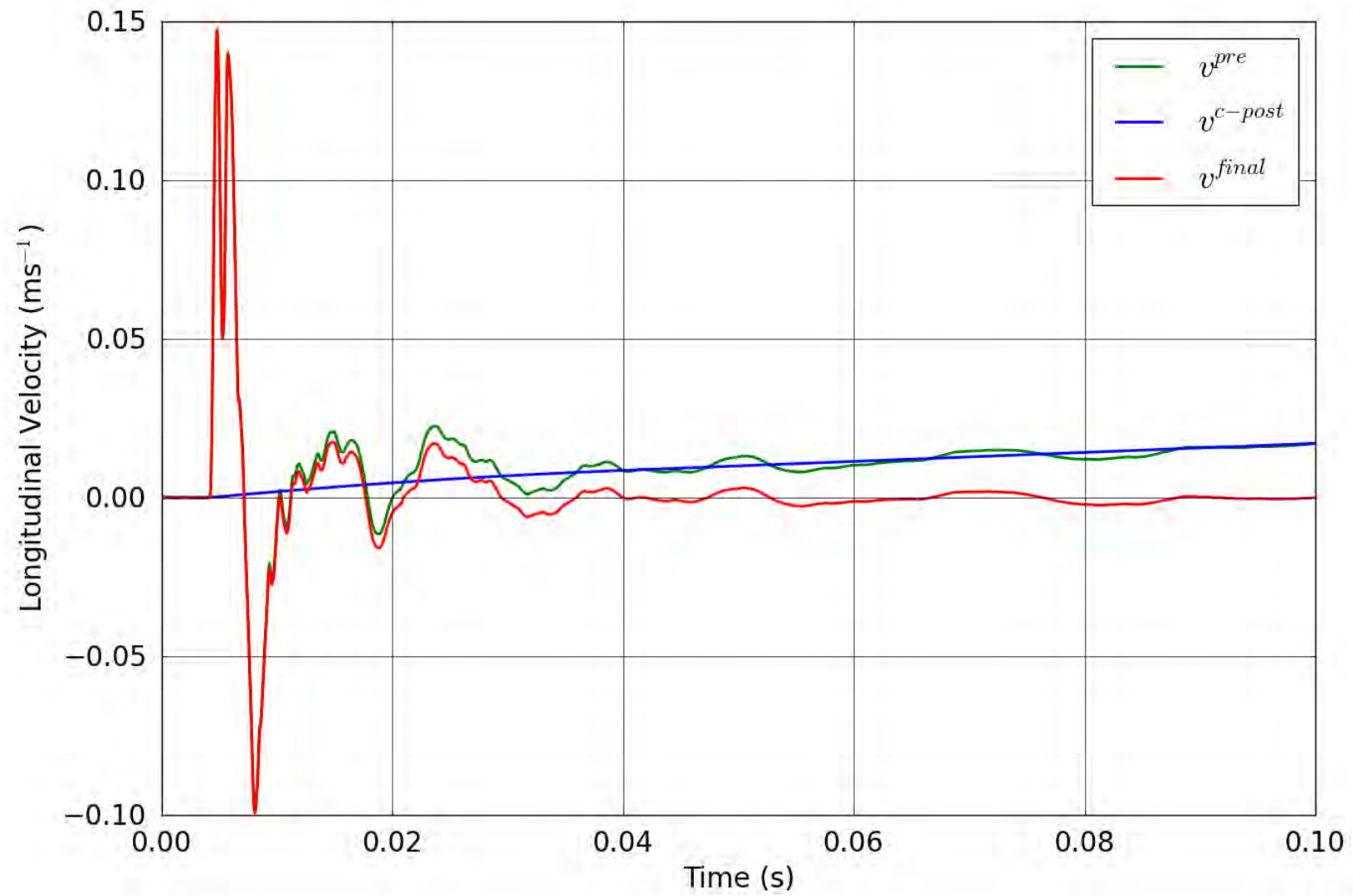Figure 44. SPE-1 Gauge 1-1-T – Tangential displacement obtained from the corrected tangential velocity.
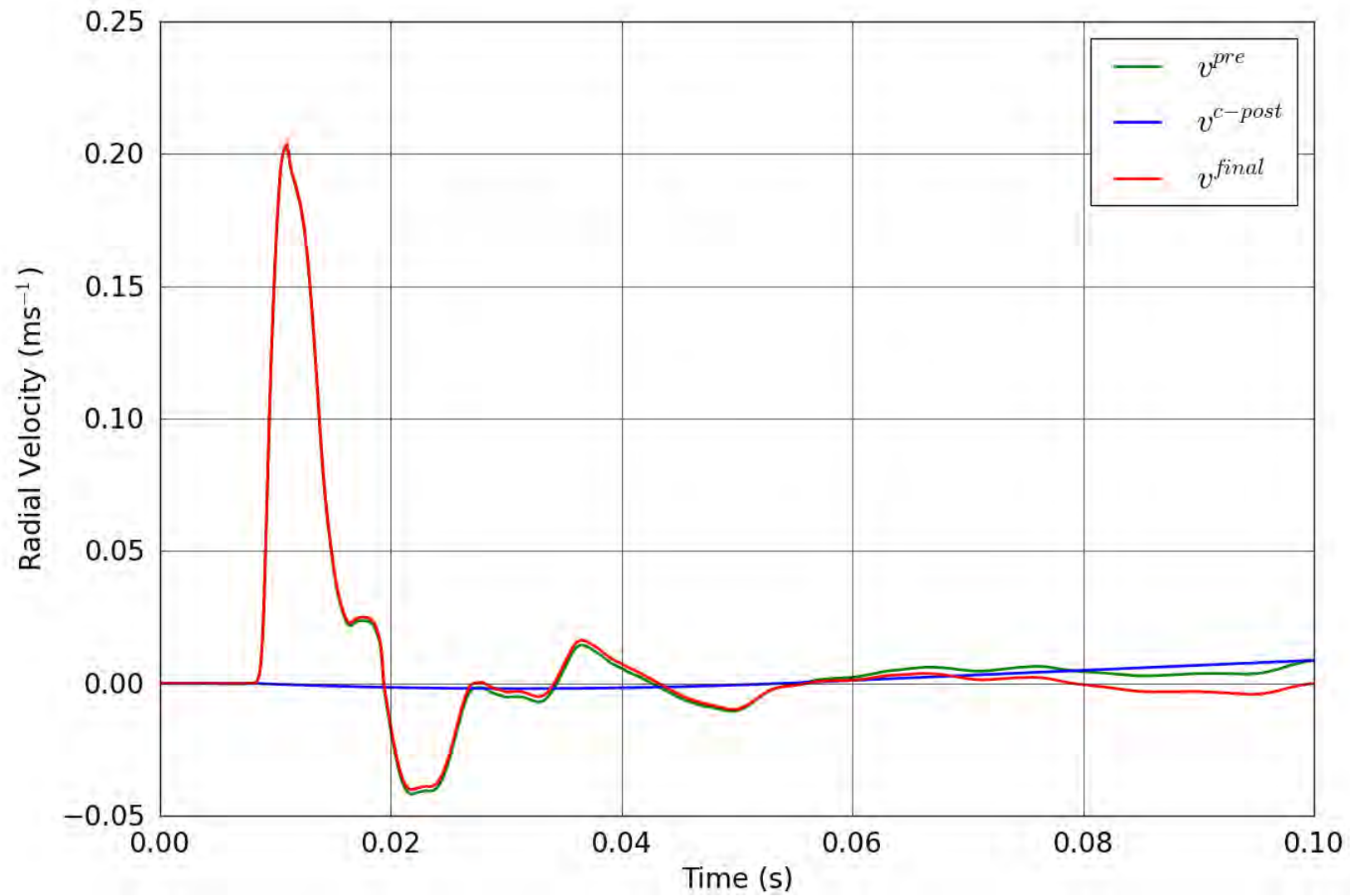
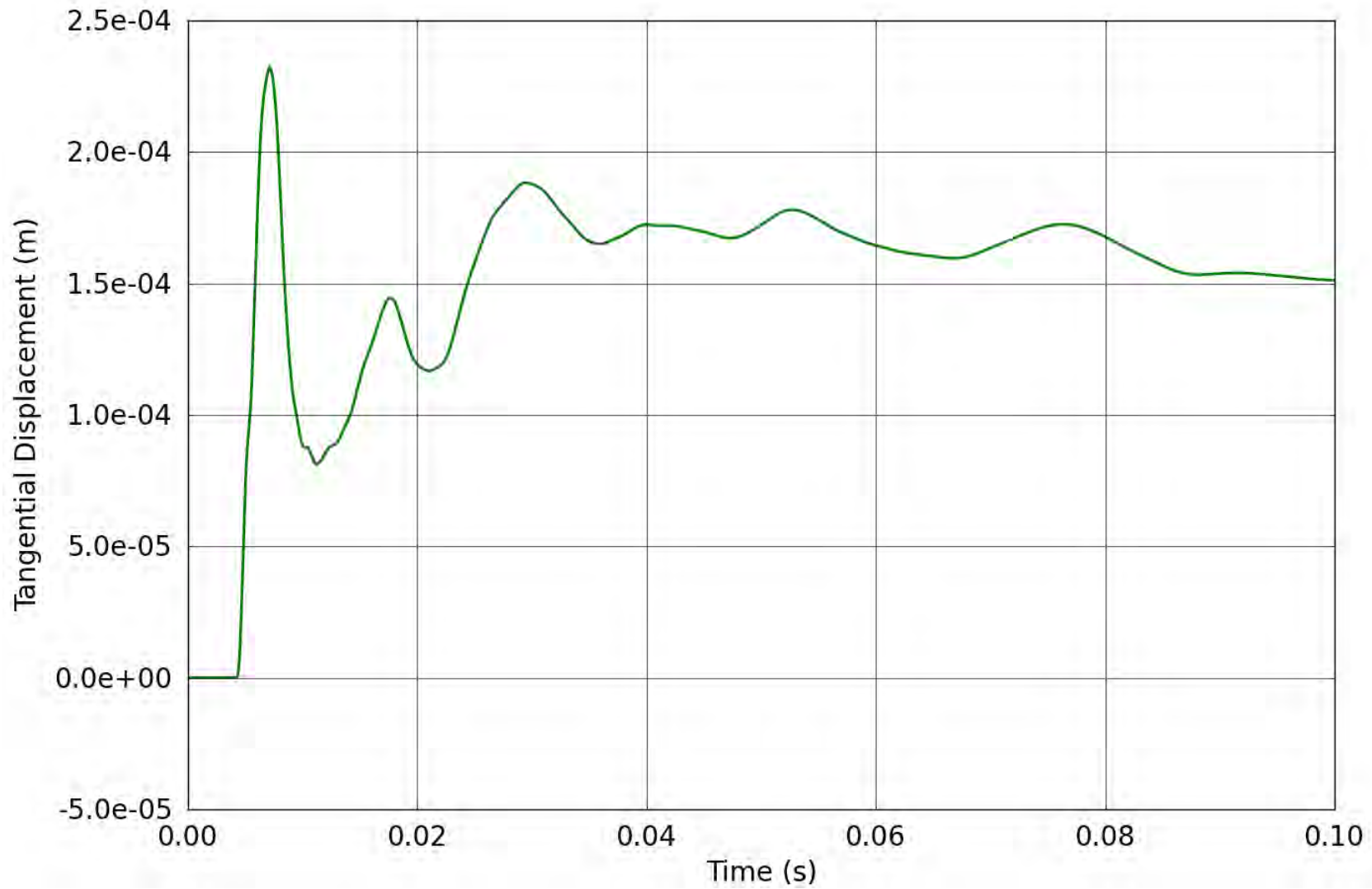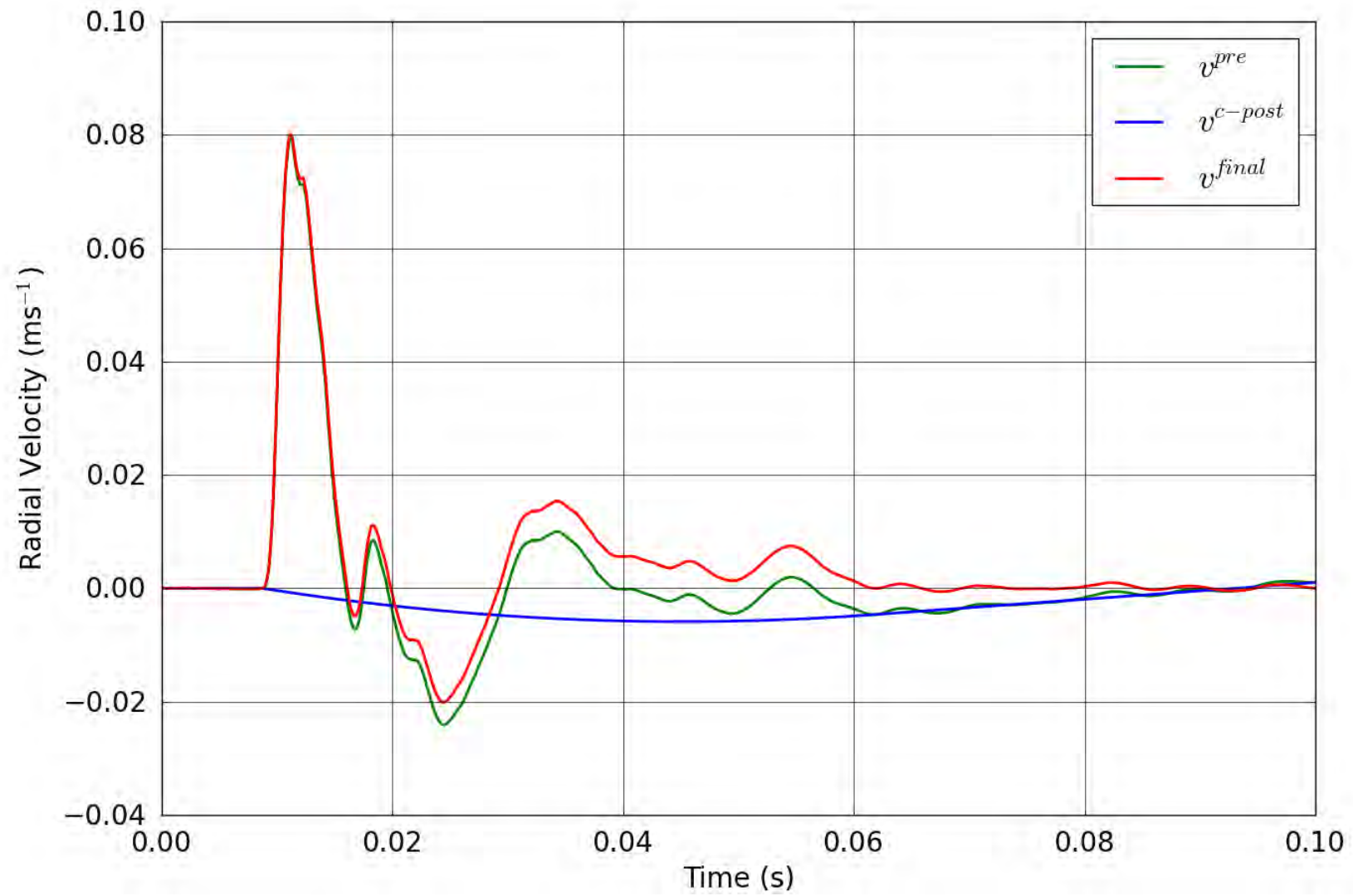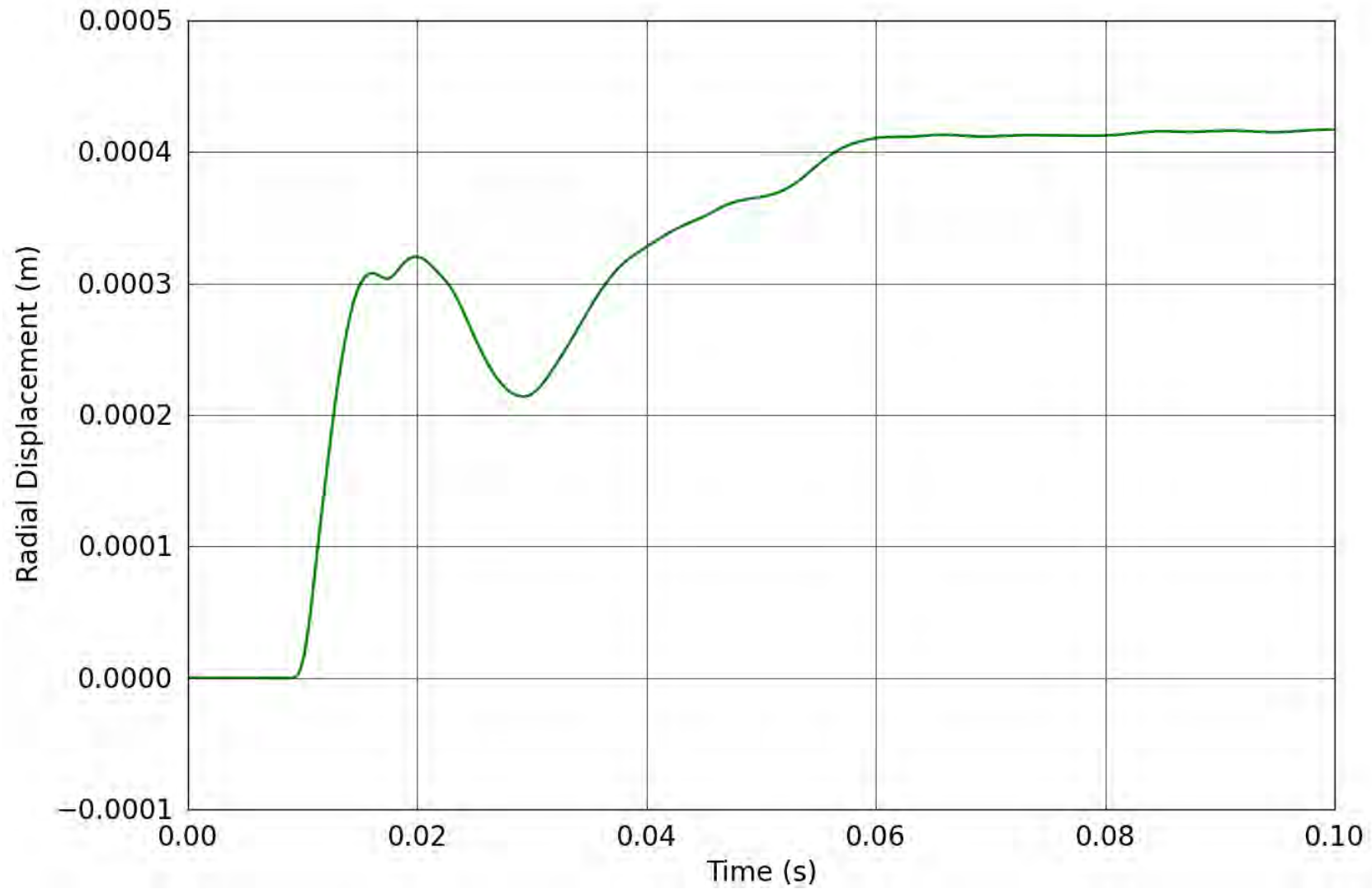Figure 45. SPE-1 Gauge 1-3-R – Correction of the radial velocity.
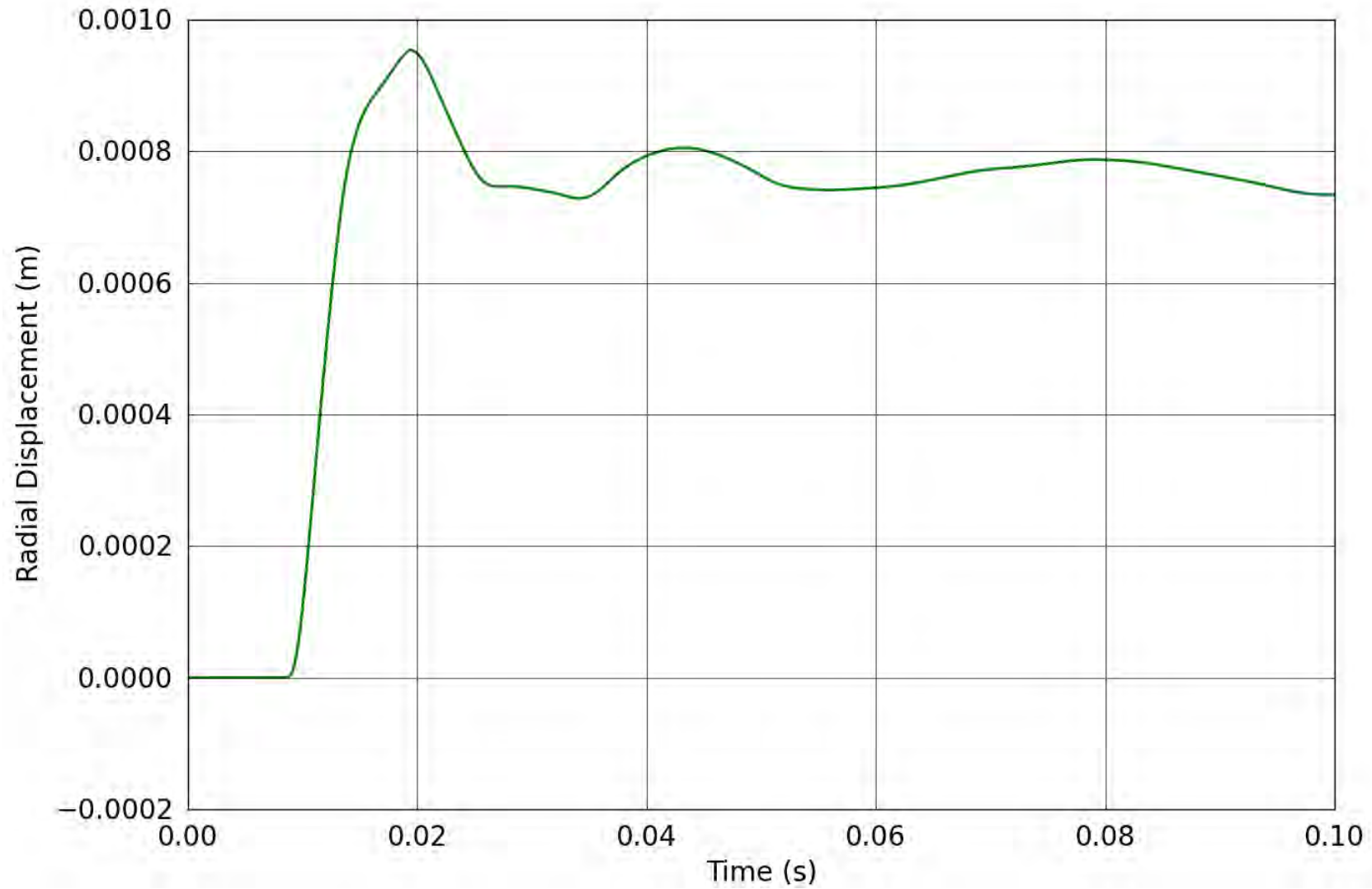
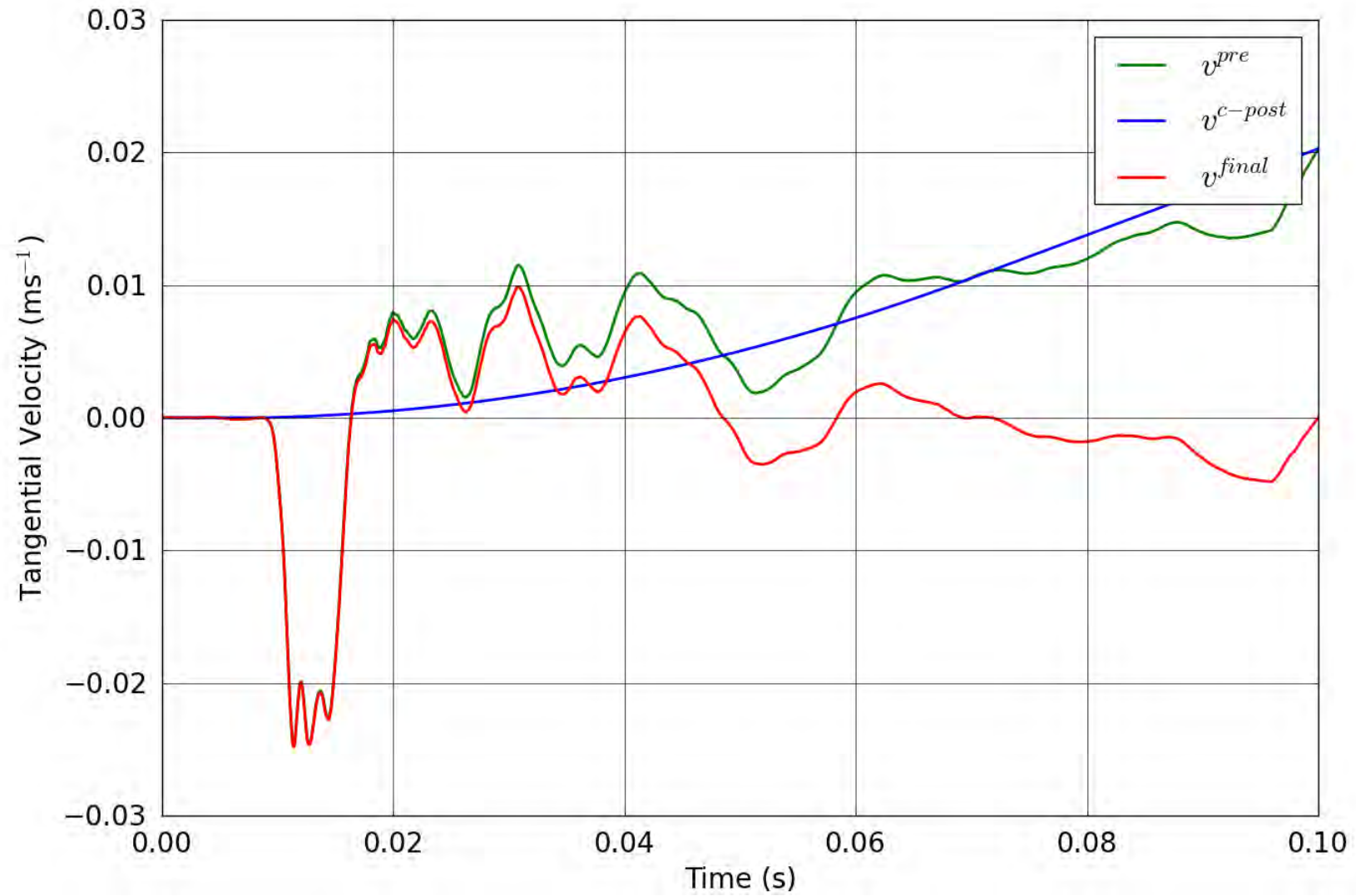Figure 46. SPE-1 Gauge 1-3-R – Radial displacement obtained from the corrected radial velocity.
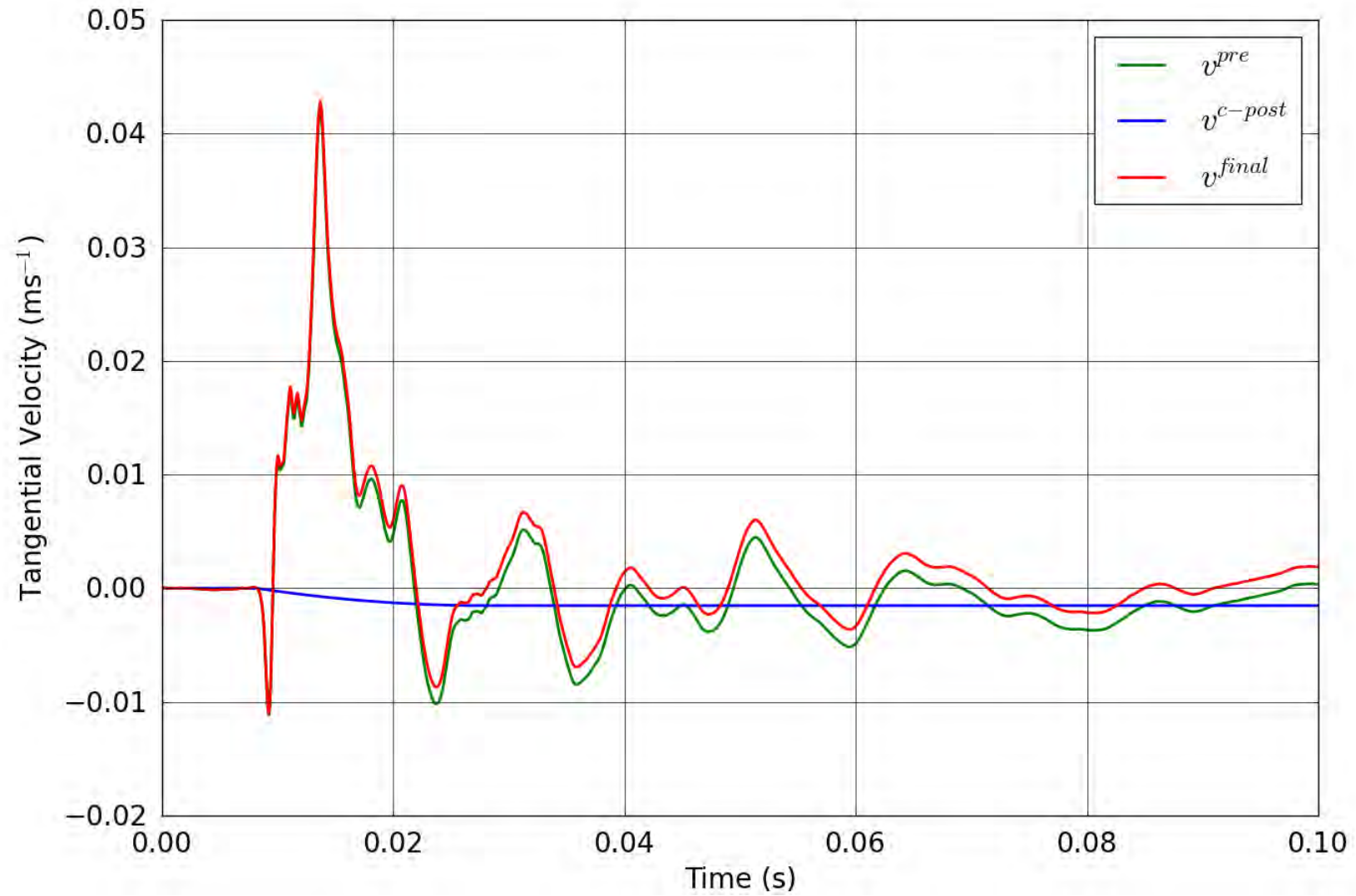
Figure 47. SPE-1 Gauge 1-3-T – Correction of the tangential velocity.
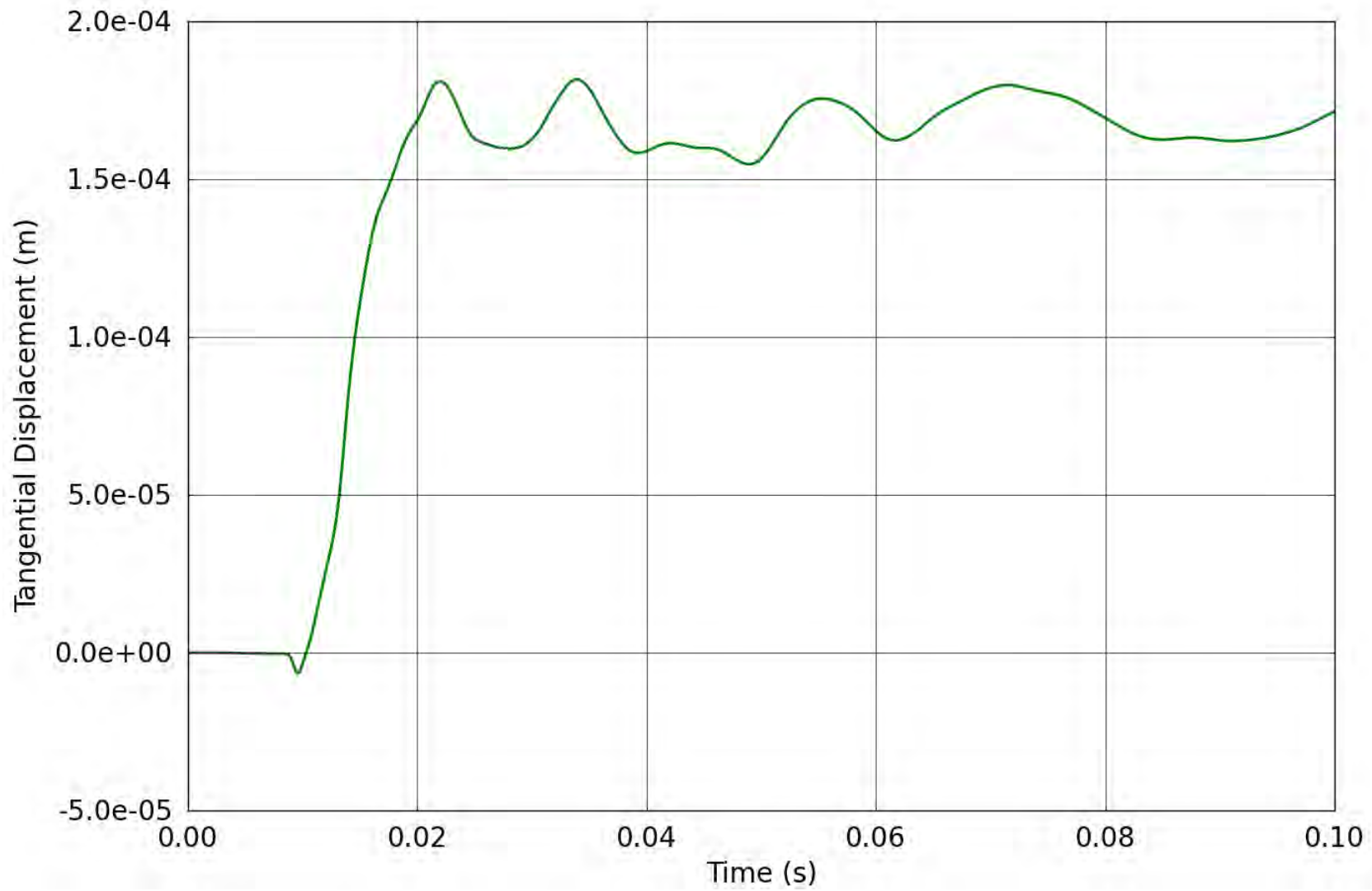
Figure 48. SPE-1 Gauge 1-3-T – Tangential displacement obtained from the corrected tangential velocity.
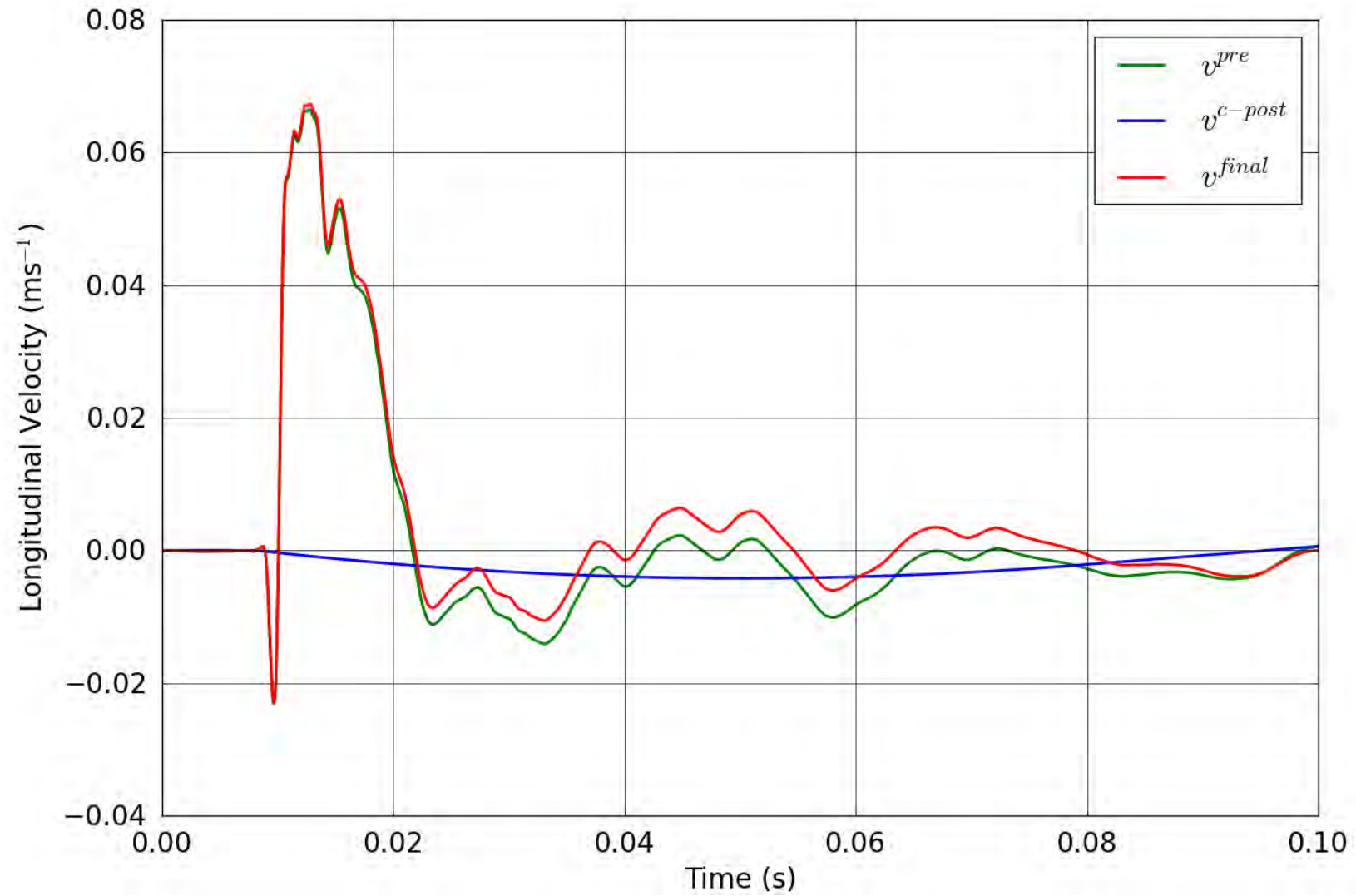
Figure 49. SPE-1 Gauge 1-3-L – Correction of the longitudinal velocity.
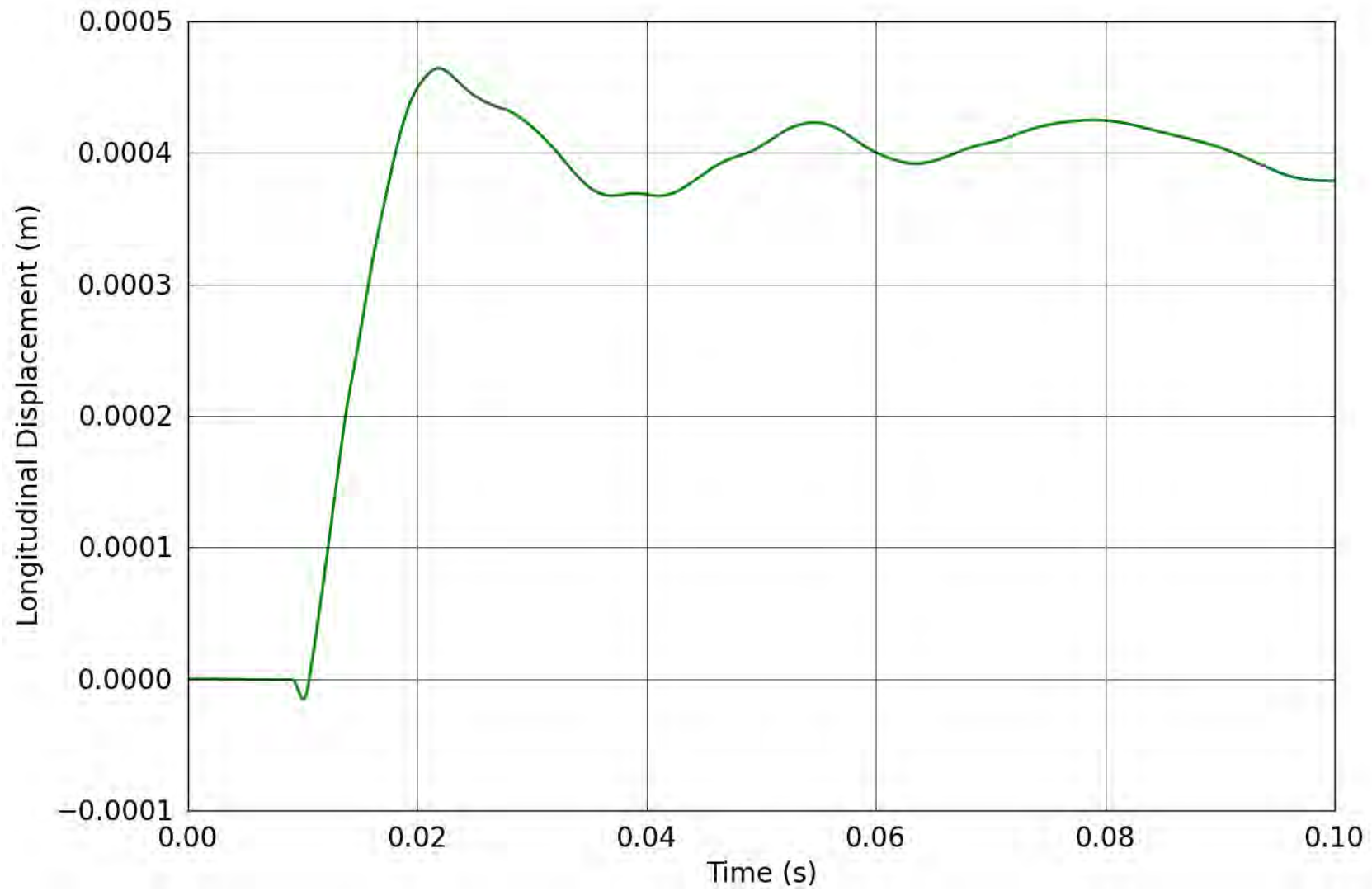
Figure 50. SPE-1 Gauge 1-3-L – Longitudinal displacement obtained from the corrected longitudinal velocity.
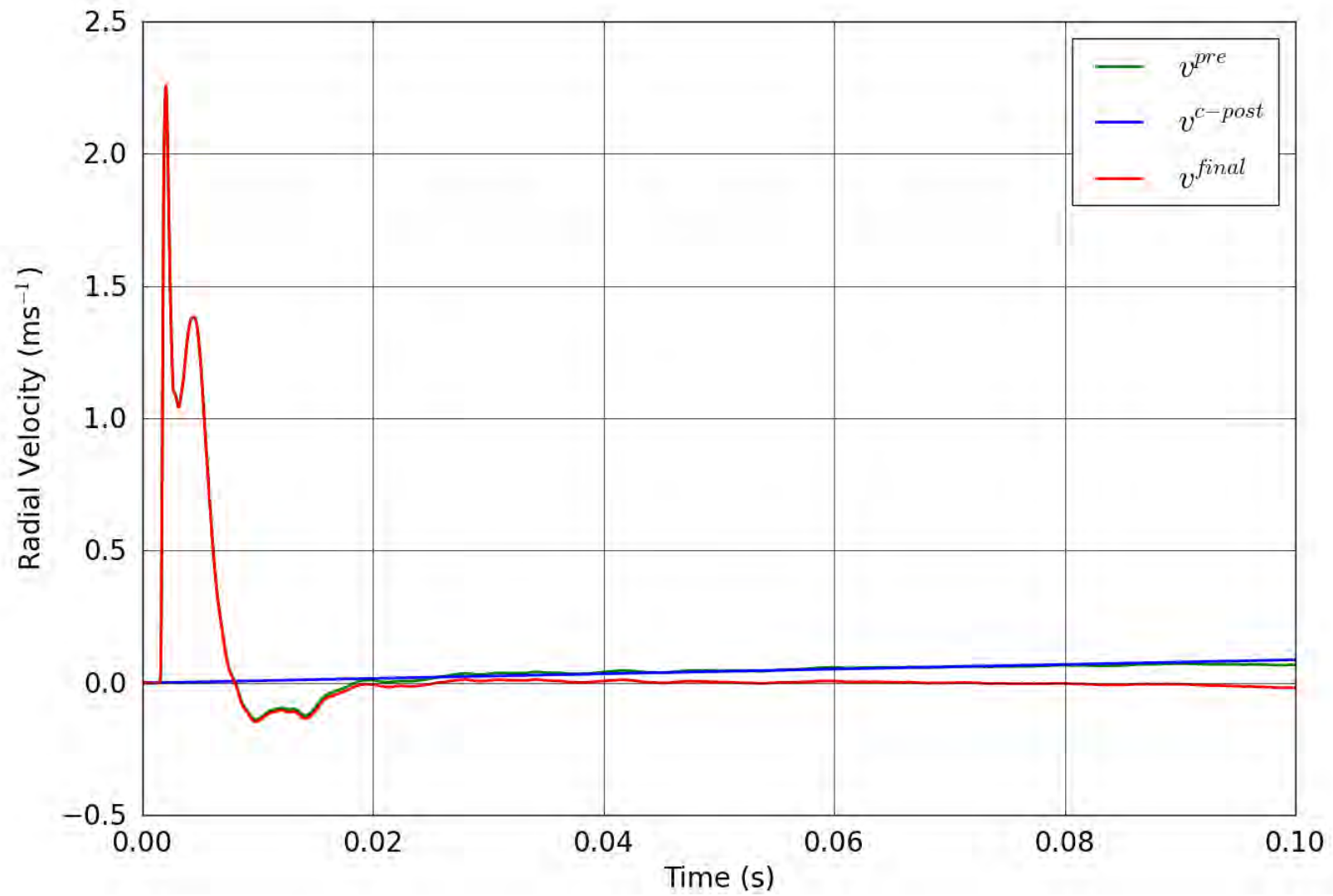
Figure 51. SPE-1 Gauge 2-1-R – Correction of the radial velocity.
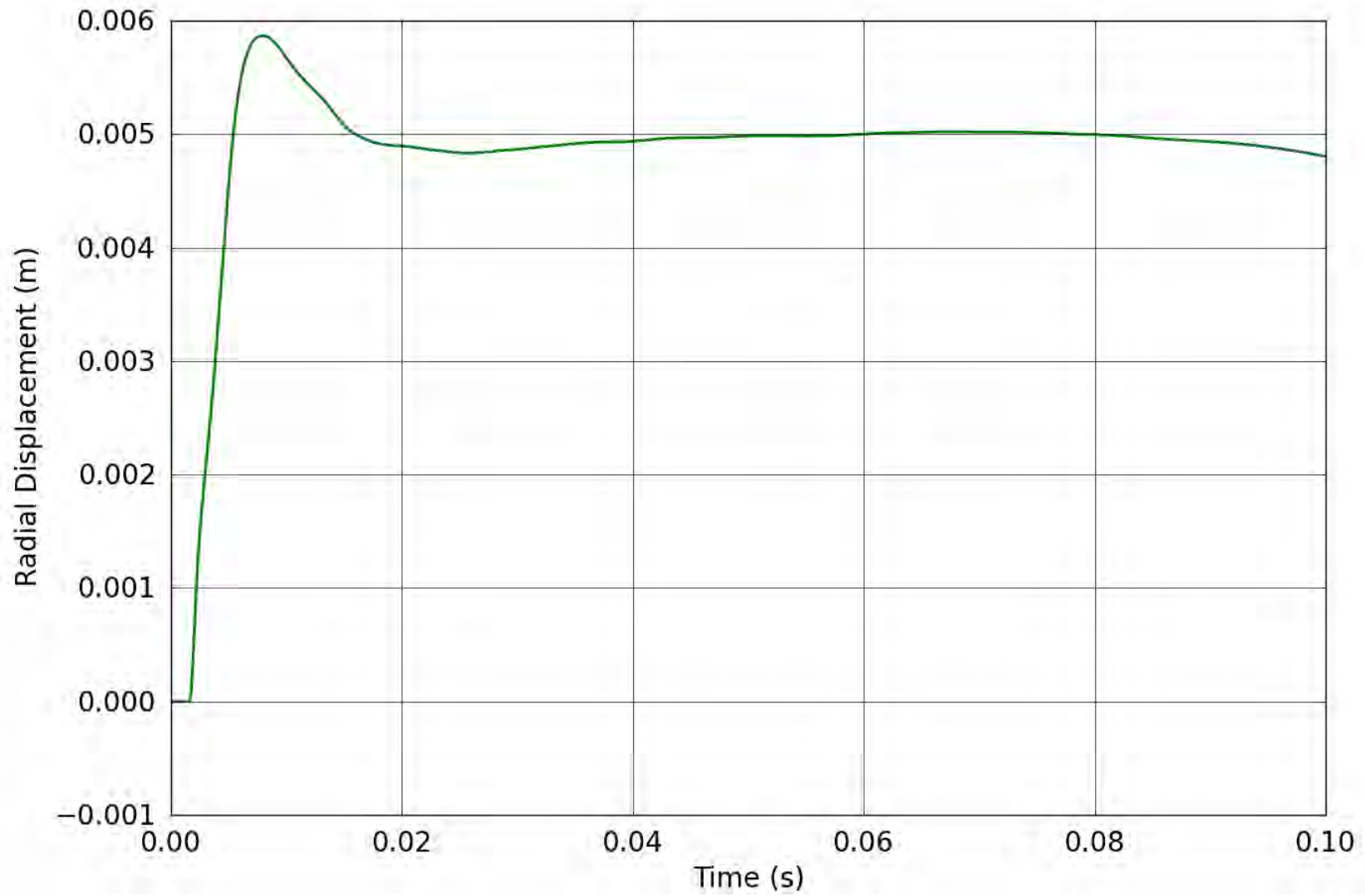
Figure 52. SPE-1 Gauge 2-1-R – Radial displacement obtained from the corrected radial velocity.
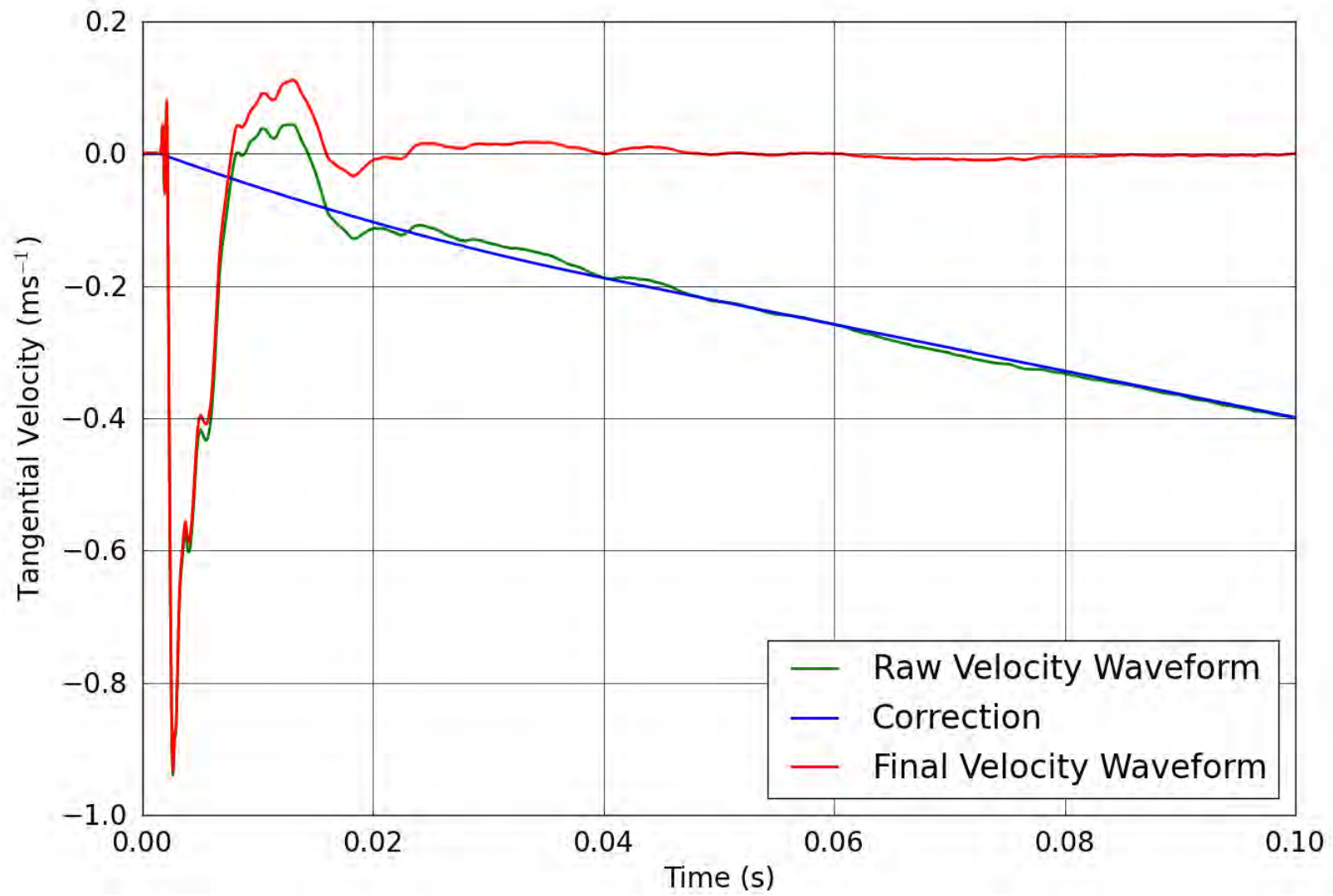
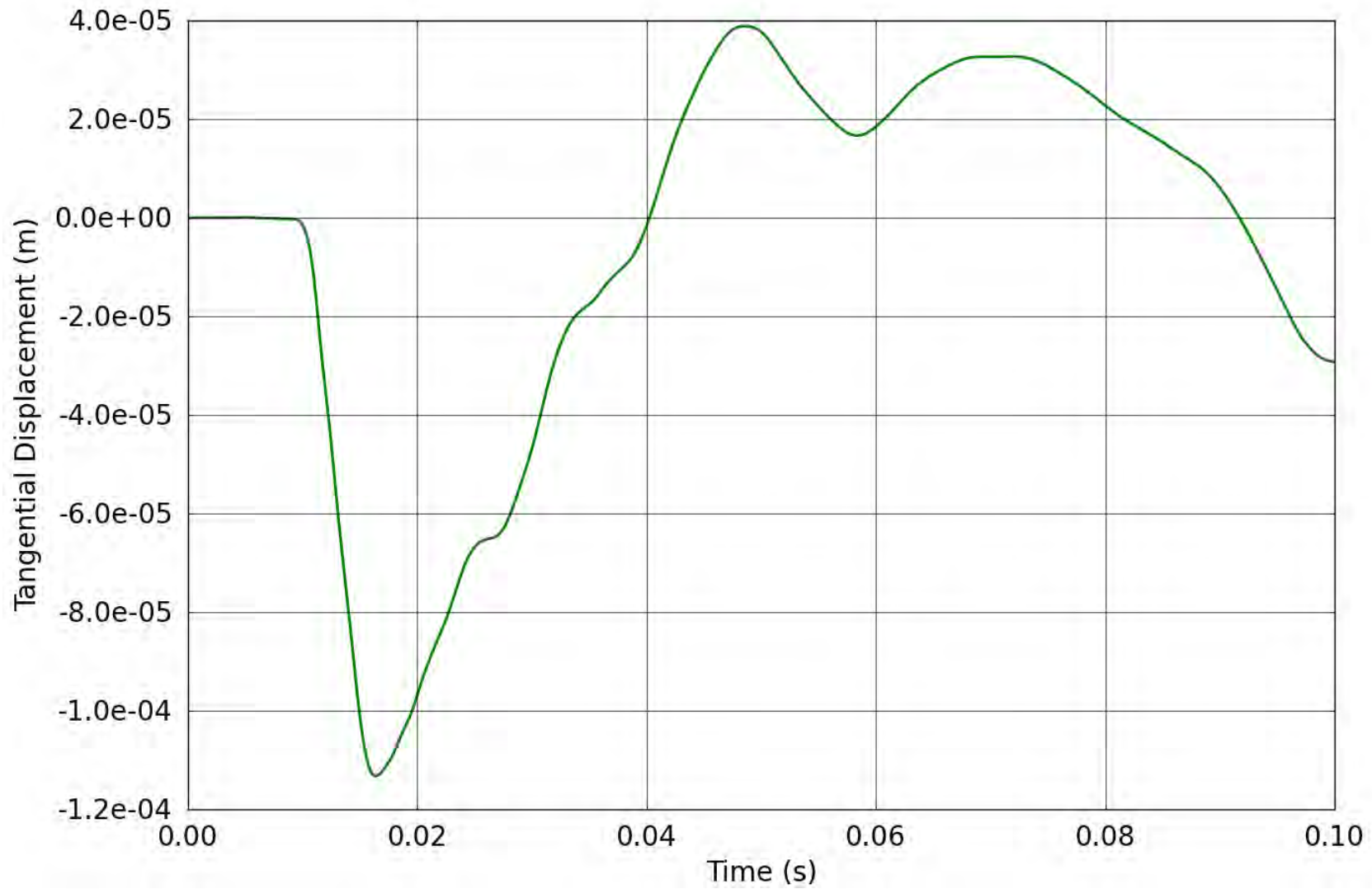Figure 53. SPE-1 Gauge 2-1-T – Correction of the tangential velocity.
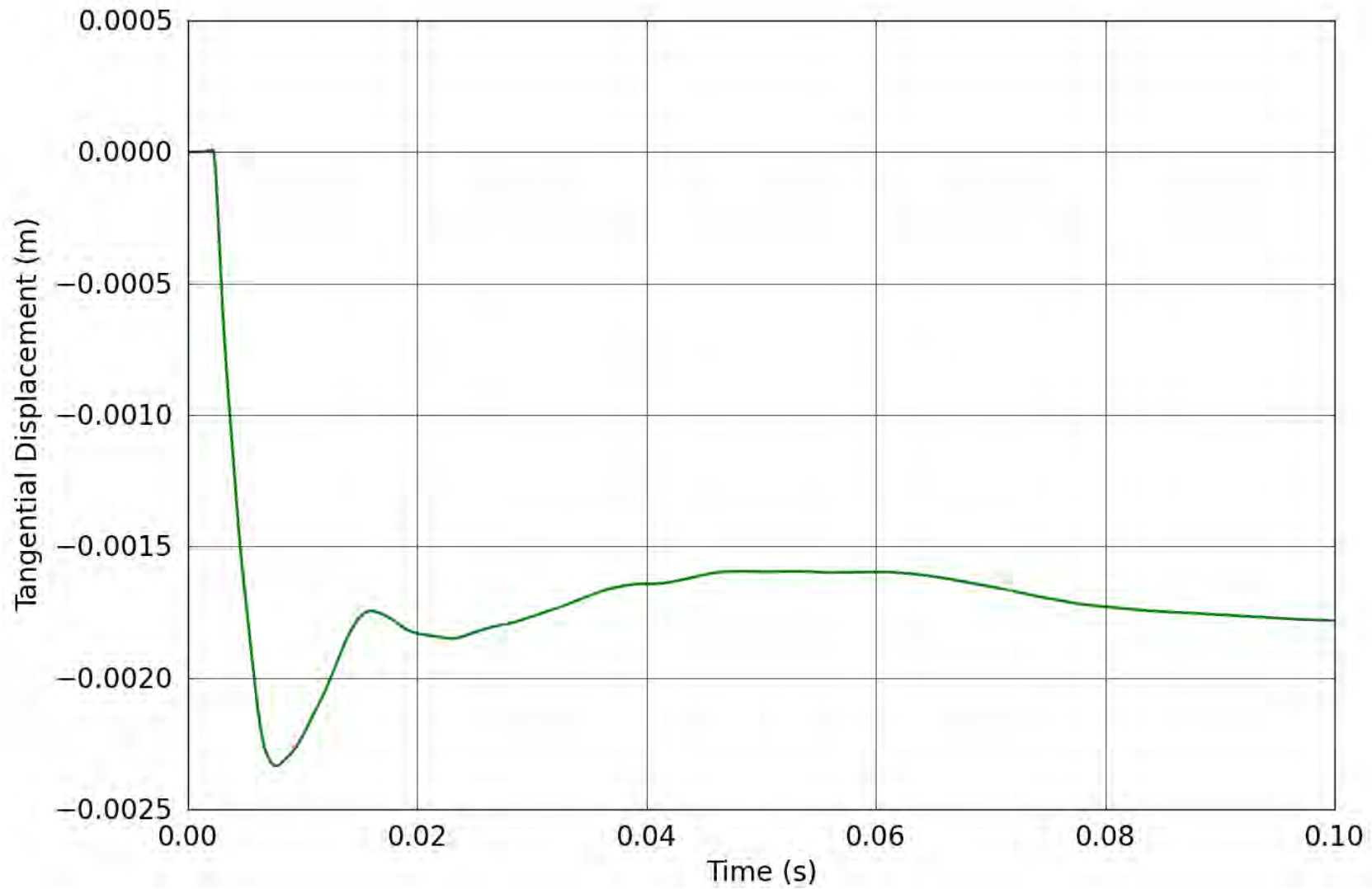
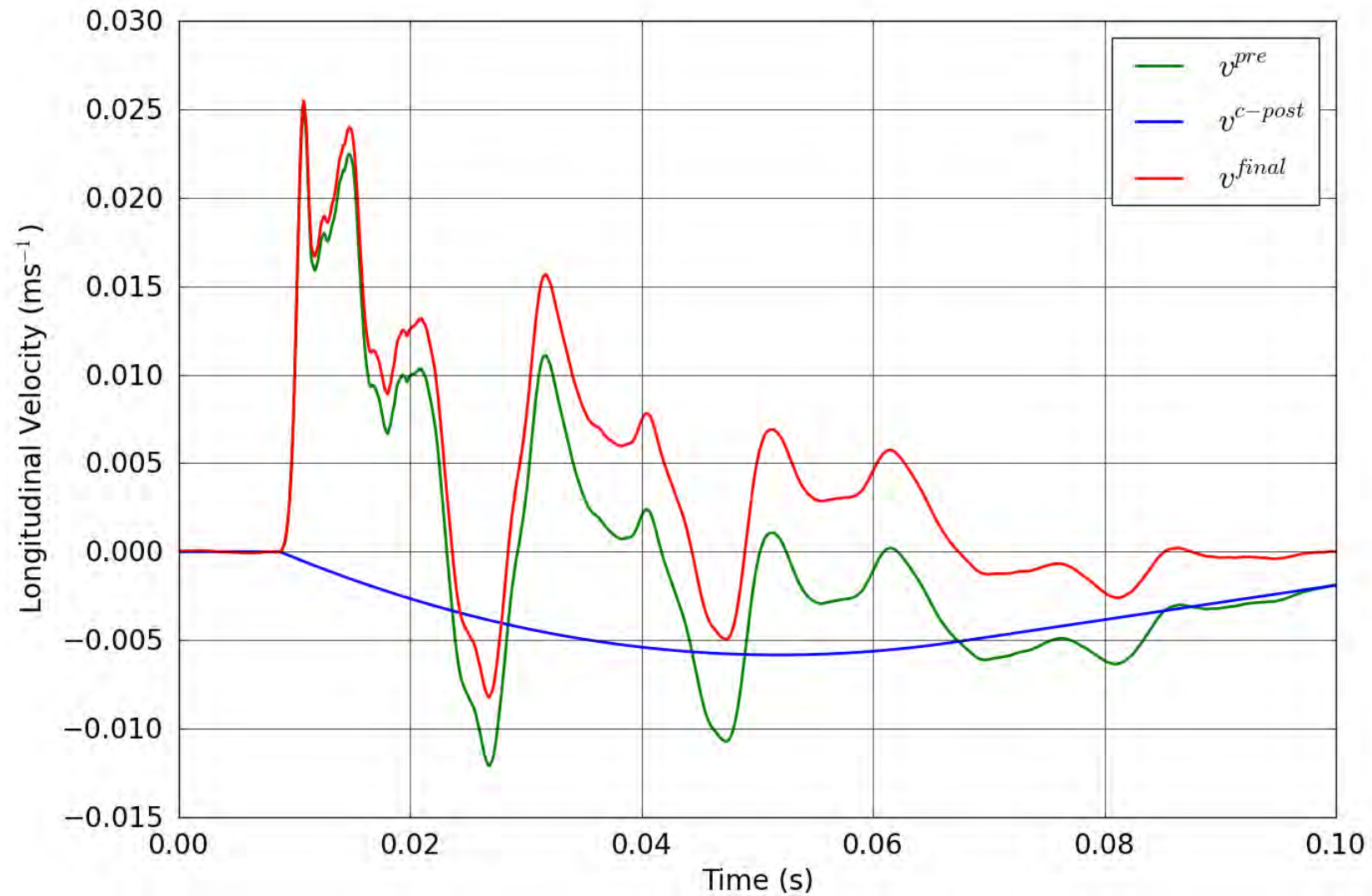Figure 54. SPE-1 Gauge 2-1-T – Tangential displacement obtained from the corrected tangential velocity.
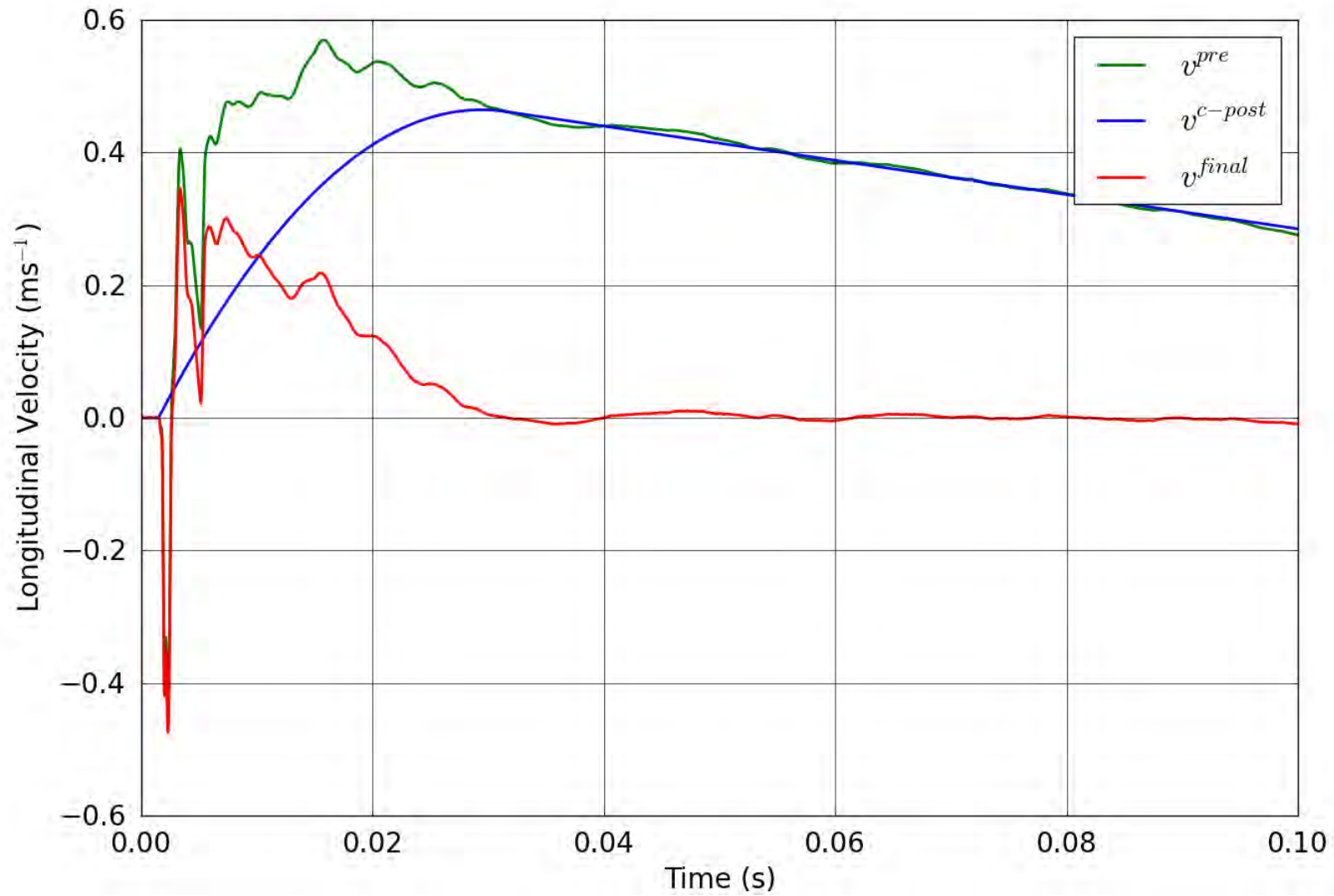
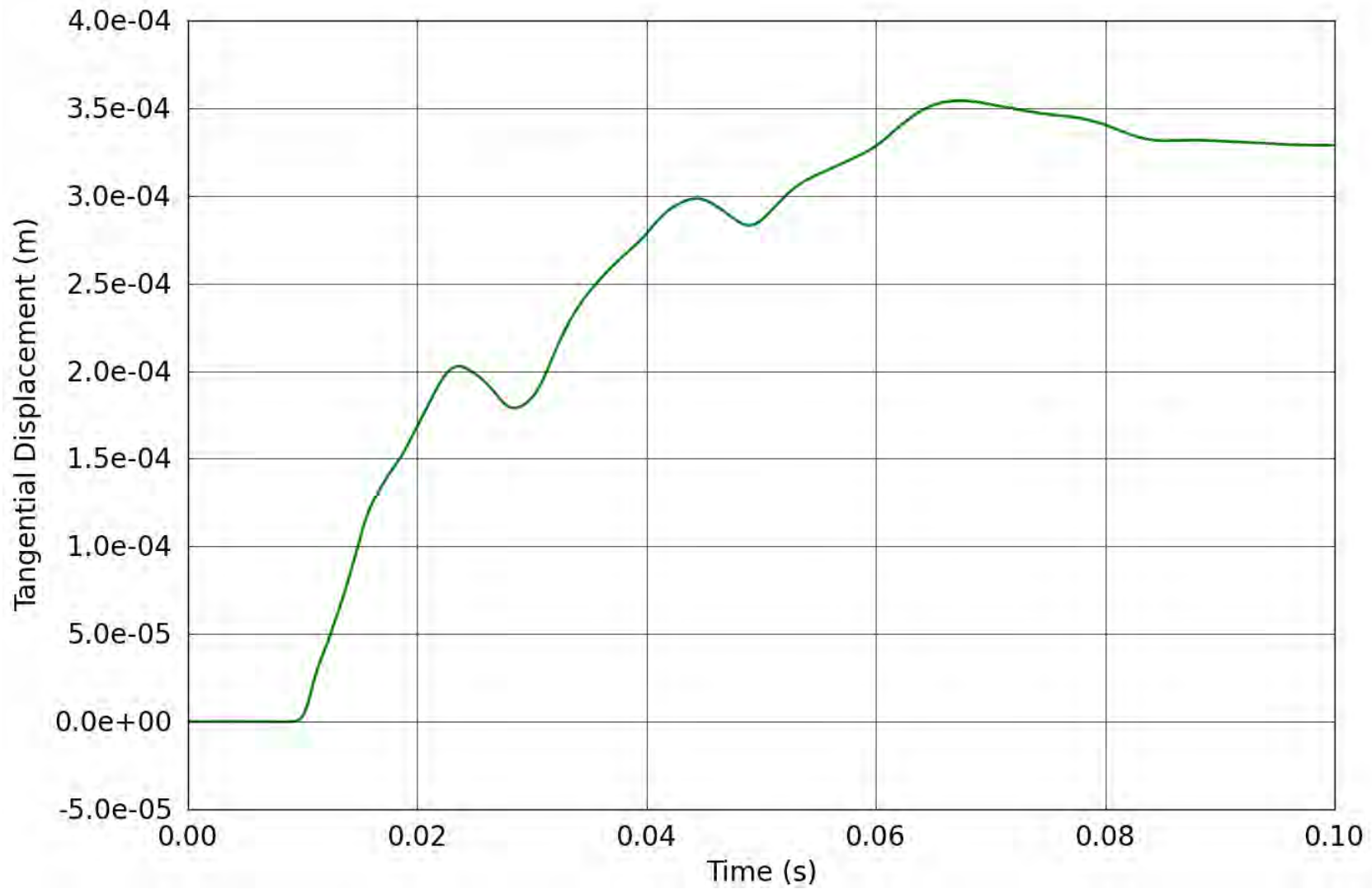Figure 55. SPE-1 Gauge 2-1-L – Correction of the longitudinal velocity.
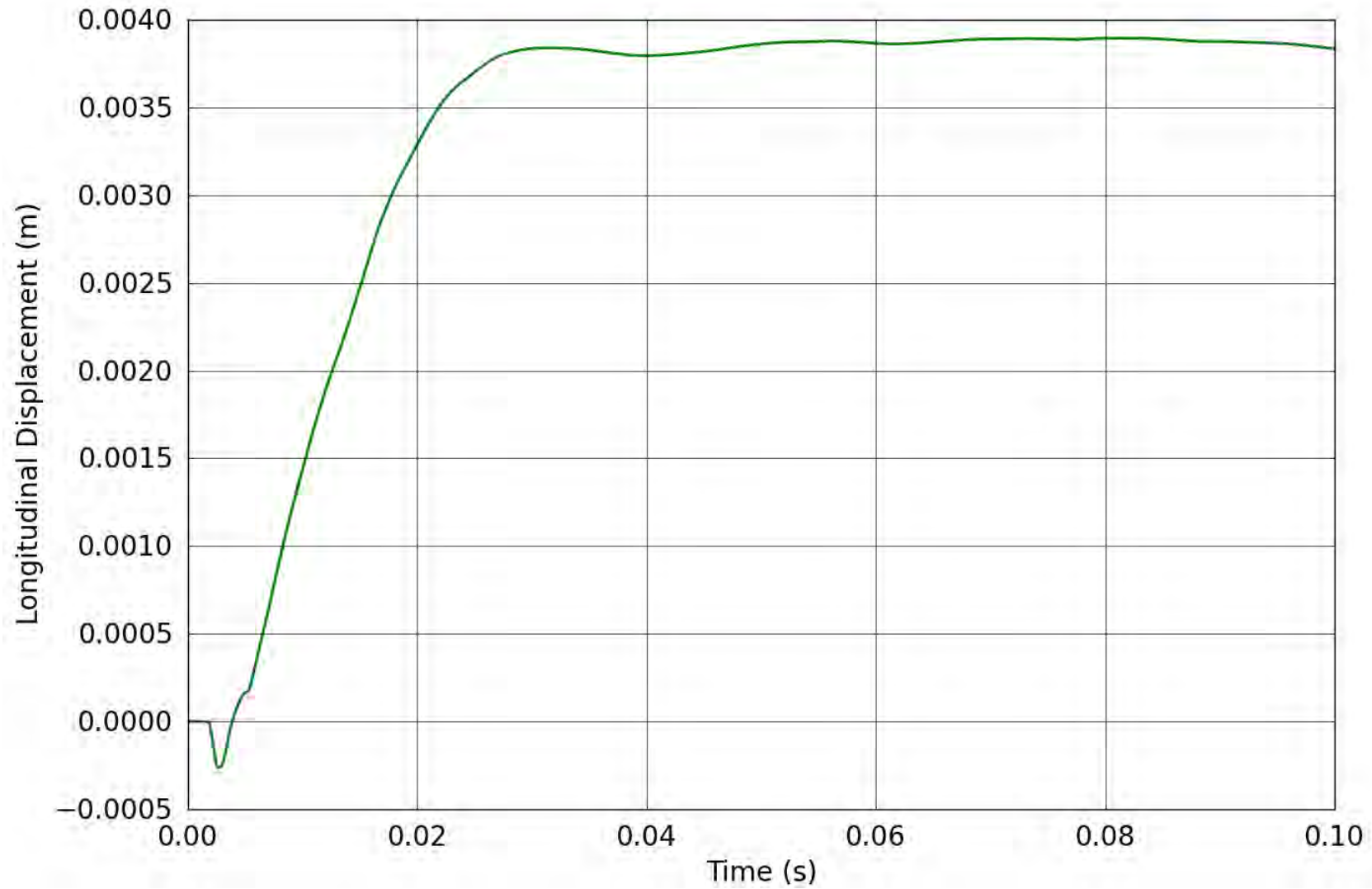
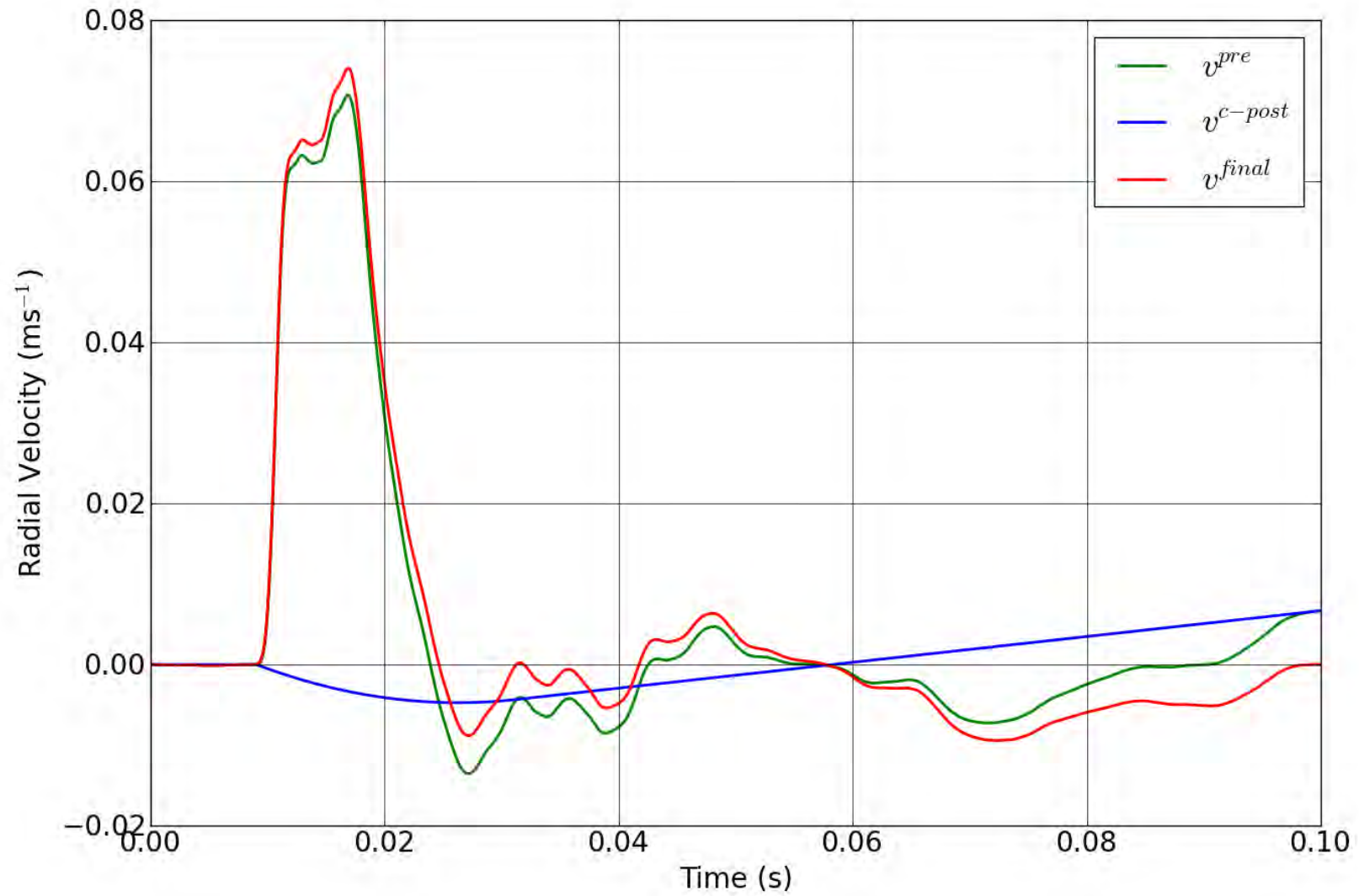Figure 56. SPE-1 Gauge 2-1-L – Longitudinal displacement obtained from the corrected longitudinal velocity.
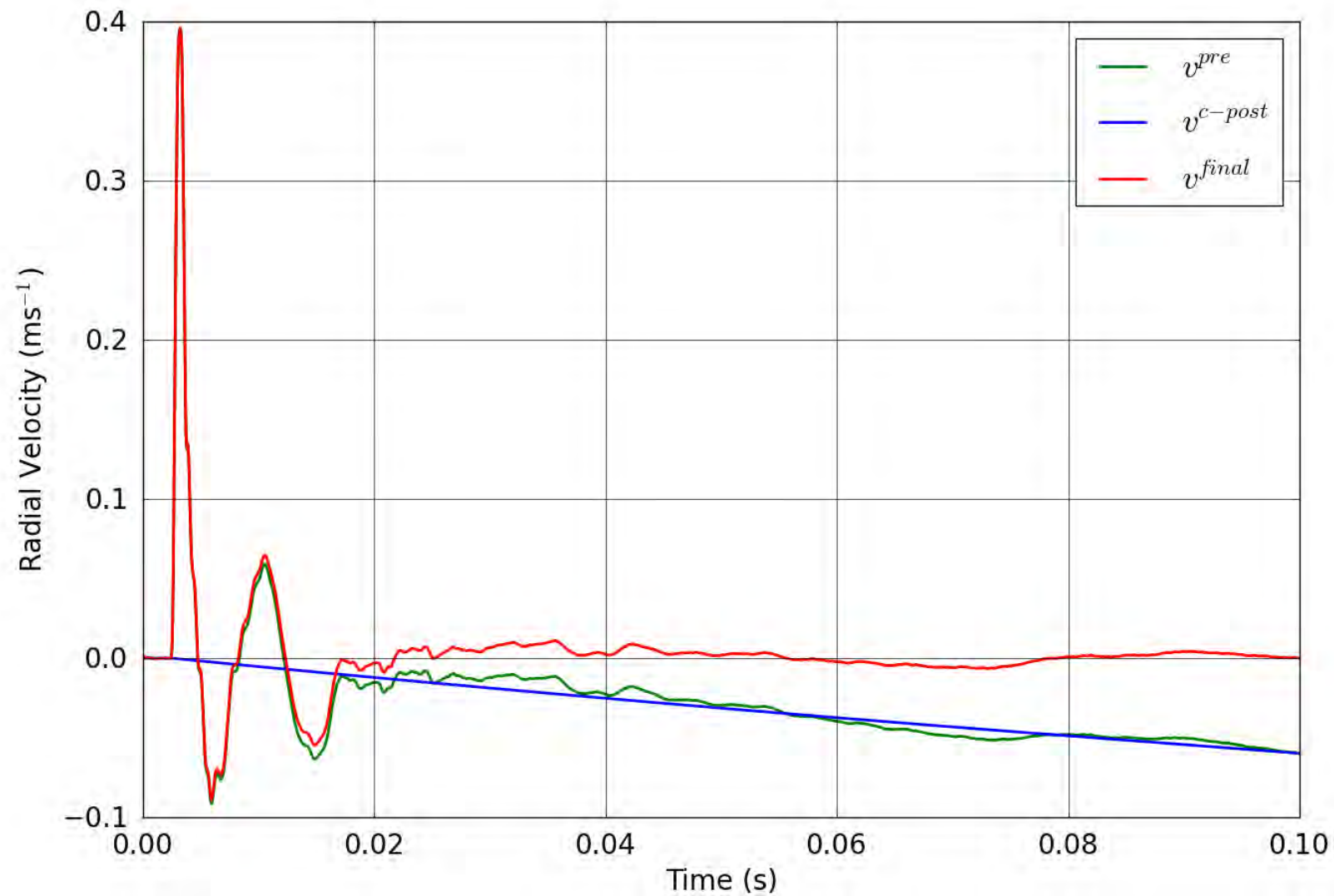
Figure 57. SPE-1 Gauge 2-2-R – Correction of the radial velocity.
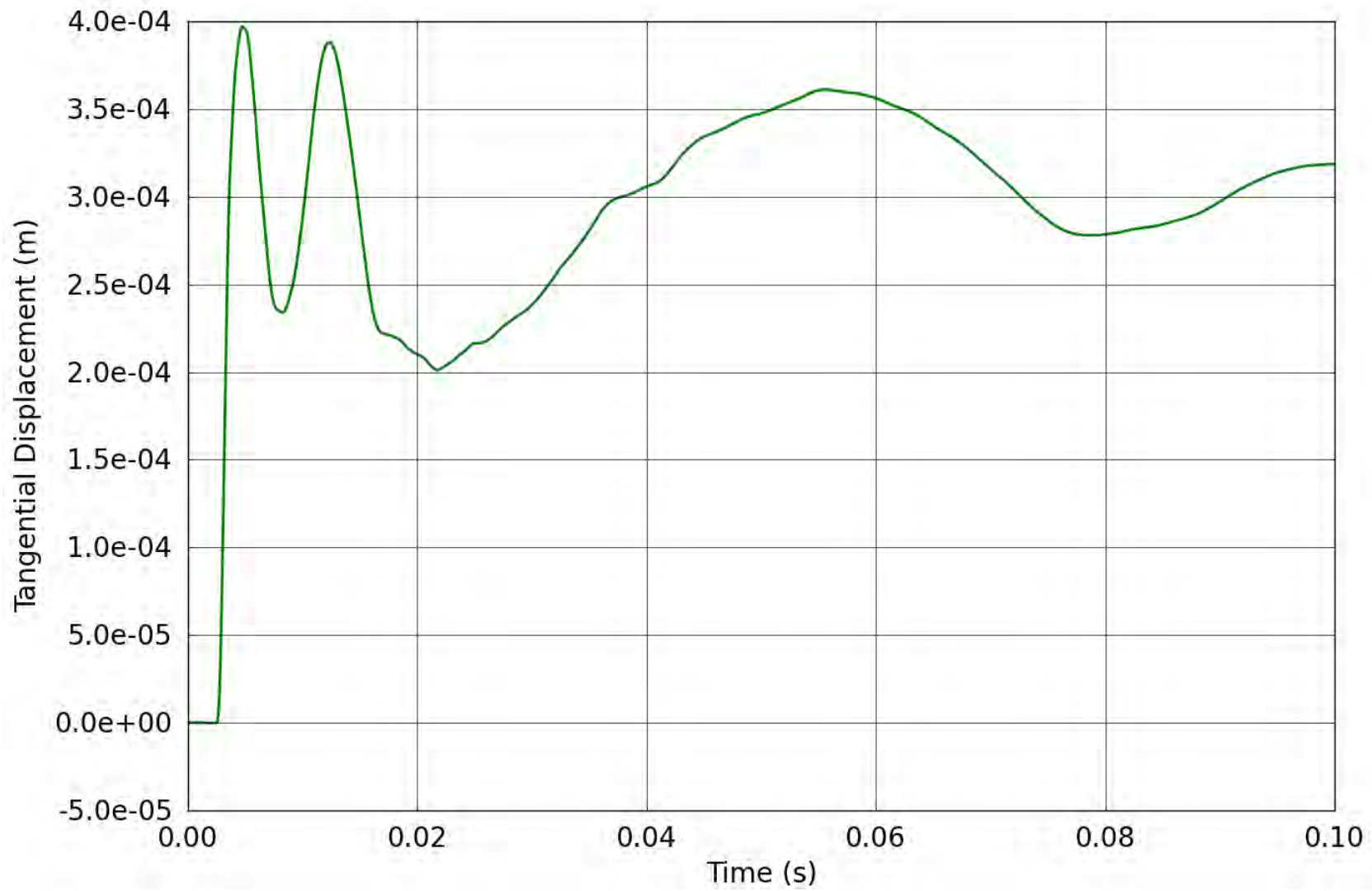
Figure 58. SPE-1 Gauge 2-2-R – Radial displacement obtained from the corrected radial velocity.
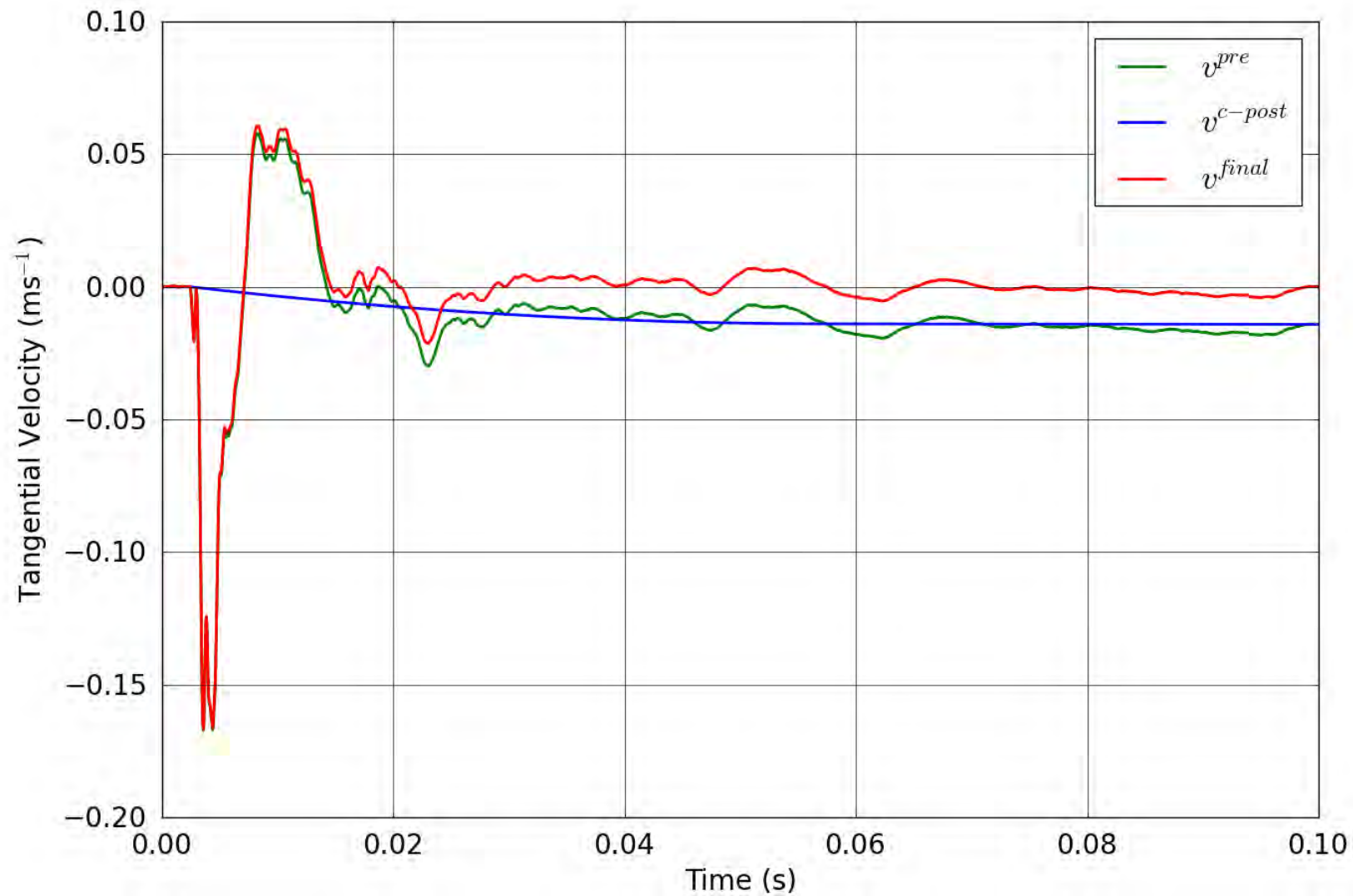
Figure 59. SPE-1 Gauge 2-2-T – Correction of the tangential velocity.
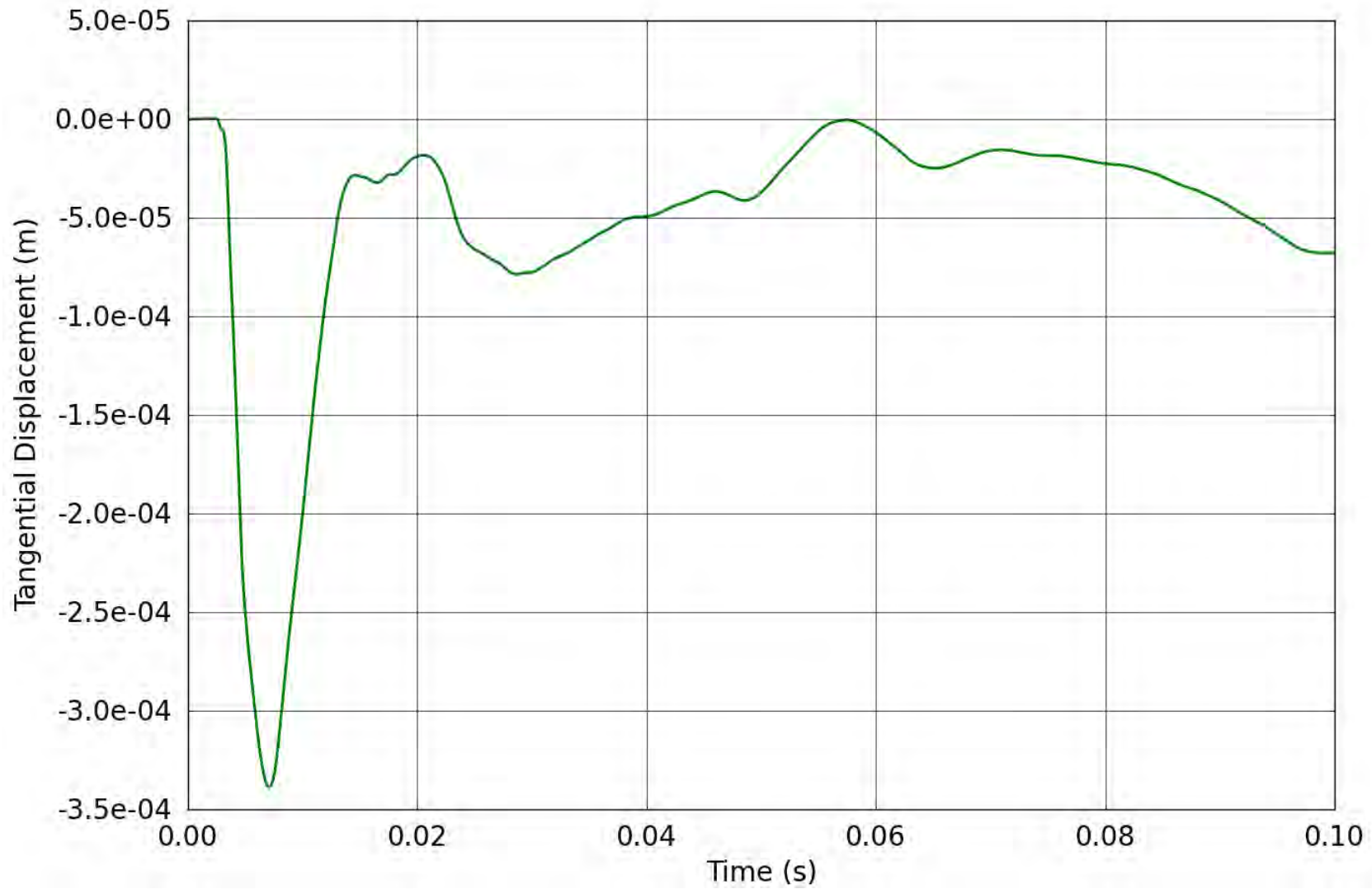
Figure 60. SPE-1 Gauge 2-2-T – Tangential displacement obtained from the corrected tangential velocity.
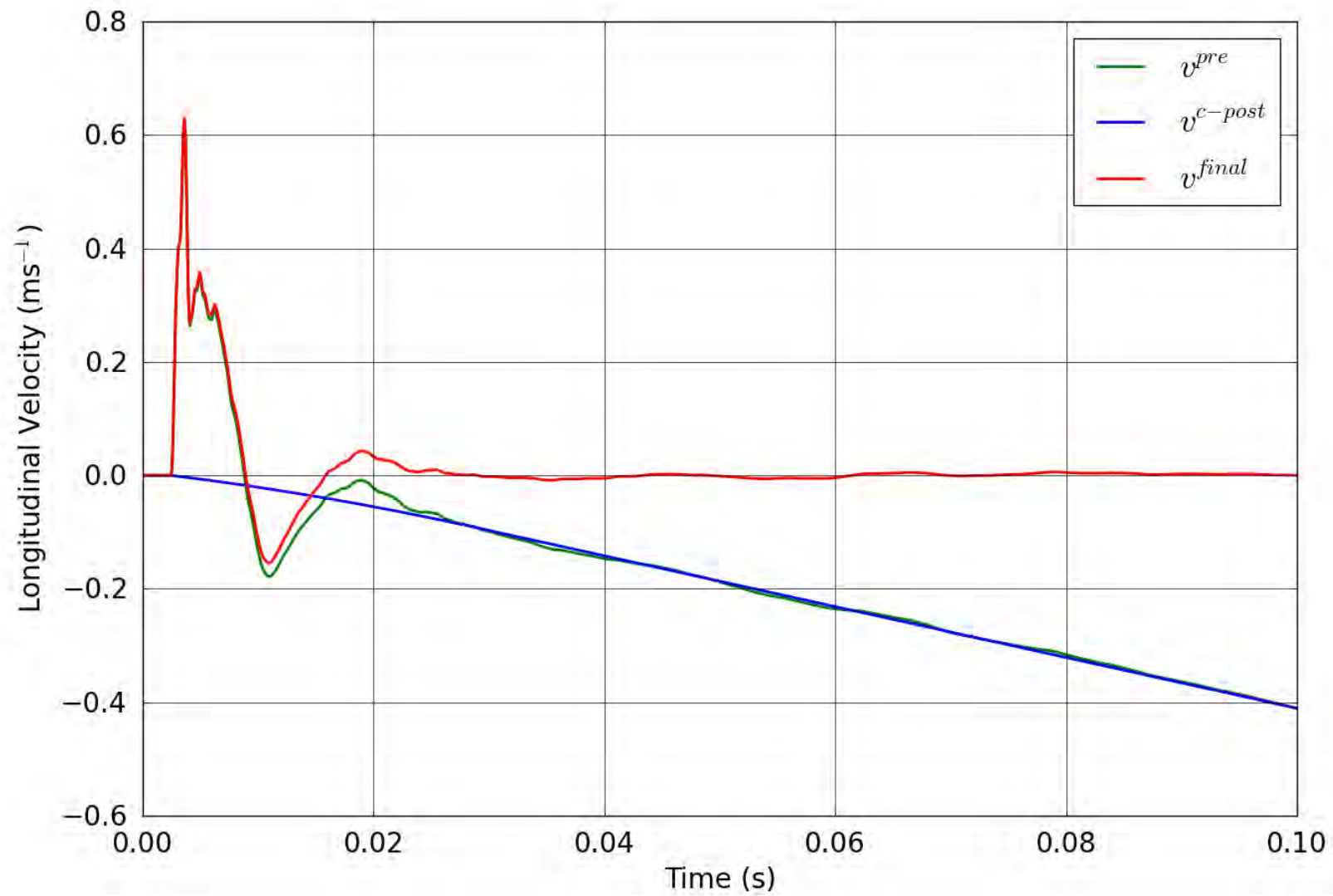
Figure 61. SPE-1 Gauge 2-2-L – Correction of the longitudinal velocity.
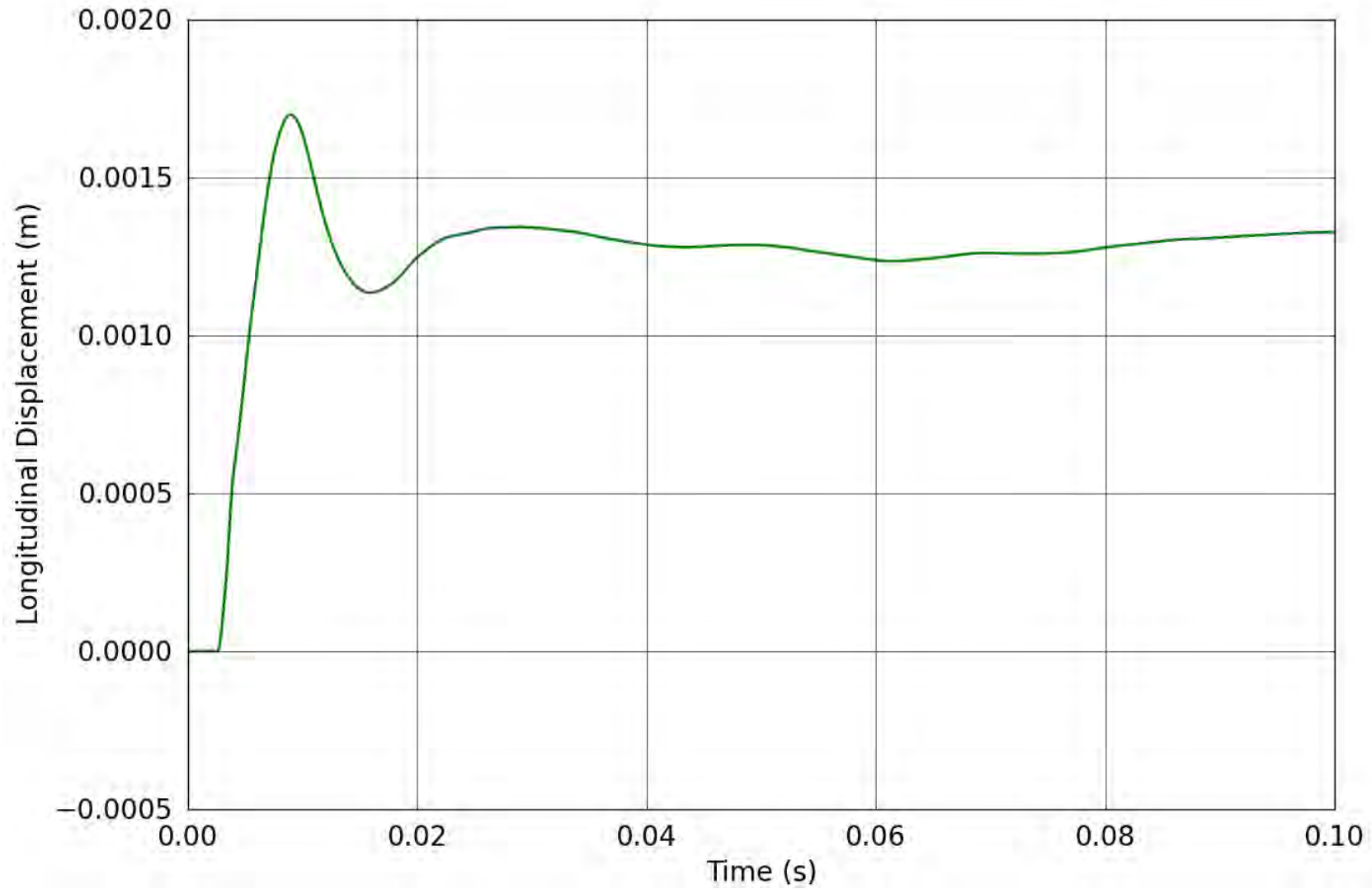
Figure 62. SPE-1 Gauge 2-2-L – Longitudinal displacement obtained from the corrected longitudinal velocity.
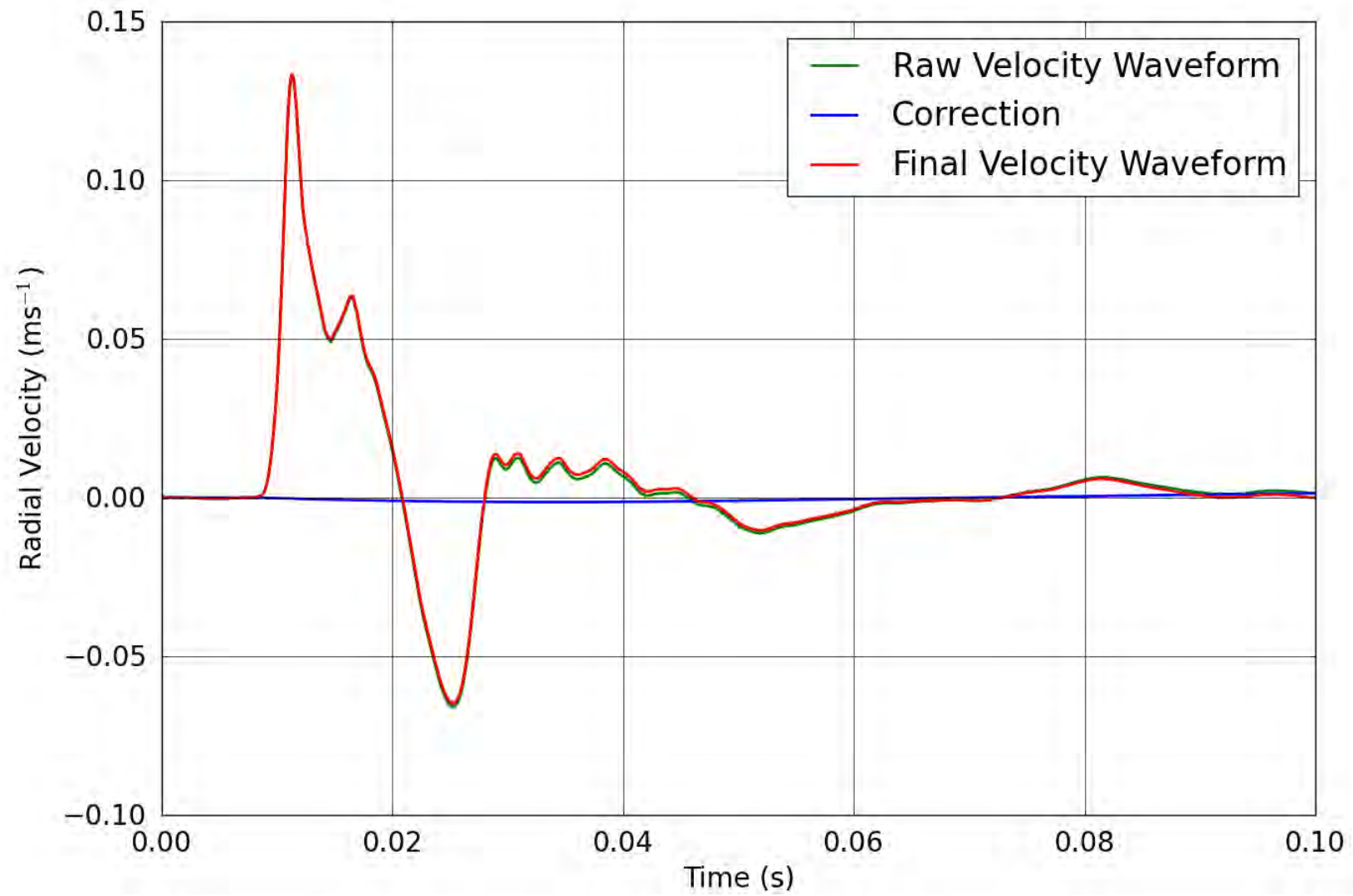
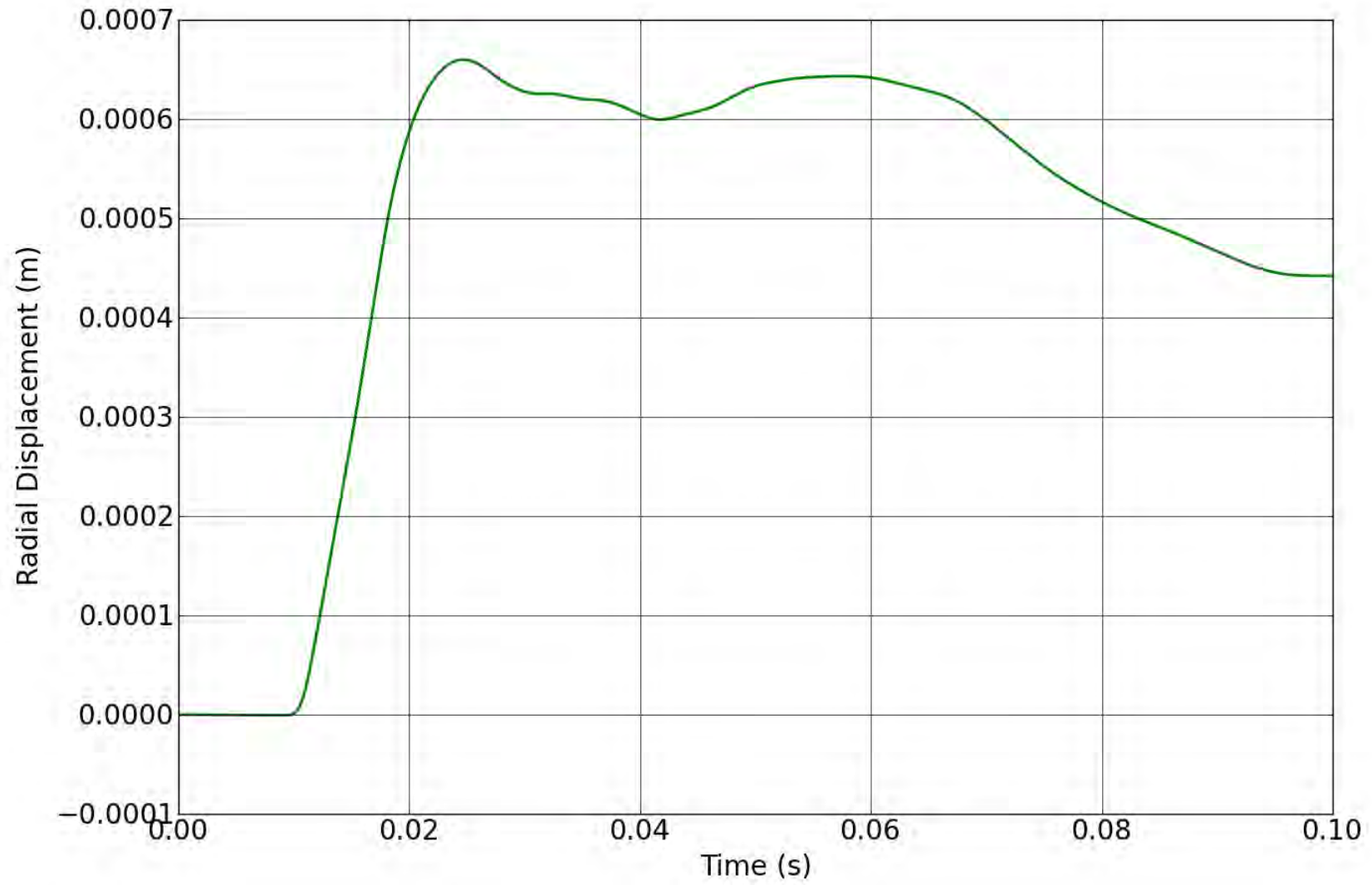Figure 63. SPE-1 Gauge 2-3-R – Correction of the radial velocity.
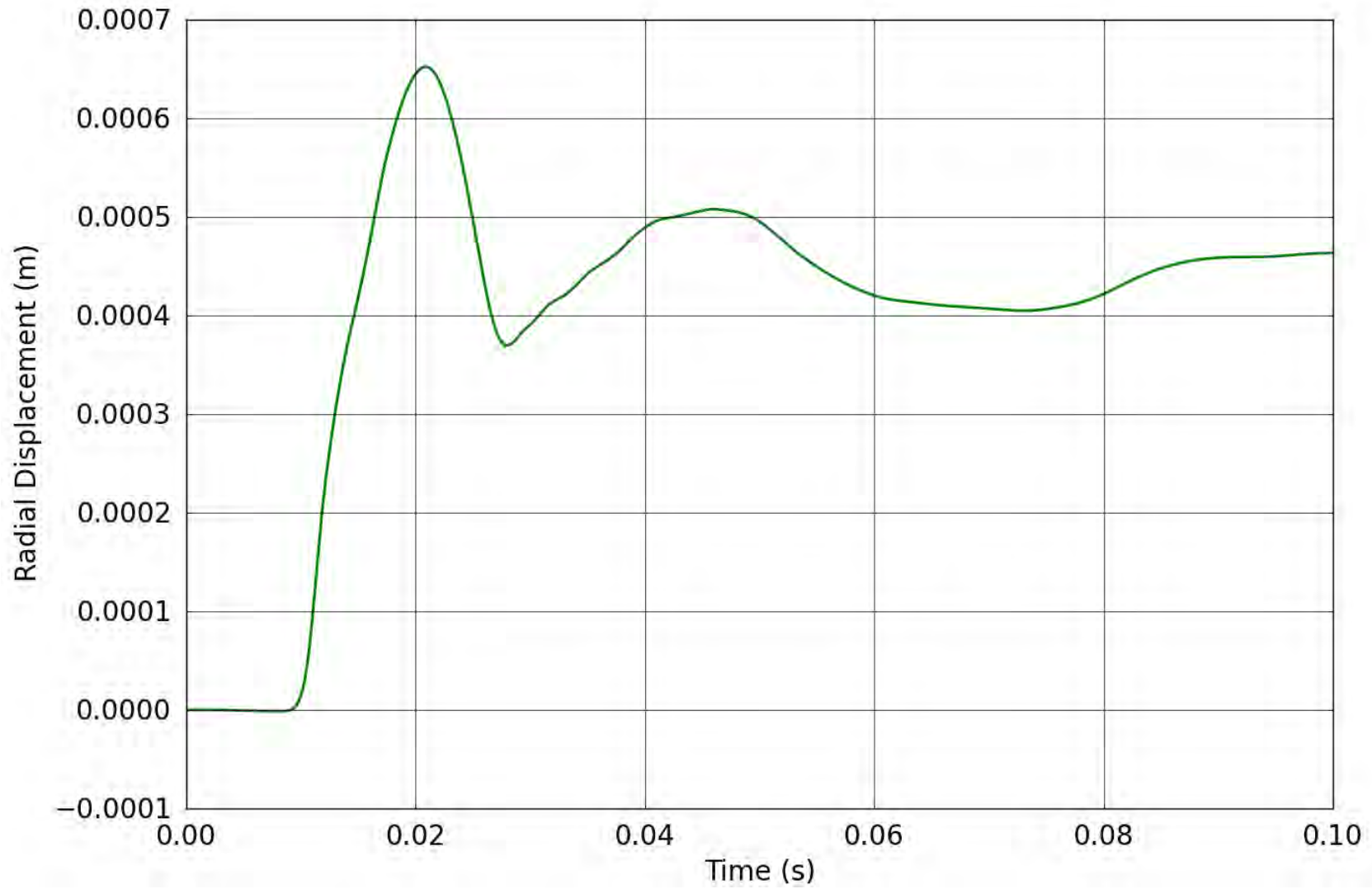
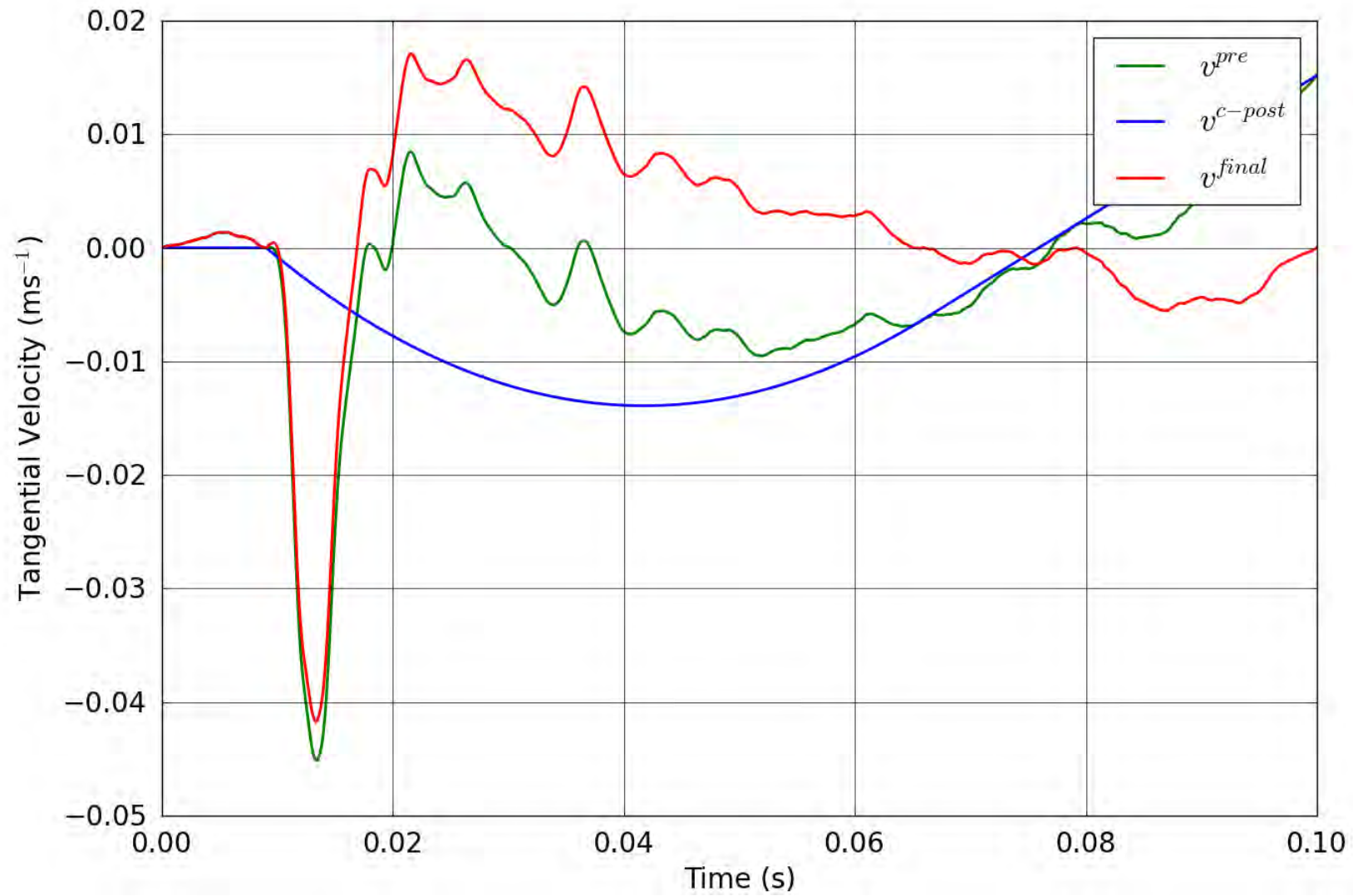Figure 64. SPE-1 Gauge 2-3-R – Radial displacement obtained from the corrected radial velocity.
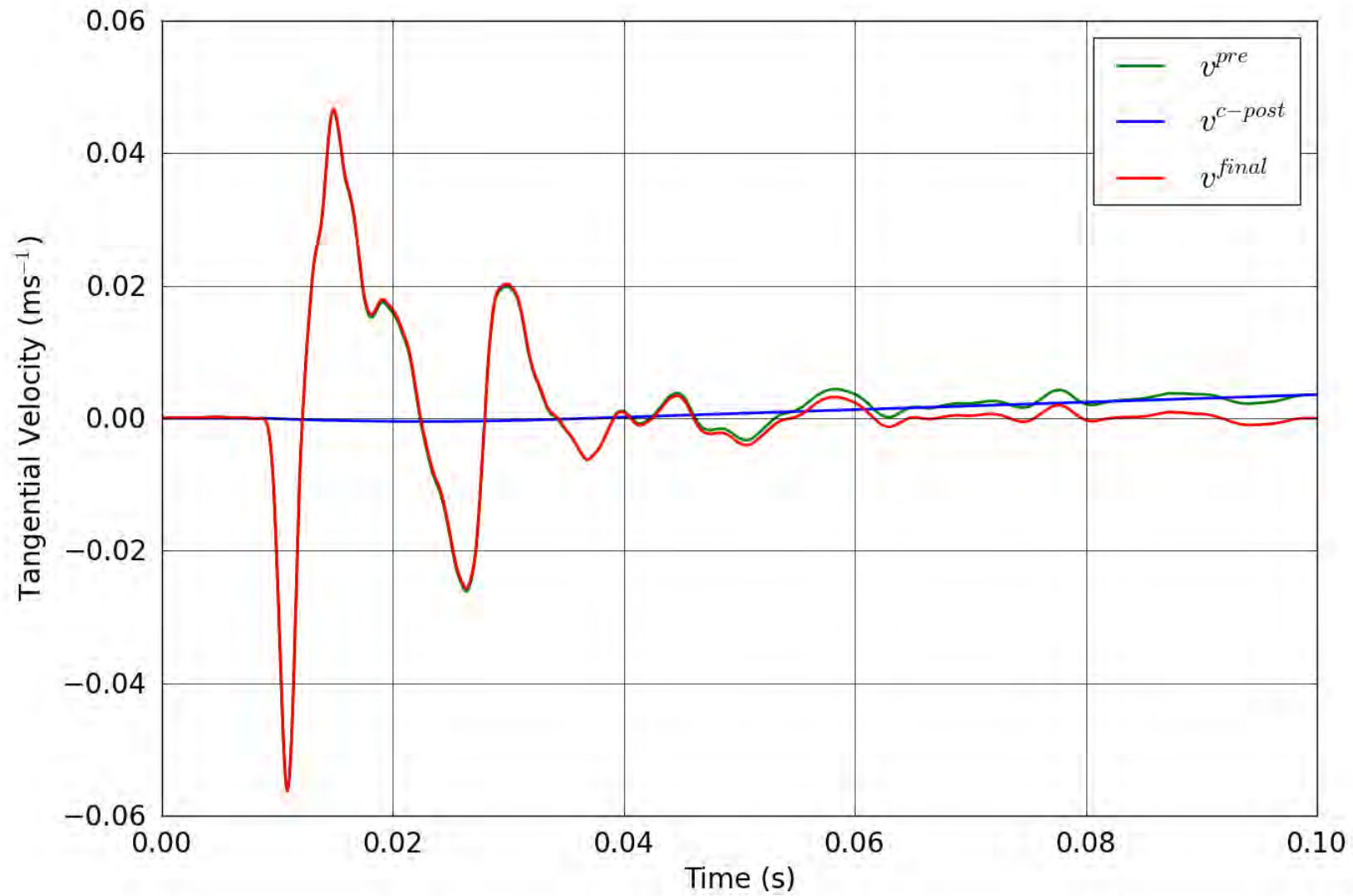
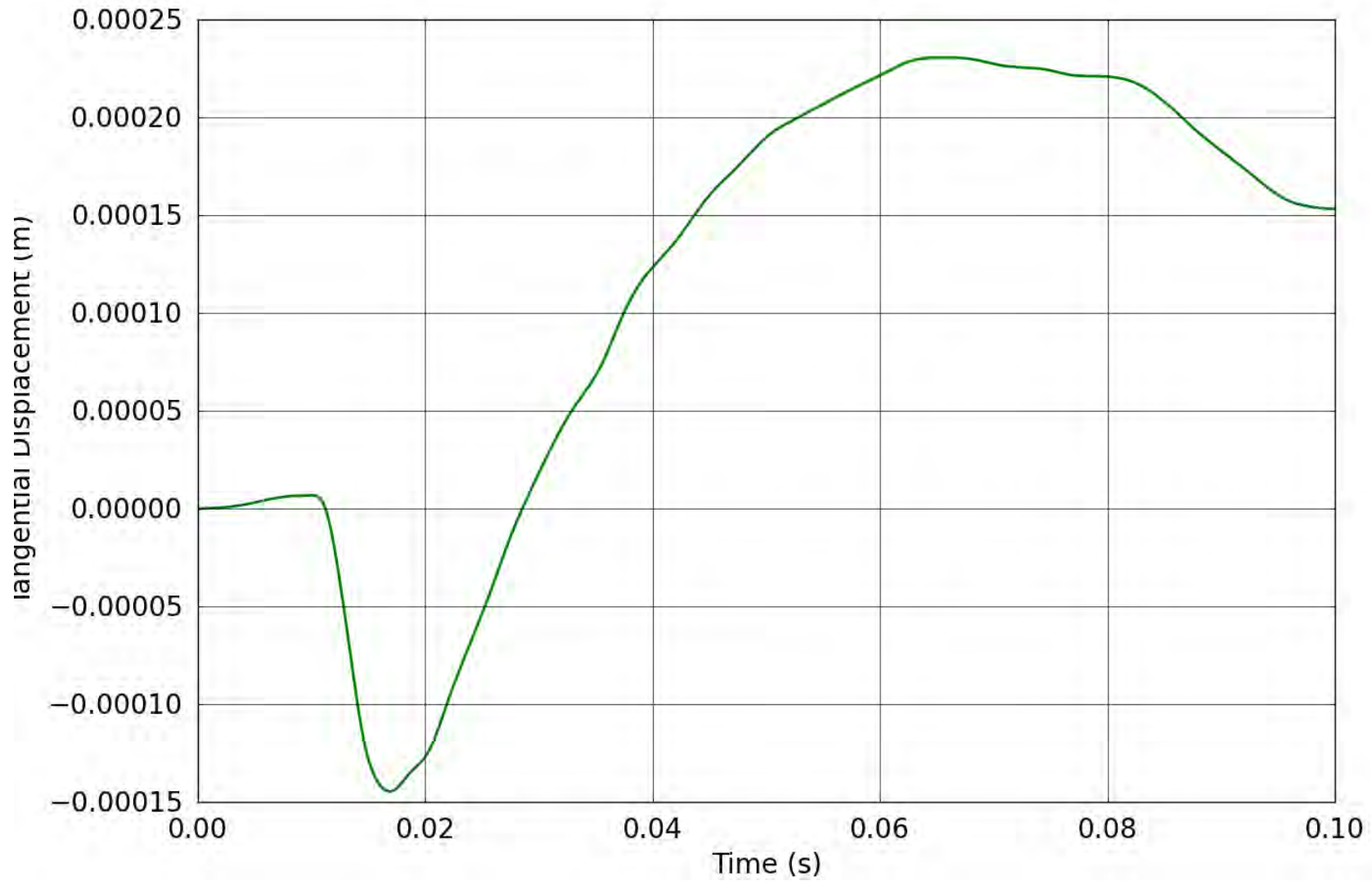Figure 65. SPE-1 Gauge 2-3-T – Correction of the tangential velocity.
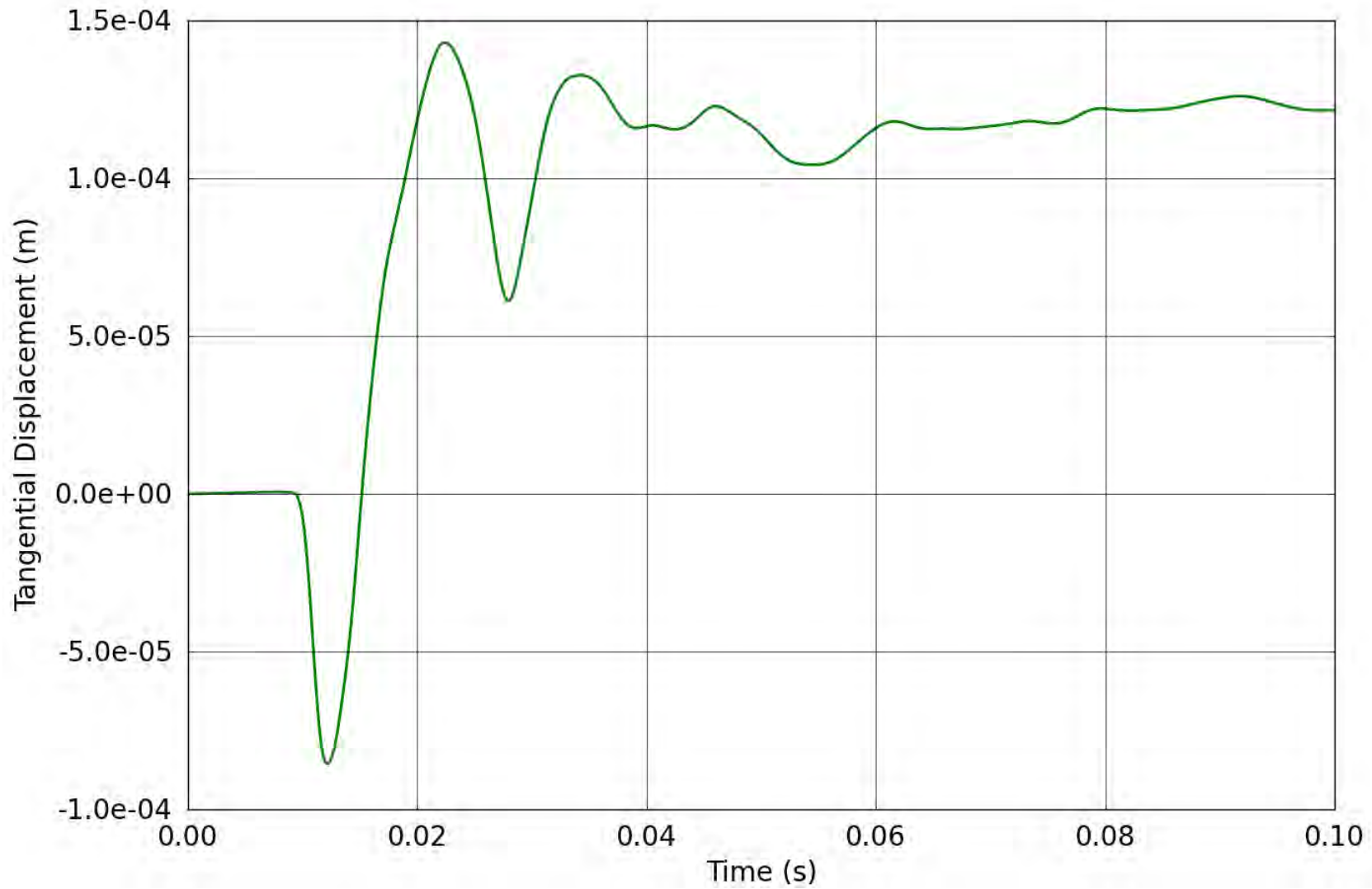
Figure 66. SPE-1 Gauge 2-3-T – Tangential displacement obtained from the corrected tangential velocity.
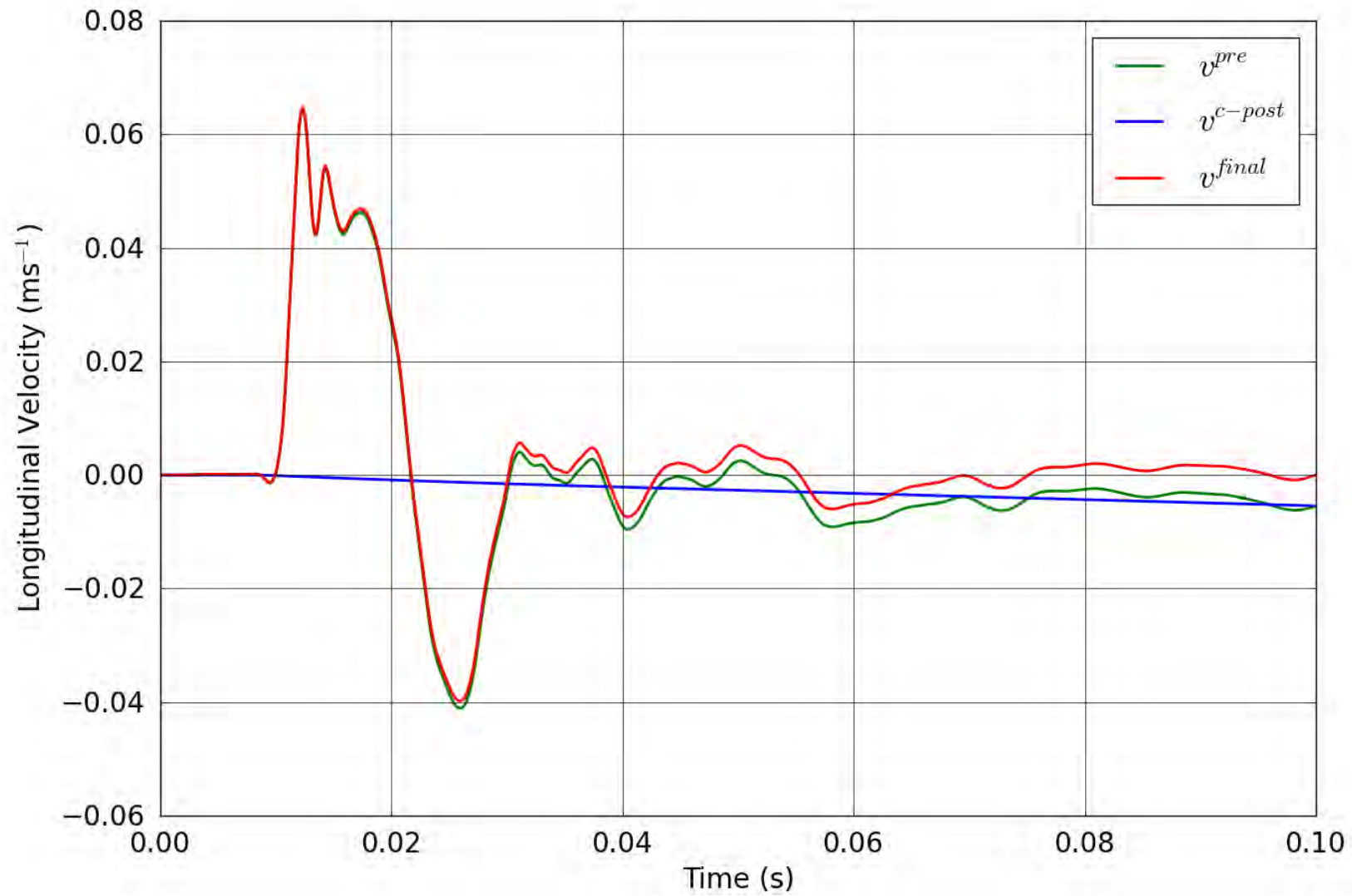
Figure 67. SPE-1 Gauge 2-3-L – Correction of the longitudinal velocity.
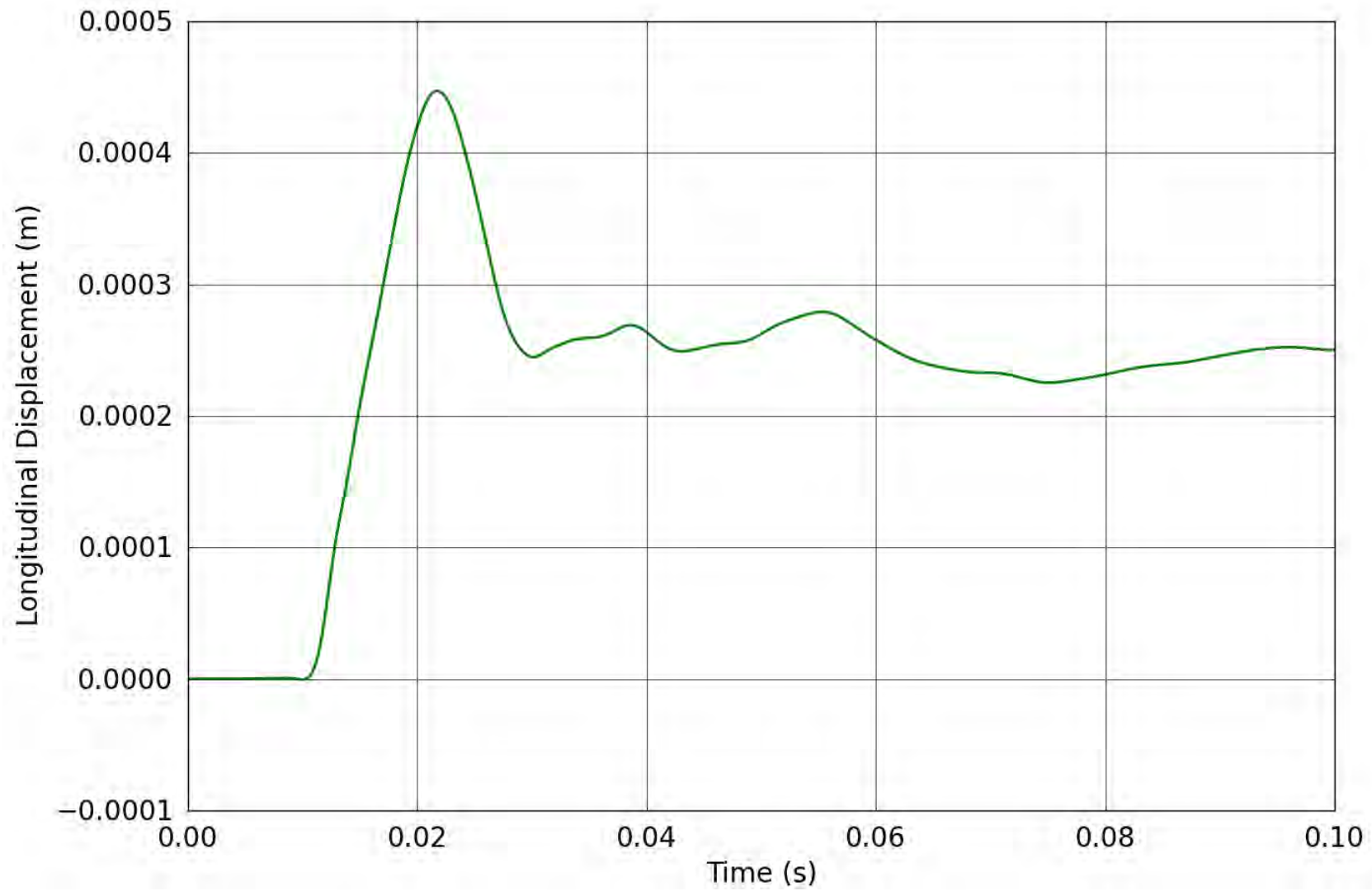
Figure 68. SPE-1 Gauge 2-3-L – Longitudinal displacement obtained from the corrected longitudinal velocity.
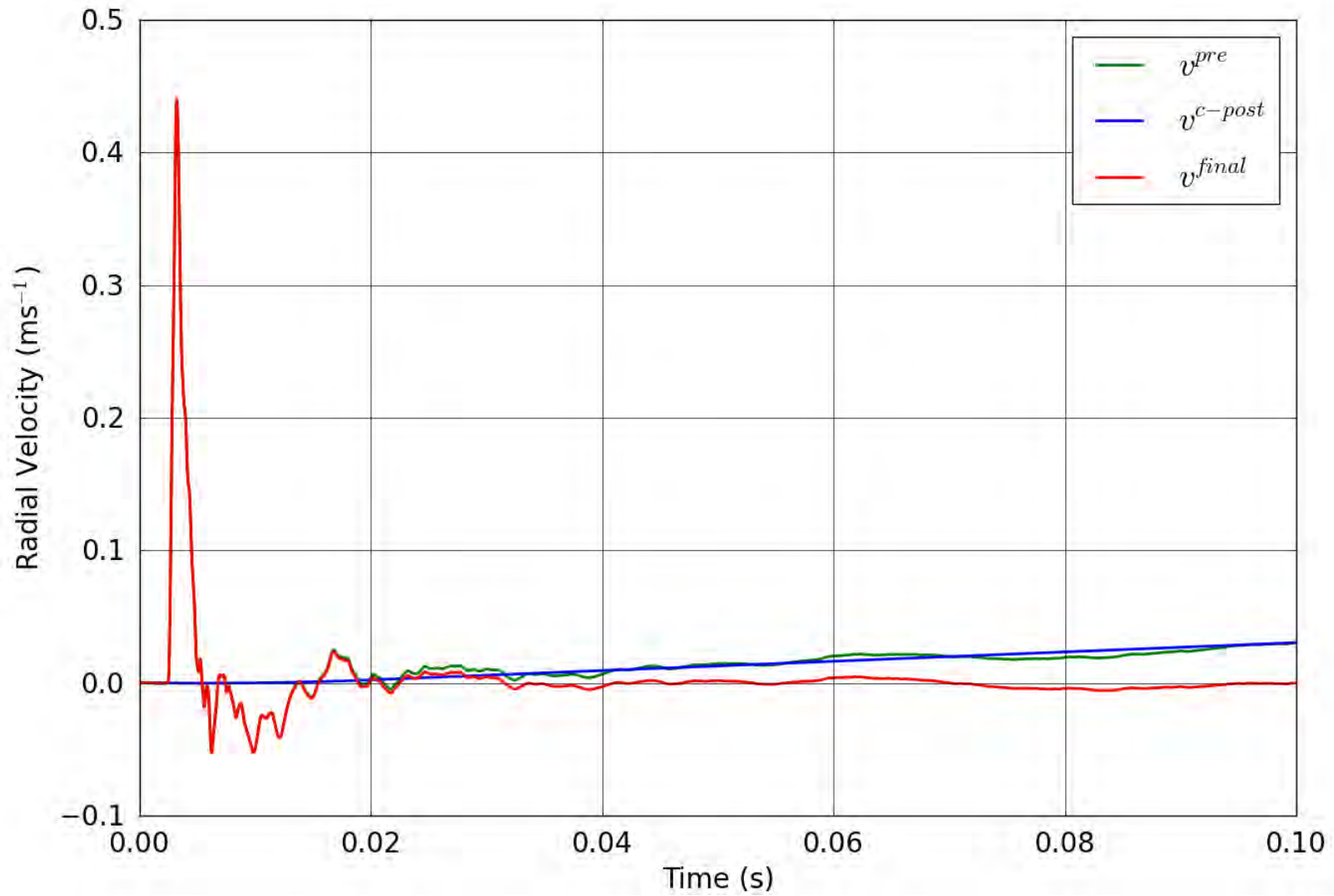
Figure 69. SPE-1 Gauge 3-2-R – Correction of the radial velocity.
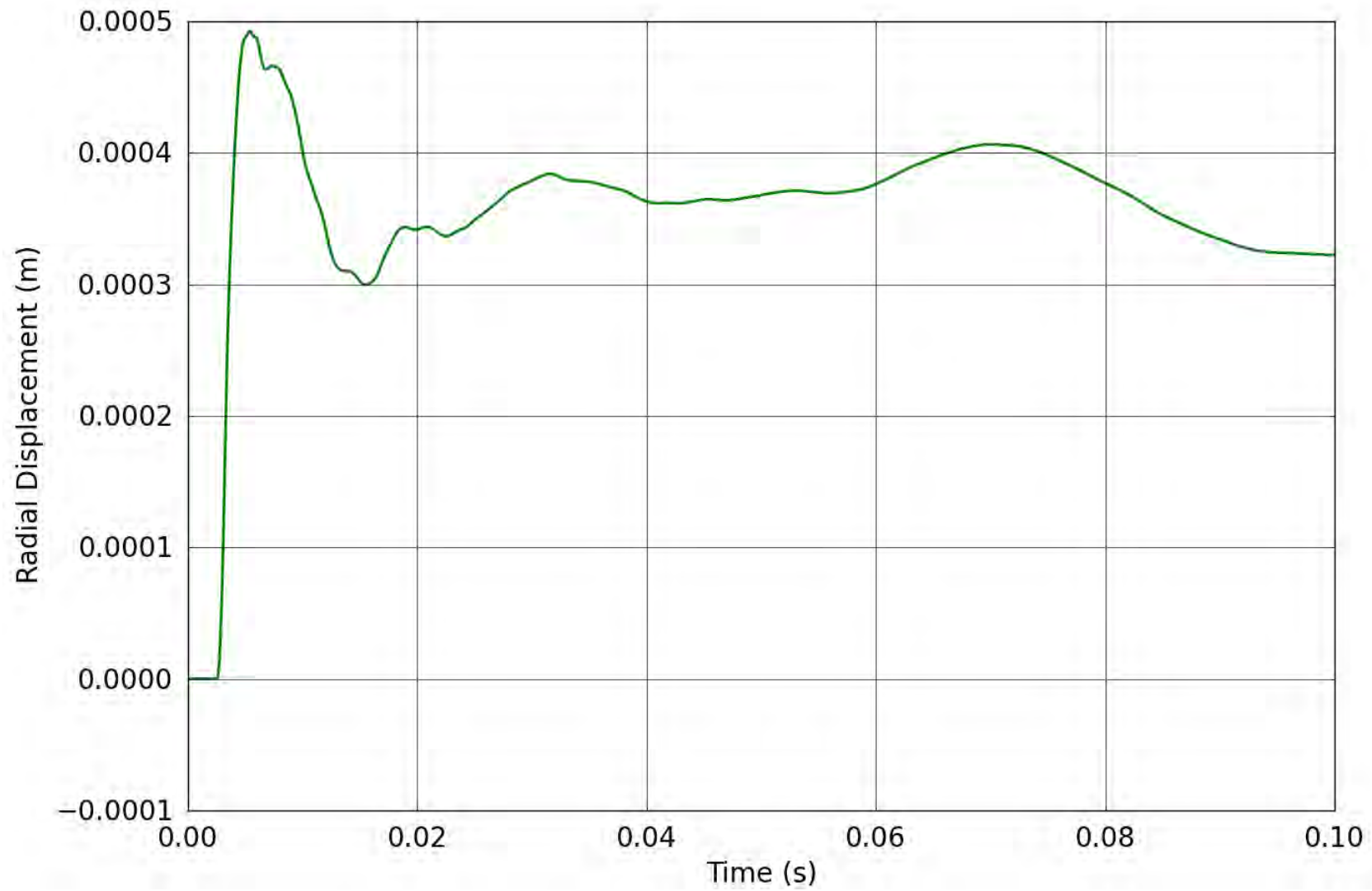
Figure 70. SPE-1 Gauge 3-2-R – Radial displacement obtained from the corrected radial velocity.
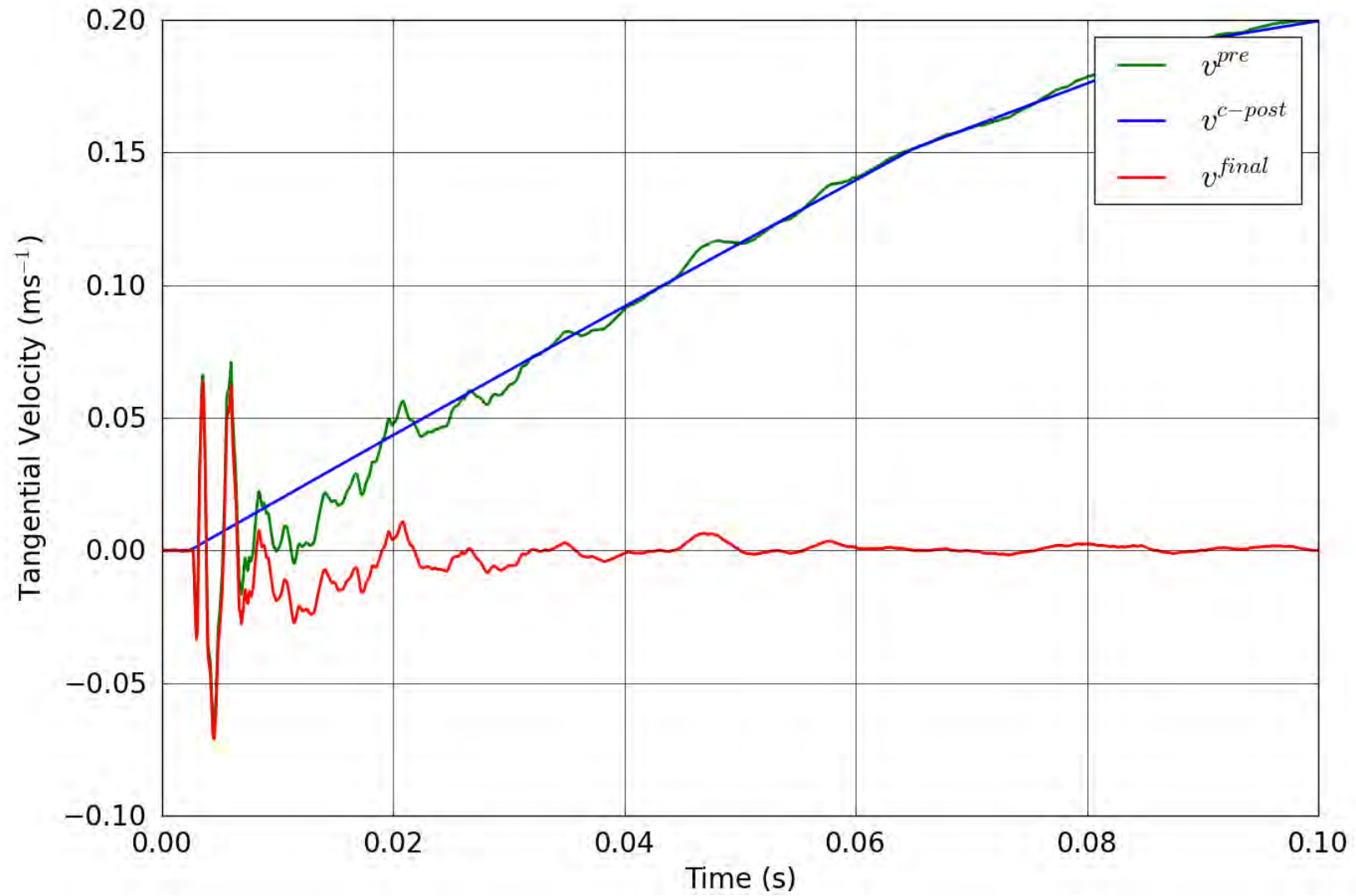
Figure 71. SPE-1 Gauge 3-2-T – Correction of the tangential velocity.
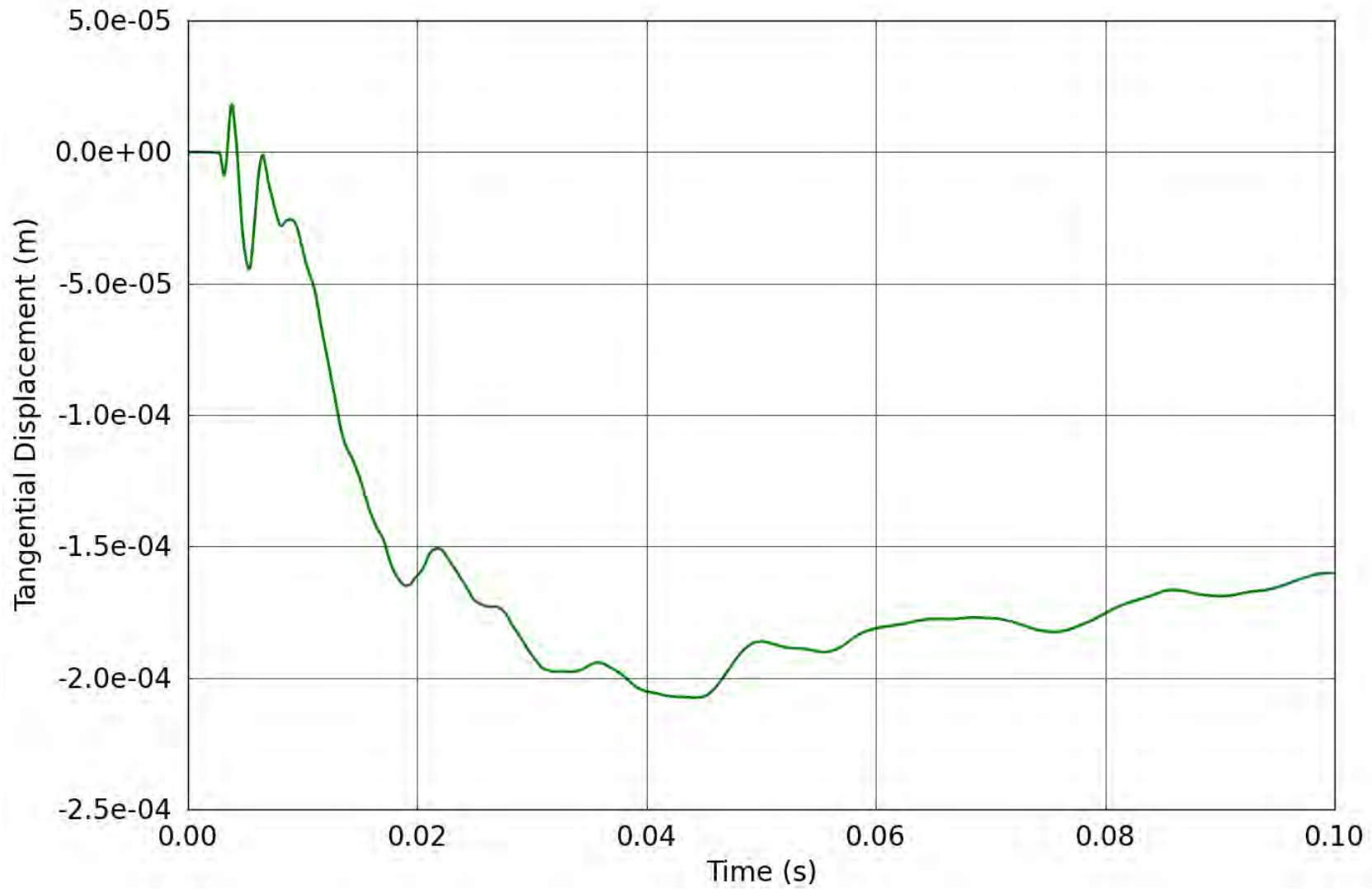
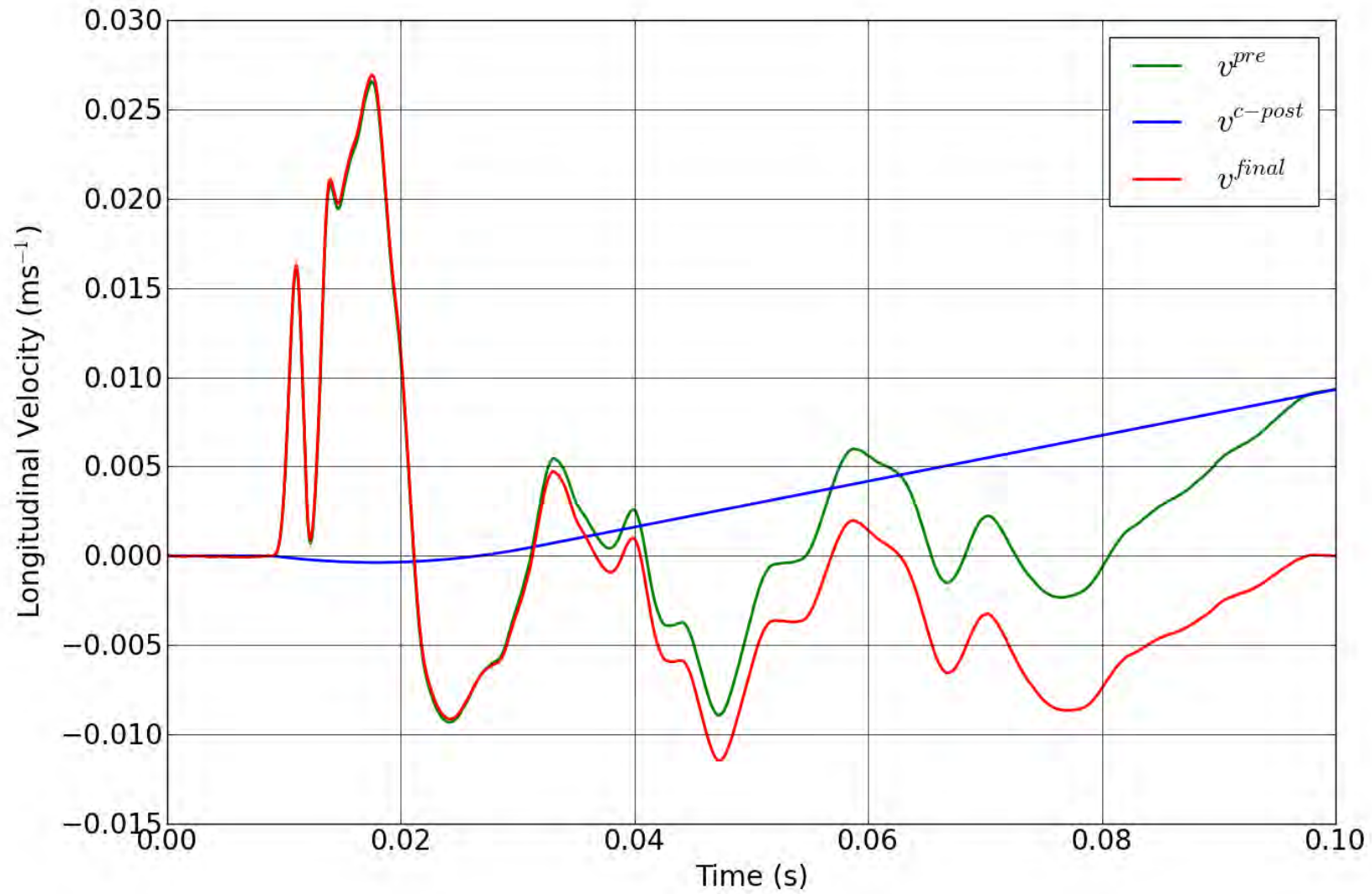Figure 72. SPE-1 Gauge 3-2-T – Tangential displacement obtained from the corrected tangential velocity.
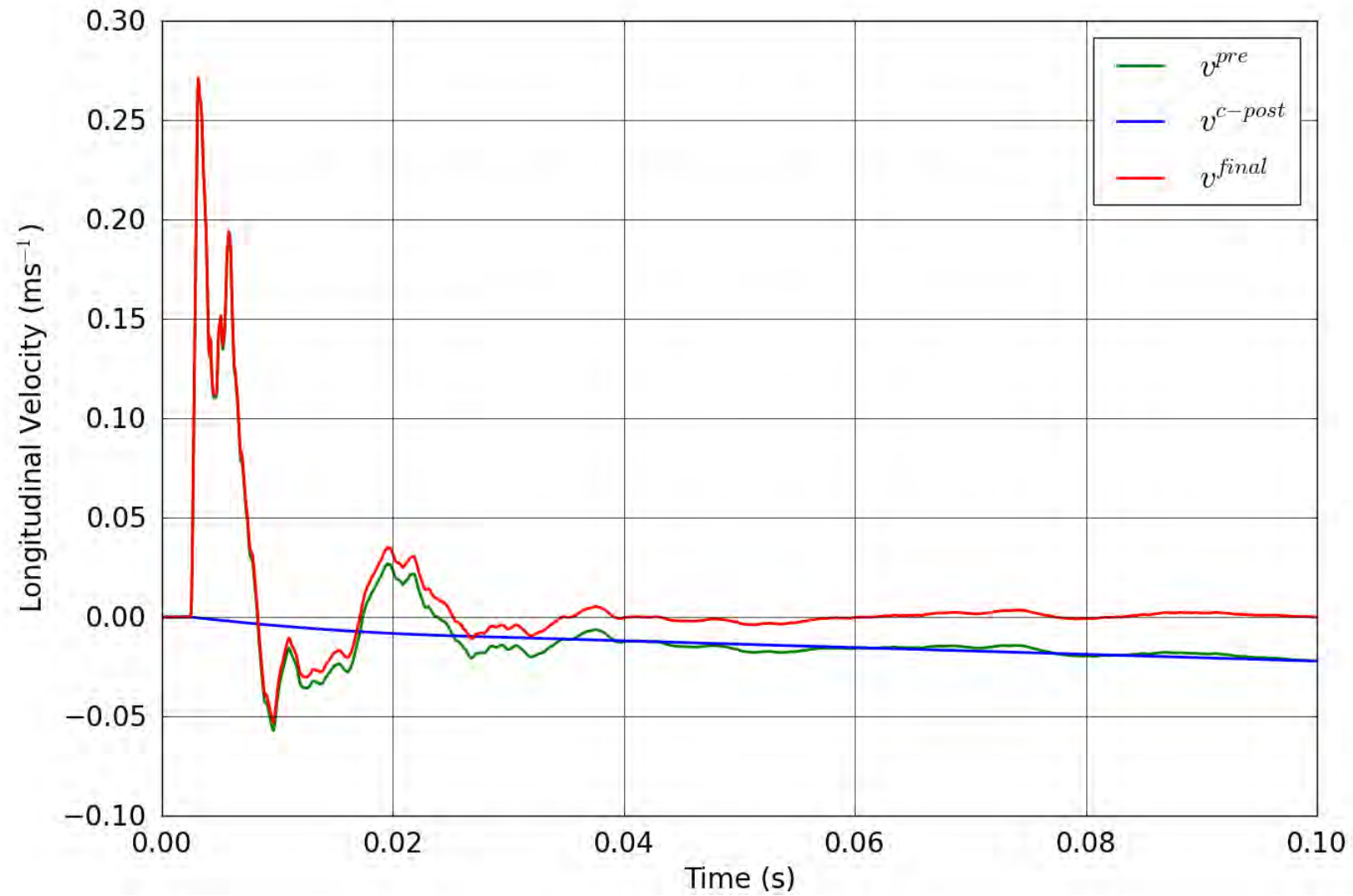
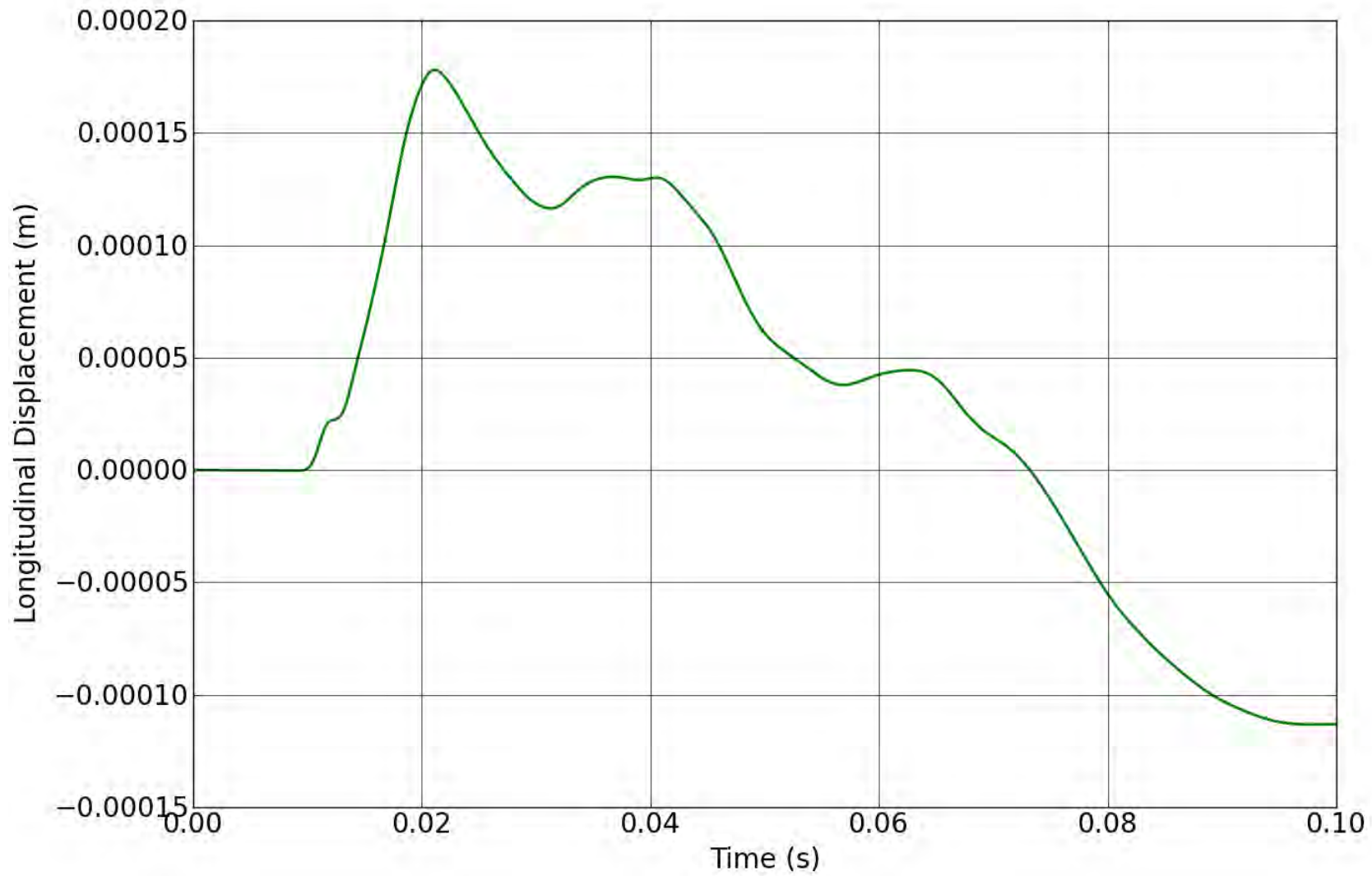Figure 73. SPE-1 Gauge 3-2-L – Correction of the longitudinal velocity.
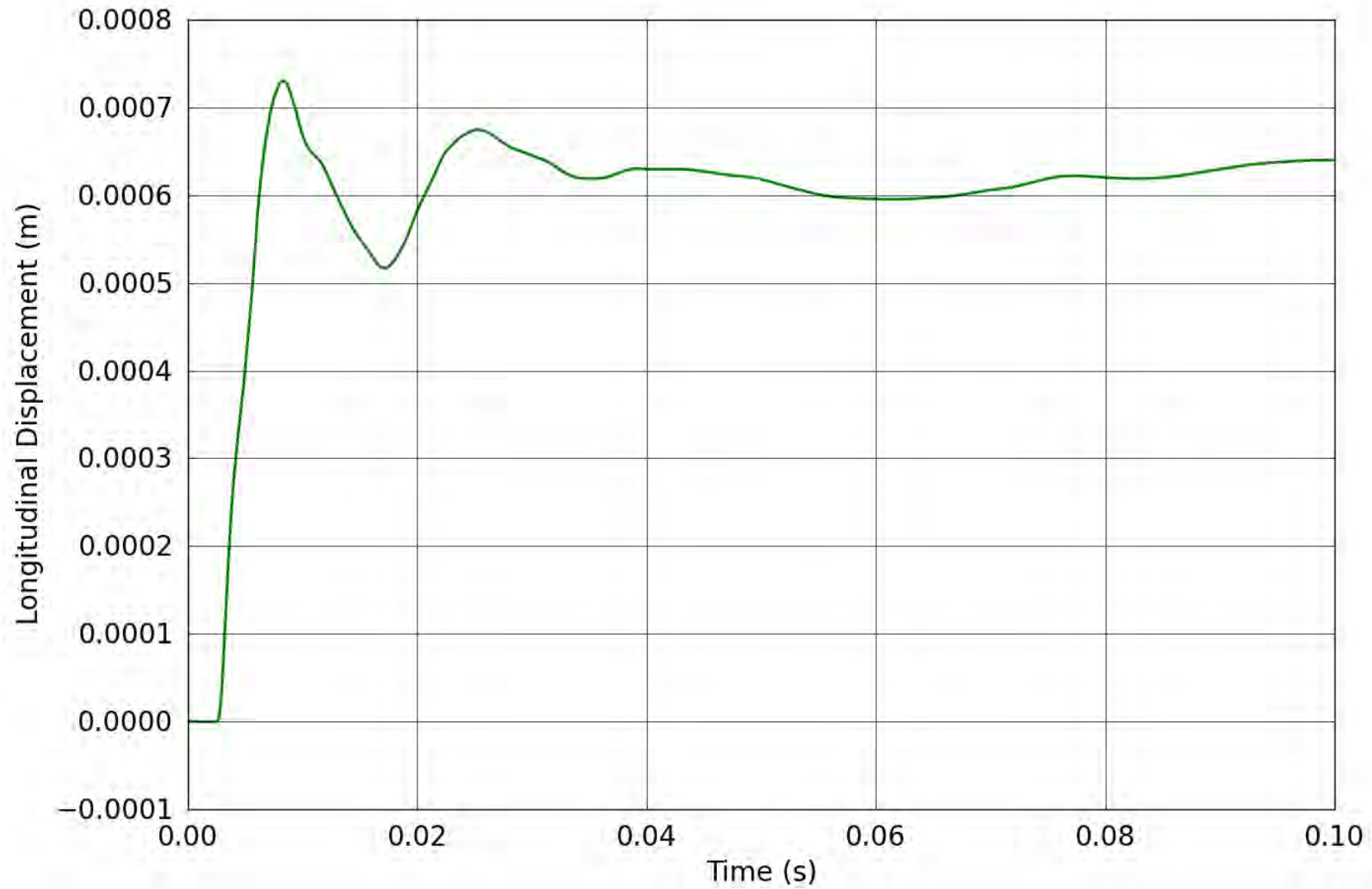
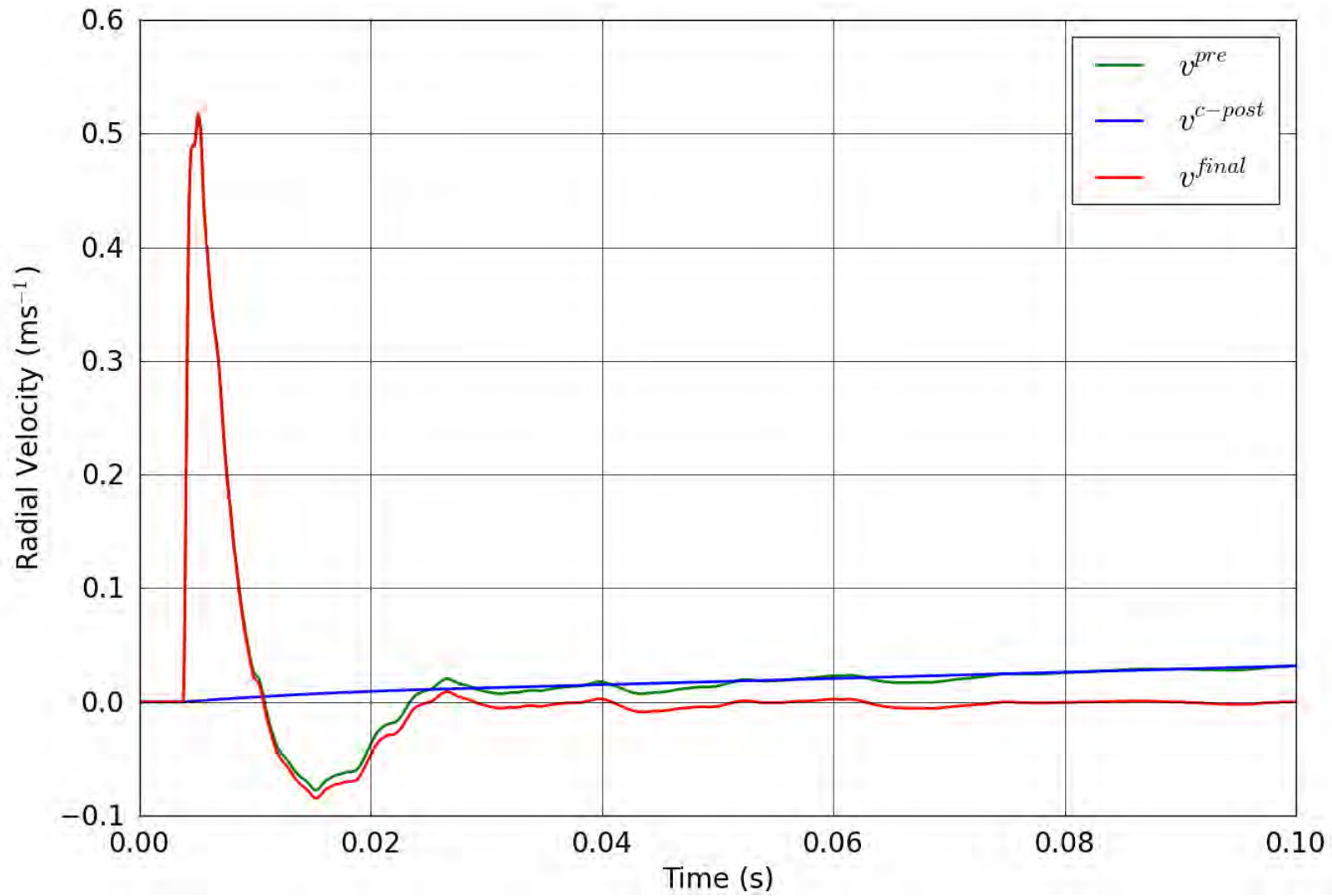Figure 74. SPE-1 Gauge 3-2-L – Longitudinal displacement obtained from the corrected longitudinal velocity.
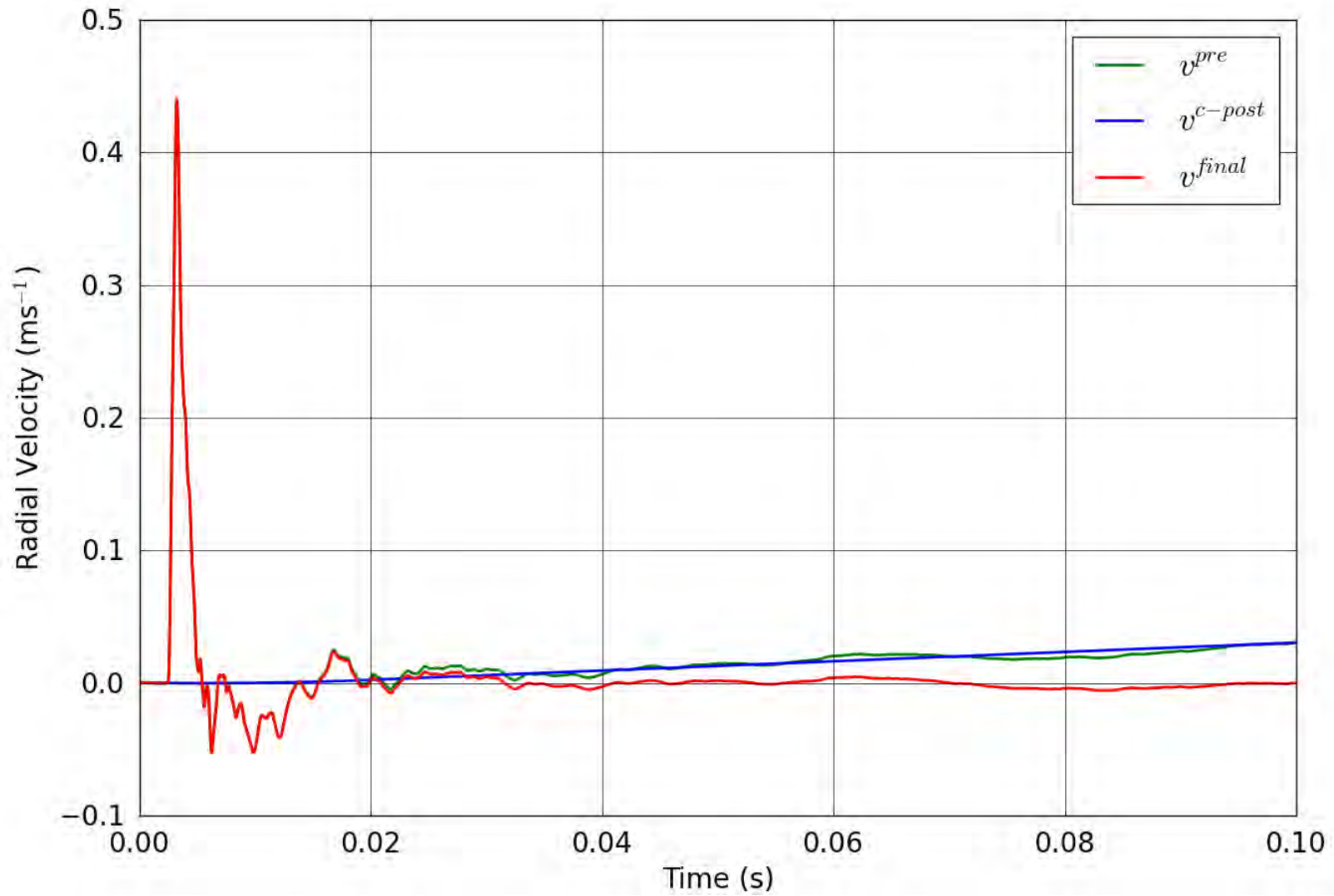
Figure 75. SPE-1 Gauge 3-2-R – Correction of the radial velocity.
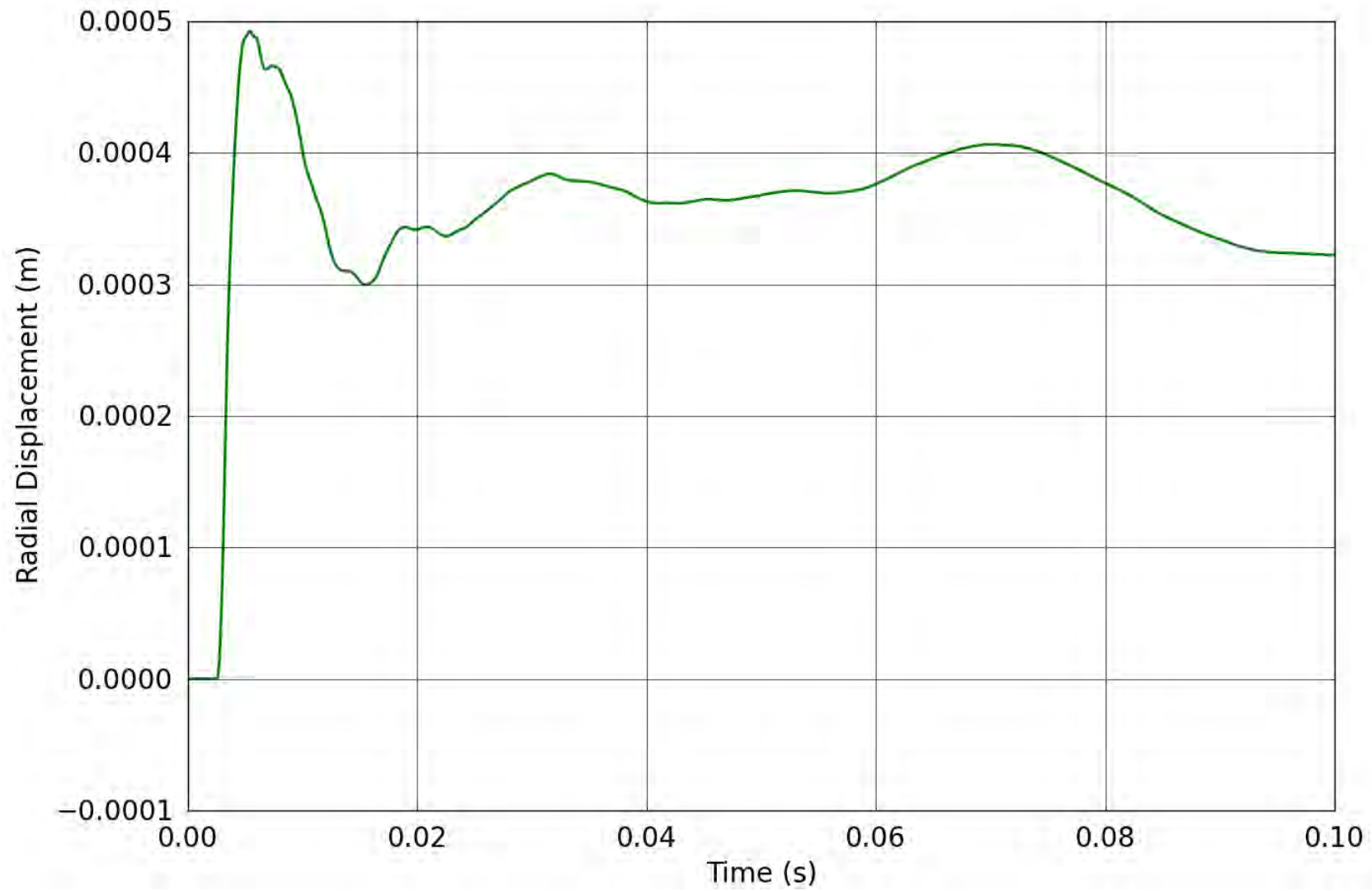
Figure 76. SPE-1 Gauge 3-2-R – Radial displacement obtained from the corrected radial velocity.
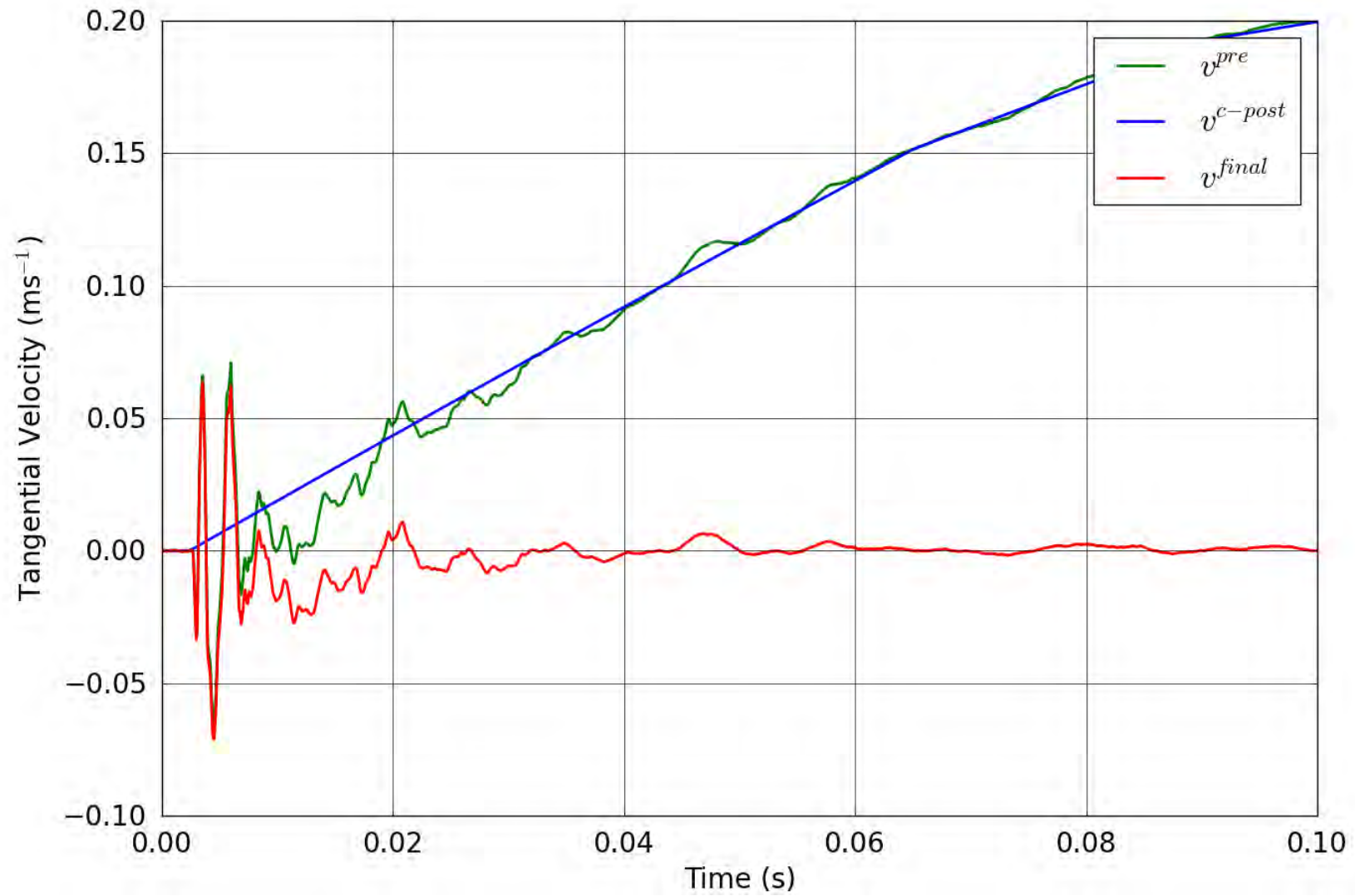
Figure 77. SPE-1 Gauge 3-2-T – Correction of the tangential velocity.
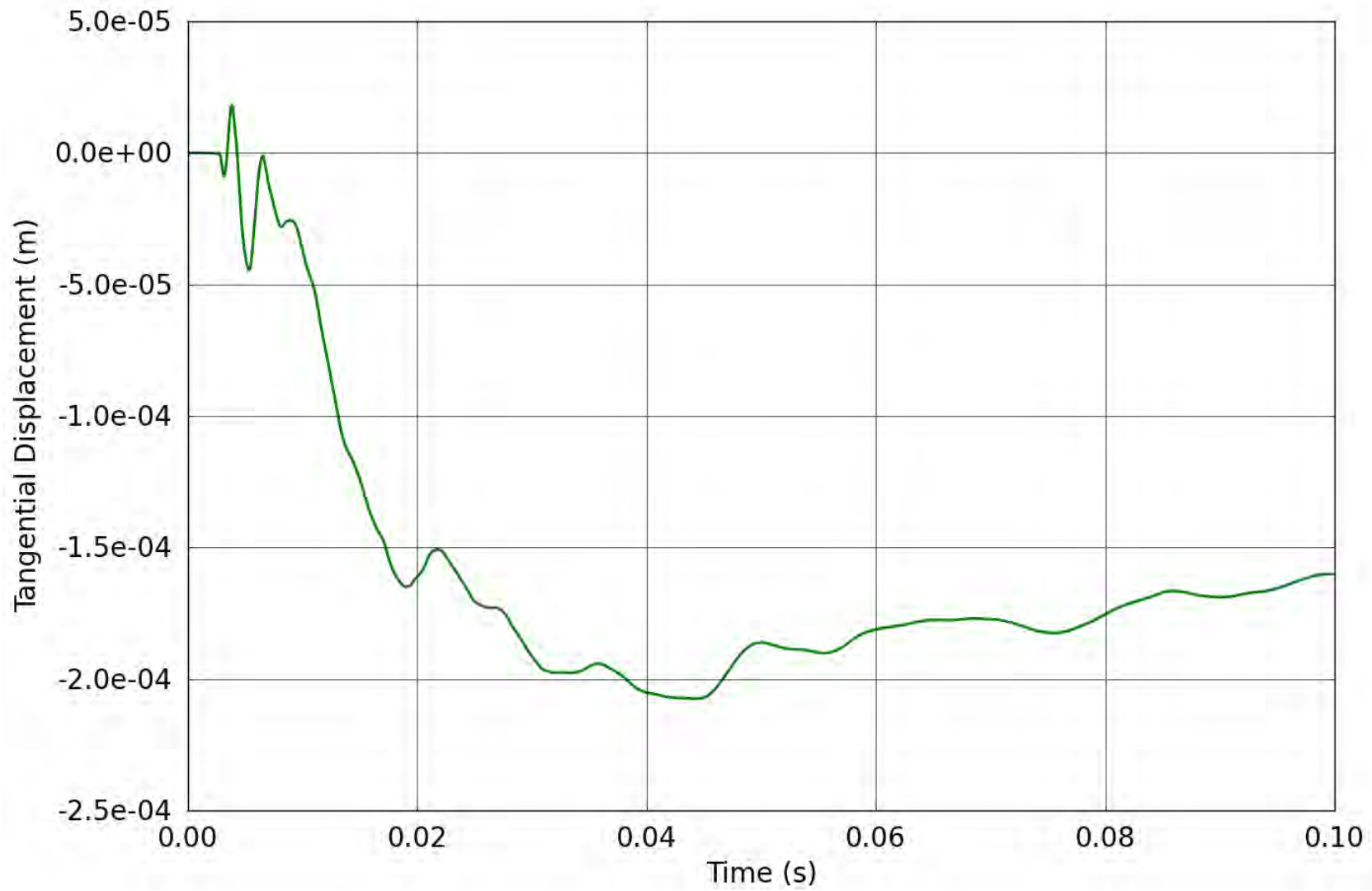
Figure 78. SPE-1 Gauge 3-2-T – Tangential displacement obtained from the corrected tangential velocity.
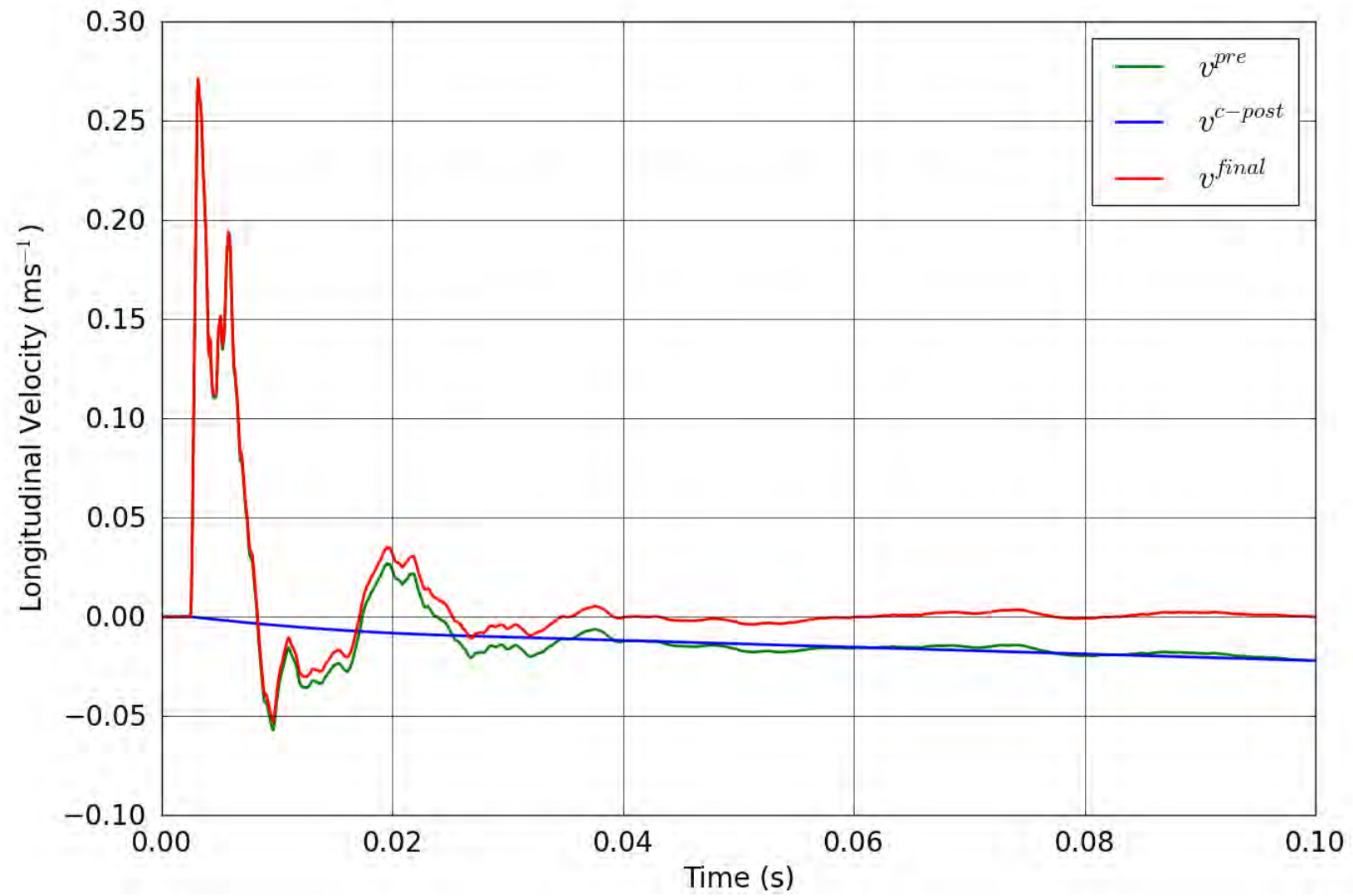
Figure 79. SPE-1 Gauge 3-2-L – Correction of the longitudinal velocity.
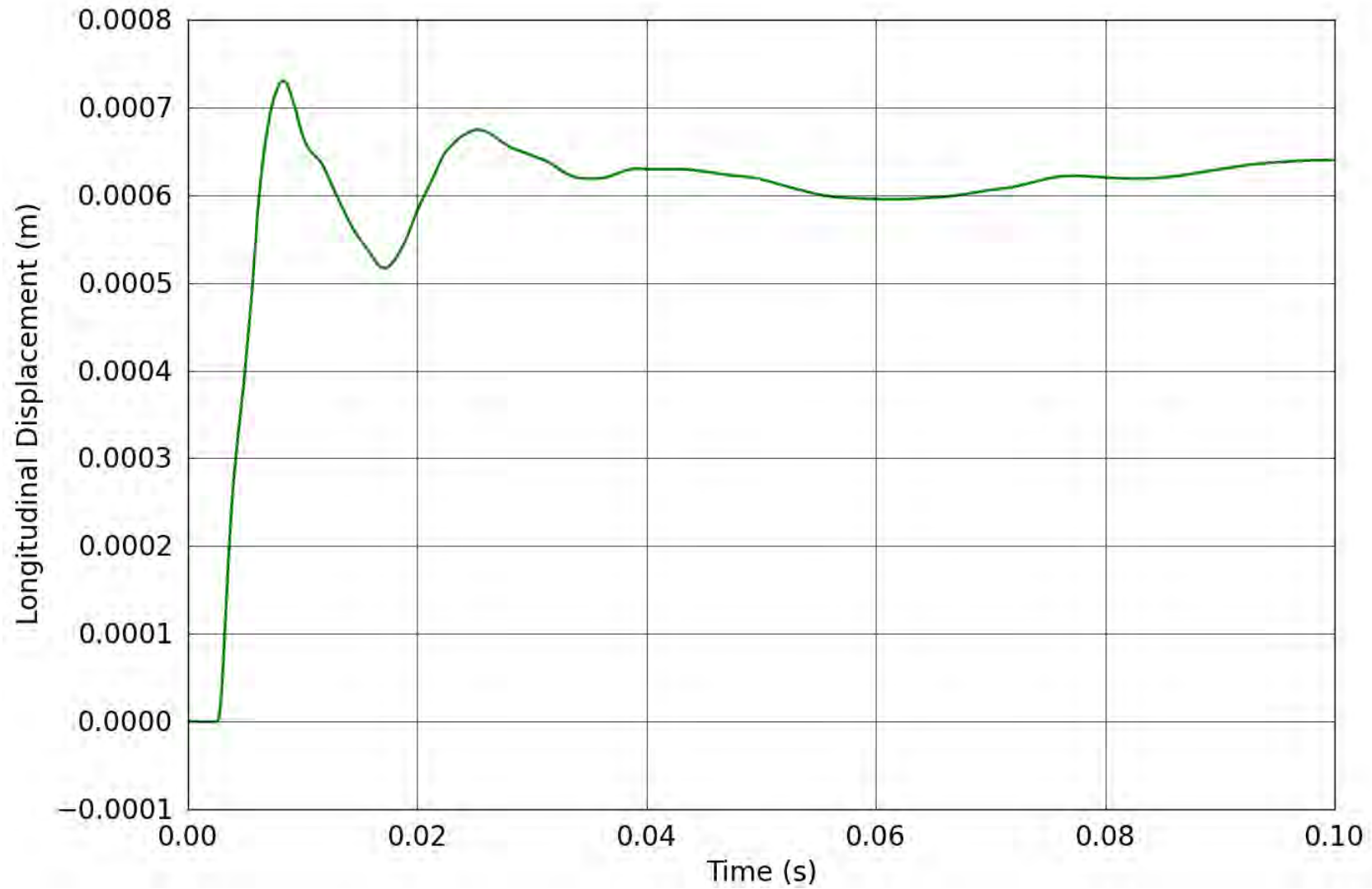
Figure 80. SPE-1 Gauge 3-2-L – Longitudinal displacement obtained from the corrected longitudinal velocity.
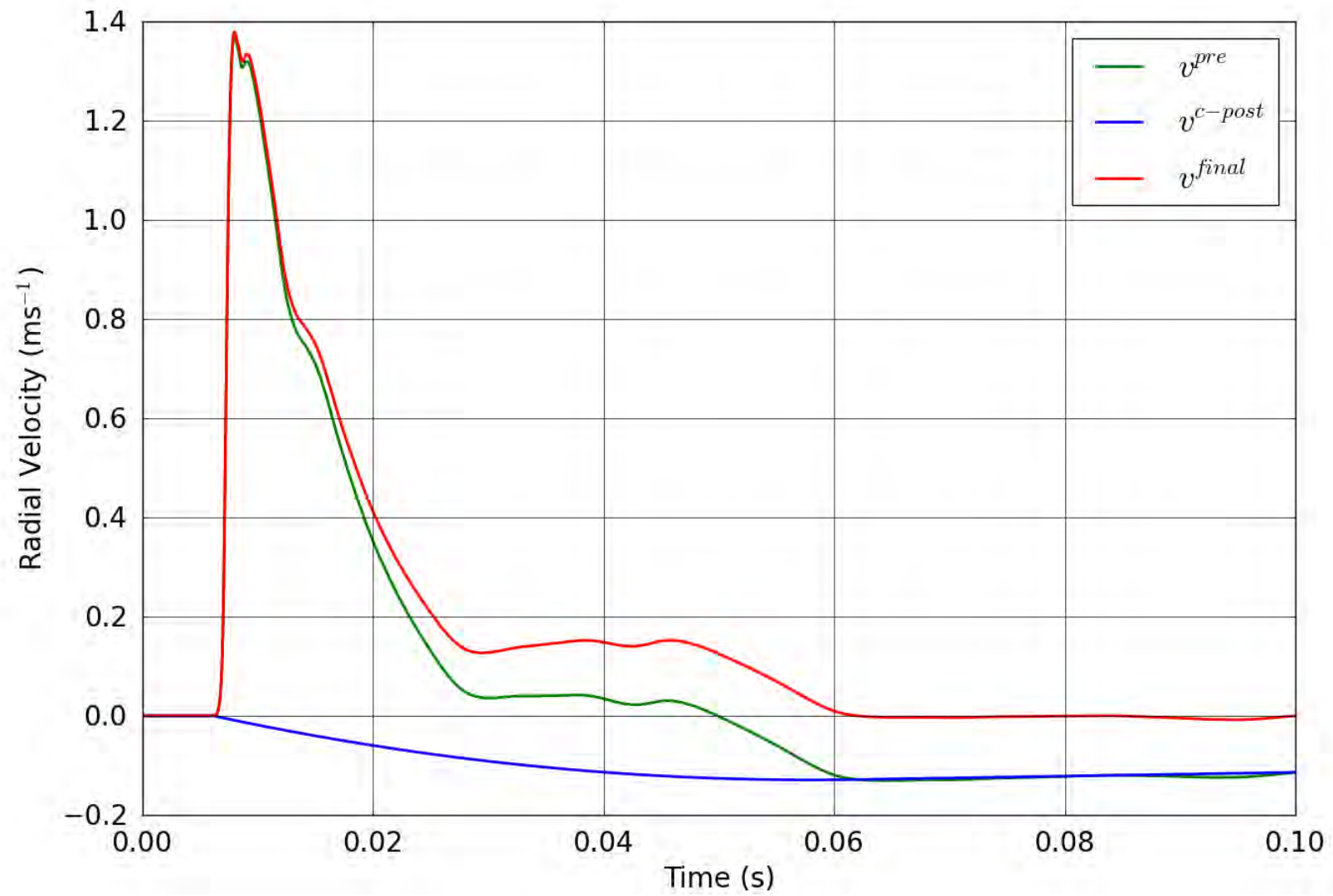
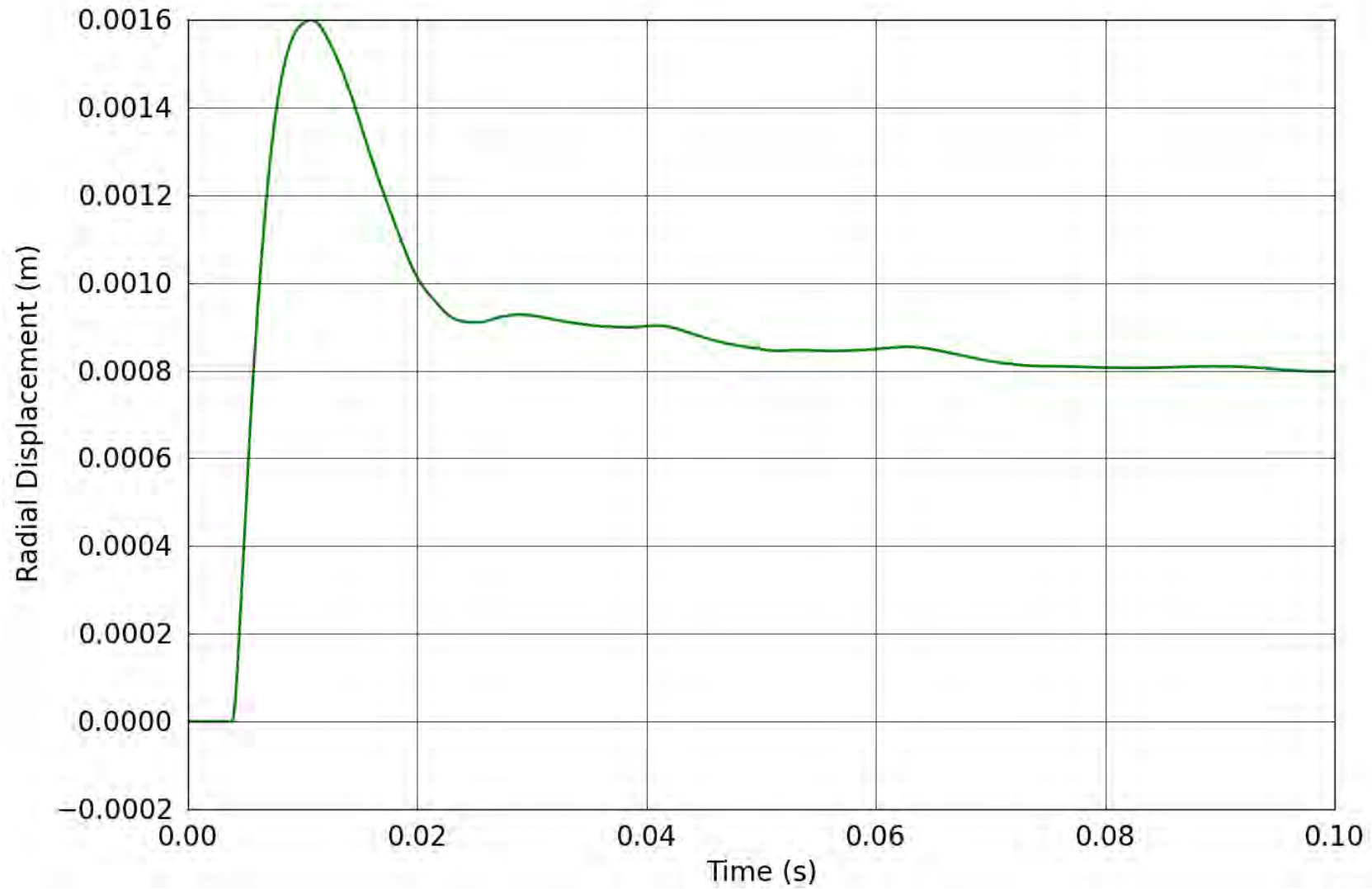Figure 81. SPE-1 Gauge 3-3-R – Correction of the radial velocity.
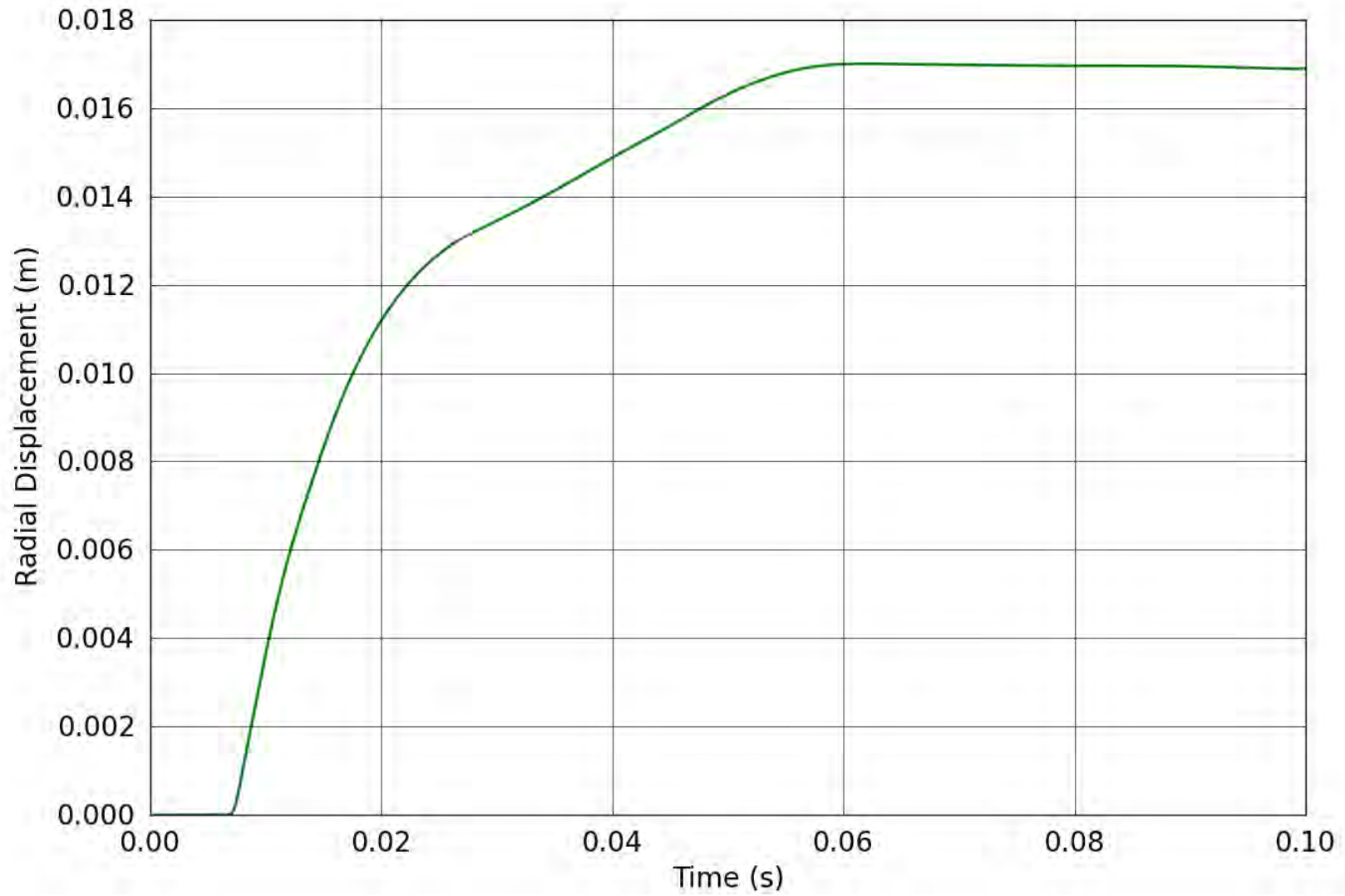
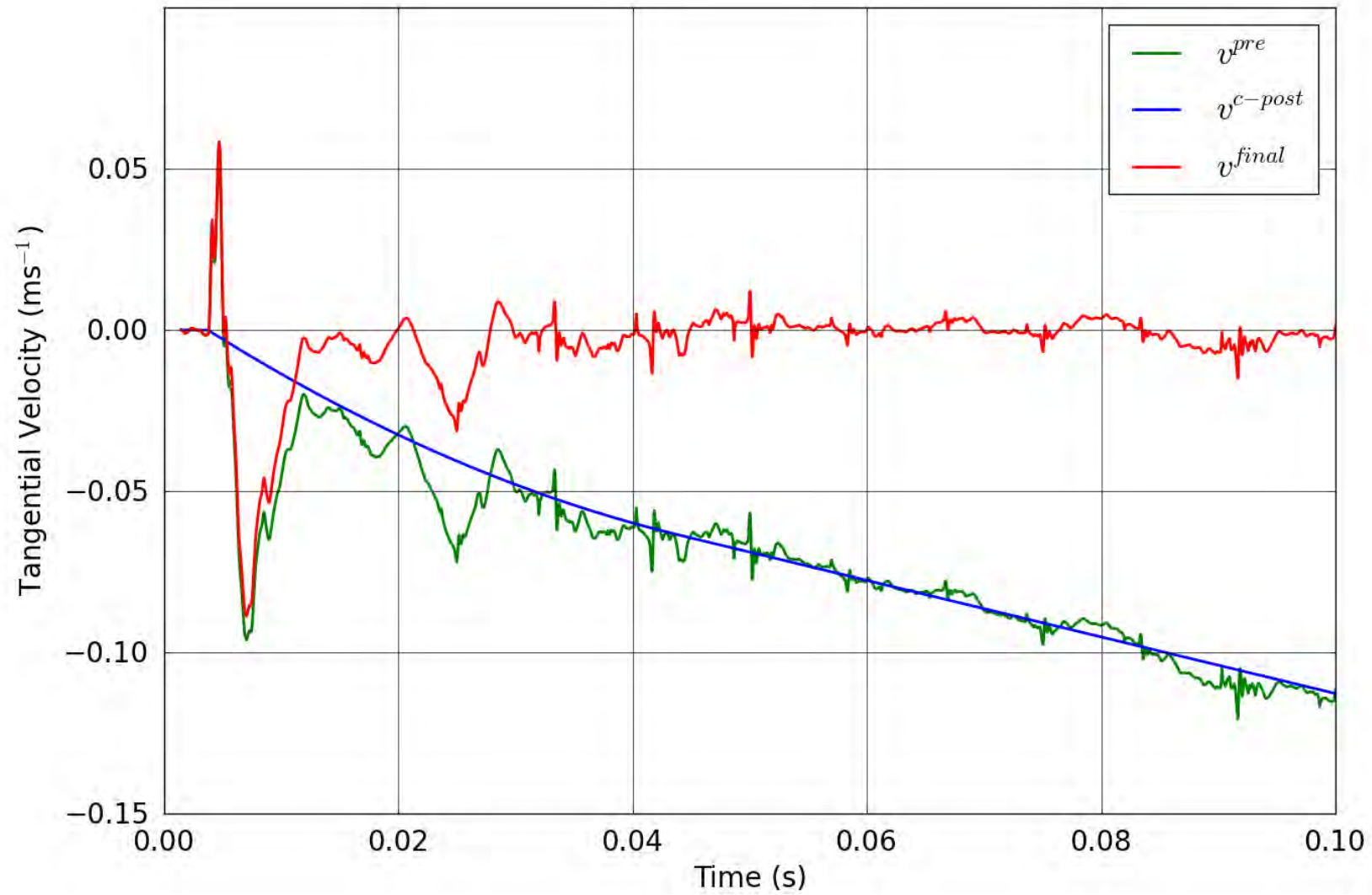Figure 82. SPE-1 Gauge 3-3-R – Radial displacement obtained from the corrected radial velocity.
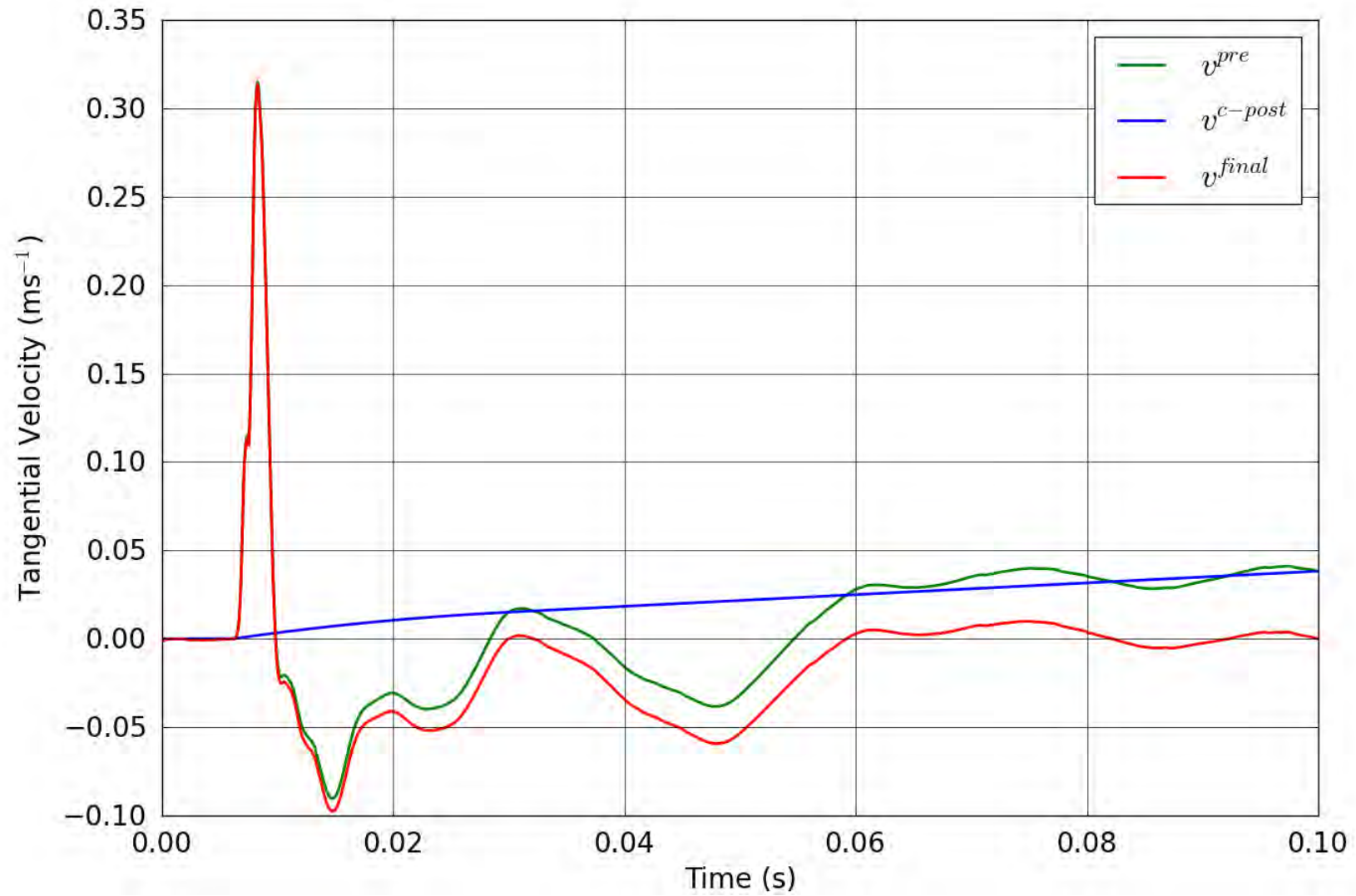
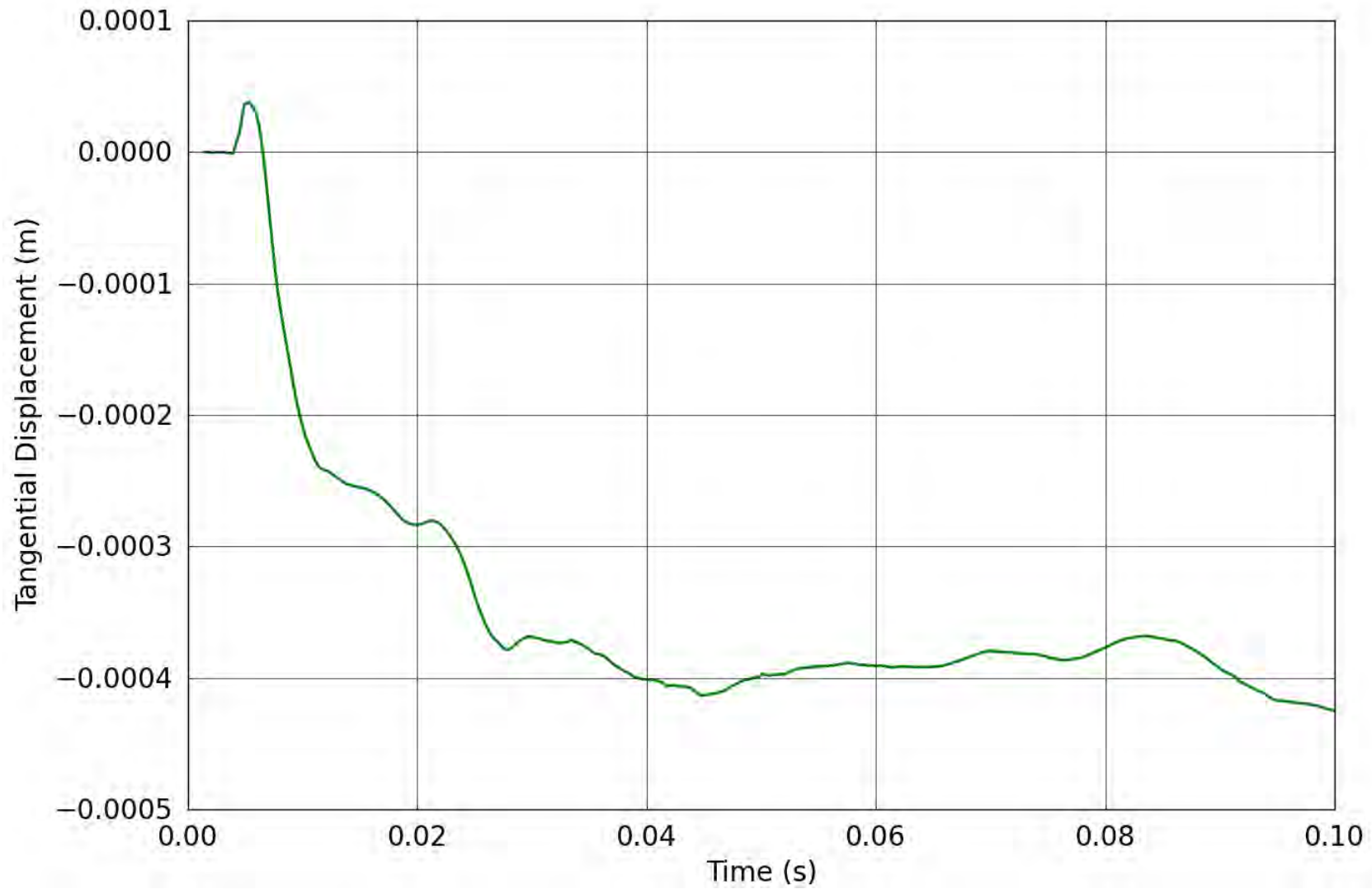Figure 83. SPE-1 Gauge 3-3-T – Correction of the tangential velocity.
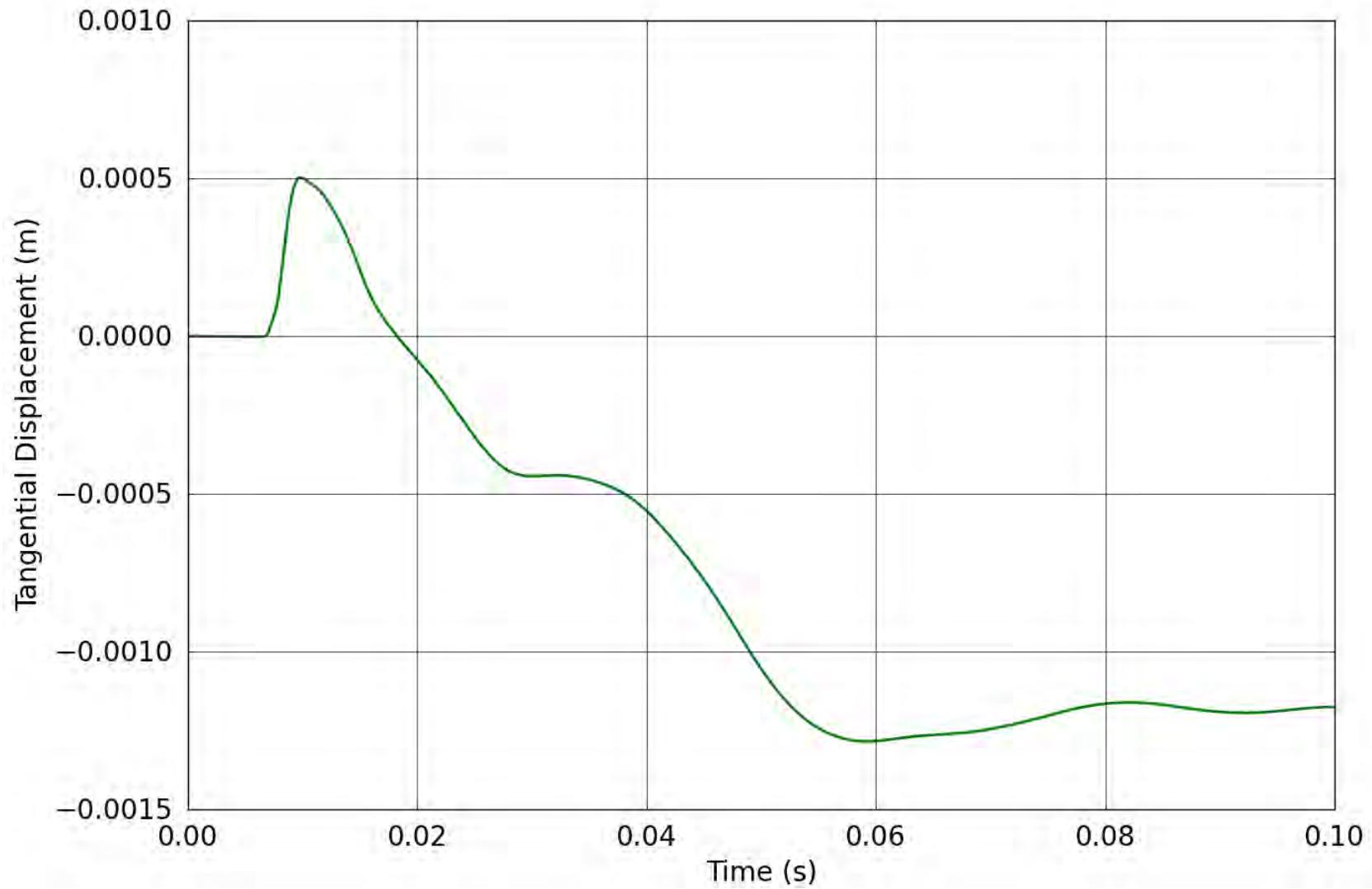
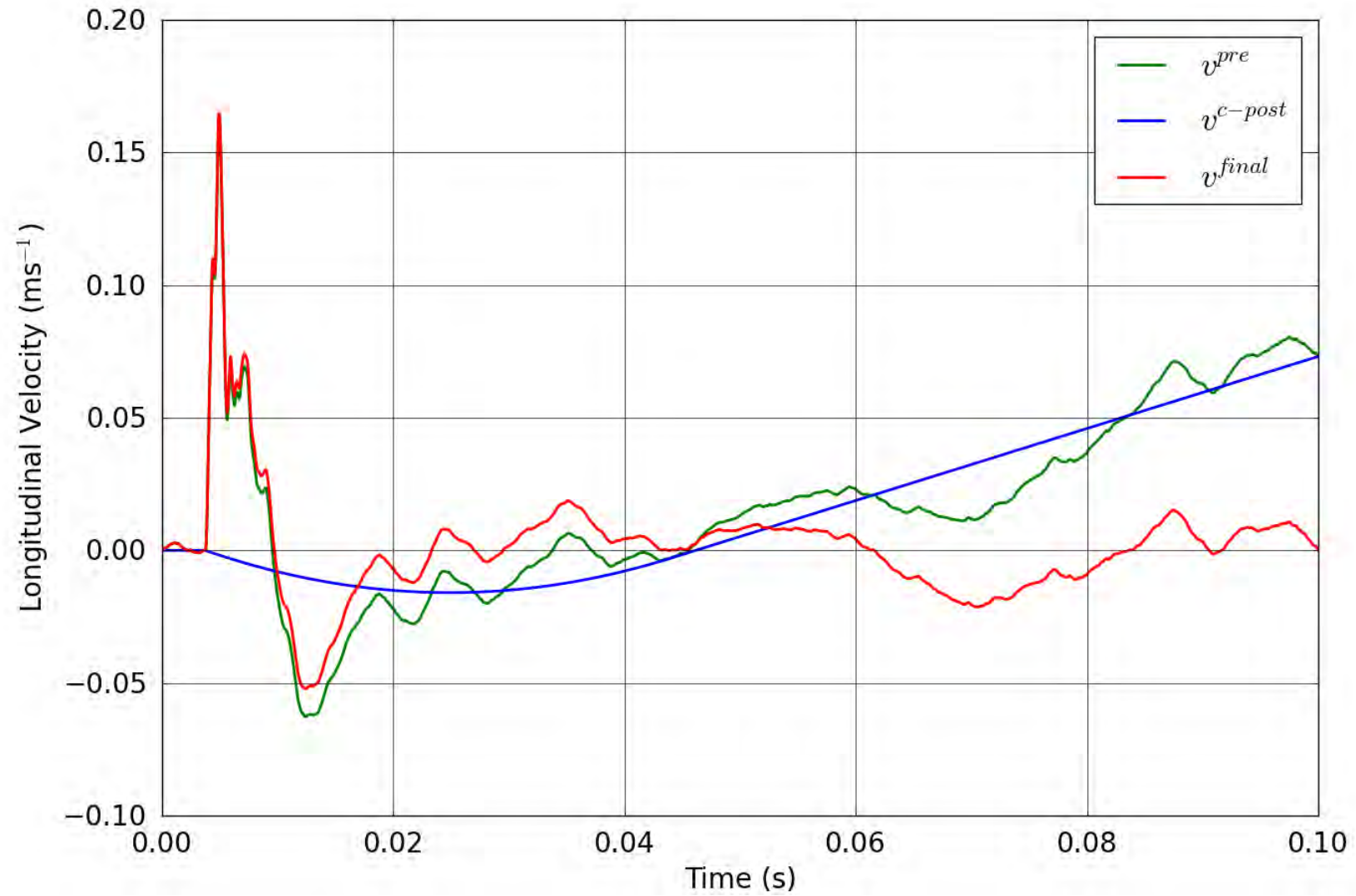Figure 84. SPE-1 Gauge 3-3-T – Tangential displacement obtained from the corrected tangential velocity.
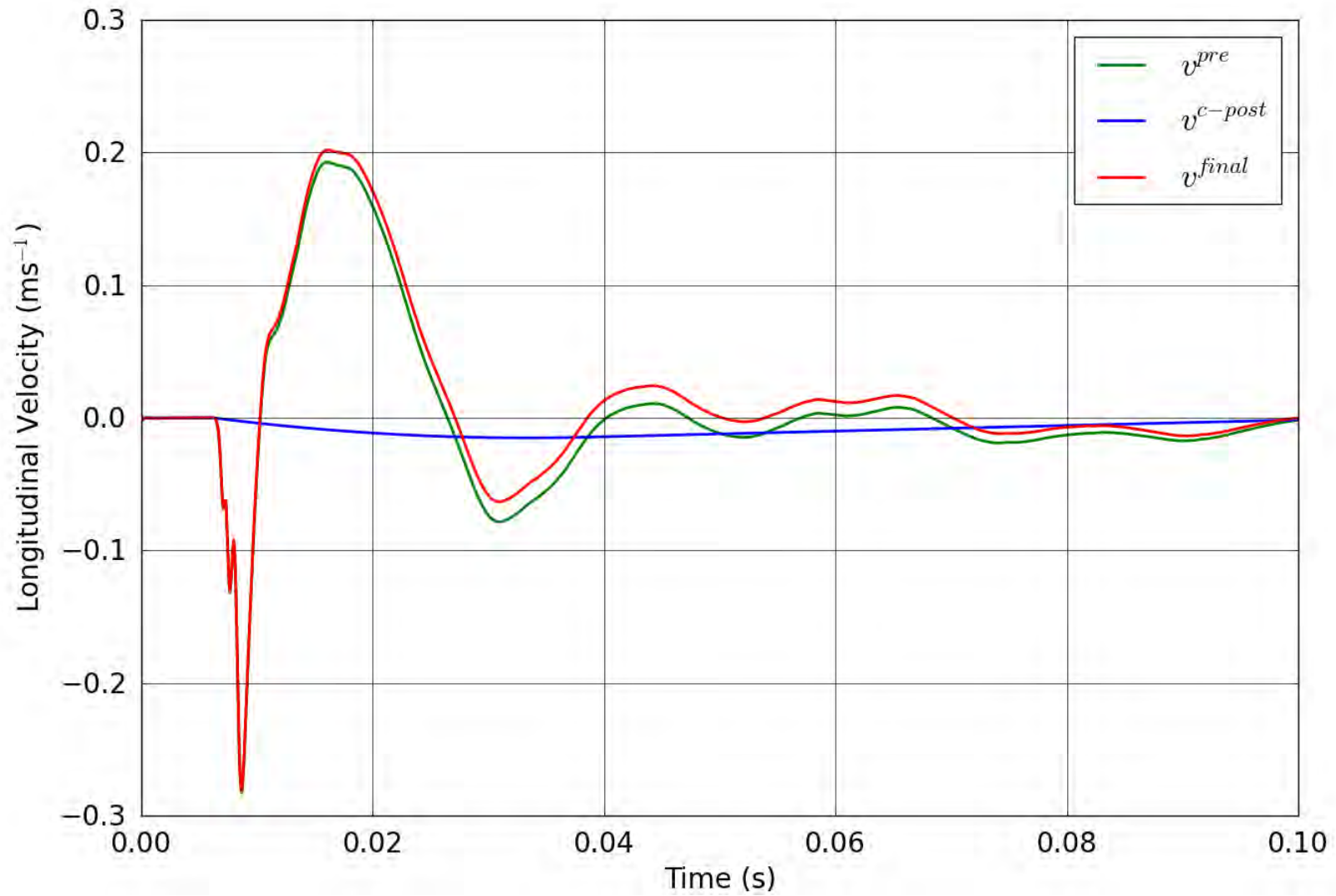
Figure 85. SPE-1 Gauge 3-3-L – Correction of the longitudinal velocity.
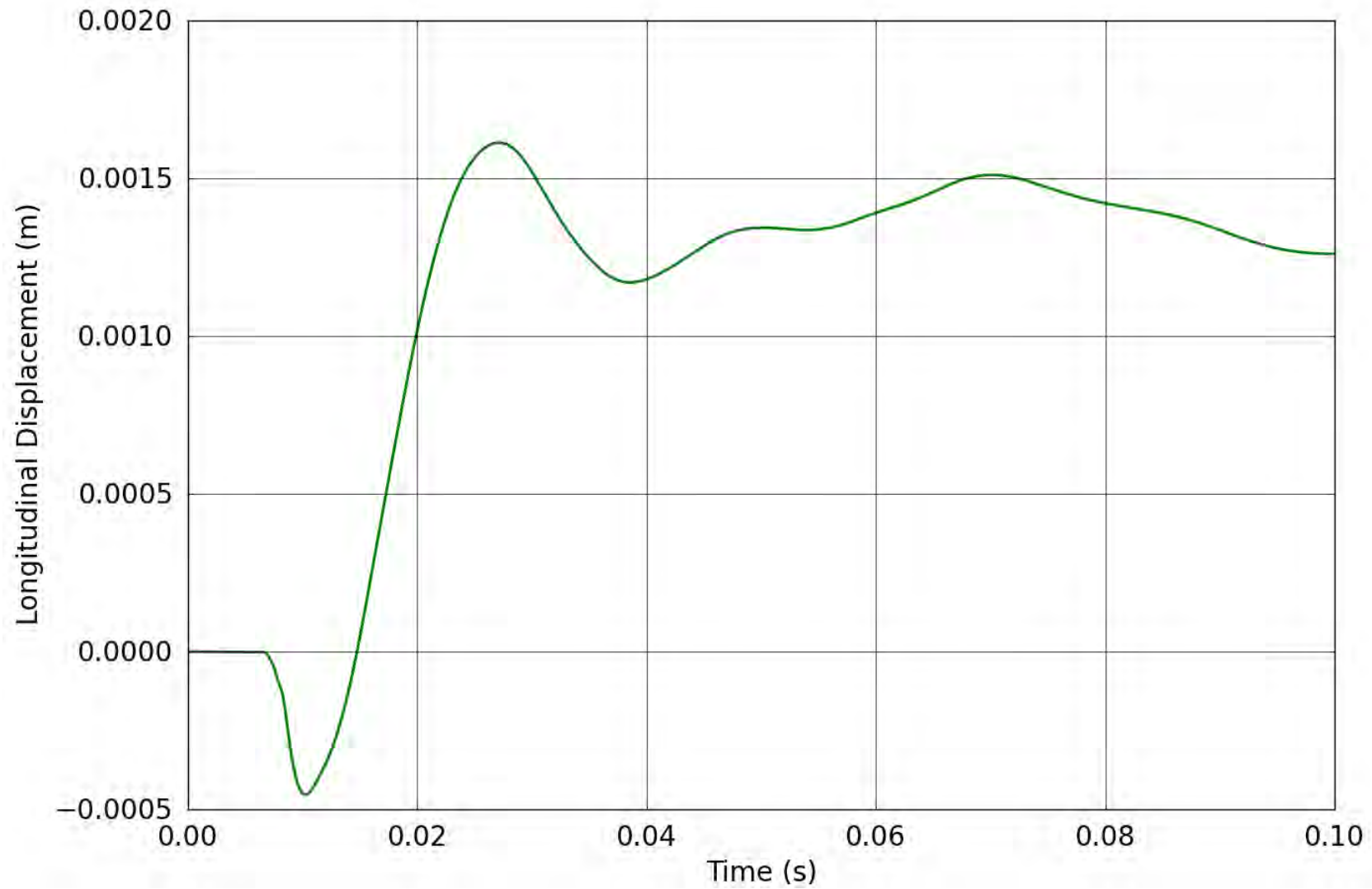
Figure 86. SPE-1 Gauge 3-3-L – Longitudinal displacement obtained from the corrected longitudinal velocity.
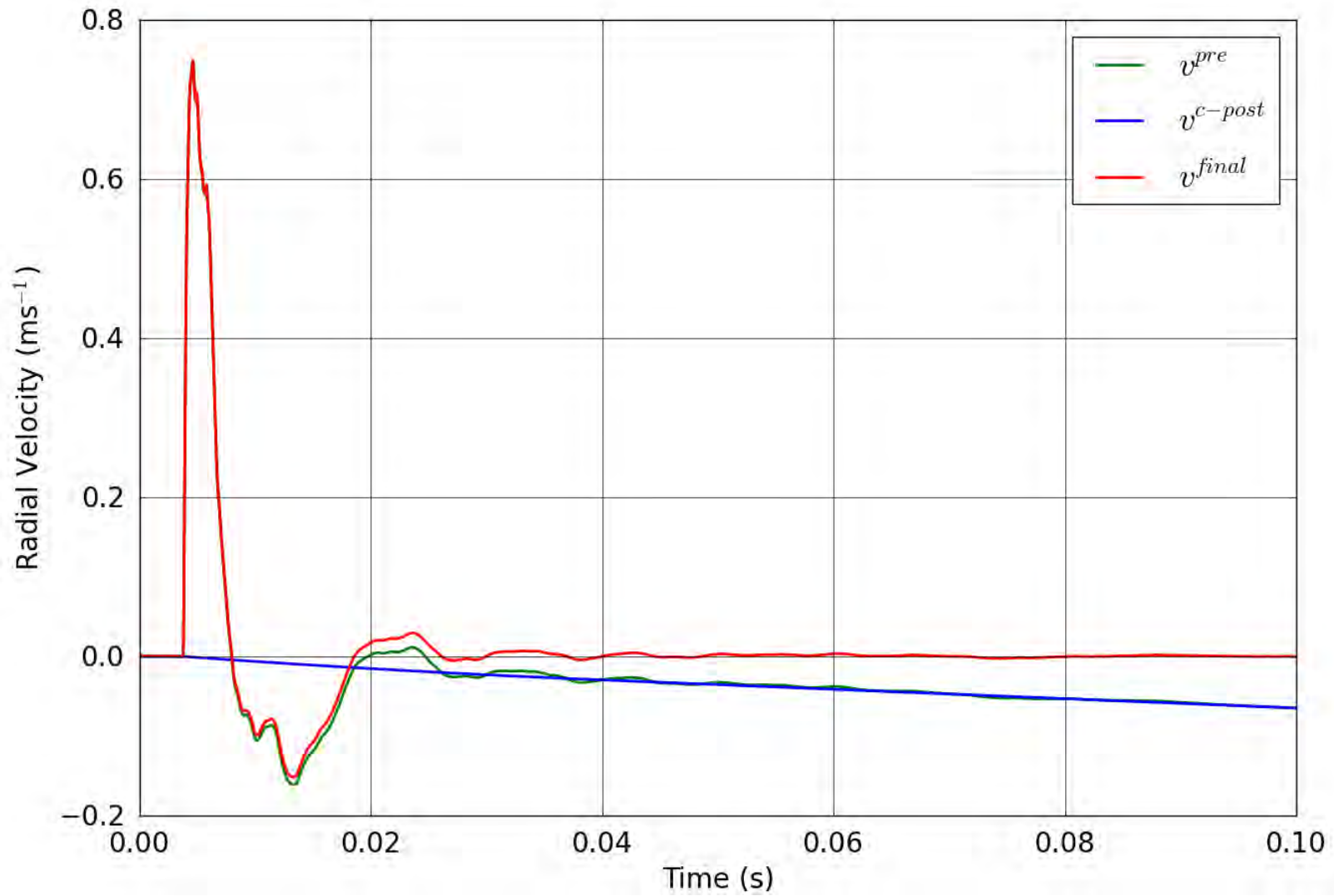
Figure 87. SPE-1 Gauge 4-1-R – Correction of the radial velocity.
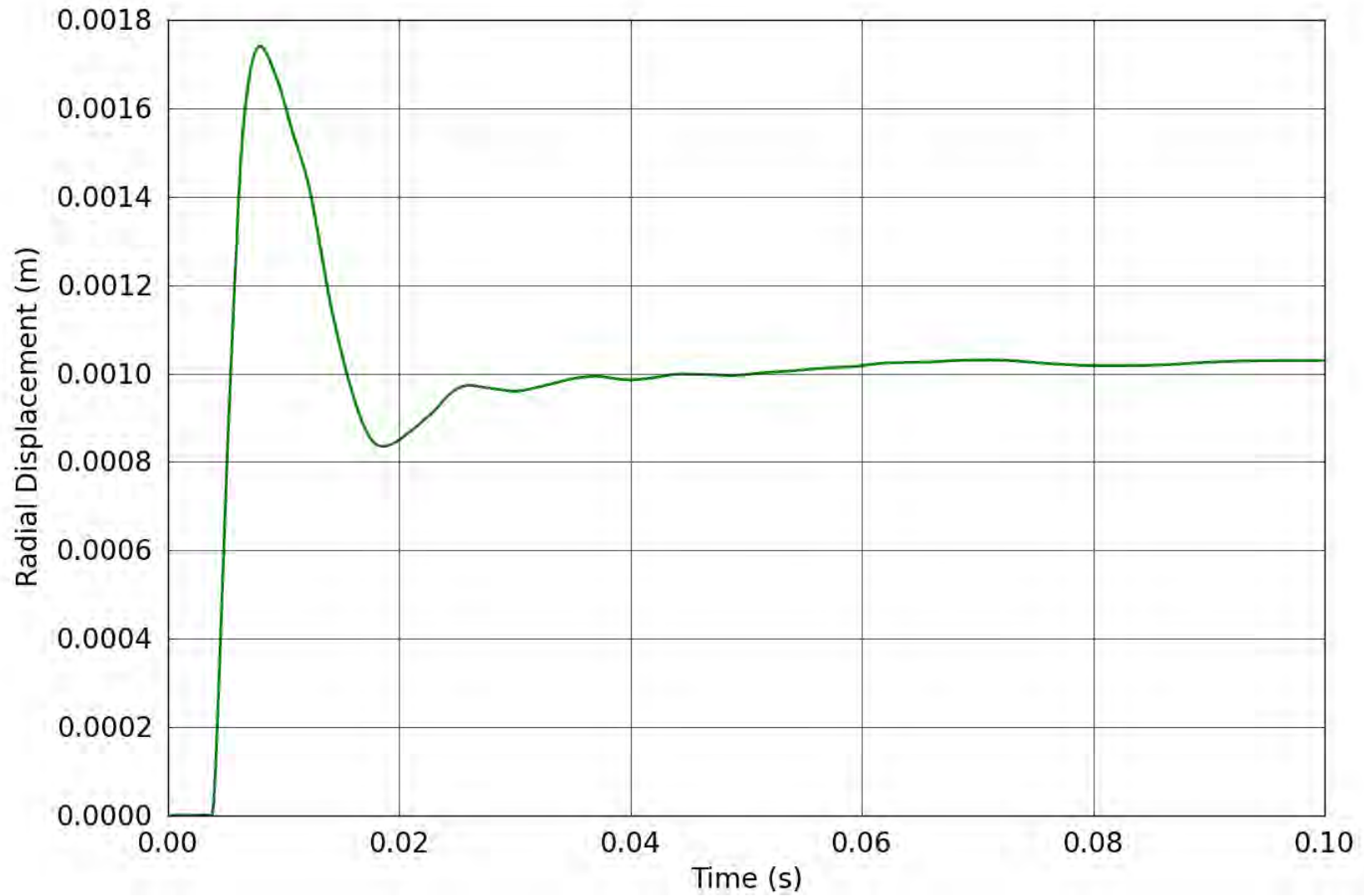
Figure 88. SPE-1 Gauge 4-1-R – Radial displacement obtained from the corrected radial velocity.
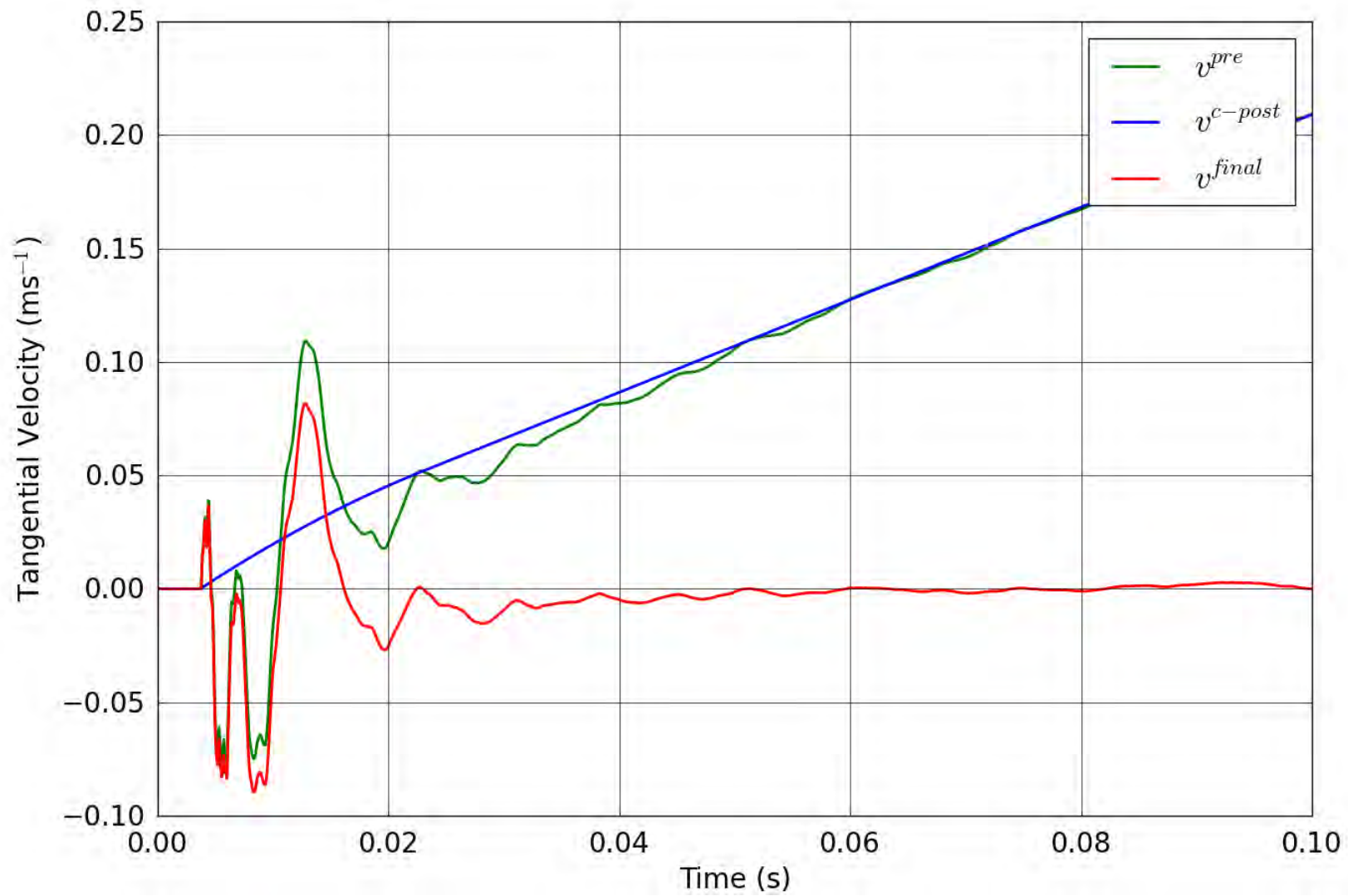
Figure 89. SPE-1 Gauge 4-1-T – Correction of the tangential velocity.
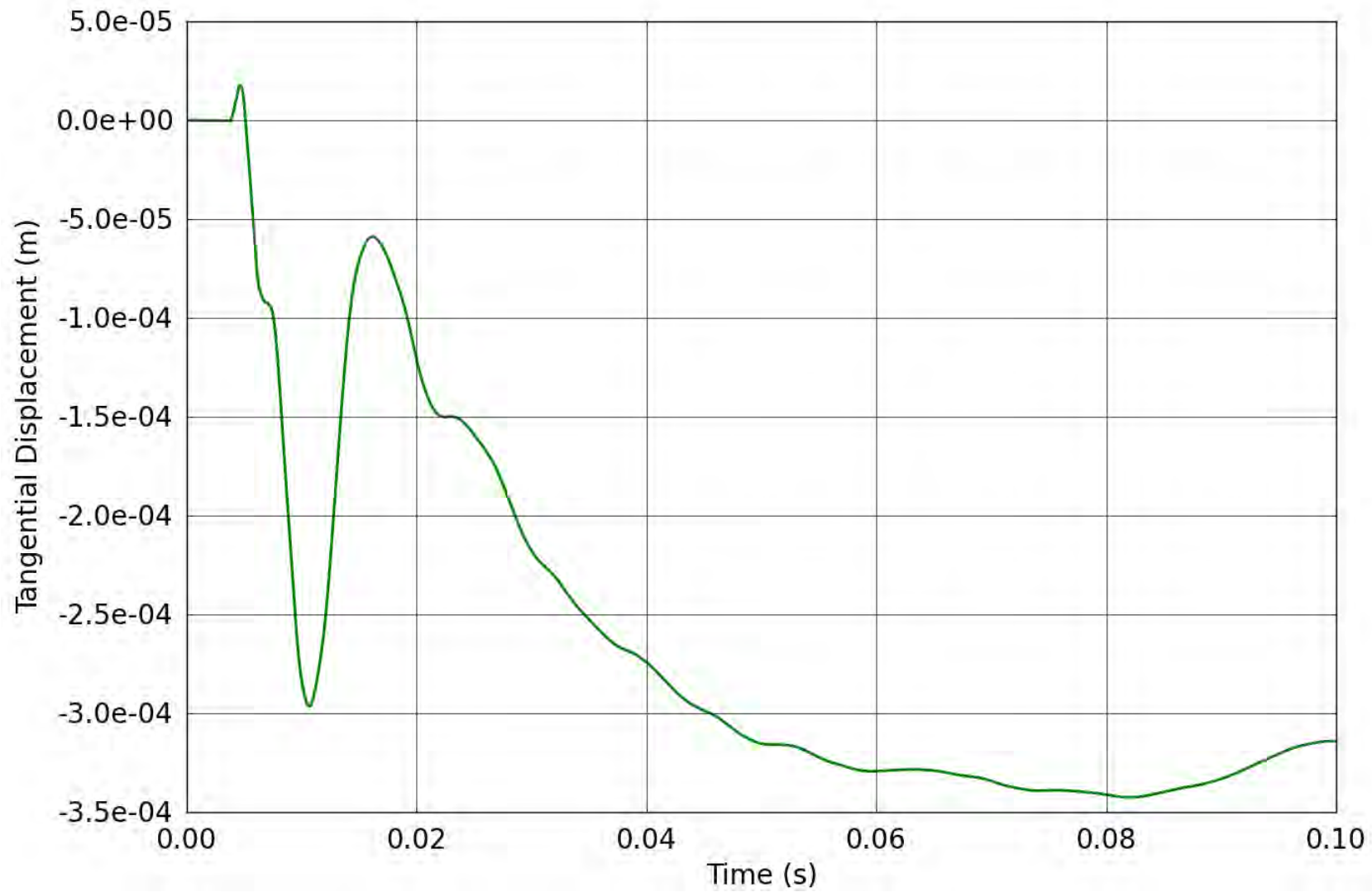
Figure 90. SPE-1 Gauge 4-1-T – Tangential displacement obtained from the corrected tangential velocity.
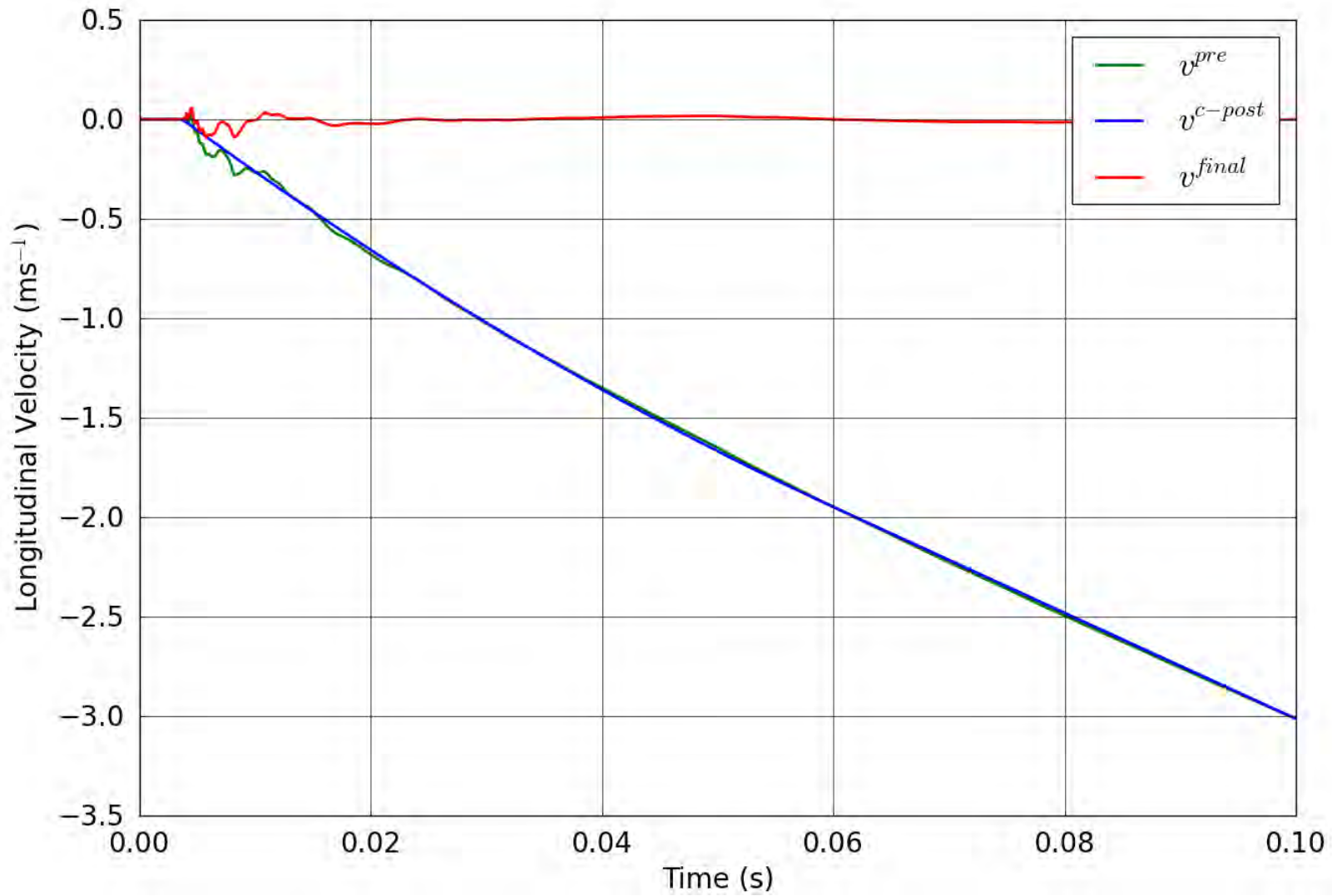
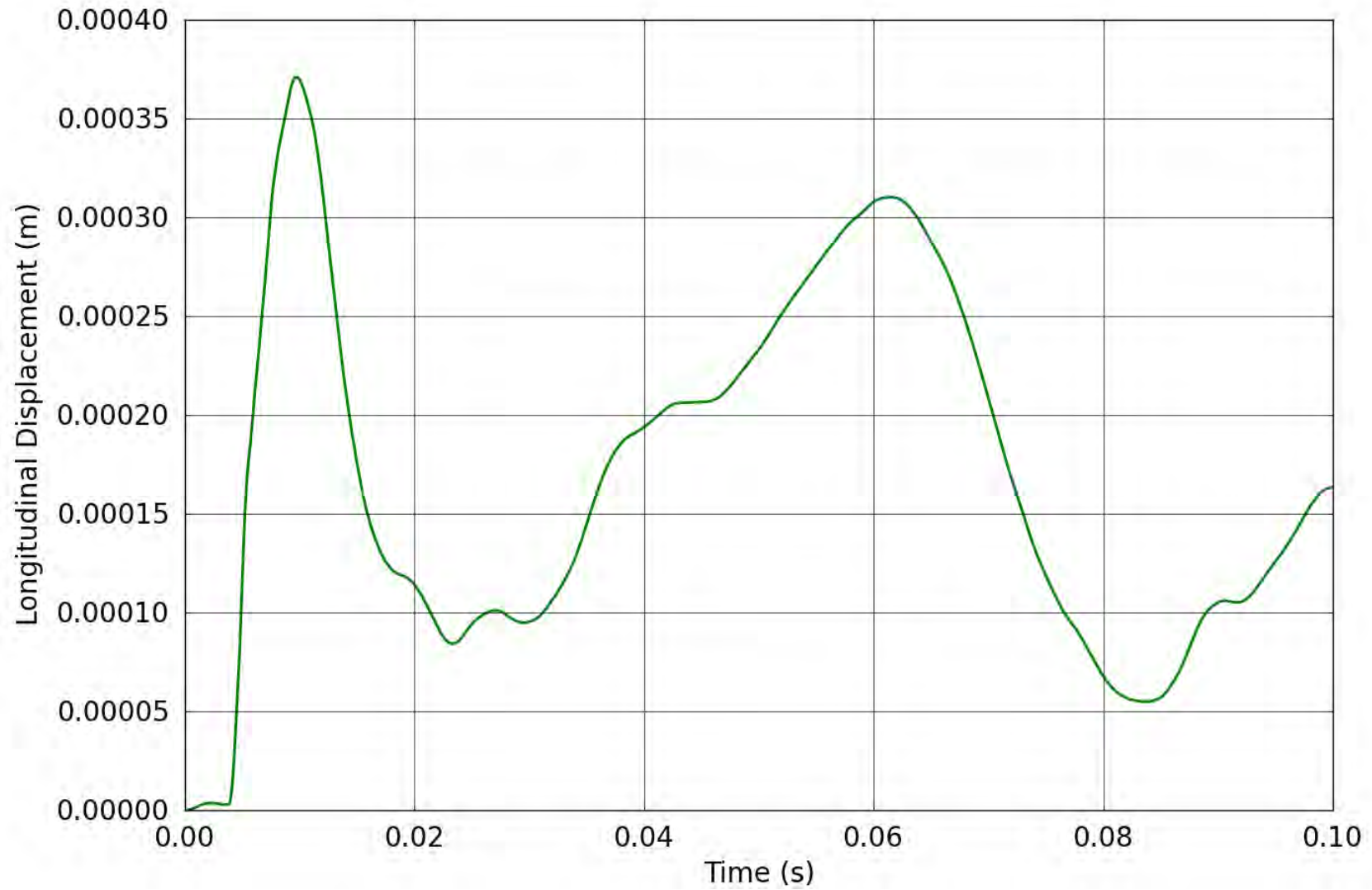Figure 91. SPE-1 Gauge 4-1-L – Correction of the longitudinal velocity.
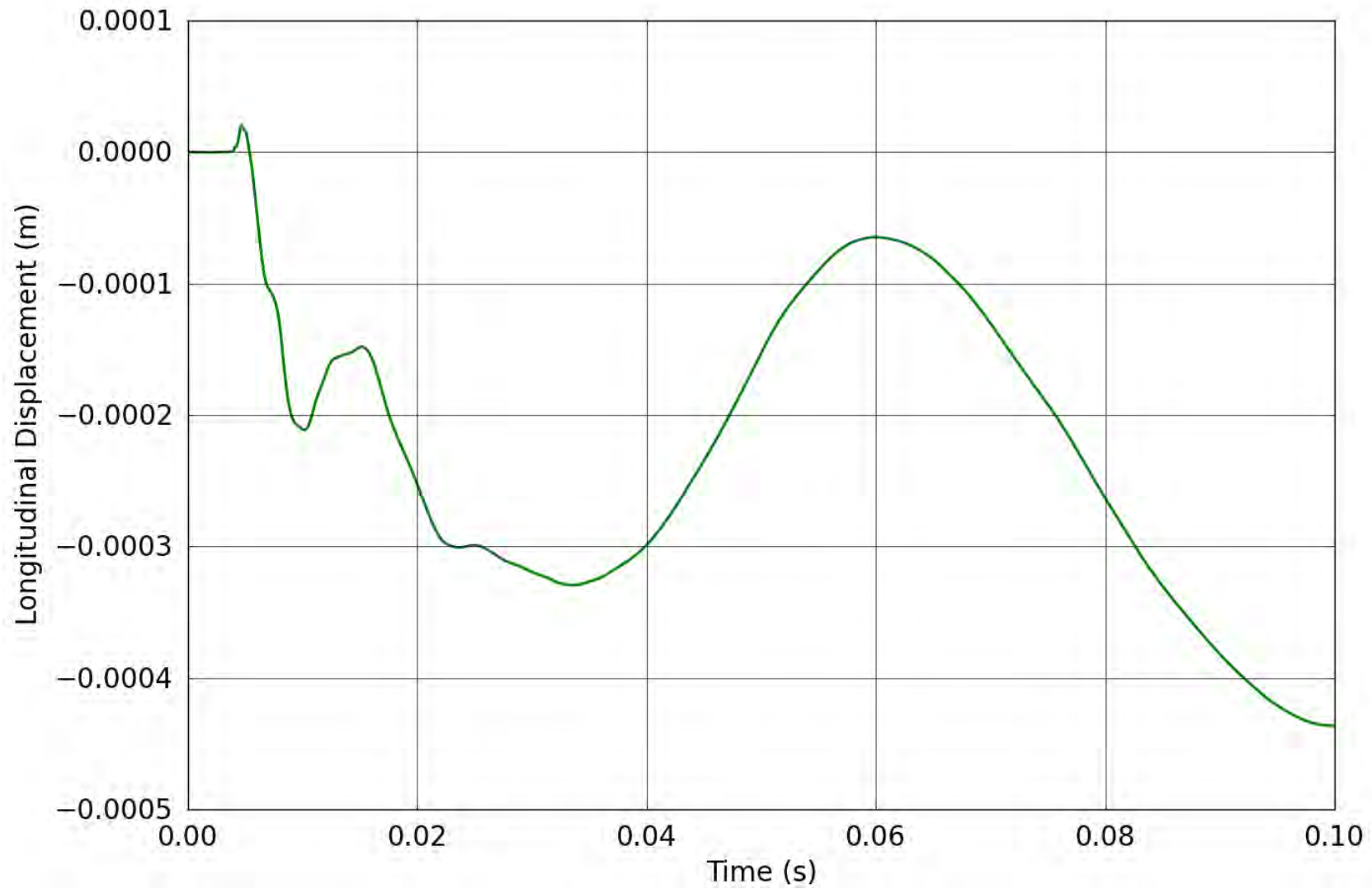
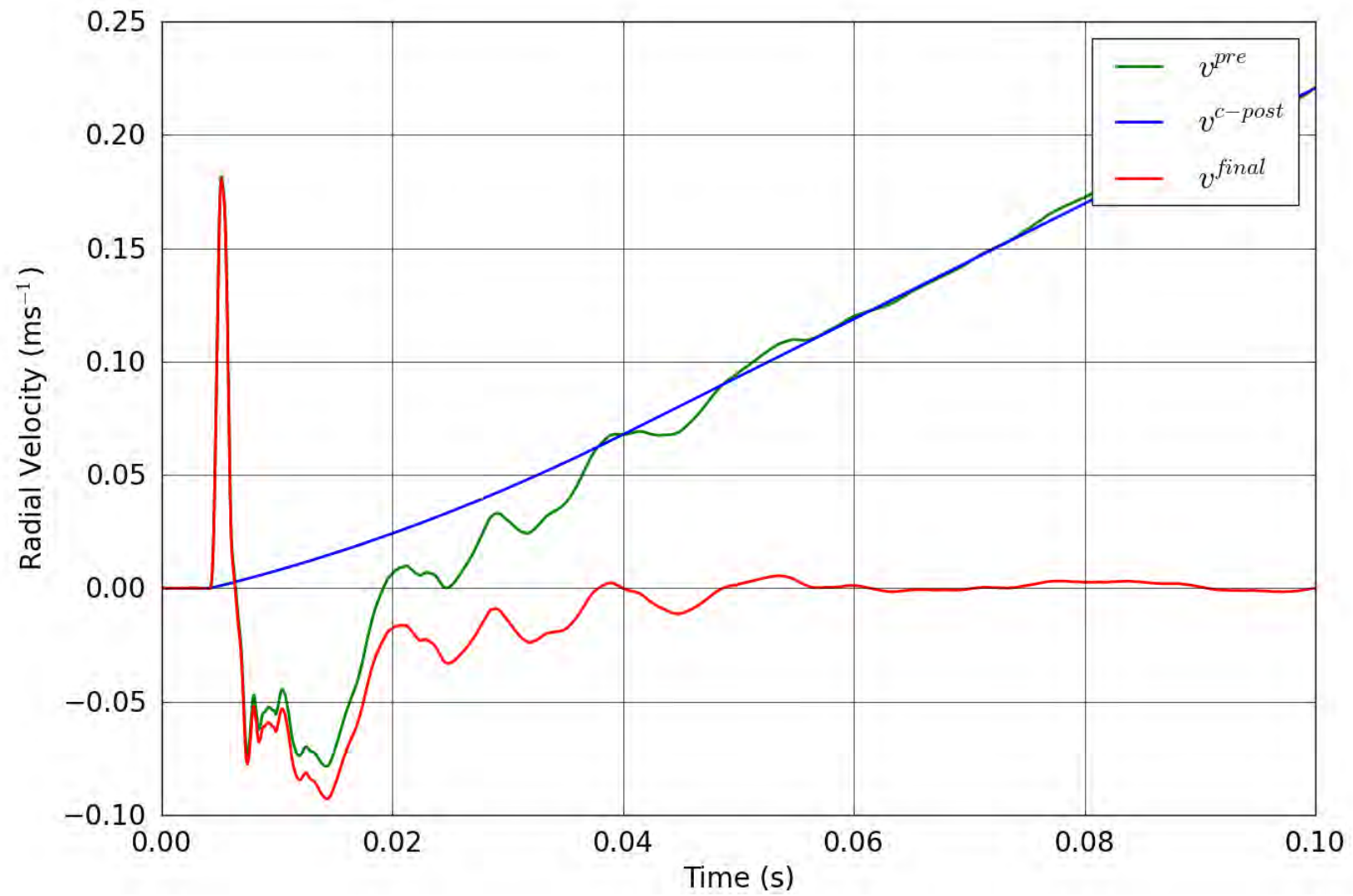Figure 92. SPE-1 Gauge 4-1-L – Longitudinal displacement obtained from the corrected longitudinal velocity.
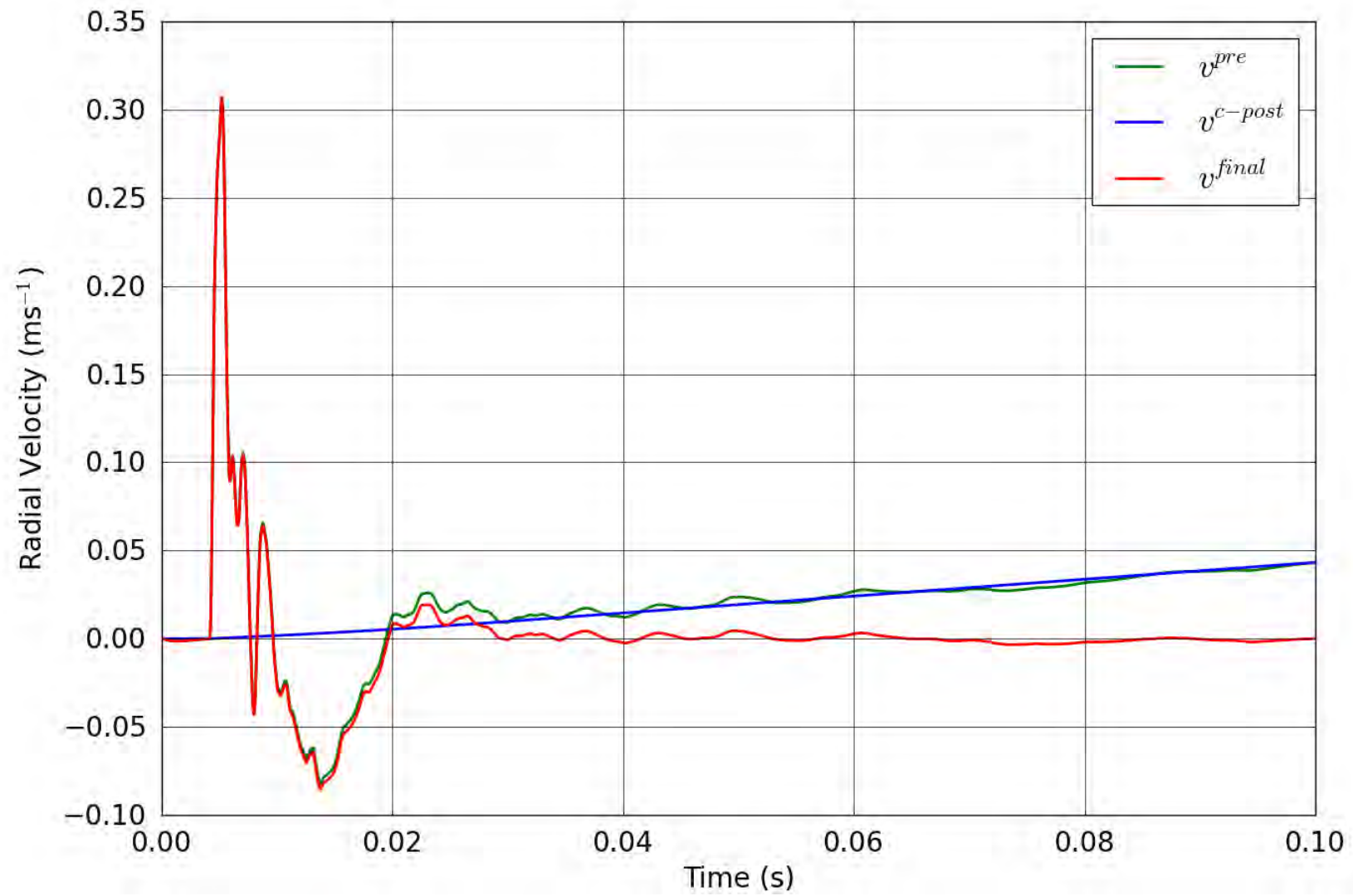
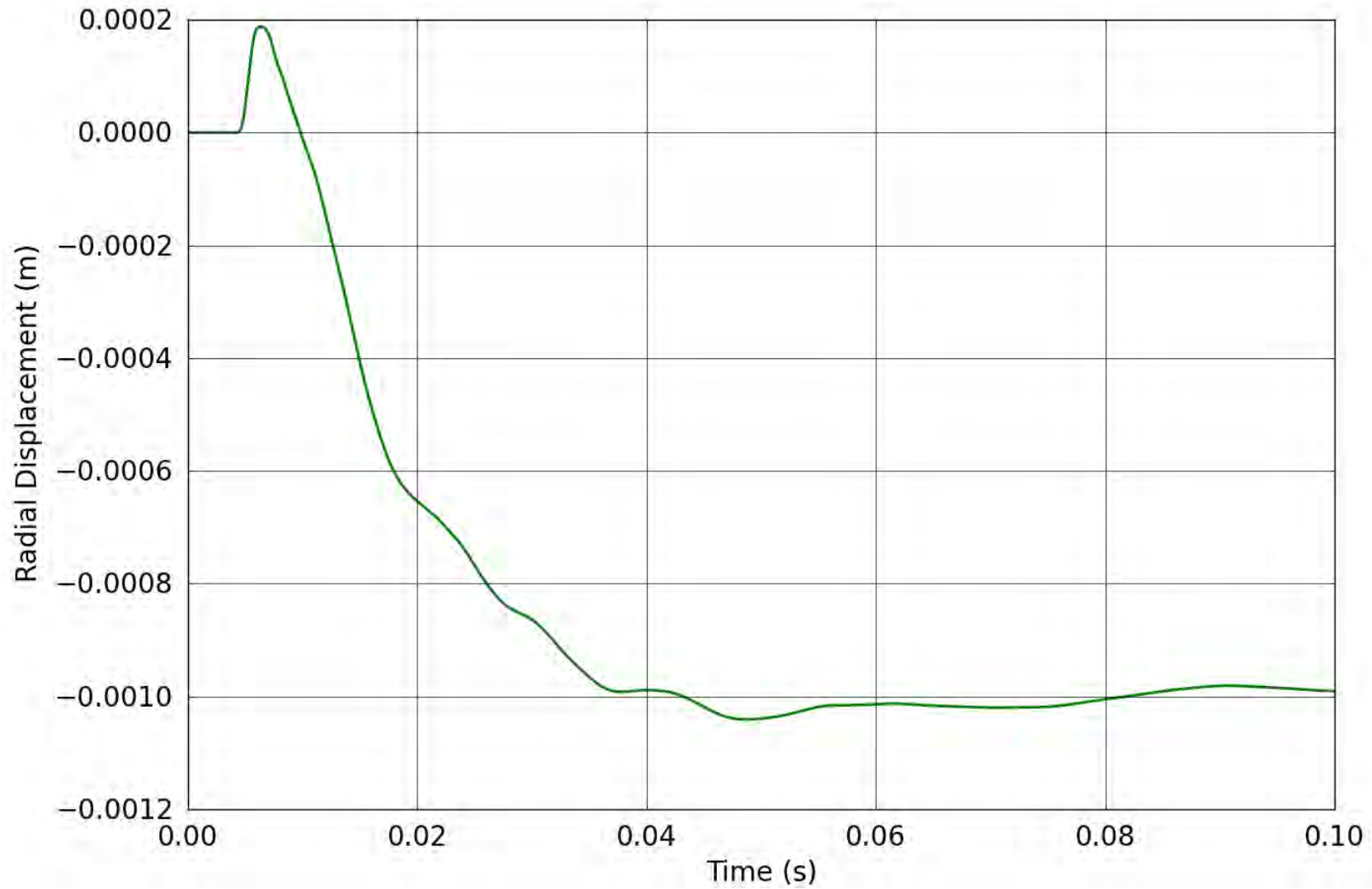Figure 93. SPE-1 Gauge 4-2-R – Correction of the radial velocity.
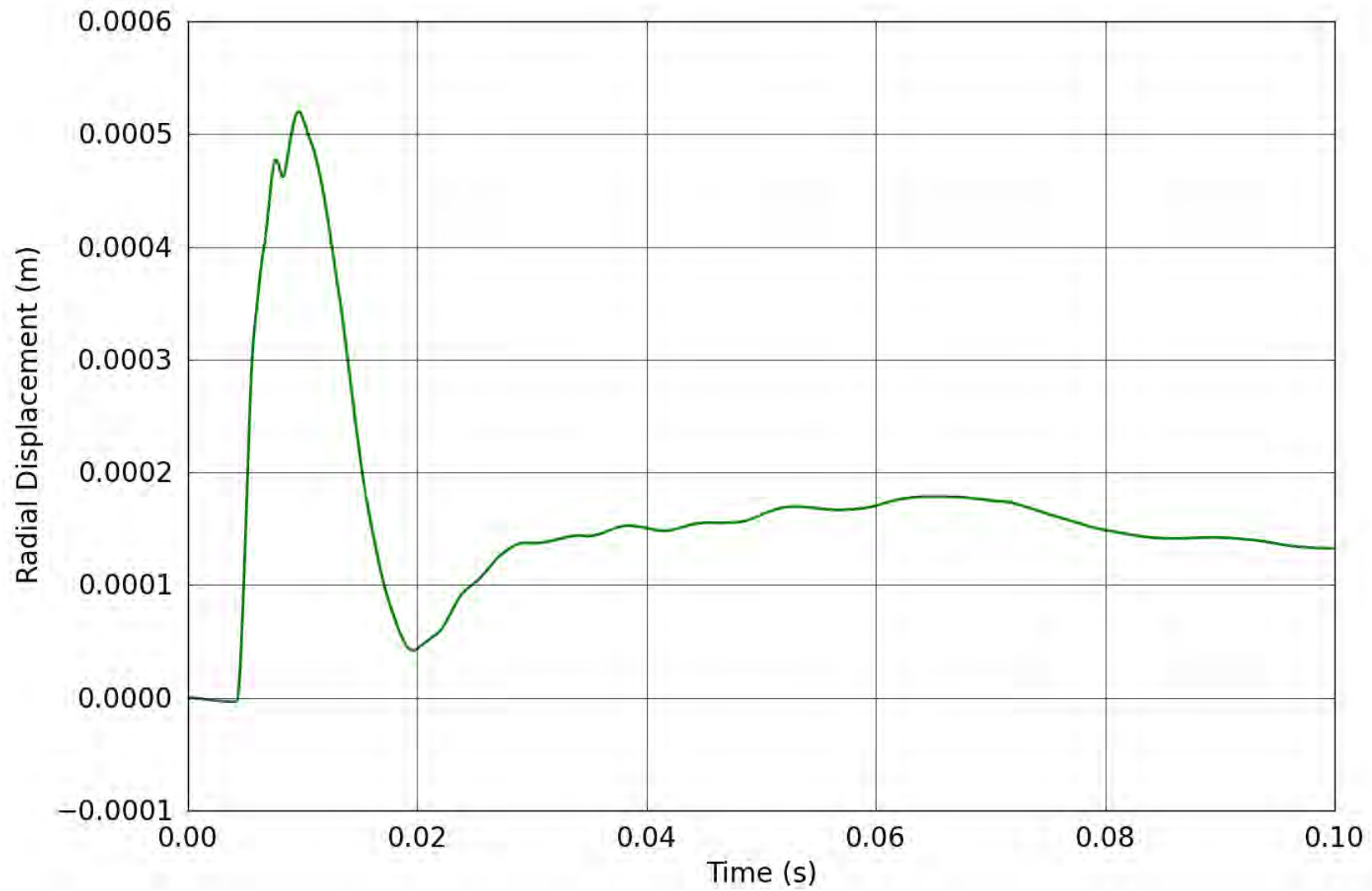
Figure 94. SPE-1 Gauge 4-2-R – Radial displacement obtained from the corrected radial velocity.
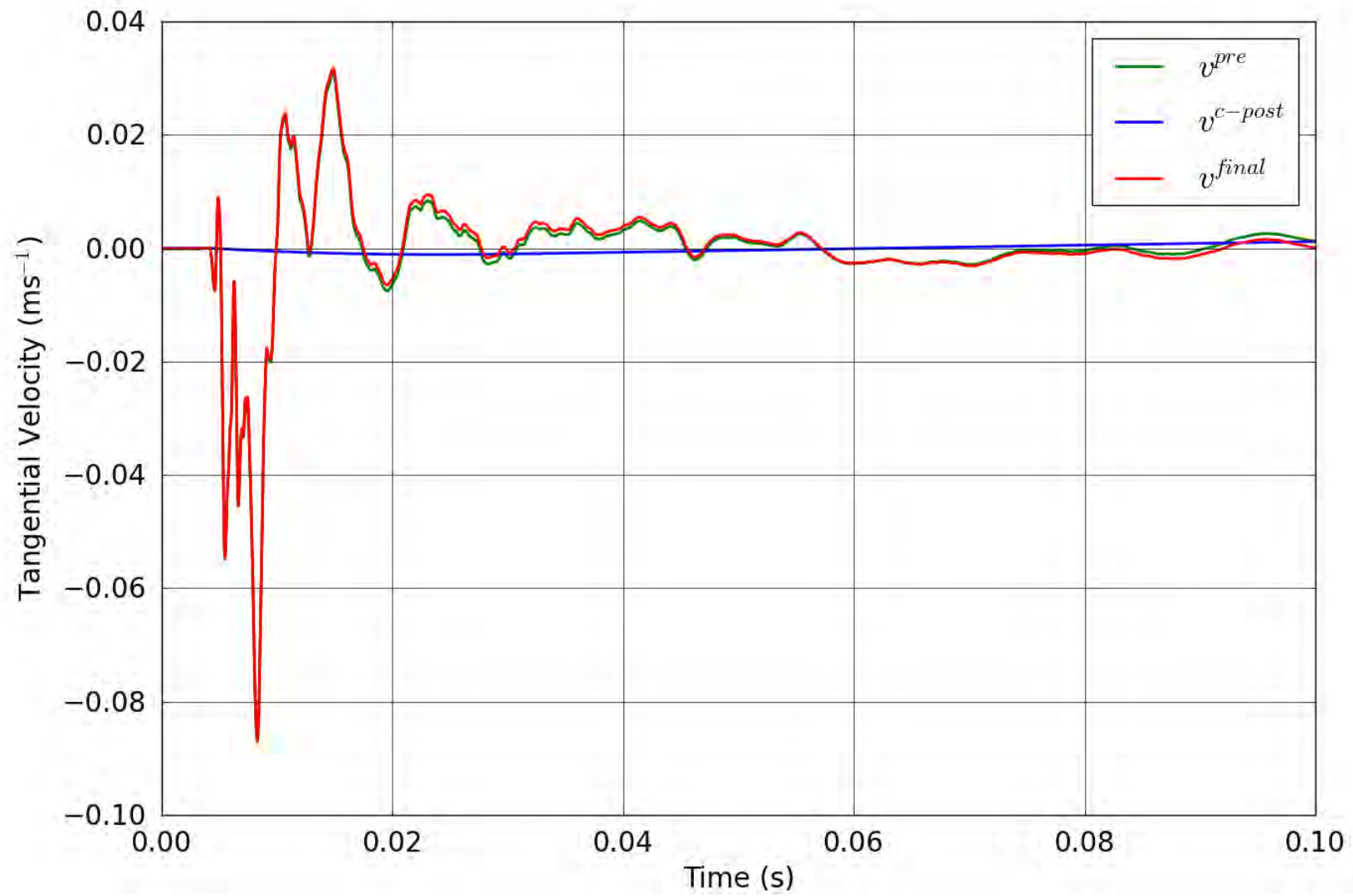
Figure 95. SPE-1 Gauge 4-2-T – Correction of the tangential velocity.
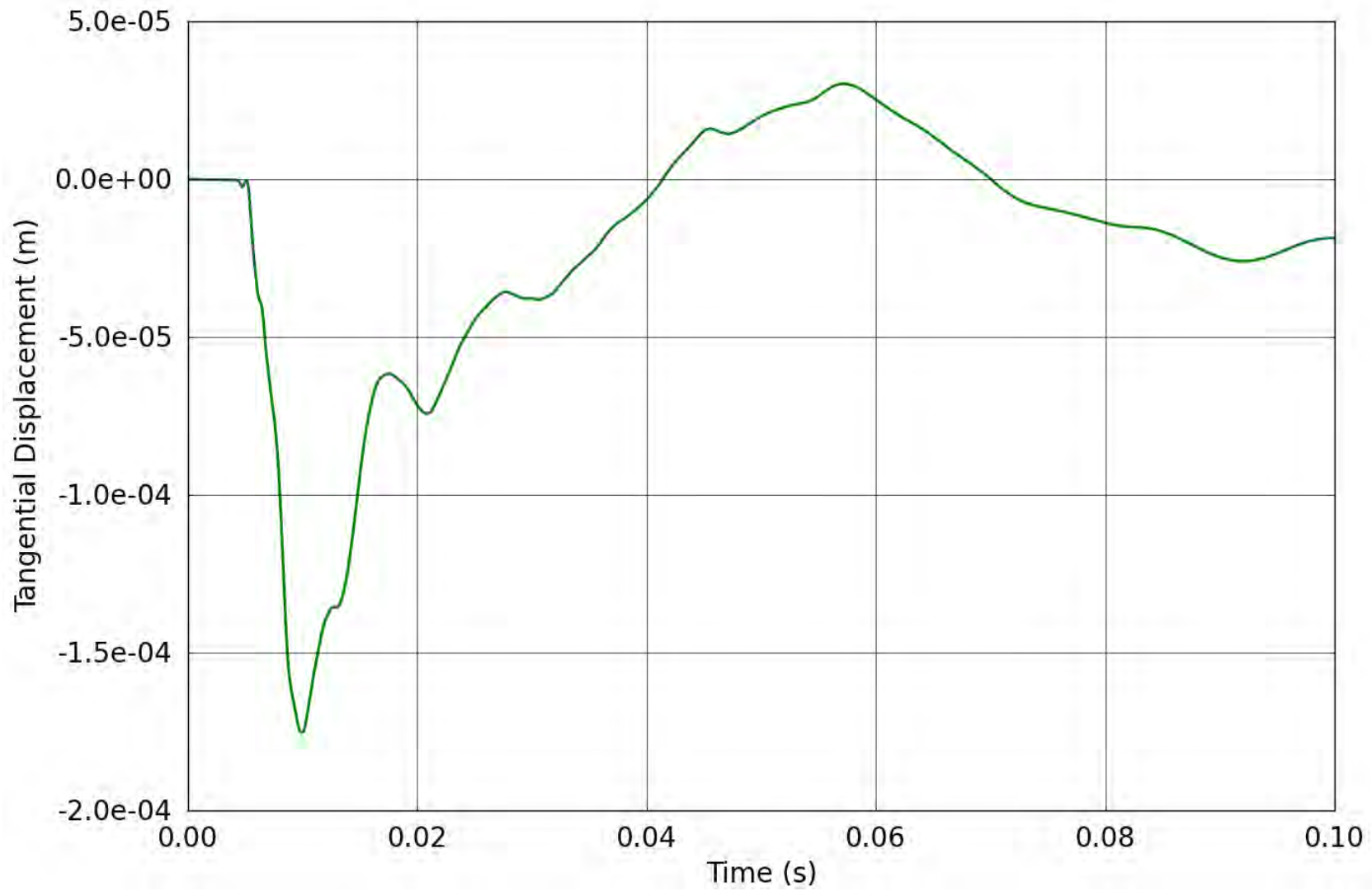
Figure 96. SPE-1 Gauge 4-2-T – Tangential displacement obtained from the corrected tangential velocity.

Figure 97. SPE-1 Gauge 4-2-L – Correction of the longitudinal velocity.

Figure 98. SPE-1 Gauge 4-2-L – Longitudinal displacement obtained from the corrected longitudinal velocity.

Figure 99. SPE-1 Gauge 4-3-R – Correction of the radial velocity.

Figure 100. SPE-1 Gauge 4-3-R – Radial displacement obtained from the corrected radial velocity.
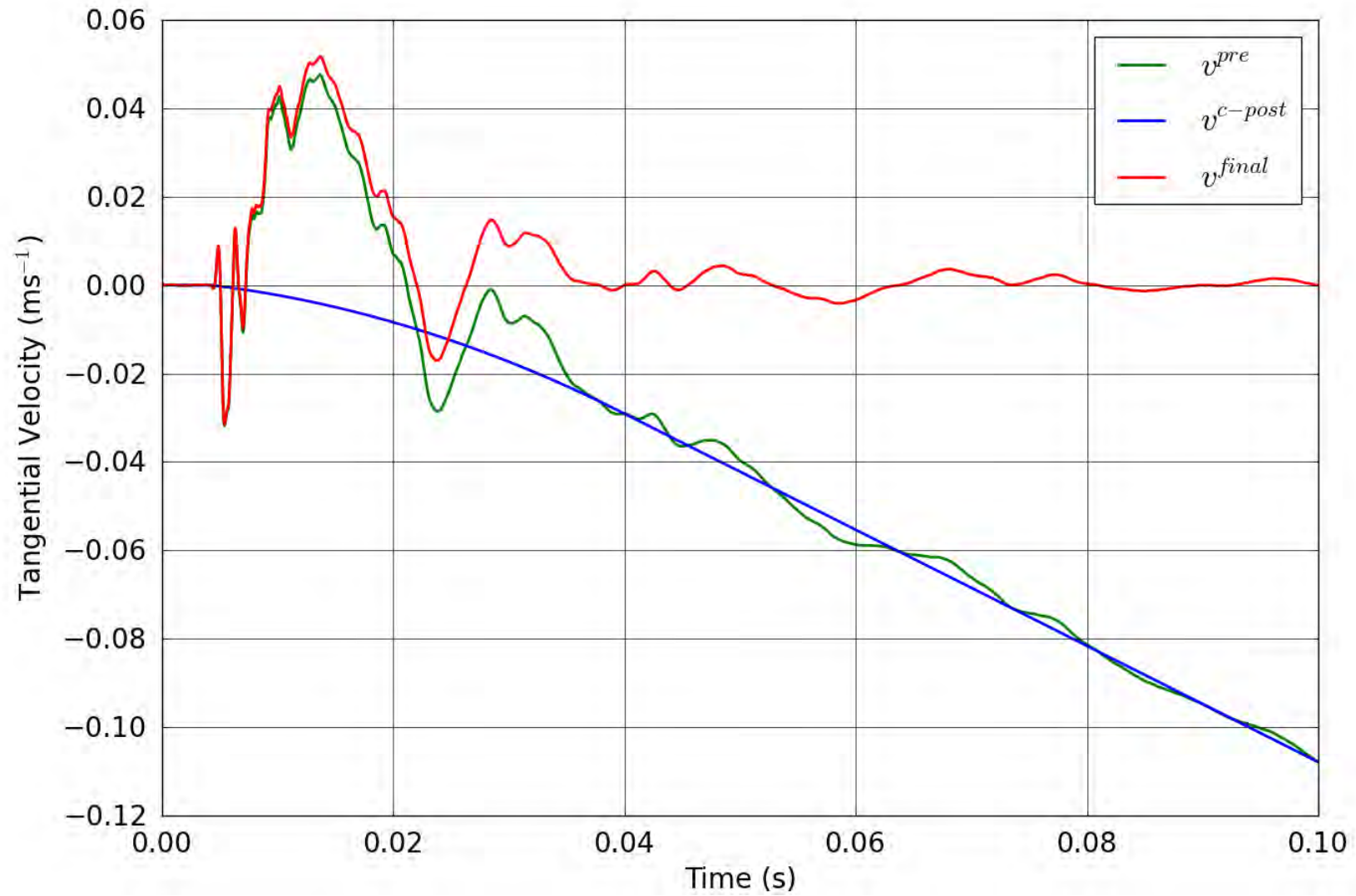
Figure 101. SPE-1 Gauge 4-3-T – Correction of the tangential velocity.
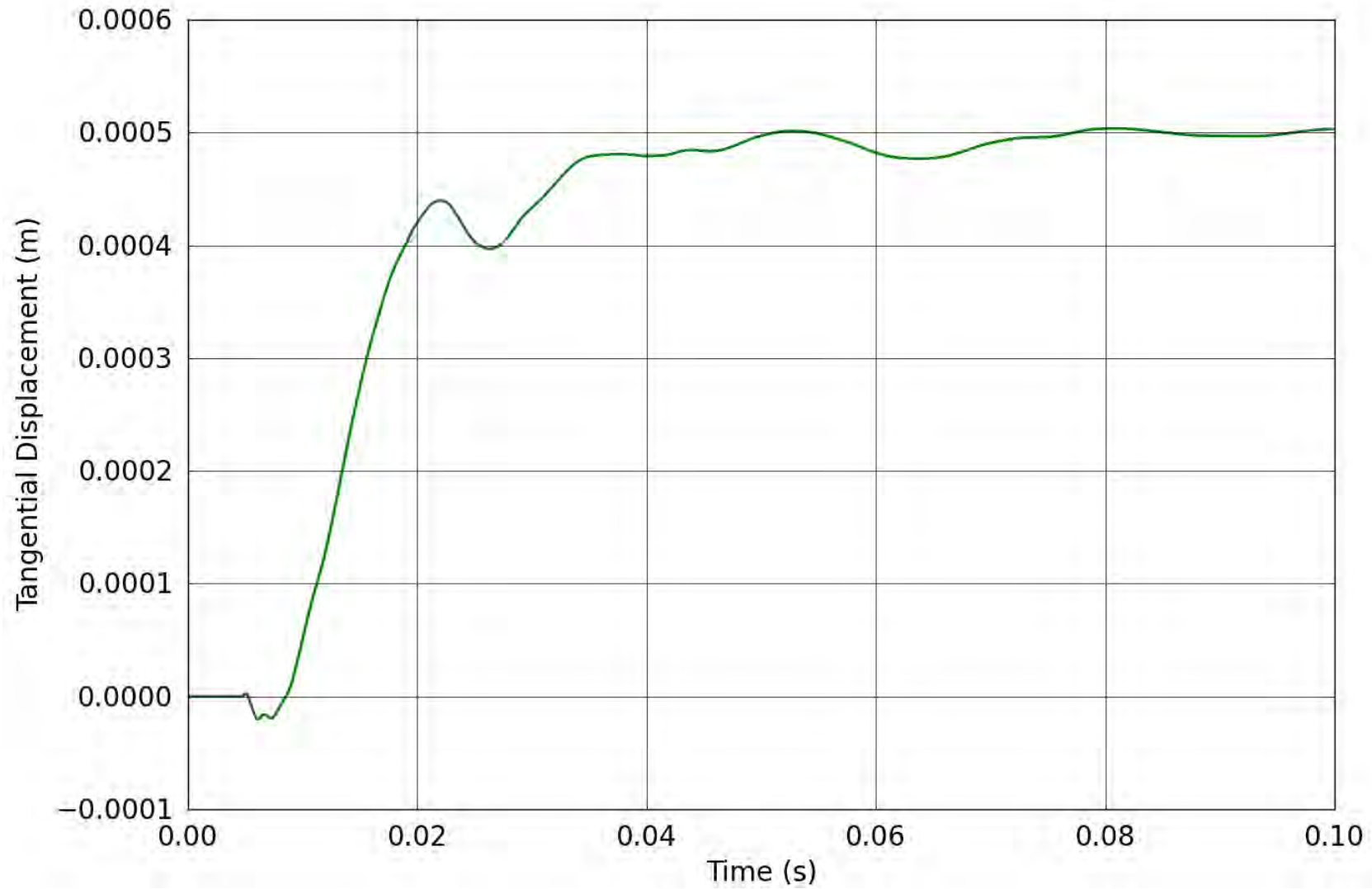
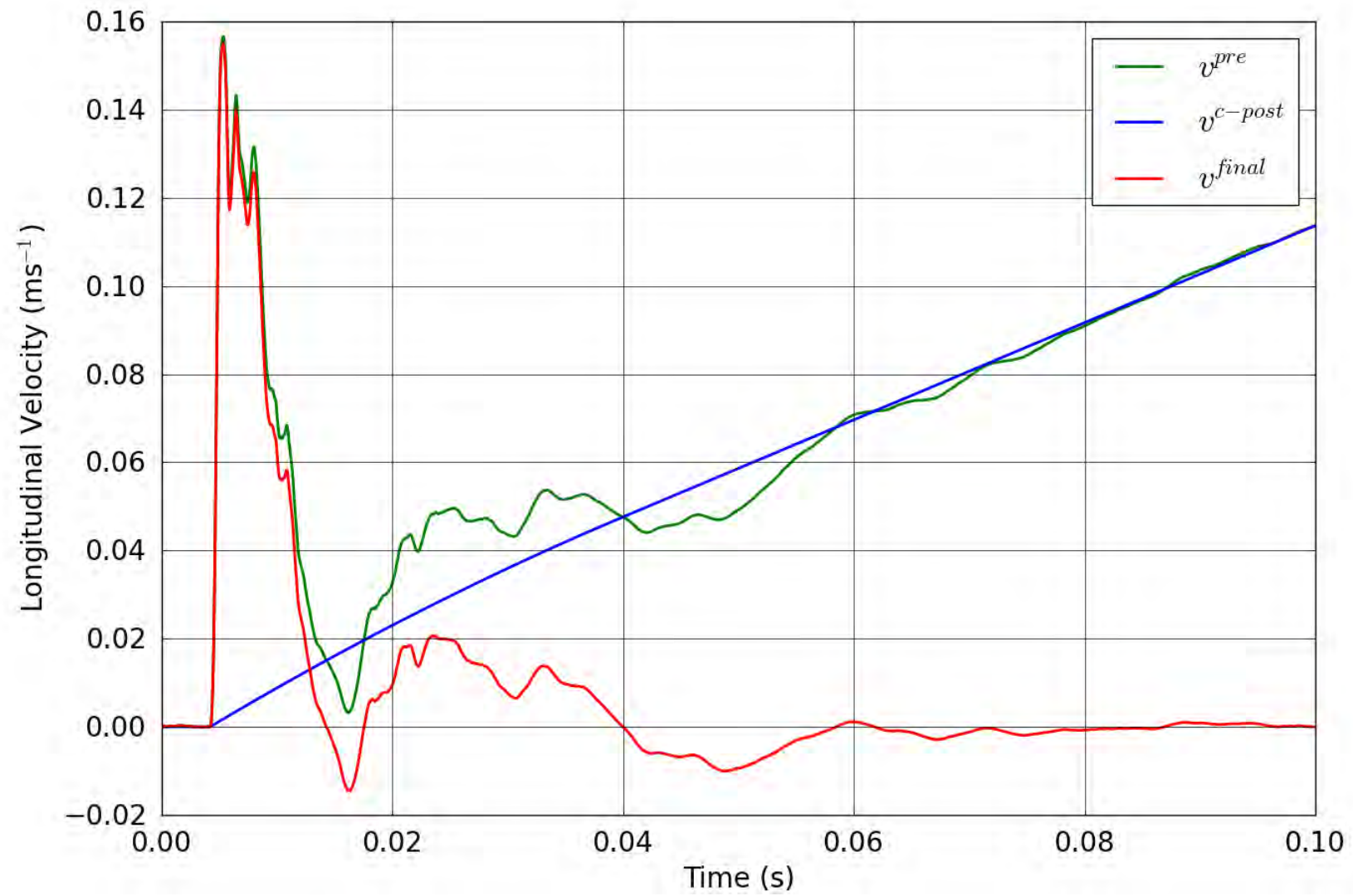Figure 102. SPE-1 Gauge 4-3-T – Tangential displacement obtained from the corrected tangential velocity.

Figure 103. SPE-1 Gauge 4-3-L – Correction of the longitudinal velocity.

Figure 104. SPE-1 Gauge 4-3-L – Longitudinal displacement obtained from the corrected longitudinal velocity.

Figure 105. SPE-1 Gauge 5-3-R – Correction of the radial velocity.

Figure 106. SPE-1 Gauge 5-3-R – Radial displacement obtained from the corrected radial velocity.

Figure 107. SPE-1 Gauge 5-3-T – Correction of the tangential velocity.

Figure 108. SPE-1 Gauge 5-3-T – Tangential displacement obtained from the corrected tangential velocity.

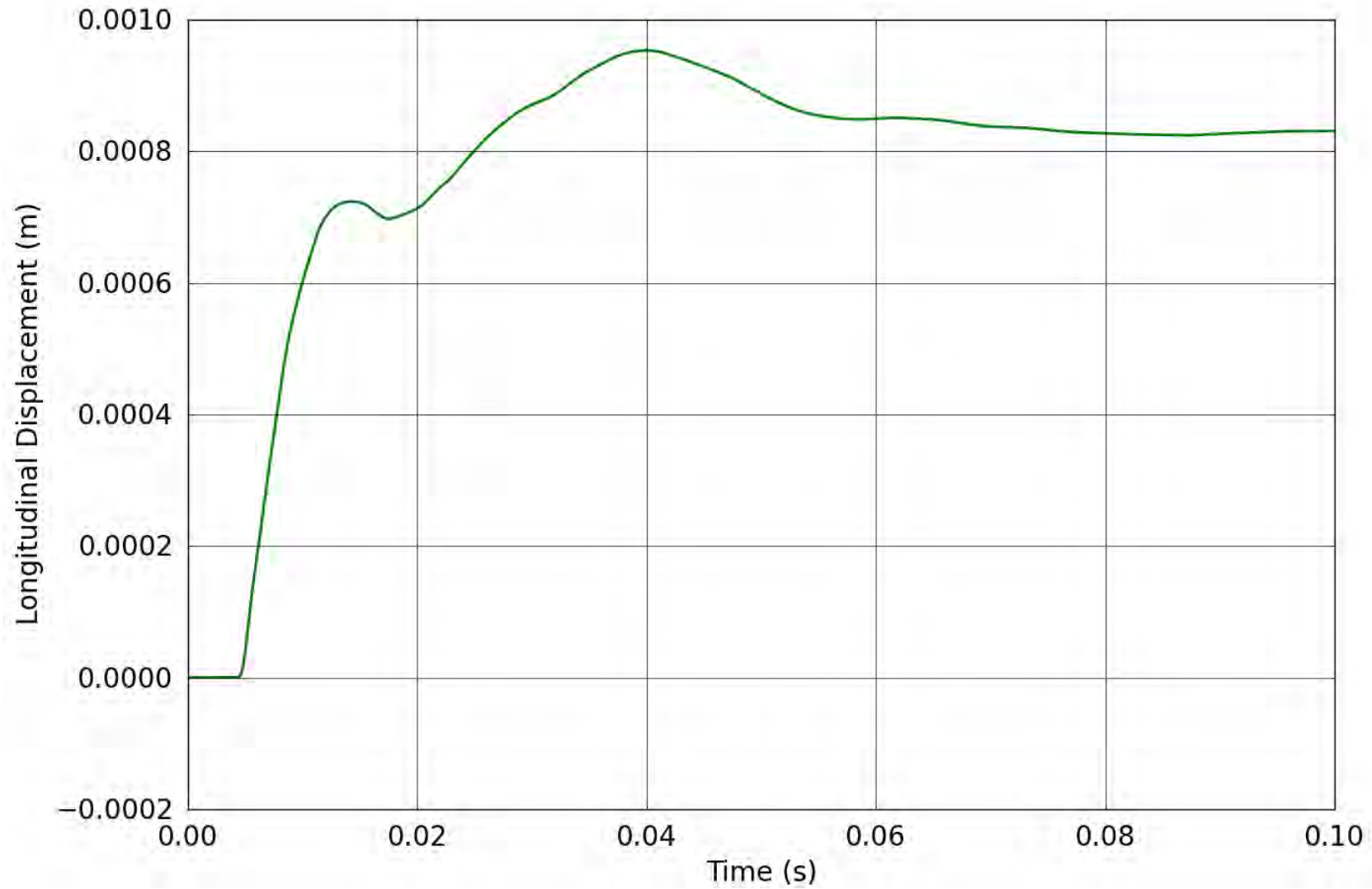Figure 109. SPE-1 Gauge 5-3-L – Correction of the longitudinal velocity.

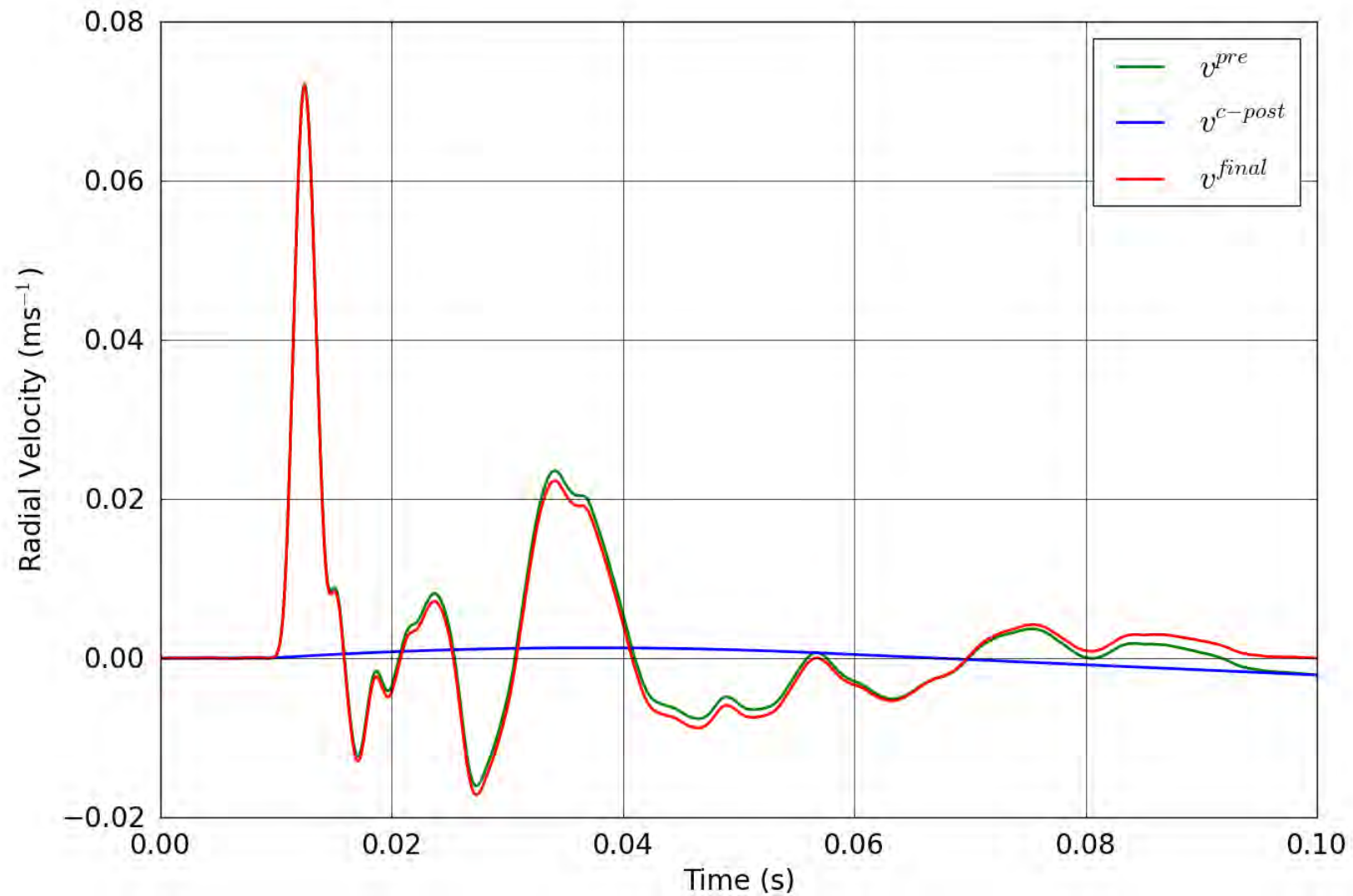Figure 110. SPE-1 Gauge 5-3-L – Longitudinal displacement obtained from the corrected longitudinal velocity.

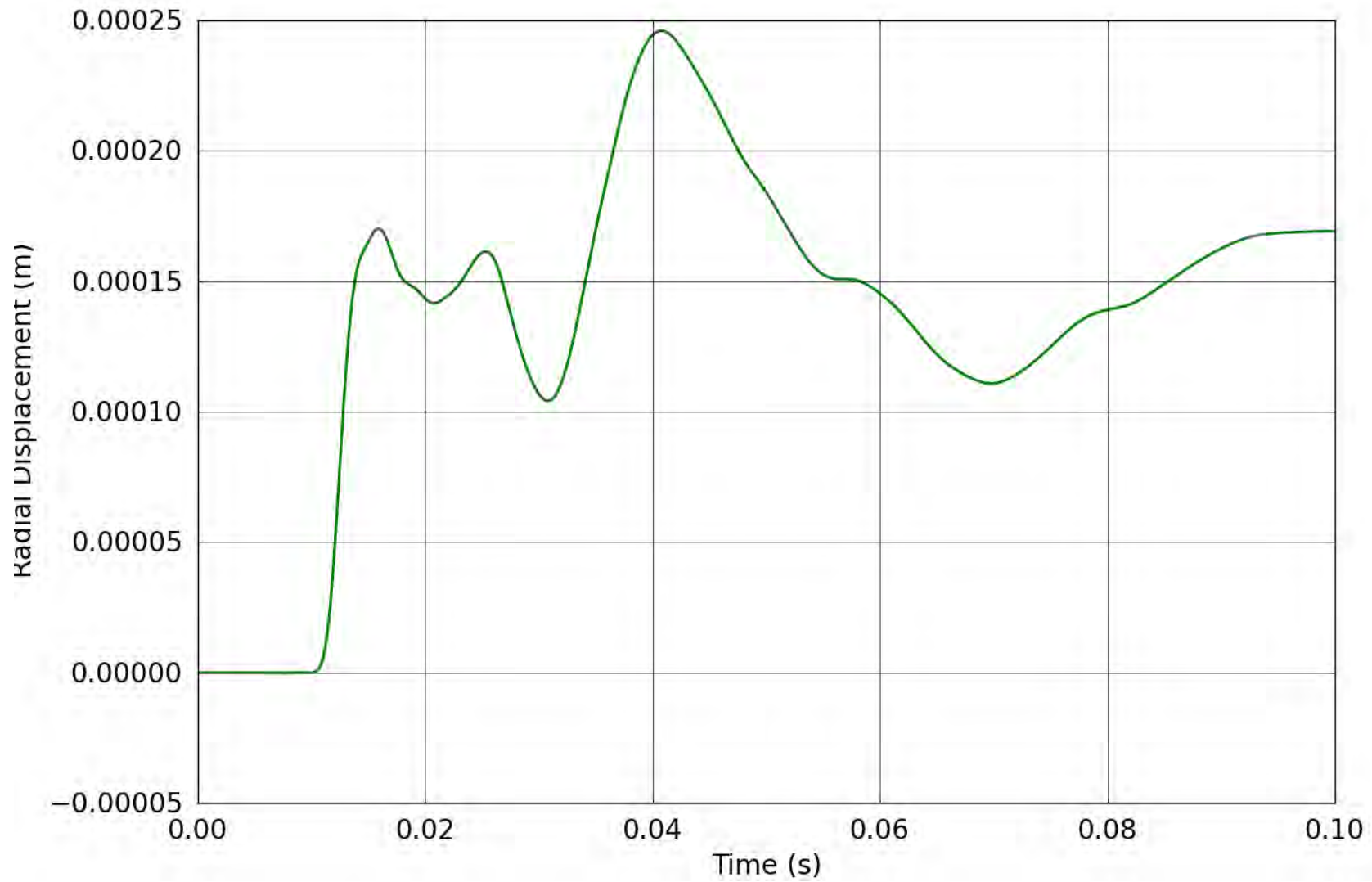Figure 111. SPE-1 Gauge 6-1-R – Correction of the radial velocity.

Figure 112. SPE-1 Gauge 6-1-R – Radial displacement obtained from the corrected radial velocity.
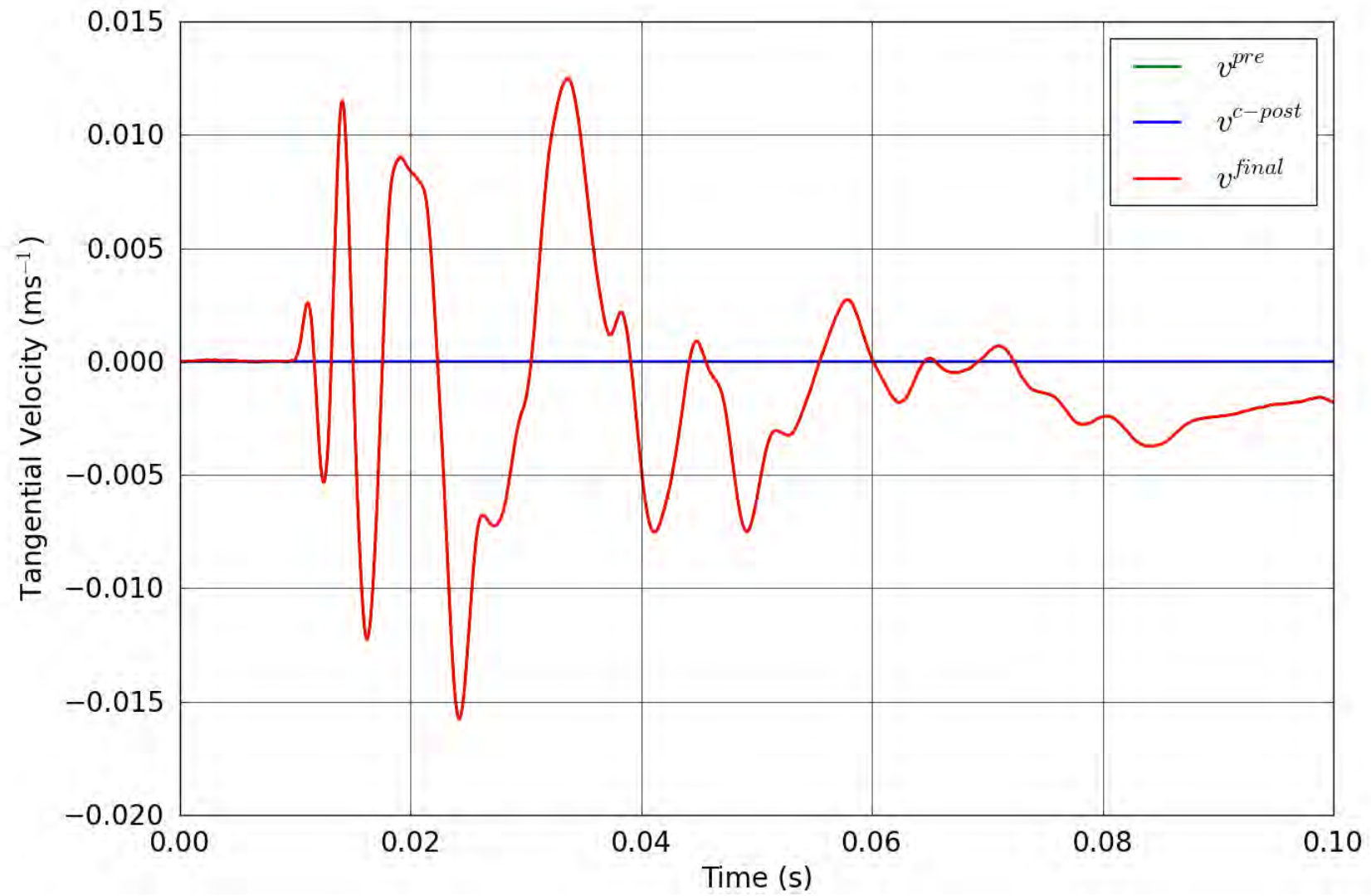
Figure 113. SPE-1 Gauge 6-1-T – Correction of the tangential velocity.

Figure 114. SPE-1 Gauge 6-1-T – Tangential displacement obtained from the corrected tangential velocity.

Figure 115. SPE-1 Gauge 6-1-L – Correction of the longitudinal velocity.

Figure 116. SPE-1 Gauge 6-1-L – Longitudinal displacement obtained from the corrected longitudinal velocity.

Figure 117. SPE-1 Gauge 6-2-R – Correction of the radial velocity.

Figure 118. SPE-1 Gauge 6-2-R – Radial displacement obtained from the corrected radial velocity.

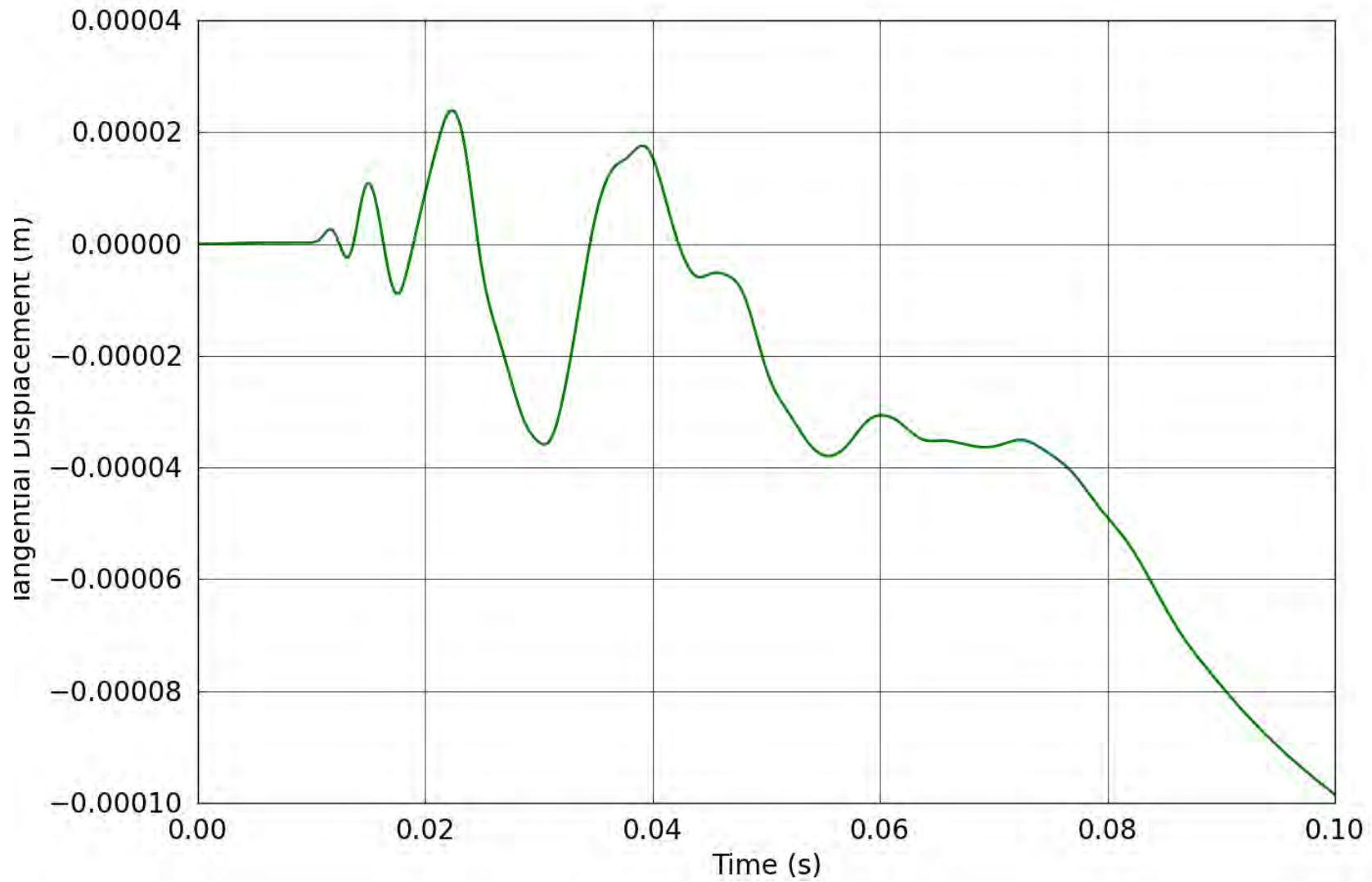Figure 119. SPE-1 Gauge 6-2-T – Correction of the tangential velocity.

Figure 120. SPE-1 Gauge 6-2-T – Tangential displacement obtained from the corrected tangential velocity.
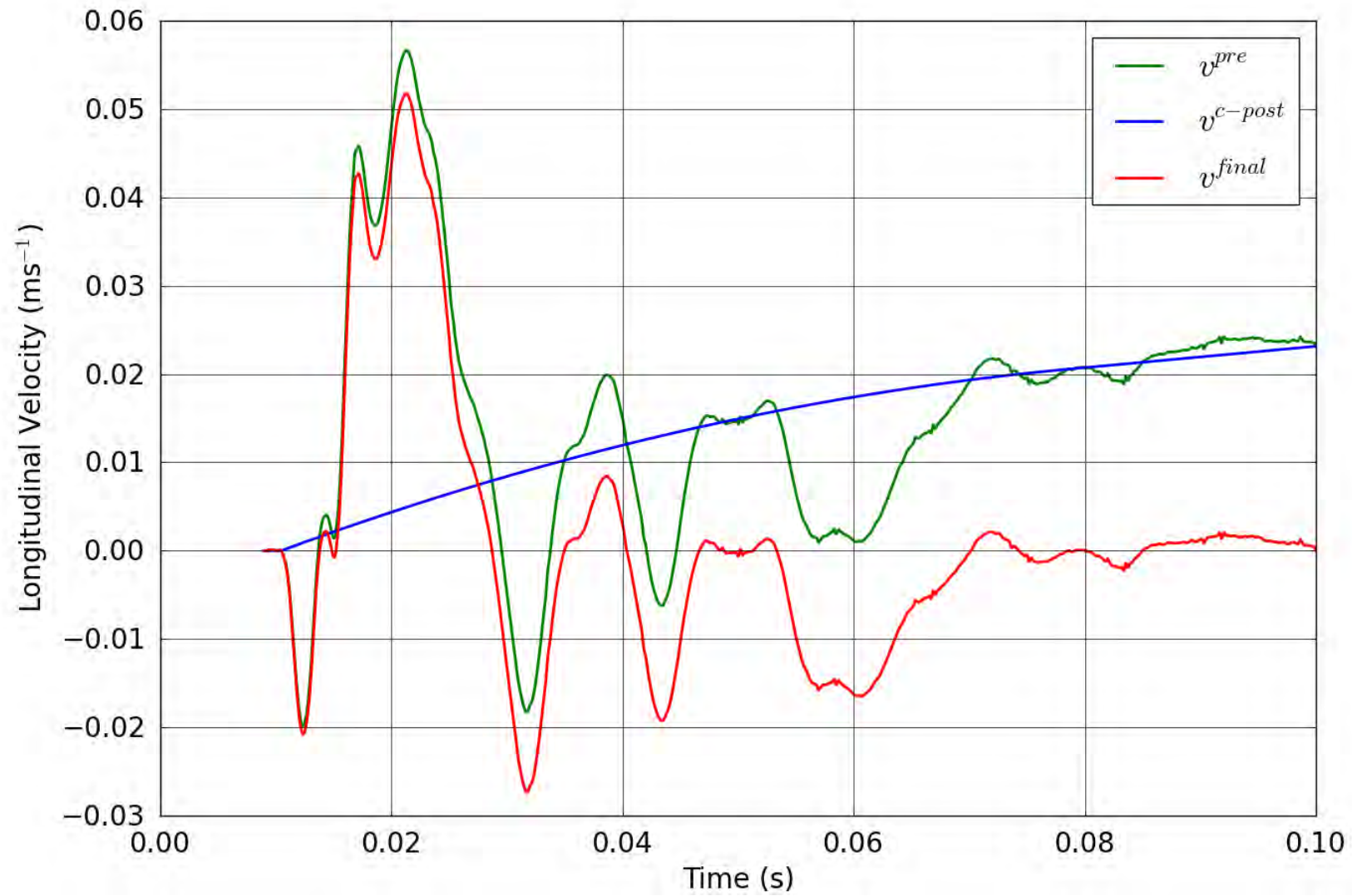
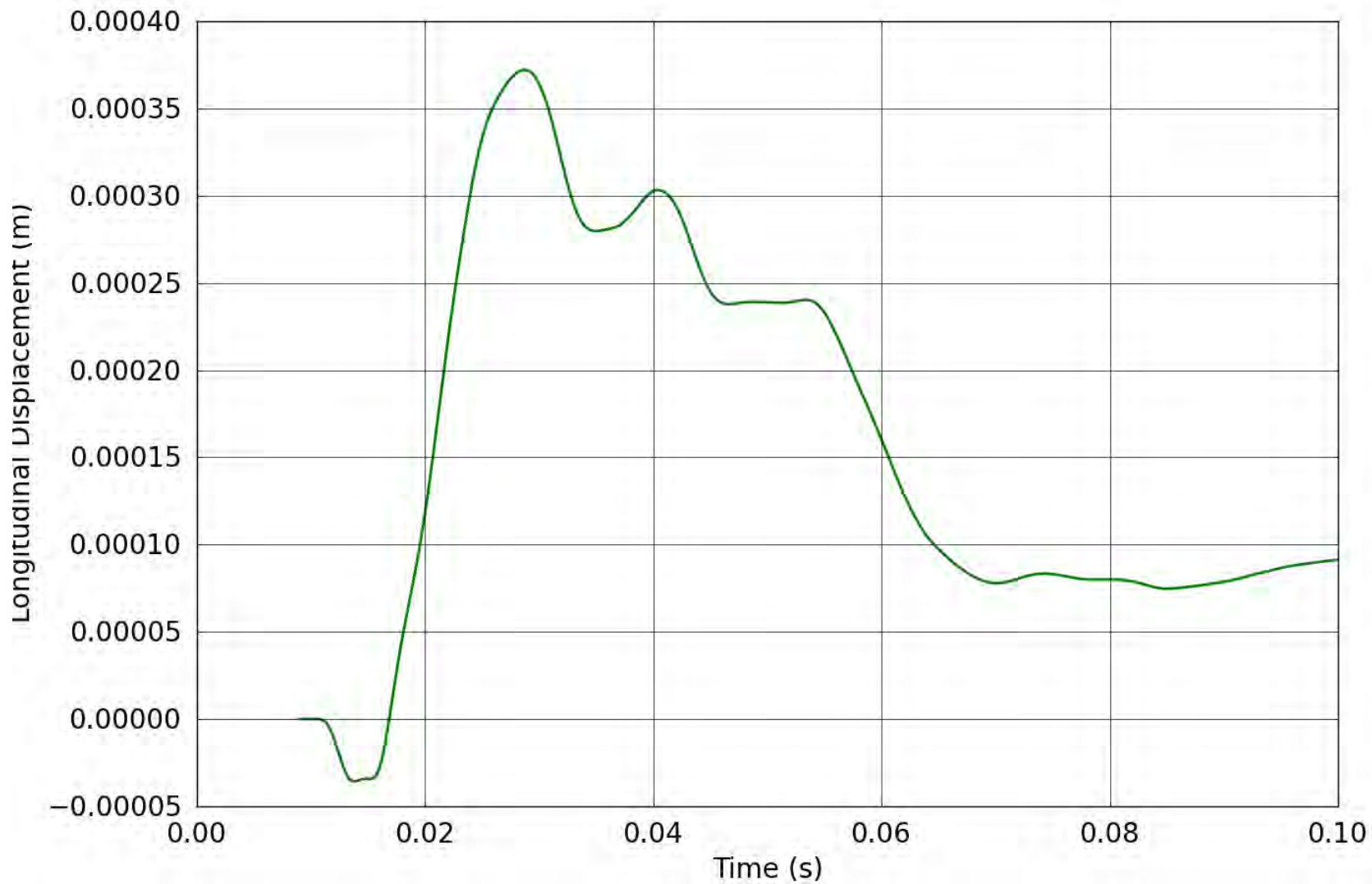Figure 121. SPE-1 Gauge 6-2-L – Correction of the longitudinal velocity.

Figure 122. SPE-1 Gauge 6-2-L – Longitudinal displacement obtained from the corrected longitudinal velocity.

Figure 123. SPE-1 Gauge 6-3-R – Correction of the radial velocity.

Figure 124. SPE-1 Gauge 6-3-R – Radial displacement obtained from the corrected radial velocity.

Figure 125. SPE-1 Gauge 6-3-T – Correction of the tangential velocity.

Figure 126. SPE-1 Gauge 6-3-T – Tangential displacement obtained from the corrected tangential velocity.

Figure 127. SPE-1 Gauge 6-3-L – Correction of the longitudinal velocity.

Figure 128. SPE-1 Gauge 6-3-L – Longitudinal displacement obtained from the corrected longitudinal velocity.

3.   REFERENCES

1. Jeff Thomsen, SPE Acceleration Component Rotations: Shock Angle Analyses for Holes 1-6 Compared to SPE-3 Holes 7-11, PowerPoint Presentation, Oct. 2012.
2. Jeff Thomsen, SPE Data Acceleration Component Rotation Methodology, PowerPoint Presentation, Oct. 2012.
3. David W. Steedman, Review of Data from Shock Physics Experiments SPE-1, SPE-2 and SPE-3: Data Corrections and Phenomenology Analysis, LA-UR-13-22561, 19 April 2013.
4. Esteban Rougier and Howard J. Patton, Quality assessment of SPE free field data based on reduced displacement potentials, LA-UR-13-20277, PowerPoint Presentation, 16 January 2013.

Appendix 9

Review of Data from Source Physics Experiment-1:

Data Corrections

Los Alamos National Laboratory Report
LA-UR-22561 (2013) prepared by D. Steedman

Review of Data from Source Physics Experiment 1: Data Corrections

The information in this appendix was extracted from
LANL publication LA-UR-13-22561 by D. Steedman

INTRODUCTION

The NNSA is conducting a series of high explosive (HE) tests – the Source Physics Experiments – at the National Nuclear Security Site (NNSS). These experiments are intended to investigate the generation of geophysical signals from controlled sources. These signals will aid in the development of physics-based models to aid in the discrimination of signals emitted from these and other possible sources, such as earthquakes and clandestine nuclear events.

The SPE events include an array of accelerometers near to the source intended to provide measurements of the strong ground motion, or "near field," regime. This report coincides with the release of these data for analysts and organizations that are not participants in this program. The report describes the various forms and location of near field data that are available.

DATA

This report coincides with the release of the data package for SPE-1. This includes the raw acceleration-time pairs recorded for all transducers. These data are in the form of time–acceleration pairs and are posted on the project data server. Files are in comma separated variables (csv) format.

This data release includes three additional sets of data histories representing each of three steps of data correction. These included, in successive order, correction for canister rotation, correction for pre-event baseline drift, and correction for baseline drift that occurs during an event. The first of these is a special case that was determined to be needed after a thorough review of data from SPE-1 and two subsequent events, SPE-2 and SPE-3. The other two corrections are standard requirements for acceleration records and were performed after this first correction was applied.

Data Corrections

Gauge Canister Rotations— An explosive event such as SPE-1 will produce a ground shock environment that is expected to follow a well-established theory of outward spherical propagation of compressive shock waves from a cylindrical, or near-spherical, source. Figure 1 provides an example of a set of velocity histories that conform to expectations at the shot depth for SPE-1. Gauge package 6-1 at the 20-m range is dominated by a large outward radial velocity with minor motion in the directions tangential (transverse and longitudinal) to the shock front.
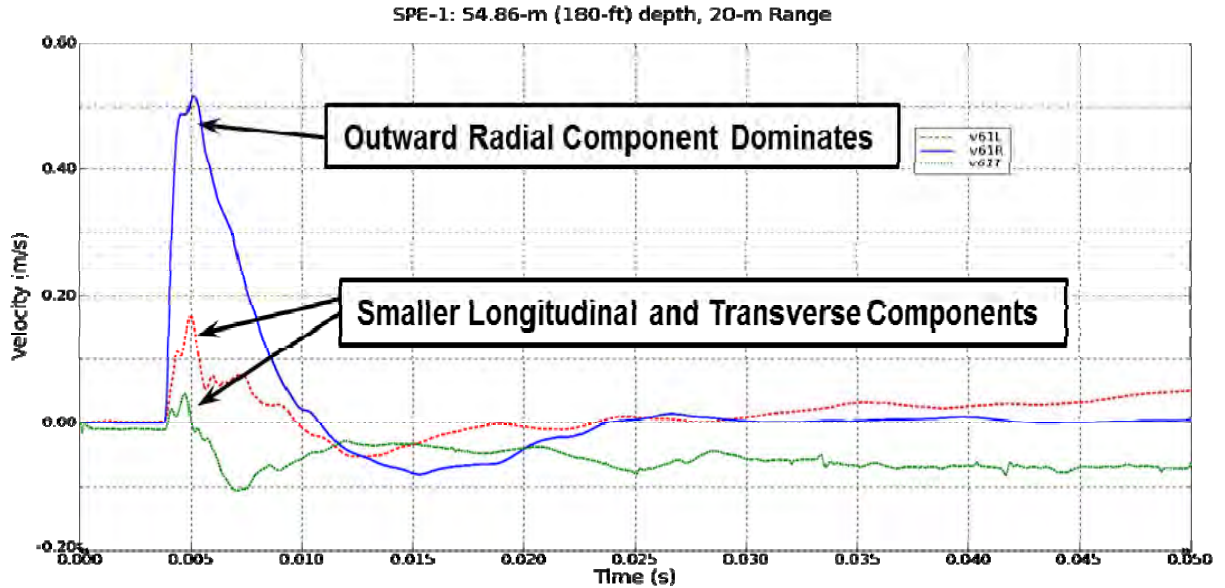
Figure 1: Consistent set of velocity histories for a cylindrical charge: gauge package 6-1.

But a review of other measurements in the SPE-1 set reveals some history sets that are not consistent with expectations. For example, while another gauge package at the same depth and range (*i.e.*, 4-1, Figure 2) shows similarly weak transverse and longitudinal components, the large radial motion is *inward*, or opposite of what one would expect from a compressive, explosively driven shock.

Another problematic response is observed in gauge package 2-1 (Figure 3) at the 10-m range at the shot depth. The radial and transverse components are similar in amplitude for this location. That is different than what is expected (*i.e.*, minor transverse component relative to the radial is expected).

The data from gauge package 3-1 (Figure 4) at the 10-m range at the shot depth is also suspect. The radial measurement in this plot is very low in magnitude and does not have the expected characteristic strong outward phase. On the other hand, the transverse component possesses a strong pulse which, notwithstanding the algebraic sign, possesses the character expected of a radial measurement.
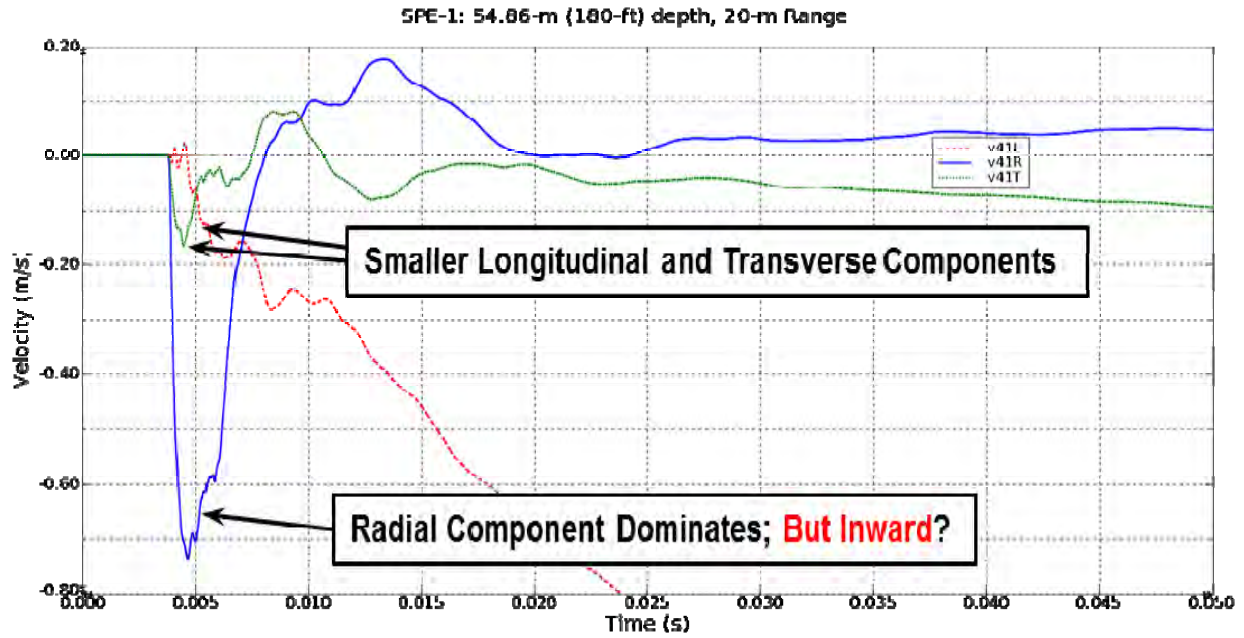
Figure 2: Consistent set of velocity histories for a cylindrical charge except for reversed direction radial: gauge package 4-1.
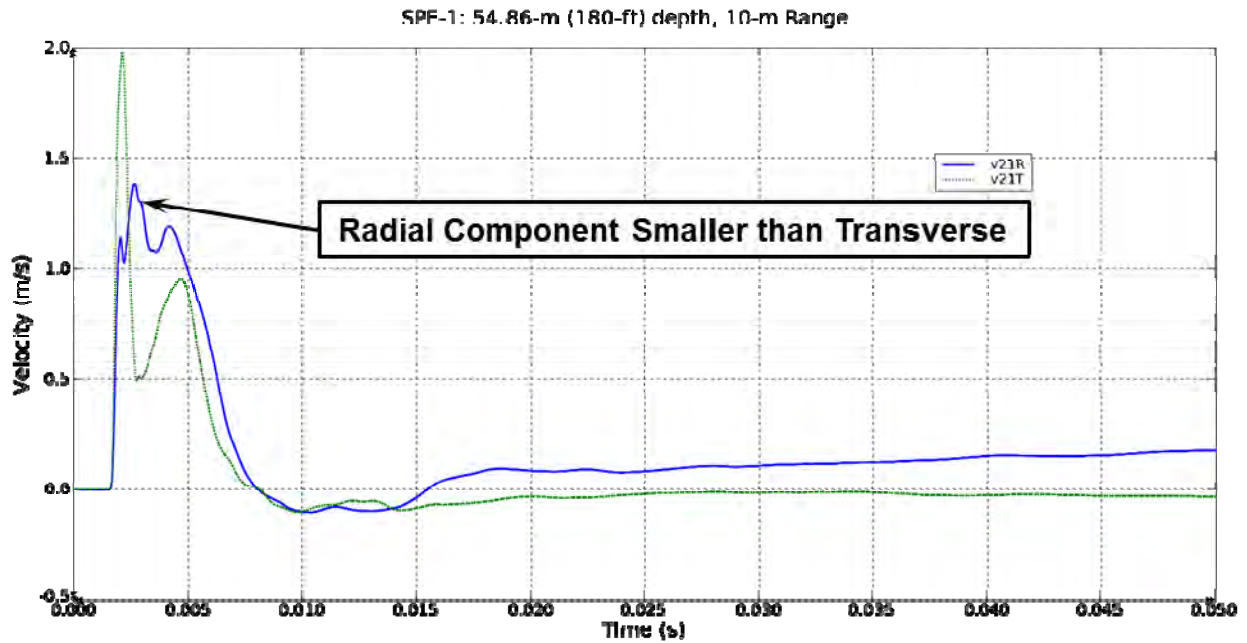

Figure 3: Inconsistent set of velocity histories for a cylindrical charge, including unexpectedly high transverse pulse relative the radial motion: gauge package 2-1.
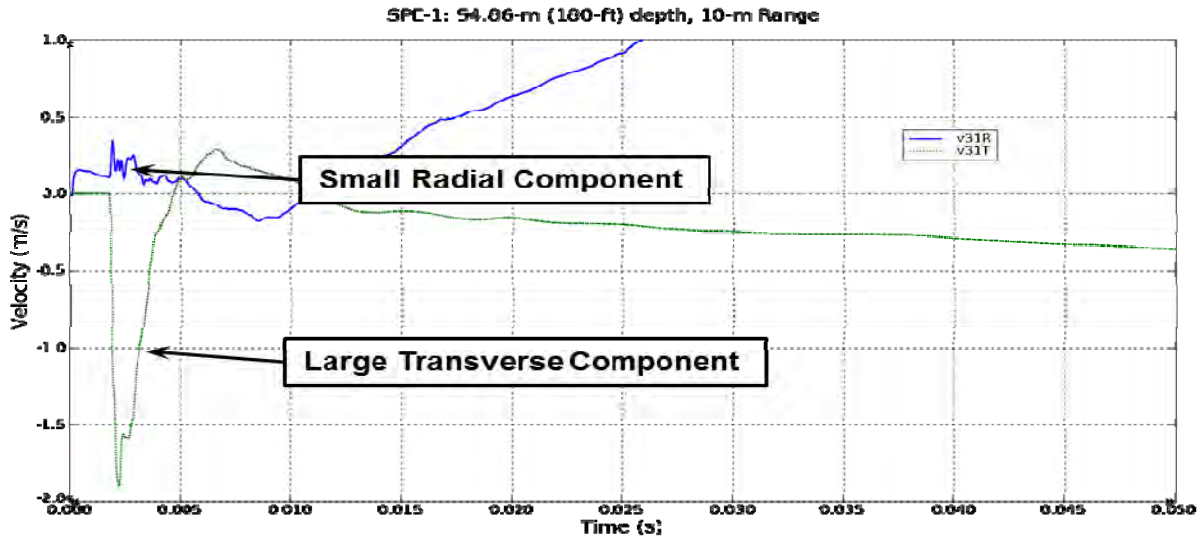
Figure 4: Inconsistent set of velocity histories for a cylindrical charge, including large transverse pulse with limited radial motion: gauge package 3-1.

Figure 3 and Figure 4 were used to illustrate relative response among the components in a given gauge package. Comparisons between data from different gauge packages also provide insight into problems with the gauges. Figure 5 includes one component from each of the gauges at the 10-m range at the shot depth. These are the radial measurement of 1-1 and the transverse components for 2-1 and 3-1 (note that we reversed the sign for the 3-1-T history). The similarity in both magnitude and character between radial and transverse measurements is unexpected. Similarly, the 2-1 radial component is nearly identical to the 1-1 transverse measurement (Figure 6). The fact that some transverse components closely track other radial components is compelling evidence of gauge rotation.
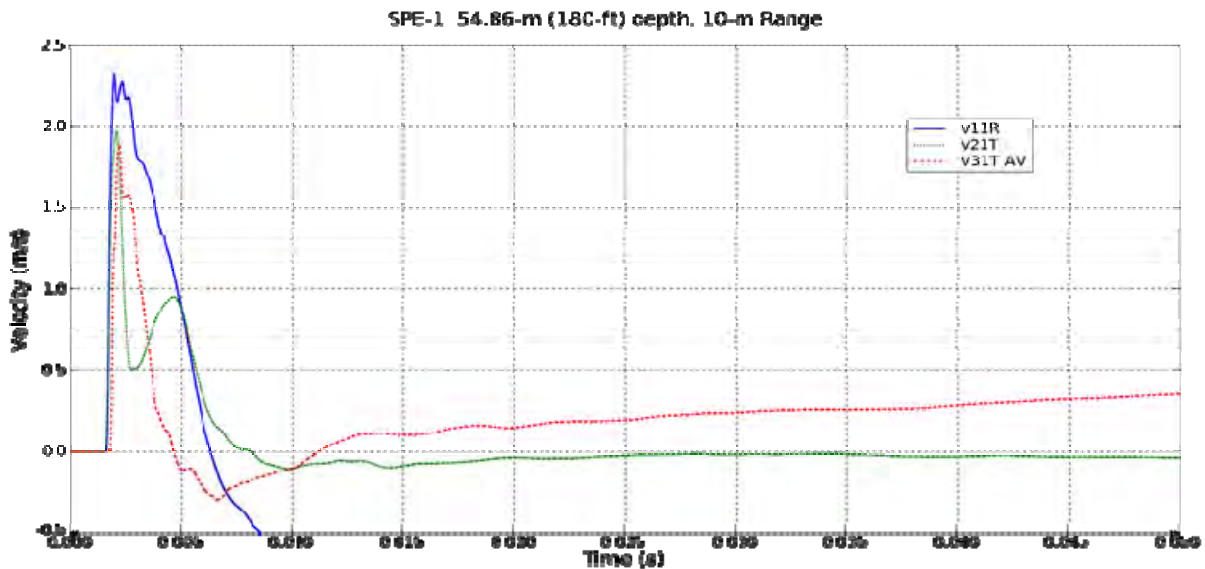

Figure 5: A radial velocity history (1-1) compared to two transverse velocity histories (2-1 and 3-1) at the same range and depth.
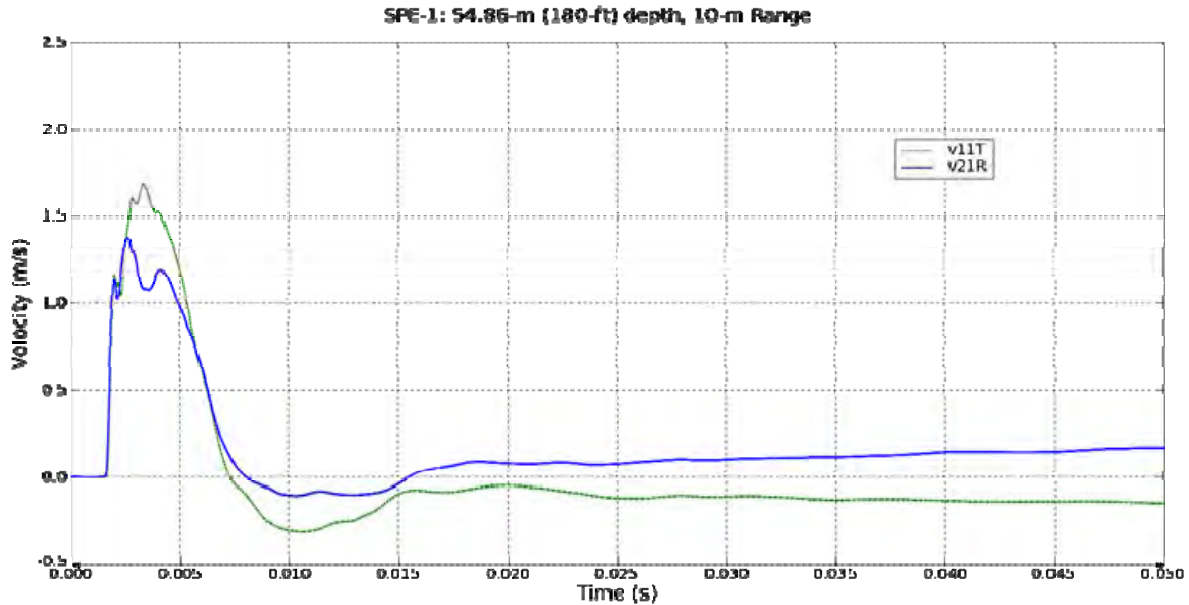
Figure 6: A radial velocity history (2-1) compared to a transverse velocity history (1-1) at the same range and depth.

Similar data anomalies are evident throughout the SPE-1 data set. These anomalies are summarized in a "stop light" chart (Figure 7) where we show all questionable canisters as red. Green represents gauge packages where no apparent anomalies were observed and black represents those locations for which no data were recovered due to inoperable gauges. A significant portion of these data are questionable.

Figure 7: Stop light chart summarizing data anomalies for SPE-1 and SPE-2.

While this report is intended to discuss the release of the SPE-1 data, it is necessary at this point to briefly introduce SPE-2, which is also illustrated in **Error! Reference source not found.**. SPE-2 was a

1172-kg SHANFO source placed at the 150-ft depth in hole U15n and fired on 25 October 2011. The same instruments were used to record this event except that some gauges failed during or after SPE-1. Additionally, due to a large gauge loss in hole 1, an identical array of gauges was placed in a new hole 1A drilled nearby to hole 1 (see Figure 8).
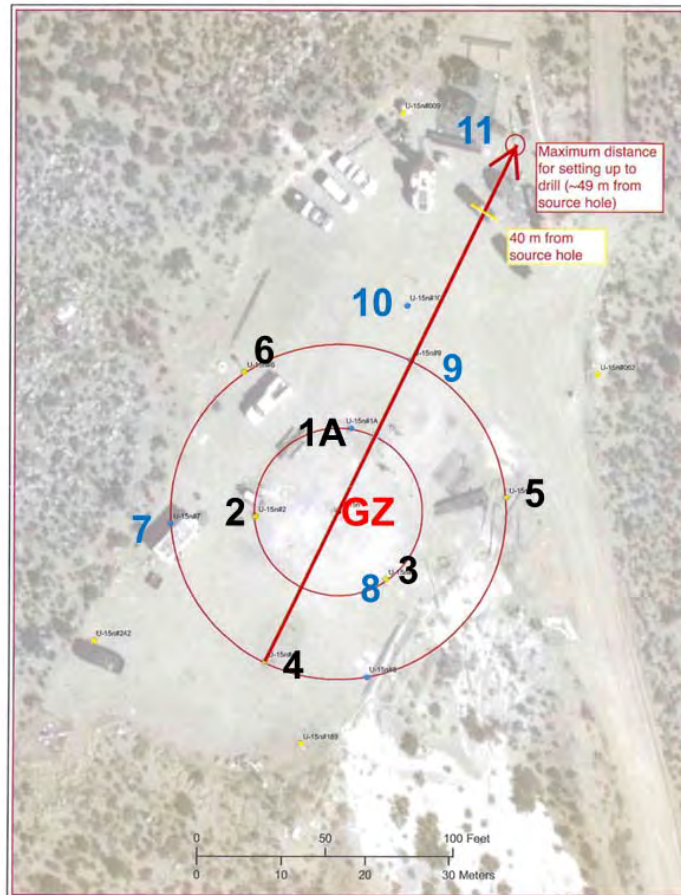

Figure 8: Instrument hole layout for SPE-3.

We will not provide examples here but the anomalies observed in SPE-1 were consistently repeated in SPE-2, as reflected in the second stop light chart in Figure 7. The two charts are consistent between the two events indicating persistence in anomalous behavior.

This includes the fact that that all gauge canisters at the 50-ft depth for both experiments performed as expected. These canisters are nearest to the surface and, thus, would have less opportunity to rotate. Finally, all canisters in the newer hole 1A appeared to yield acceptable data. These replacement gauges were placed with better quality control than the older canisters (Ref. 3).

The reader is referred to Reference 1 and Reference 2 for a comprehensive review of all data from these two events

Based on these observations the test team determined that it would be prudent to include extra gauge canisters for the next test in the series, SPE-3. SPE-3 was slightly smaller (1064.71 kg of SHANFO) than, but placed at the same location as, SPE-2 and fired on 24 July 2012.

These new canisters served two purposes: to provide redundant data for questionable canisters and to fill-in for areas of the test bed where more data coverage was desired. Figure 8 illustrates the layout of these new holes, numbered 7, 8, 9, 10, and 11. Holes 7 and 8 on the 20-m and 10-m rings, respectively, and hole 11, 45 m from the charge hole, had canister depths identical to the older holes; that is, at 50 ft, 150 ft, and 180 ft from the ground surface. Hole 9 on the 20-m ring had canisters at those depths as well as at 90 ft and 120 ft from the ground surface. Hole 10 was a slant hole drilled from the surface location indicated through the SPE-2 charge center, and had a single radial (*i.e.*, in the line of the hole axis) transducer at a distance of 12 m from the charge.

Comparisons between the data from these two events provide adequate evidence into whether some canisters in holes 1 through 6 rotated during placement. For example, Figure 9 presents the data for the radial and transverse transducers (there were no longitudinal transducers active) from canister 6-1 for shots SPE-2 and SPE-3. This canister provides reasonable data in that a large outward radial measurement is accompanied by a relatively small transverse component. The records for both components are consistent between the two events.
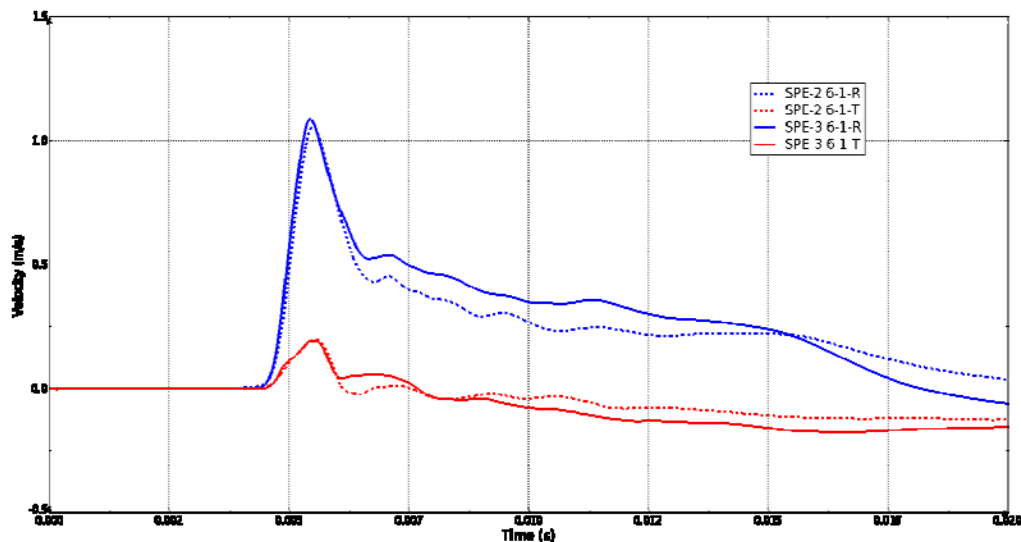

Figure 9: All data components recorded by canister 6-1 from both SPE-2 and SPE-3.

Figure 10 presents the data for these same tests from canister 2-1 where the relative magnitudes between radial and transverse components were previously described to be questionable (Figure 3). As in SPE-1, the transverse component is larger than the radial component which is inconsistent with the response expected. The significant longitudinal component is a reasonable response as the canister is located 45° below the shot point and so the spherically propagating shock will have a significant vertical component. All of the records for canister 2-1 are consistent between the two events.
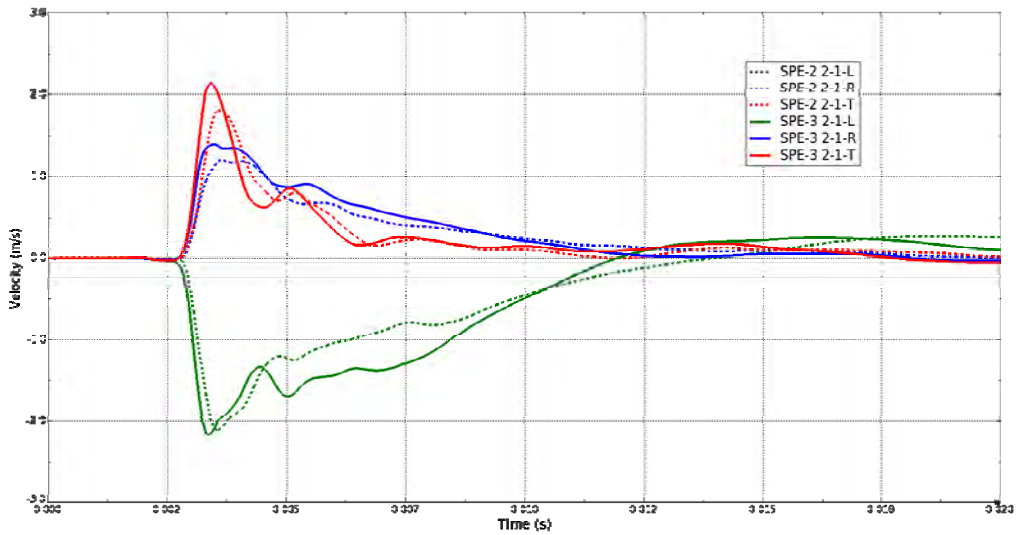
Figure 10: All data components recorded by canister 2-1 from both SPE-2 and SPE-3.

Figure 11 includes SPE-2 and SPE-3 data for canister 6-2 which was dominated completely by the supposed transverse measurement with apparently inconsequential motion in the radial direction. Again, the histories for all transducers are consistent between events but inconsistent with expectations.
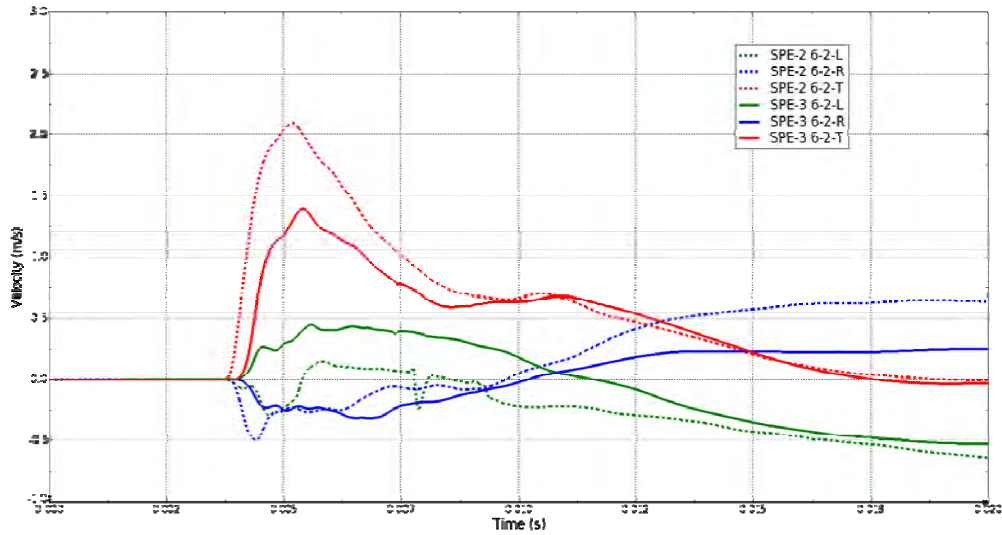

Figure 11: Velocity histories from location 6-2 for SPE-2 and SPE-3.

The above examples used data from three canisters to display consistency between two events with identical locations and nearly identical yields. It is an important observation that one of these (6-1) had reasonable radial-to-transverse component amplitude comparisons while the other two (2-1 and 6-2) provided unexpectedly high transverse magnitudes relative to their respective radial magnitudes. This provides evidence that SPE-3 was a reasonable replication of SPE-2, thus allowing comparisons between

SPE-3 histories from questionable canisters and those from the redundant newer canisters. In other words, the quality of the data from questionable gauges can be judged by the data recovered from the redundant gauges.

For example, reference to Figure 8 reveals that hole 7 was drilled on the 20-m ring on the same radial as hole 2 on the 10-m ring. But while canister 2-1 (Figure 10) appeared to experience questionable transverse-to-radial magnitudes, canister 7-1 (Figure 12) reveals a set of histories that is fully consistent with a shock environment dominated by radial motion (*i.e.*, large radial component accompanied by an insignificant transverse contribution). Canister rotation is a reasonable explanation of the canister 2-1 response.
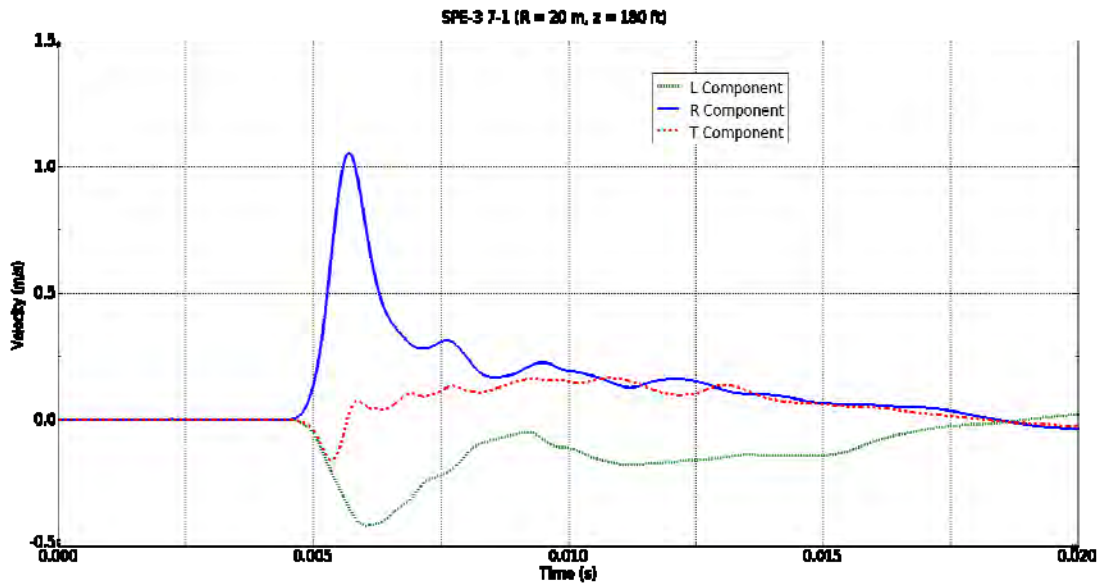

Figure 12: Velocity histories from location 7-1 for SPE-3.

Another example is the comparison in Figure 13 between data from older canister 3-2 and newer canister 8-2 which is nearby on the same radius ring. The 3-2 canister transducers were inoperable for SPE-3 and so those data are from SPE-2; the data at 8-2 are from SPE-3. Other comparisons have already established consistency between those two events, and so comparison between these two nearby canisters is relevant. Specifically, location 3-2 displays uncharacteristically high transverse negative amplitude accompanied by an insignificant radial record. But location 8-2 experienced a high outward radial velocity and a low magnitude transverse velocity. It is unrealistic that the shock environment can change by such a large amount in the short distance between hole 3 and hole 8 and this difference must be explained by rotation of canister 3-2 during installation.
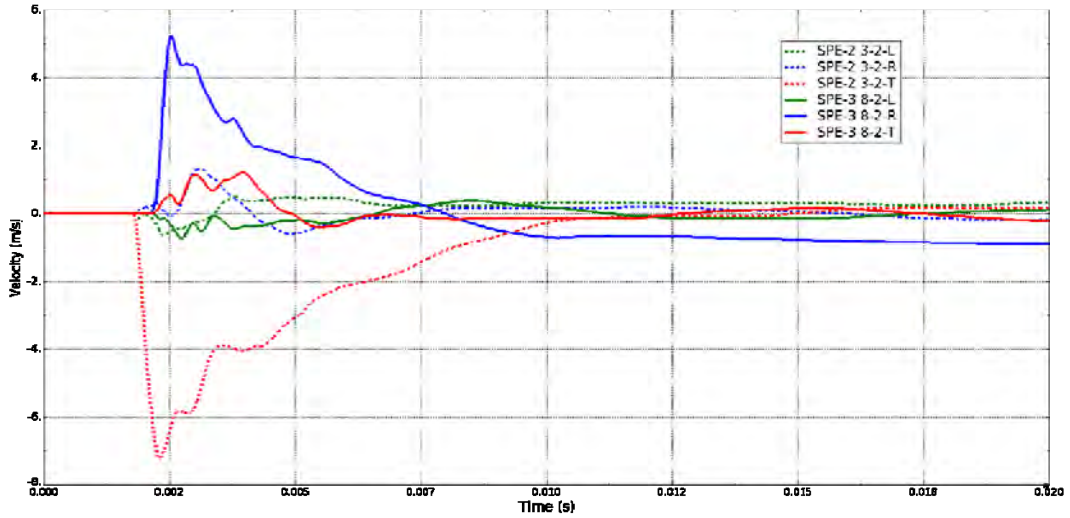
Figure 13: Velocity histories from location 3-2 for SPE-2 and location 8-2 for SPE-3.

Finally, reference to Figure 8 shows that older hole 6 is roughly in the middle of an arc between newer holes 7 and 9 on the 20-m ring. Canister 7-2 (Figure 14) and canister 9-2 (Figure 15) have reasonable relative radial and transverse motions while canister 6-2 (Figure 16) is unreasonable in this respect. It is unlikely that the azimuth to hole 6 would have such a significant difference in the environment relative to the azimuths on either side.
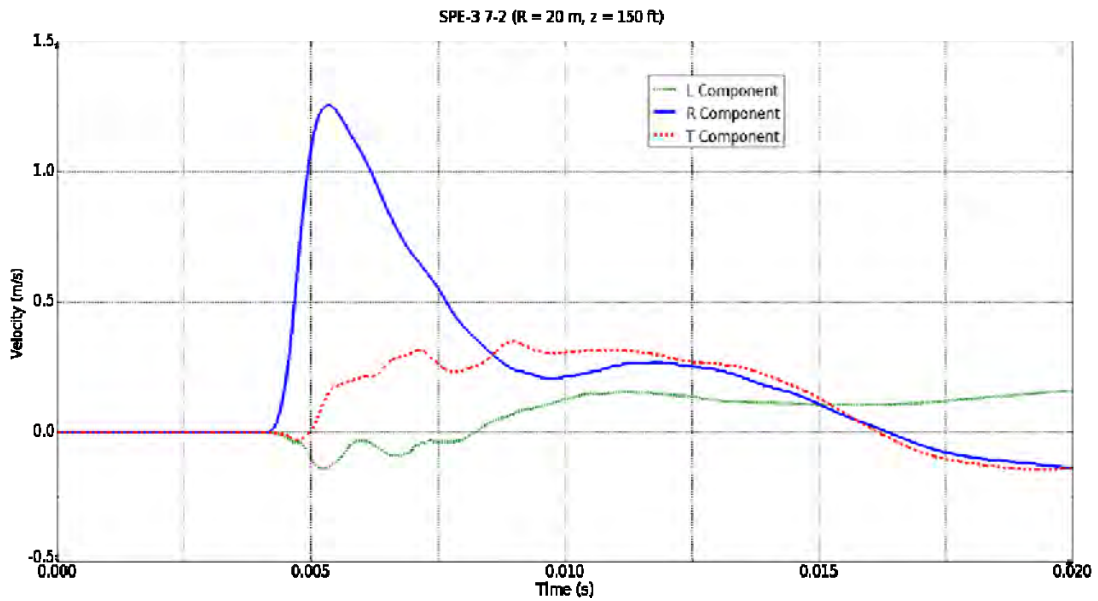

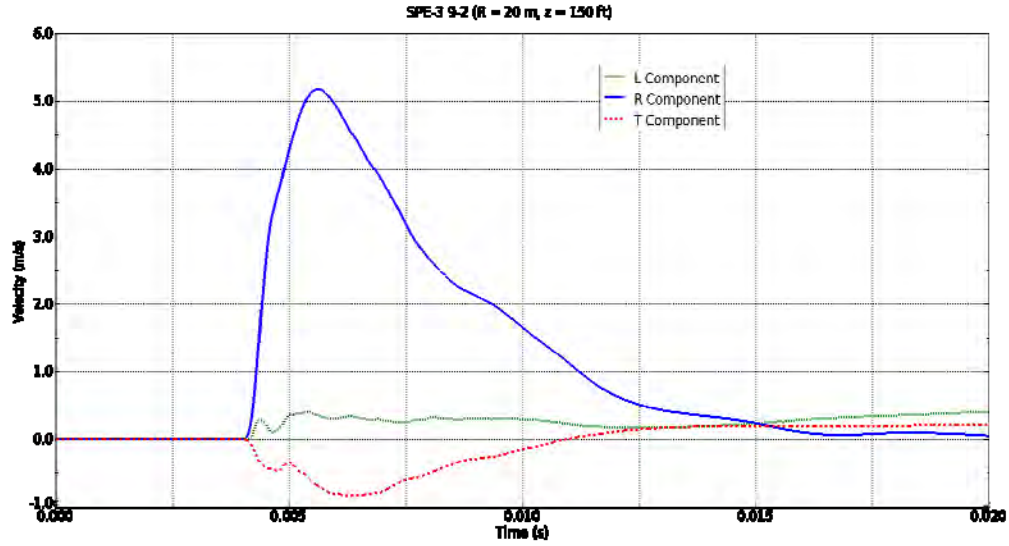**Figure 14: Velocity histories from location 7-2 for SPE-3.**

Figure 15: Velocity histories from location 9-2 for SPE-3.
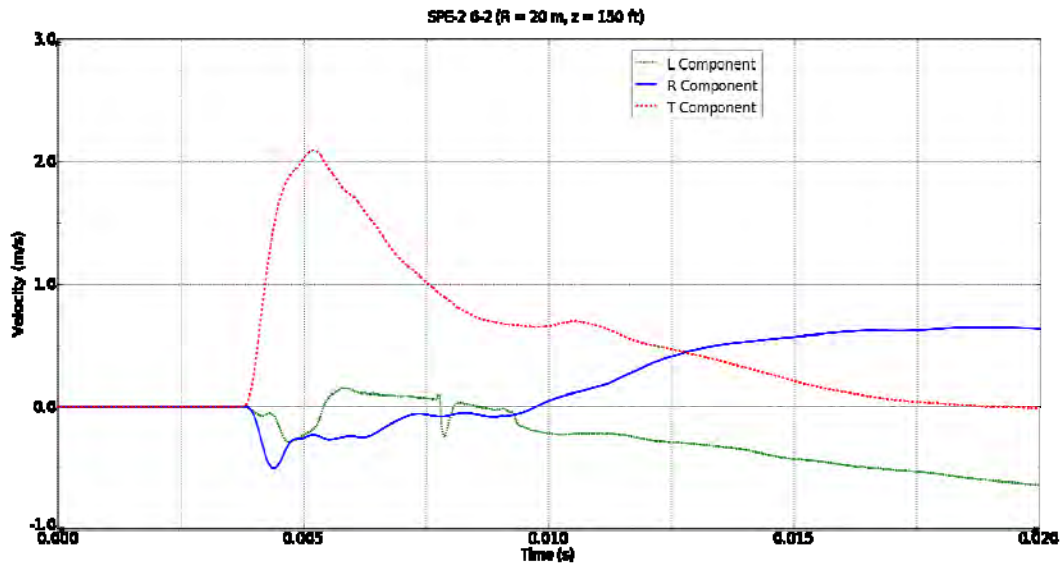
Figure 16: Velocity histories from location 6-2 for SPE-3.

The above discussion reviewed the relative horizontal components of canister histories. The general premise is that for a spherical or cylindrical explosive source the shock environment should be dominated by outward radial motion, with smaller contributions in the orthogonal tangential directions. Reference 4 presents more comparisons of these data that will not be repeated here. Instead, the full SPE-3 data set is summarized by plotting the radial peak velocity vs. the tangential peak velocity for every canister in Figure 17.

Figure 17: Peak radial velocity vs. peak transverse velocity for all canisters in SPE-3

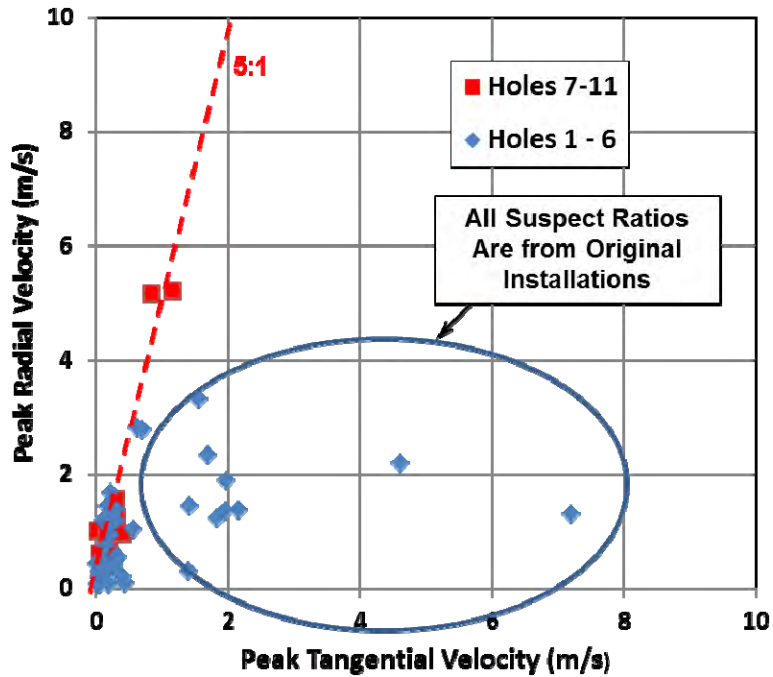A fit to the data from only the newer holes suggests that the transverse velocity is about 20% of the radial velocity (*i.e.*, radial is five times the transverse). This is also true of a subset of the older canisters. However, a number of locations have peak transverse velocities that are equal to or greater than the respective peak radial velocity. All of those data points represent older installations. The response of all canisters installed using high quality control (holes 7 through 11) is clearly dominated by radial motion.

A final summary of these data can be seen in Figure 18 which is an updated version of the "stop light" chart shown earlier. It repeats the chart from SPE-2 and includes a similar chart for SPE-3 including both the older and the newer canisters. The figure illustrates: 1) the older gauge response was consistent between the two events and 2) all new gauges provided reasonable data.

These findings were presented in a briefing (Ref. 4) to the SPE Subject Matter Experts (SME) panel and subsequently to the National Center for Nuclear Security (NCNS) Executive Advisory Board (EAB). The recommendation that the radial and transverse data from those gauges be corrected for rotations was accepted by both of these review groups.

Reference 5 describes the correction methodology, while Reference 6 includes the magnitudes of those corrections. Both of these documents are available on the project data server. The records resulting from these corrections are posted on the data server.
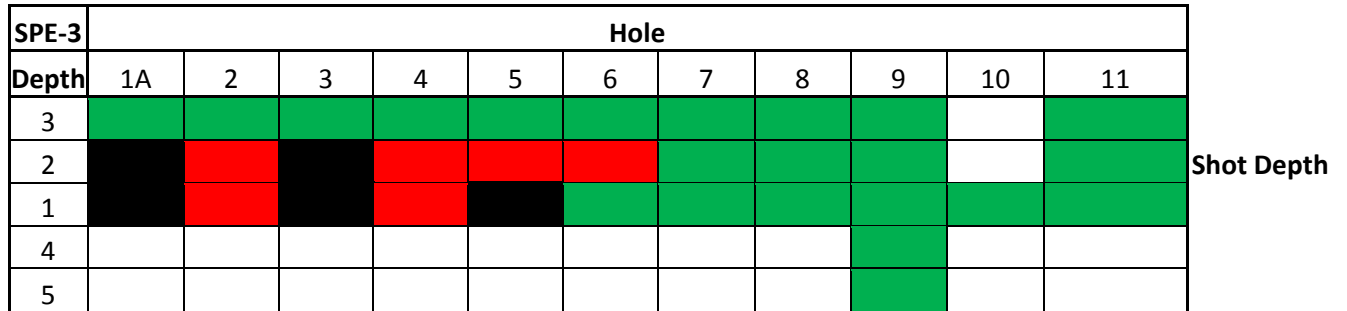
SPE-2	Hole						
Depth	1A	2	3	4	5	6	
3	🟩	🟩	🟩	🟩	🟩	🟩	
2	🟩	🟥	🟥	🟥	🟥	🟥	**Shot Depth**
1	🟩	🟥	⬛	🟥	⬛	🟩	

Legend
No Anomalies Observed
Apparent Gauge Rotation
No Data

SPE-3	Hole											
Depth	1A	2	3	4	5	6	7	8	9	10	11	
3	🟩	🟩	🟩	🟩	🟩	🟩	🟩	🟩	🟩		🟩	
2	⬛	🟥	⬛	🟥	🟥	🟥	🟩	🟩	🟩		🟩	**Shot Depth**
1	⬛	🟥	⬛	🟥	⬛	🟩	🟩	🟩	🟩	🟩	🟩	
4									🟩			
5									🟩			

Figure 18: Figure 19: Stop light chart summarizing data for SPE-2 and SPE-3 including new gauge canisters.

Pre-Event Zero-Shift Corrections— When examining data obtained from accelerometers a zero-shift is often observed both prior to and during an event. In a piezoresistive sensor pretest "zero-shifts" may be due to the sensor being out of balance or thermal effects. This type of zero-shift is generally easy to correct as it is normally a uniform shift from what should be zero amplitude; that is, before the shot there should be no motion).

This is typically inconsequential to acceleration character and amplitude. However, velocity is achieved through integration of these acceleration records, and the shift in acceleration can translate into a significant cumulative error. This error can measurably alter the velocity peak amplitude and outward phase to an extent that can change the assessment of the ground shock environment caused by the explosive event.

Consequently, to facilitate analysis of velocity from these records we provide baseline corrected acceleration records for these transducers. These corrections were made by reading the digital data record up to fiducial. As these data should be null, or zero acceleration, the average of these pre-fiducial data is representative of the DC shift. This average value is subtracted from the entire raw data record to generate a new data file for each measurement corrected for zero-shift.   Reference 7 describes the magnitudes of shift applied to all data.

Users are welcome to perform their own corrections to the data, or to operate on the uncorrected data as they see fit. We provide corrected data records on the data server to facilitate consistency among analyses. Any alternate approaches to data corrections should be documented by the user. We note

here that the velocity records used to describe the canister rotation analysis in the prior section included zero-shift corrections.

During Event Zero-Shift Corrections— Zero-shifts occurring during an event pose a larger problem and are less tractable than the pre-event zero-shift. Accelerometer data that never returns to baseline, or zero, will result in continually increasing, or decreasing depending on the shift direction, velocity and displacement while, in reality, a static equilibrium state must be achieved. But these shifts are harder to correct.

The shift can reflect several possible phenomena, or combination of phenomena. These include overstressing the piezoelectric crystals, physical movement in the sensor parts, excessive base strain, excessive cable motion, or overloading the signal conditioning. There is not a straight forward way to correct for these phenomena and we recommend caution in accomplishing these corrections and in using the resulting displacements for analysis, such as in the Reduced Displacement Potential (RDP) analysis discussed in Reference 8.

Reference 7 includes a discussion of corrections made for this second drift. Basically, a reasonable estimate was made on the correction required to bring the late-time velocity to a zero-amplitude baseline. Some degree of judgment was required to make these adjustments and so they must be viewed with caution. Nevertheless, an additional set of data with these corrections applied is available on the project data server.

REFERENCES

1. Steedman, D. W., "LANL Review of SPE-2 Near Field Velocity Data," Presented to the SPE SME Data Review, Los Alamos National Laboratory, Los Alamos, NM, January 2012.
2. Steedman, D. W., "Supplement to: LANL Review of SPE-2 Near Field Velocity Data," Presented to SPE Data Review Team, Los Alamos National Laboratory, Los Alamos, NM, January 2012.
3. Shah, K., personal communication, 2011
4. Steedman, D. W., Shah, K., and Hemming, X., "Review of SPE Near Field Accelerometer Data," Presented to the NCNS Executive Advisory Board, 13 September 2012
5. Thomsen, J., "SPE Data Acceleration Component Rotation Methodology," Applied Research Associates, Albuquerque, NM, 22 October 2012.
6. Thomsen, J., "SPE Acceleration Component Rotations: Shock Angle Analyses for Holes 1-6 Compared to SPE-3 Holes 7-11," Applied Research Associates, Albuquerque, NM, 31 October 2012
7. Rougier, E., "SPE-1 Baseline Shift Corrections," Los Alamos National Laboratory, Los Alamos, NM, May 2013.
8. Rougier, E., and Patton, H.J.," Quality Assessment of SPE Free Field Data Based on Reduced Displacement Potentials," LA-UR-13-20277, Los Alamos National Laboratory, Los Alamos, NM, 16 January 2013.